

---

This item was submitted to [Loughborough's Research Repository](#) by the author.  
Items in Figshare are protected by copyright, with all rights reserved, unless otherwise indicated.

## Ion mobilities in capillary electrophoresis

PLEASE CITE THE PUBLISHED VERSION

PUBLISHER

© Andrew McKillop

PUBLISHER STATEMENT

This work is made available according to the conditions of the Creative Commons Attribution-NonCommercial-NoDerivatives 2.5 Generic (CC BY-NC-ND 2.5) licence. Full details of this licence are available at:  
<http://creativecommons.org/licenses/by-nc-nd/2.5/>

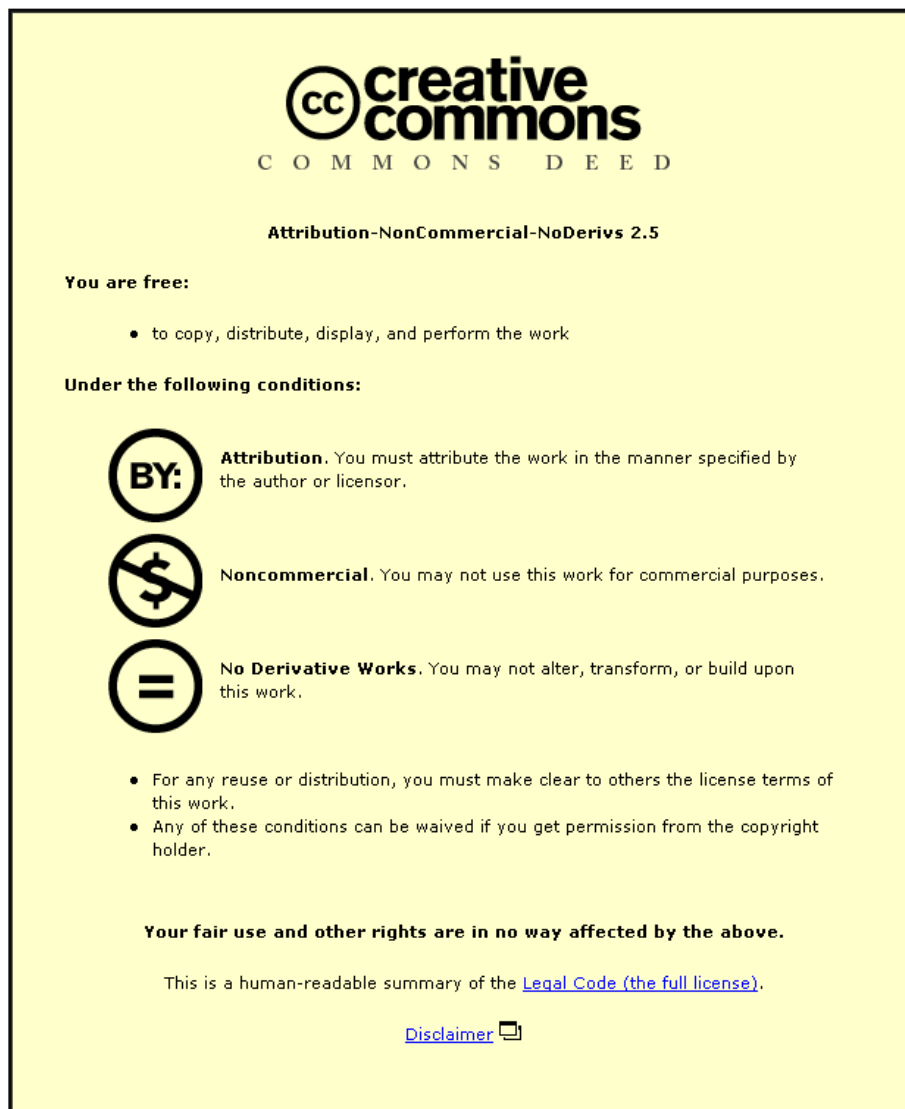
LICENCE

CC BY-NC-ND 2.5

REPOSITORY RECORD

McKillop, Andrew G.. 2019. "Ion Mobilities in Capillary Electrophoresis". figshare.  
<https://hdl.handle.net/2134/28235>.

This item was submitted to Loughborough University as a PhD thesis by the author and is made available in the Institutional Repository (<https://dspace.lboro.ac.uk/>) under the following Creative Commons Licence conditions.



For the full text of this licence, please go to:  
<http://creativecommons.org/licenses/by-nc-nd/2.5/>



**Pilkington Library**

Author/Filing Title ..... McKillop, A.G.

Accession/Copy No. .... 040147168

Vol. No. .... Class Mark ..... T

~~26 JUN 1998~~

LOAN COPY

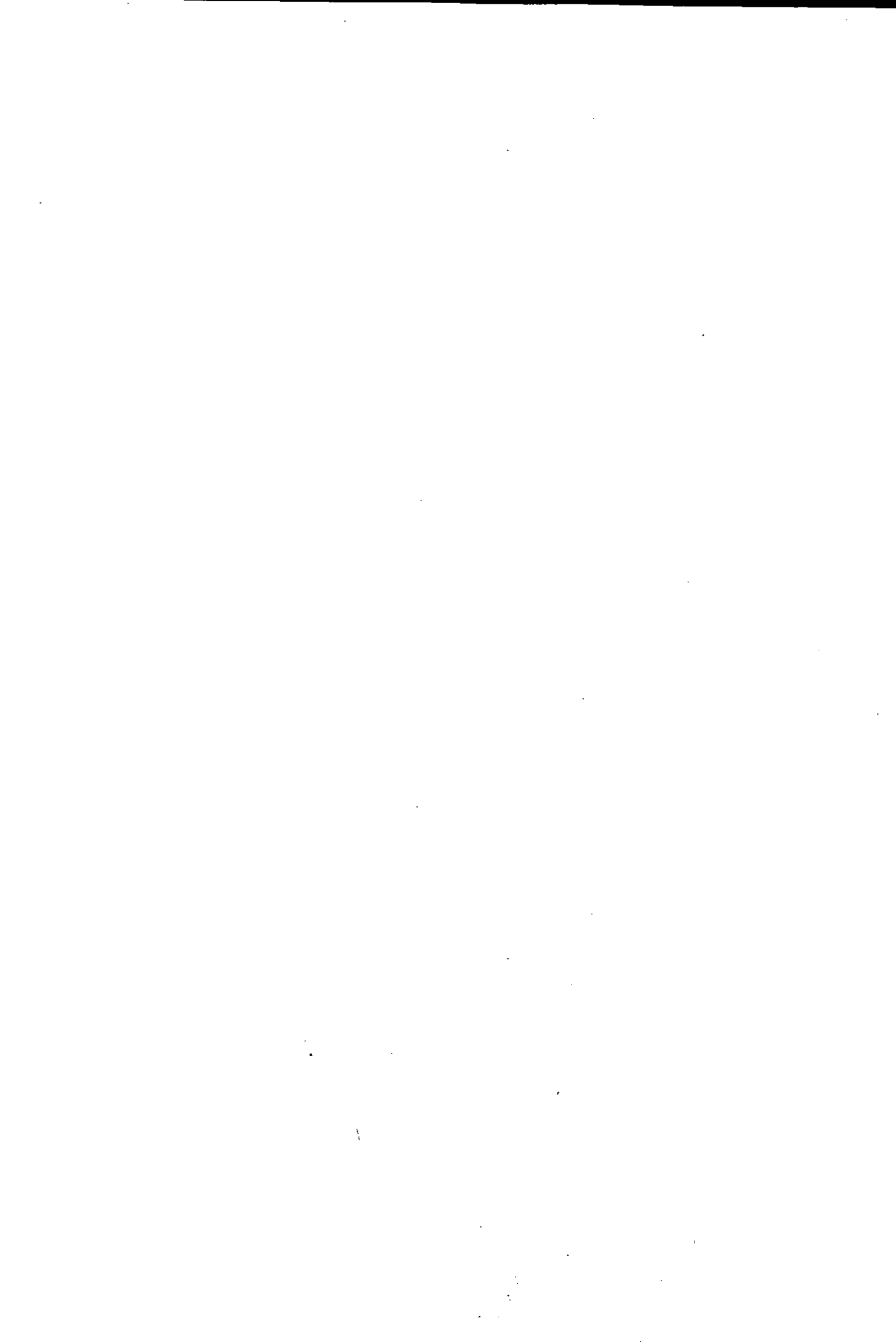
26 JUN 1998

25.6.99

0401471683



BADMINTON RR  
18 THE HALES  
SYSTEM  
LEICESTER LE  
ENGLAND  
TEL: 0116 260  
FAX: 0116 269



# ION MOBILITIES IN CAPILLARY ELECTROPHORESIS.


By Andrew McKillop.

A Doctoral Thesis  
submitted in partial fulfilment of the  
requirements for the award of Doctor of  
Philosophy of Loughborough University.

September 1996.

Supervisor: Professor R.M. Smith  
Department of Chemistry

© Andrew McKillop 1996.

	Loughborough UNIVERSITY
Date	July 97
Class	
040147168	

99100128

## **ABSTRACT.**

### **Ion Mobilities in Capillary Electrophoresis.**

**Andrew Gordon McKillop.**

**September 1996.**

The project has investigated the electrophoretic mobilities of sets of model compounds to determine the effects of size and shape on ion mobilities. Methods were developed for the analysis of compounds in order to quote accurate electrophoretic mobilities. Using the obtained electrophoretic mobilities, mobility orders were correlated with structural properties.

The analysis of the first group of compounds, the alkyipyridines, showed that differences in electrophoretic mobility were obtained for structural isomers at low pH where the compounds are all fully charged. Mobility orders were found to have no relation to the ionisation constants of compounds and the relationship between the mobility order of compounds at low pH and at higher pH values where separation is controlled by the ionisation constants was investigated for the six dimethylpyridine isomers.

Structural properties of the alkyipyridines were investigated with a view to prediction of mobility from such properties. Literature relationship accounted for the size of ions but isomers were not accounted for. An approach to modelling the separations of the alkyipyridines was presented. The centre of charge of analytes were calculated based on the Hückel charge distribution model and the centre of mass of the compounds was calculated. The ions were considered to be restricted in their rotation in the applied electric field and two molecular radii related to this property were calculated:  $R_{rot}$  - the radii swept out due to unrestricted rotation and  $R_i$  - distance between centre of mass and centre of charge related to the ability of an analyte to rotate against the applied electric field. Using these values and the Van der Waals' radii of the molecules, multi-linear regression was used to produce a regression equation predicting the mobility of analytes. This equation was tested on other alkyipyridines.

The electrophoretic mobilities of some alkyilanilines were also determined by capillary electrophoresis. Their mobilities were found to be generally lower than corresponding sized alkyipyridines, and it is thought that these lower mobilities were due to the amine groups being able to interact more strongly with counterions in solution. Primary amines had lower mobilities than secondary amines. The mobility orders of the dimethylanilines had some similarities with the alkyipyridines.

The final set of compounds that were investigated were some alkyibenzoic acids. The electrophoretic mobility of these compounds were found to be generally lower than the mobilities of corresponding alkyipyridines. The mobility order of structural isomers was found to differ than the orders observed for the other sets of compounds and this may be due to increased interactions with counterions. The chromatographic retentions of alkyibenzoic acids in alkyl bonded capillaries was also investigated.

## **Acknowledgements.**

I would like to thank my supervisor Roger Smith for his help and guidance throughout the past three years. Also, I would like to thank Ray Rowe and Steve Wren for support and useful discussions throughout the project and the encouragement to follow my chosen career.

My colleagues, Paul Desmond, Arjinder Ubi and Rob Burgess have provided me with help and friendship in the laboratory during my project as well as the numerous visiting and project students who are too numerous to mention. Thanks also to the Analytical technicians, Bev Cooper and Elaine Till for their help and patience. Thanks also to fellow chemists Mark Evans and Ian Begley for friendship. Thanks to Doug Bray at Zeneca who helped me with viscosity measurements and to the modelling group at Mereside who also provided support.

A special thanks to my girlfriend Vivienne who has had to cope with all the pressures associated with the writing of this thesis and has provided strong support throughout. Numerous friends both new and old have also played a part over the past three years. Thanks to Simon, Darren, Justin, Barney, Chris, Kerr, George, Paul, Kate, Ian, Rob, Biff, Brian.

Finally I'd like to thank my family Mum, Dad, Fiona and Morag for their support over the past three years and indeed throughout my whole education.

I feel that I have been fortunate with the friends and colleagues I have been associated with over the last three years. I hope that as my life enters a new chapter, these associations may continue.





2.1	Introduction	26
2.2	Capillary Electrophoresis	26
2.2.1	Chemicals	26
2.2.2	Apparatus	26
2.2.3	Methods for Alkylpyridine separations	27
2.2.4	Methods for Alkylbenzoic acid separations	28
2.3	Molecular Modelling	29
2.3.1	Equipment	29
2.3.2	Methods	30
2.4	Potentiometric Titration	32
2.4.1	Chemicals	32
2.4.2	Apparatus	33
2.4.3	Method	33
2.5	pKa Estimation	34
2.5.1	Equipment	34
2.6	NMR Spectroscopy	35
2.7	NMR Spectroscopy	35
2.8	Rheometry	35
3.	<b>Evaluation of Fundamental Parameters.</b>	<b>36</b>
3.1	Introduction	36

3.2	Analysis and Markers at pH 2.5	36
3.2.1	The repeatability of migration times	36
3.2.2	Measurement of electroosmotic mobility	38
3.2.3	Pyridine as an internal standard	42
3.2.4	Summary	48
3.3	The Effects of Temperature at pH 2.5	49
3.3.1	Power dissipation experiments	49
3.3.2	Estimation of capillary temperature	51
3.3.3	Summary	54
3.4	Analysis at pH 8.5	55
3.4.1	Analysis and markers at pH 8.5	55
3.4.2	Effects of temperature	58
3.5	Summary	59
4.	<b>Separations of Alkylpyridines.</b>	<b>60</b>
4.1	Introduction	60
4.2	Separations at low pH	60
4.3	The Effects of Ionic Strength	65
4.3.1	General Trends	65
4.3.2	Electroosmotic Mobility	66
4.3.3	Electrophoretic Mobility	66
4.3.4	Effects of Ionic Strength on Separations	67
4.4	The Effects of Temperature	70

4.5	Separation of the Dimethylpyridines across the pH range.	72
4.5.1	Introduction	72
4.5.2	Separations at pH 2.5	72
4.5.3	Prediction of mobility from pKa values	74
4.5.4	Separation at pH 6.5	77
4.6	Separations of Z and E 2-(3-pentenyl)pyridine	79
4.7	Summary	83
<b>5.</b>	<b>Separations of Substituted Benzenes.</b>	<b>84</b>
5.1	Introduction	84
5.2	Separations of Alkylbenzoic Acids	84
5.2.1	Separations at high pH	84
5.2.2	BICINE buffer	85
5.2.3	Lithium borate buffer	87
5.2.4	Alkyl bonded capillaries	89
5.3	Retention of Alkylbenzoic Acids in Alkyl Bonded Capillaries	90
5.3.1	Fused silica capillary separations	91
5.3.2	C1 capillary separations	92
5.3.3	C18 capillary separations	94
5.3.4	Effect of Organic Modifier	96
5.3.5	Pressure driven separations	97
5.3.6	Separation of neutral compounds	100

5.4	<b>Separations of Alkylanilines</b>	<b>101</b>
5.5	<b>Multi-functional compounds</b>	<b>103</b>
	5.5.1 Separation at pH 2.5	103
	5.5.2 Separation at pH 8.5	104
5.6	Summary	106
<b>6.</b>	<b>Modelling of the Alkylpyridine Separations.</b>	<b>107</b>
6.1	Introduction	107
6.2	Existing models	107
	6.2.1 Offords' parameter	107
	6.2.2 The Van der Waals' model	109
6.3	Molecular Properties of the Analytes and their Relationship with Electrophoretic Mobility	111
	6.3.1 The relaxation effect and charge distribution	111
	6.3.2 The electrophoresis effect and restricted rotation	113
	6.3.3 Analyte-analyte interactions	114
6.4	A Model for Restricted Rotation of Analytes	114
6.5	Multi-Linear Regression Analysis	118
	6.5.1 Van der Waals' model	118
	6.5.2 Van der Waals' model including $1/R_{rot}$	119
	6.5.3 Van der Waals' model including $1/R_i$	119

6.5.4	Van der Waals' model including $1/R_{\text{rot}}$ and $1/R_i$	119
6.5.5	Effects of ionic strength	122
6.6	Extensions to other Analytes	124
6.6.1	Other positional isomers and longer chain alkylpyridines	124
6.6.2	Chain branching	130
6.6.3	2-(3-pentenyl)pyridine	132
6.7	Modelling of Aminoalkylpyridines	134
6.7.1	Van der Waals' model	134
6.7.2	Relationship with molecular mass	138
6.7.3	Separations of Isomers	139
6.8	Summary	143
7.	<b>Modelling of Substituted Benzenes and Related Compounds</b>	<b>144</b>
7.1	Introduction	144
7.2	Alkylanilines	144
7.2.1	Literature relationships and comparisons with the alkylpyridines	144
7.2.2	Modelling of the Dimethylanilines	147
7.3	Aminoalkylbenzenes	149
7.4	Dual Functionality Compounds	151

<b>7.5</b>	<b>Study of the Alkylbenzoic Acids</b>	<b>153</b>
7.5.1	Literature Relationships	153
7.5.2	Shape Modelling of the Alkylbenzoic Acids	159
<b>7.6</b>	<b>Summary</b>	<b>163</b>
<b>8.</b>	<b>Conclusions</b>	<b>164</b>
	<b>References</b>	<b>166</b>
	<b>Appendix I</b>	<b>173</b>
	Electrophoretic Mobility Data	
	<b>Appendix II</b>	<b>182</b>
	Survey of Ionisation Constants	
	<b>Appendix III</b>	<b>187</b>
	HPLC of the Dimethylpyridines	
	<b>Appendix IV</b>	<b>200</b>
	Poster and Presentations	
	<b>Publications</b>	

# Chapter 1.

## Introduction.

### 1.1 History of Capillary Electrophoresis

Electrophoresis is defined as the migration of charged particles, colloidal particles or ions through a solution under the influence of an electric field [1]. The separation of compounds by applying a voltage to a gel support matrix has long been established as an important separation technique for biomolecules [2]. The use of capillaries as the separation chamber is a relatively more recent development and can be traced back to the thesis of Virtanen [3] who in 1974 showed that it was possible to achieve separations of alkali cations by free zone electrophoresis in small diameter (200-500  $\mu\text{m}$  internal diameter) Pyrex tubing. Mikkers, Everaerts and Verheggen [4] described the use of Teflon tubes (200  $\mu\text{m}$  internal diameter) and demonstrated that by using only a small amount of analyte, a symmetrical peak shape could be achieved.

The work that inspired the separation science community was that of Jorgenson and Lukacs in 1981 [5] where CE was performed in open-tubular glass capillaries of 75  $\mu\text{m}$  internal diameter. Injection was achieved by electromigration giving a narrow injection band and detection was performed by means of fluorescence detection. Such conditions allowed Jorgenson and Lukacs to achieve symmetrical peaks and efficiencies in excess of 400 000 theoretical plates  $\text{m}^{-1}$  for runs of under 30 minutes. This landmark in the development of the instrumental technique demonstrated all the advantages of capillary electrophoresis: namely relatively short migration times, cheapness, extremely small sample capacity, environmentally friendly buffers and high efficiencies of separation.



Many problems still remained, such as the need for an automatable and quantitative injection technique, the requirement of flexible and sensitive means of detection to accommodate a broad spectrum of analytes and the problems of band broadening due to thermal gradients within capillaries. The challenge to the scientific community was established and CE saw explosive growth in the following 15 years. The development of commercially available automated instrumentation [6-13] has eliminated many of the problems faced by early workers.

Features of CE such as high separation efficiency, reasonable sensitivity, short separation times and simplicity have led to the rapid development of capillary electrophoresis in the analysis of small molecules [14-16] including the analysis of analytes of pharmaceutical interest [17-21].

## 1.2 Basic Theory of Electrophoresis.

### 1.2.1 Electrophoretic Mobility.

In capillary electrophoresis, ions are separated according to their differential velocity in an electric field, either by attraction or repulsion. When an ion of charge  $q$  is subjected to an electric field of strength  $H$ , it is acted on by a force  $qH$ , causing the ion to accelerate. In liquids this acceleration will continue until it is exactly balanced by a frictional force  $f$ , causing the particle to reach a constant terminal velocity  $v$ . The equilibrium conditions can be represented by the general equation (1.1) [22],

$$qH = \frac{kT}{D} v = fv \quad (1.1)$$

where  $D$  is the diffusion constant of the particle,  $k$  is the Boltzmann constant and  $T$  is the temperature. The terminal (or steady state) velocity of the particle  $v$  is dependent on the applied field. The ability to migrate, the

electrophoretic mobility  $\mu_e$  is defined as the velocity per unit field strength and is given by equation (1.2).

$$v = \mu_e H \quad (1.2)$$

Therefore the quotation of electrophoretic mobility has the advantage over ion velocity of being independent of field strength. In terms of mobility, equation (1.1) can thus be rewritten (1.3).

$$\mu_e = \frac{qD}{kT} = \frac{ZeD}{kT} \quad (1.3)$$

where  $Z$  is the unit charge on the ion and  $e$  is the electronic constant. This equation is widely applicable, as it is independent of shape and size of particle. However, diffusion constants are rarely available for chosen experimental conditions.

The common theory adopted in capillary electrophoresis has been to assume that the frictional force experienced by an analyte is given by Stokes' Law [23], thus the mobility of ions is given by equation (1.4),

$$\mu_e = \frac{q}{6\pi\eta r} \quad (1.4)$$

where  $q$  is the charge on the analyte,  $r$  is the hydrodynamic radius of the analyte and  $\eta$  is the viscosity of the separation medium. Equation (1.4) can also be derived from electrostatic theory for the limiting case where the charged particle is so small that it does not distort the applied electric field [24]. For the case where the charged particle is so large that the electric field is everywhere tangential to its surface the equation is similar except for the factor

$6\pi$  is replaced by the factor  $4\pi$ . The numerical value is a function of geometry and experimental results are often fitted by the experimental assignment of a value between  $4\pi$  and  $6\pi$ .

Thus in the simplest form of CE (open tubular or capillary zone electrophoresis) the two principal factors that influence the electrophoretic mobility of analyte's are their charge and size. Equation (1.4) is a measure of a spherical analytes speed of movement through the buffer solution within the capillary.

### 1.2.2 Electroosmotic Flow.

The buffer is also transported through the capillary by the phenomena known as electroosmotic flow, which occurs in addition to the migration of ions in the capillary. The electroosmotic flow (EOF) is defined as the bulk flow of liquid in the capillary [1] and occurs as a consequence of the surface charge on the interior of the capillary wall. The EOF can allow the separation of cations and anions within the same run in capillary electrophoresis [25].

In a fused silica capillary, the ionised silanol groups at the capillary wall are balanced by a layer of positive ions in the vicinity of the capillary surface forming a zeta potential ( $\zeta$ ) at the capillary wall. When a voltage is applied to the capillary the loosely bound layer of cations is free to move towards the cathode causing a bulk flow of liquid within the capillary. An exact expression for  $\mu_{eof}$  [26] (1.5) is,

$$\mu_{eof} = \frac{\epsilon\epsilon_0\zeta}{\eta} \quad (1.5)$$

where  $\eta$  is the buffer viscosity,  $\epsilon$  is the dielectric constant and  $\epsilon_0$  is the permittivity of free space. The EOF is highly dependent on the pH of the electrolyte buffer [27] because of effect of pH on the surface charge of the silanol groups within the capillary (Figure 1.1).

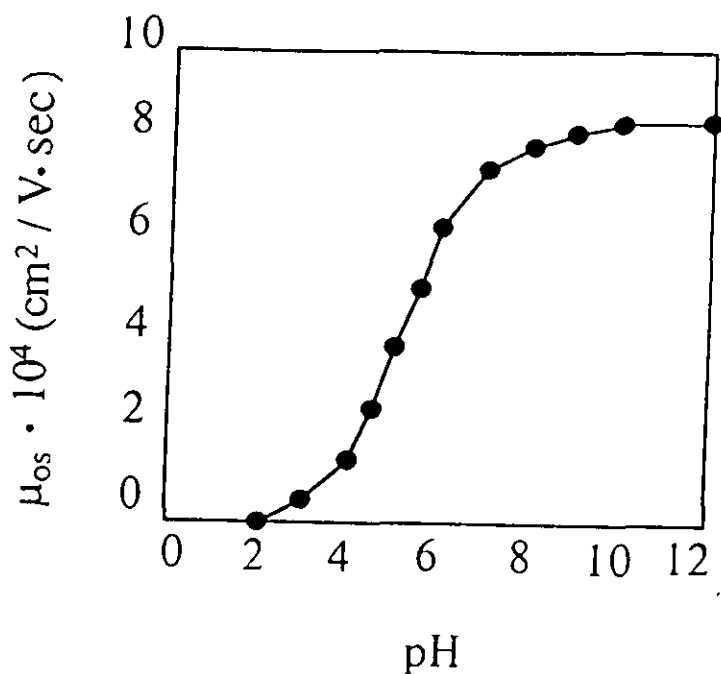


**Figure 1.1** Dependence of EOF on pH for a fused silica capillary.  
Reproduced from [27]

The fundamental properties of the fused silica capillary were investigated by Salomon *et al.* [28]. The potential induced by the capillary surface is compensated by positive ions over an effective distance  $x$  (perpendicular to the wall), such that the electroosmotic mobility can be re-written as

$$\mu_{eof} = \frac{Qx}{\eta} \quad (1.6)$$

where  $Q$  is the charge per unit area at the interface between capillary wall and the buffer solution and  $x$  is the thickness of the counterion layer. The thickness of the counter ion layer was derived to be a sum of a compact layer of fixed thickness  $d_o$  and the Debye-Hückel thickness [29] which is related to the square root of ion concentration (1.7),

$$x = d_o + \frac{1}{K' \sqrt{[M^+]}} \quad (1.7)$$

$[M^+]$  is the ion concentration and  $K'$  is equal to  $3.2 \text{ e}^{-9} \text{ m}^{-1} (\text{mol l}^{-1})^{-1/2}$  for a dilute aqueous system at 25 °C.

The model was tested by measuring the electroosmotic flow in a 20 mM 2-(N-morpholino)ethanesulfonic acid (MES) - 8 mM sodium hydroxide buffer and a non-linearity of EOF against  $[\text{NaOH}]^{-1/2}$  was observed at low buffer concentrations. This non-linearity was accounted for by the fact that the charge  $Q$  is also a function of buffer concentration due to the absorption of buffer ions [30]. Cations are known to adsorb to silica surfaces and can be held by forces in addition to electrostatic attraction, however the mechanism is not well understood [30]. A simple adsorption mechanism was investigated and the electroosmotic flow was found to be inversely proportional to  $[\text{NaOH}]$  at low concentrations, with curvature at higher concentrations. Thus, a model involving both absorption and electrostatic interaction was developed and fitted well with experimental results (1.8),

$$\mu_{\text{eof}} = \frac{Q_o}{\eta(1 + K_{\text{wall}}[M^+])} \left( d_o + \frac{1}{K' \sqrt{[M^+]}} \right) \quad (1.8)$$

The effects of other parameters were also investigated [28]. Buffer cation has a large effect on electroosmotic flow [31]. The addition of organic

modifiers are known to lead to changes in the EOF [32-36], with methanol leading to a reduction in EOF. The reduction of EOF by methanol has been attributed to the shielding of charged sites from one another by methanol molecules.

The EOF is also sensitive to coating on the capillary surface. Coated capillaries such as alkyl bonded or polyacrilamide have less free  $\text{SiO}^-$  groups available to form the electrical double layer [37] and also absorption of cations is greatly reduced. This makes these capillaries ideal for the analysis of complex samples susceptible to absorption of analytes such as biological matrices or polymer samples [38,39].

### 1.2.3 The Effects of Temperature in Capillary Electrophoresis.

The application of an electric field to a buffer filled capillary leads to Joule heating within the capillary. This heating can lead to a variety of effects which can influence the quality of separations. For biological samples, performing separations using rigid gels was the most common approach to eliminate heating affects. The gel support materials anti-convective properties and the application of low electric fields lead to reduced heating effects thus producing satisfactory results [2]. However, the ability to work with and detect samples in capillaries of less than 200  $\mu\text{m}$  [3-5] has led to a powerful alternative to gel electrophoresis. The high surface area to volume of small capillaries allows sufficient heat dissipation at high electric field strengths to avoid excessive temperature rises. However, the effects of temperature can still be detrimental and so must be evaluated. Joule heating effects can be divided into three main categories.

### Natural Convection.

The bulk flow of liquid due to density differences in neighbouring regions of fluid is known as natural convection, and can be due to differences in either composition or temperature of the electrolyte solution [23]. A parameter used to evaluate the effects of natural convection is the dimensionless Rayleigh number,  $Ra$  [40] (1.9).

$$Ra = \frac{R_1^4 g}{\eta \alpha} \left( \frac{\Delta \rho}{\Delta r} \right) \quad (1.9)$$

where  $R_1$  is the radius of the electrophoresis chamber,  $g$  is the acceleration due to gravity,  $\eta$  is the viscosity of the separation medium,  $\alpha$  is the thermal diffusivity of the medium and  $\Delta \rho / \Delta r$  is the density change per unit of radial distance caused by heating. If  $Ra \ll 1$ , then convective flow is negligibly small, and if  $Ra$  is in the region of 1 then natural convection becomes significant. Thus by reducing the Rayleigh number convective effects can be reduced.

Historically, the first attempt to reduce natural convection was to superimpose a composition-induced density gradient using sucrose [41]. A horizontal tube rotated about its longitudinal axis also hinders thermal convection [42,43]. Another proposed method but not widely applicable would be to perform electrophoresis in outer space thus reducing the gravity term in equation (1.9). This method may be a future approach to preparative scale electrophoresis.

However, the method of widest applicability for reducing the Rayleigh number is to perform separations in capillaries, thus reducing the  $R_1$  term. This method is particularly successful due to the power relationship between  $Ra$  and the radius of the separation chamber  $R_1$ .

### Intracapillary Temperature Profile.

The heat generated due to the application of electric fields must be lost through the walls of the capillary to surroundings. Thus, an intracapillary temperature profile is generated under electrophoresis. For the types of capillary used in CE (Figure 1.2) heat must be lost at the interfaces between buffer and the fused silica wall, between the fused silica and polyimide coating and between the polyimide coating and surroundings.

The difference in temperature between the centre of the capillary and the boundary with the fused silica is described by the laws of thermal conduction [44-46] and is given by expression (1.10).

$$T_0 - T_1 = \frac{S_e R_1^2}{4k_b} \quad (1.10)$$

where  $T_0$  is the temperature at the centre of the capillary,  $T_1$  is the temperature at the fused silica wall,  $S_e$  is the rate of power generation within the control volume per unit volume and  $k_b$  is the thermal conductivity of the buffer.  $S_e$  is given by  $I^2/\kappa_e$  where  $I$  is the current density and  $\kappa_e$  is the electrical conductivity of the buffer. The intracapillary temperature profile has a parabolic shape (Figure 1.3) and leads to the electrolyte buffer viscosity being higher at the walls of the capillary than the centre. These viscosity differences can lead to band broadening of peaks due to migration of compounds at different rates (equation 1.4) at the centre and walls of the capillary. The usual way of controlling this form of band broadening is to keep the ionic strength of the electrolyte solution low and thus the amount of heat generation within the capillary to a minimum.



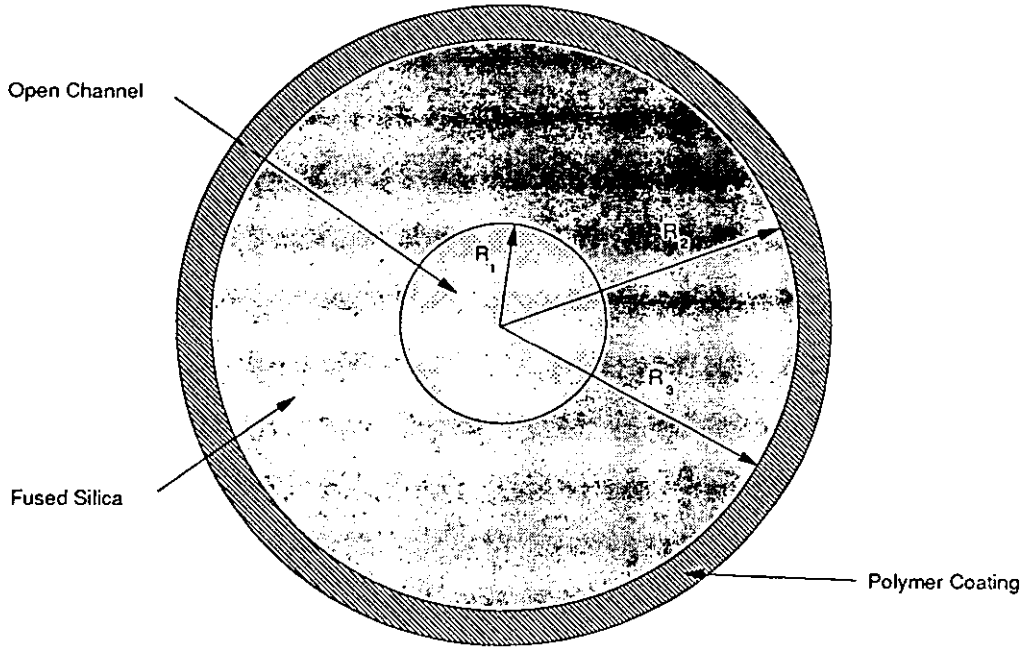


*Figure 1.2 Schematic diagram of a typical capillary cross section where  $R_1$ ,  $R_2$  and  $R_3$  are the radii of the open channel, fused silica and polymer coating respectively.*

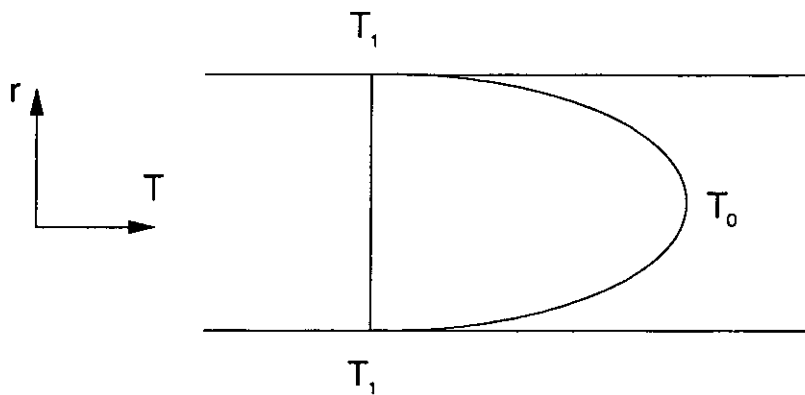


*Figure 1.3 Parabolic intracapillary temperature profile.  $T_1$  is the temperature at the fused silica wall and  $T_0$  is the temperature at the centre of the capillary.*

### Overall Temperature Rise.

In order to accurately determine the temperature within a capillary under conditions of natural and forced convection, it is necessary to use heat conduction and convection equations of heat transfer [44-46]. For steady state heat conduction from composite cylinders, the heat equation reduces to equation (1.11).

$$T_0 - T_a = \frac{SeR_1^2}{2} \left( \frac{1}{2k_b} + \frac{1}{k_g} \ln\left(\frac{R_2}{R_1}\right) + \frac{1}{k_p} \ln\left(\frac{R_3}{R_2}\right) + \frac{1}{R_3 h} \right) \quad (1.11)$$

where  $T_a$  is the actual average temperature within the capillary,  $k_g$  and  $k_p$  are the thermal conductivities of the fused silica (glass) and polyimide coatings respectively,  $h$  is the capillary-surroundings heat transfer coefficient and  $R_1$ - $R_3$  are as Figure 1.2.

The relationship is a summation relating to heat transfer across each interface. Knox and McCormack [47] calculated the temperature difference within the capillary bore (i.e. ignoring the final term in the summation) to be 1.05 K using typical values for buffer thermal and electrical conductivities. This contrasted with an experimental value [48] of 34.1 K. The discrepancy was accounted for since the capillary was cooled by natural convection. For such a system by far the greatest drop in temperature occurs between the outer capillary wall and surrounding fluid [49]. Typical values for the capillary-surroundings heat coefficient  $h$  were estimated by Jones and Grushka [50] to be 263 W/m<sup>2</sup>°C for an air velocity of 2 m/s and an air temperature of 25 °C. A value of 10,000 W/m<sup>2</sup>°C would be typical for a liquid heat transfer medium. Thus the temperature rise within the capillary in a liquid cooled CE instrument is much smaller than for a corresponding CE cooled either by forced convection or natural convection. Knox and McCormack [47] calculated that

for typical conditions, the maximum power dissipation in a liquid cooled capillary could be 391 W/m compared to 2.13 W/m for air, although it is never likely that such high power levels would ever be reached.

The methods for the determination of temperature within capillaries described above use indirect information, such as the current data and information about the electrical and thermal properties of the materials, to determine the temperature rise within capillaries under electrophoresis. Direct methods of determining temperature within capillaries have also been investigated. Wätzig [51] used a cobalt (II) solution which has thermochromic properties to measure temperature changes by a shift in the UV spectrum of the buffer. The effectiveness of the cooling system was investigated in reaching equilibrium temperatures was investigated and results indicated temperature rises of several degrees Kelvin despite thermostatic control, which was in agreement with theoretical calculations for a liquid cooled system.

Using Raman thermometry based on the temperature dependence of the water O-H stretch equilibrium, the temperatures within a fused silica capillary were probed by Davis *et al.* [52]. The capillary was cooled by natural convection and intracapillary temperatures ranging from 25 °C to 70 °C were observed over the range of buffers and electric fields used. Differences between local temperatures and average capillary temperatures were observed at all operating conditions.

In summary, heating within capillaries occurs due to current flow. Such effects can lead to dramatic changes in the separation conditions and so it is desirable to cool the capillaries. Most commercial CE apparatus have forced air or liquid cooling systems to minimise the effects of heating [6-13].

### 1.3 Separations of Small Molecules by Free Solution Capillary Electrophoresis.

#### 1.3.1 Range of Applications.

Features such as high separation efficiency, reasonable sensitivity, short separation times and simplicity have led to the investigation of free solution capillary electrophoresis by many workers [14-16]. The range of substances analysed is wide, from small molecules to larger molecules such as polymers and biomolecules. Small molecules and ions have been analysed by CE for a wide range of applications, ranging from inorganic analysis to pharmaceutical analysis [17-21].

#### 1.3.2 Separations of Small Molecules.

The electrophoretic mobility of compounds is governed by the factors in equation (1.4) describing the mobility of spherical analytes. External factors such as the temperature of the background electrolyte and therefore its viscosity affect electrophoretic mobilities, however the only analyte dependant factors on electrophoretic mobility are the charge on the analyte and the size of the analyte. The shapes of analytes are considered in section 1.4. Therefore to achieve relative changes in the separations of analytes by free solution capillary electrophoresis, the analyst can adjust the charge on compounds by varying the pH of the background electrolyte or exploit differences in the size of analytes. It is not possible to separate neutral molecules without adding complexing agents [53] to perform electrokinetic chromatography.

For separations exploiting differences in the charge on analytes Terabe and co-workers studied the separation of isotopic  $^{16}\text{O}$  and  $^{18}\text{O}$  benzoic acids as examples of closely related compounds [54]. An optimum pH for separation was calculated to be  $(\text{p}K_{\text{a}} - \log 2)$  based on the theoretical resolution equation

in CE. The effects of applied voltage and capillary length were also investigated. Optimisation of pH in the separation of the methylpyridines was studied by Wren [55], who predicted that the maximum charge difference between two species could be calculated by taking the average of their  $pK_a$  values. At the point of maximum charge difference between the species the best separation should be obtained and this was shown using the isomeric methylpyridines as an example. For the basic methylpyridines increasing electroosmotic flow was shown to deteriorate separations due to the time windows available for separation being reduced. Separation of the methylpyridines was improved by the use of a cationic surfactant to suppress electroosmotic flow. Friedl and Kenndler investigated resolution as a function of the pH of the buffer for multivalent ions, including the benzenedicarboxylic acids [56]. It was determined that resolution depended on two terms, the ratio of the electrophoretic mobilities and an efficiency term. Based on the  $pK_a$  values and the actual mobilities the resolution was calculated across the pH range and compared with experimental data.

Physico-chemical constants can also be determined by free solution CE. An advantage of a separation technique such as CE for determining such constants is that possible impurities can be separated from the substance of interest. Ionisation constants are readily determined by CE by investigating the change in electrophoretic mobility of analytes with changes in the pH of the background electrolyte. Beckers *et al.* [57] described the determination of  $pK_a$  values for a weak monovalent acid. The effect of the partial charge on the migration rates has also been used to determine ionisation constants at low solute concentrations [58]. By studying the change in electrophoretic mobility across the pH range,  $pK_a$  values between 2.55 and 5.26 were determined to within 0.03 pH units for analyte concentrations less than 100  $\mu\text{M}$ .

Diffusion coefficients ( $D$ ) and frictional coefficients (the inverse of diffusion coefficient) of analytes are also related to their electrophoretic

mobilities. The frictional coefficients and pKa values of four diuretics were correlated with their electrophoretic mobilities by Jumpannen *et al.* [59]. The self diffusion coefficients and the frictional coefficients of clopamide, ethacrynic acid, hydrochlorothiazide and acetazolamide were determined by pulse gradient spin-echo (PGSE) nuclear magnetic resonance spectroscopy, where a field gradient is used to tag molecules at a certain time, they are allowed to diffuse during the lapse time and the positions of the molecules are then determined by the application of a second field gradient pulse. However, the determination of diffusion coefficients for compounds is more usually calculated from the measured peak widths [60, 61], as band broadening is also controlled by diffusion. By calculating diffusion constants in this way, the assumption that diffusion and migration are governed by the same mechanism (which is only a rough approximation) is avoided.

One of the main groups of small ions that have been separated by free solution CE is are inorganic anions and cations [62]. Inorganic ions are particularly important in water analysis and the ions of the alkali metals [63, 64], alkali earth metals, ammonium ions [65] and heavy metals [66, 67] have been analysed and found to generally have high mobilities. One feature of the alkali metals is that the lower atomic weight metals have lower mobilities than their size would predict, since their hydrated radii are larger due to high charge densities. Similarly, inorganic anions such as bromide, bromate, iodide, iodate, nitrate and selenite anions have been separated by CE [68]. Thus CE can be used for many of the applications performed routinely by ion chromatography.

Organic acids are sufficiently soluble to be separated by CE [69-72]. Of the other techniques available to the analyst, gas chromatography is unsuitable due to the non-volatile nature of the acids, and reversed phase HPLC often requires ion pair reagents or ionisation suppression. In a typical example Brumley and Brownrigg [72] studied the electrophoretic behaviour of some 56 aromatic organic acids by both free zone electrophoresis and micellar

electrokinetic chromatography. Separations were achieved at pH 8.3 which in most cases was well above the  $pK_a$  values of the analytes.

The effect of experimental parameters on the separation of *p*- and *m*-aminobenzoic acids was investigated by Nielen [73]. The pH was varied between 4.0 and 6.0 and the optimum resolution was found to be close to the  $pK_a$  values of the analytes. Because these analytes have two  $pK_a$  values, a reversal in migration order was observed at low pH with co-migration at pH 4.2.

## **1.4 The Effects of Size and Shape on Electrophoretic Mobility.**

### **1.4.1 Effects leading to the retardation of ions.**

Of the examples of applications for CE already presented, compounds are separated based on the differences between charge and size of compounds. Factors related to the shapes of compounds has also been shown to lead to the separation of non-spherical compounds by CE [74-76]. The separation of analytes by differences in shape may be attributed to the differences in the frictional forces experienced on them. Analytes are retarded by two primary effects known as the relaxation effect [77] and the electrophoretic effect [77] which contribute to the size relationship. As ions move through a liquid they experience a frictional force due to collisions with the liquid molecules, however ions in solution are under non-ideal conditions, therefore they cannot be considered to be moving independently of one another. Thus, each ion in solution can be considered to be surrounded by a relatively higher proportion of ions carrying opposite charge due to coulombic forces [77, 78].

Relaxation Effect.

When a potential is applied to a positive ion, it moves with mobility  $\mu_e$  towards the cathode, and the surrounding anions are continually reforming in the environment around it. It takes a finite time for the anionic environment to reform thus an asymmetric distribution of the ions results (Figure 1.4). The electrical attraction between the asymmetric charged atmosphere and the ion reduces the overall speed of the ion. This is known as the relaxation effect .

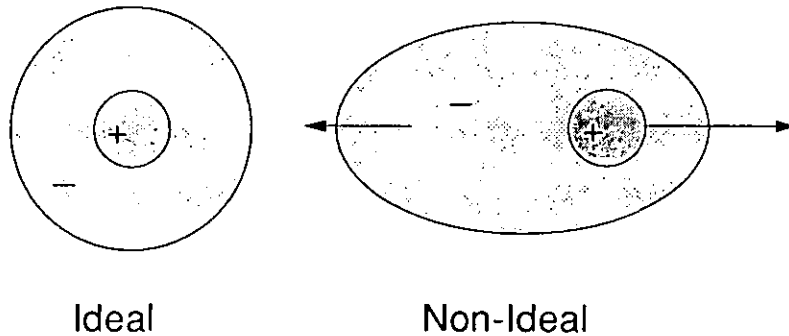


**Figure 1.4** *The distribution of ions under ideal conditions where no voltage is applied and under non-ideal conditions where the applied voltage leads to the movement of ions and an asymmetric distribution of ions.*



### Electrophoresis Effect.

The viscous force opposing the motion of the ion is equal to the product of the frictional coefficient and the velocity of the ion. The counterions in the vicinity of the central ion are moving in the direction opposite to the central ion and are carrying with them their molecules of solvation. Therefore the solvent in the immediate vicinity of the central ion has a net motion in the direction opposite to the motion of the central ion (Figure 1.5), and thus a stronger viscous environment is experienced by the central ion. Thus, the electrophoretic effect retards the motion of the central ion.

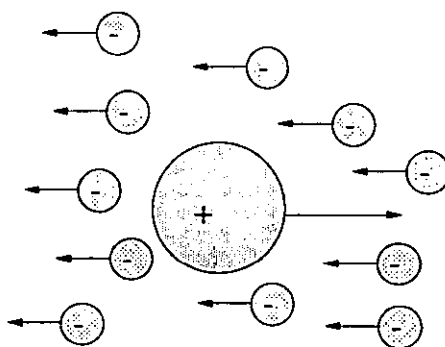


**Figure 1.5** *The strong viscous environment experienced by the analyte ion due to the movement of counterions in an opposing direction.*

### 1.4.2 The Modelling of Size and Shape Effects.

Before the advent of capillary electrophoresis, paper electrophoresis [79] provided a means of separating analytes by their electrophoretic mobilities and the properties of such separations closely resembles free solution capillary electrophoresis. Investigations of the size/shape effects under these conditions led to a number of publications.

When considering the electrophoretic mobility of peptides on paper, Offord suggested that the retarding force caused by the electrophoresis effect could be accounted for by considering the force to be related to a function of the effective surface area ( $M^{2/3}$ ) of the peptide [80]. Thus a semi-empirical equation for mobility was suggested for spherical analytes (1.12),

$$\mu_e = \frac{k' Z}{M^{2/3}} \quad (1.12)$$

where  $\mu_e$  is electrophoretic mobility of the peptide,  $Z$  is the charge on the peptide,  $M$  is the molecular weight of the peptide and  $k'$  is a constant.

However many analytes are not of spherical shape and based on the assumption that the frictional resistance to the passage of an ellipsoid is greater than that of a sphere of the same volume Cantor and Schimmel [81] suggested the use of different indices to account for different shapes of analytes (Table 1.1). In this case the shape of a sphere was modelled as  $M^{1/3}$  and all other shapes led to higher frictional coefficients, thus the index was varied from 1/3 to 1.

**Table 1.1**                      **Molecular shape indices.**

Molecular Model	Proportionality Relationship
Solid sphere	$f \sim M^{1/3}$
Statistical ball	$f \sim M^{0.5 \text{ to } 0.6}$
Broad planar disc	$f \sim M^{2/3}$
Long cylinder	$f \sim M^{0.8}$
Porous Ball	$f \sim M^1$

Perrin derived equations relating the frictional resistance to the ratio (b/a) of the semiaxes (a,b) of a prolate or oblate ellipsoid [82]. The results are usually described as a frictional ratio ( $f/f_o$ ). Edward and Waldron-Edward proposed a semi-empirical method for the calculation of the mobilities of small organic ions [83]. They proposed that free solution mobility of ions in infinitely dilute aqueous solution at 25 °C can be given by the equation (1.13).

$$\mu_e = \frac{1.14 \times 10^{-3} \times Zf}{r_w f_o} \quad (1.13)$$

where  $r_w$  is the van der Waals' radius (Å) of the ion, Z is the ionic charge in electronic units, and  $f/f_o$  is the frictional ratio for non-spherical molecules (unity for spheres, less than unity for prolate ellipsoids and greater than unity for oblate ellipsoids).

### 1.4.3 Separations of Isomeric Compounds.

Chadwick and Hsieh reported the separation of *cis*- and *trans*- double bond isomeric compounds by capillary electrophoresis [74]. Separation of fumaric acid and maleic acid could be achieved at pH 8.5 where the compounds existed as dianions. Separation at pH 4.0 was also achieved, but without baseline resolution. Baseline separation of all-*trans*-retinoic acid and 13-*cis*-retinoic acid was achieved, the retinoic acids being of interest as they serve as visual pigments in photoreception and phototransduction (Figure 1.6).

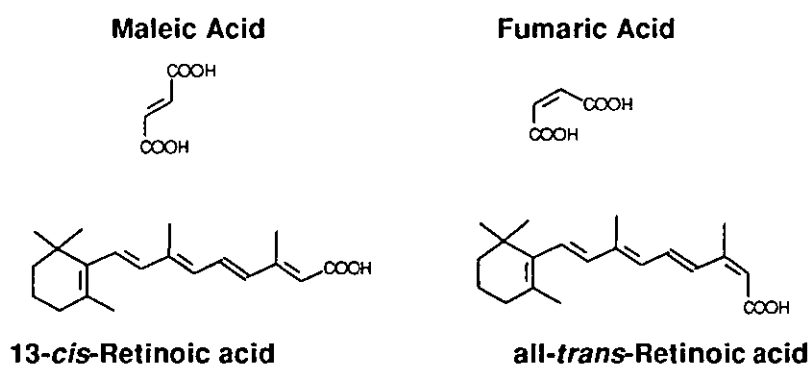


**Figure 1.6** *Fumaric acid, maleic acid, all-trans-retinoic acid and 13-cis-retinoic acid*

The differences in electrophoretic mobility of the analytes were attributed to the isomers possessing different hydrodynamic radii. By considering the mobility of the analytes the hydrodynamic radii of the molecules could be calculated.

In the separation of codeine and its by-products by capillary zone electrophoresis [75], it was noted by Korman *et al.* that the closely related by-products thebaine and 6-methylcodeine could be separated (Figure 1.7).



migration times of 3.81 mins, 3.77 mins and 3.73 mins for 2-hydroxybenzoic acid, 3-hydroxybenzoic acid and 4-hydroxybenzoic acid respectively.

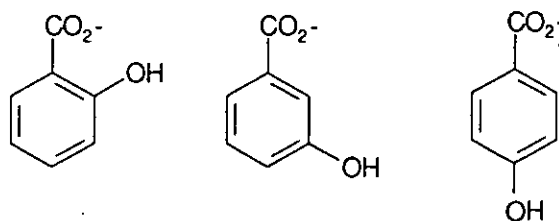


**Figure 1.8** The hydroxybenzoic acids.

Similar migration orders were obtained for the chlorobenzoic acids and nitrobenzoic acids. Also the hydroxyphenylacetic acids (Figure 1.9) were separated and migration times of 3.73 mins, 3.55 mins and 3.54 mins were obtained for 2-hydroxyphenylacetic acid, 3-hydroxyphenylacetic acid and 4-hydroxyphenylacetic acid respectively.

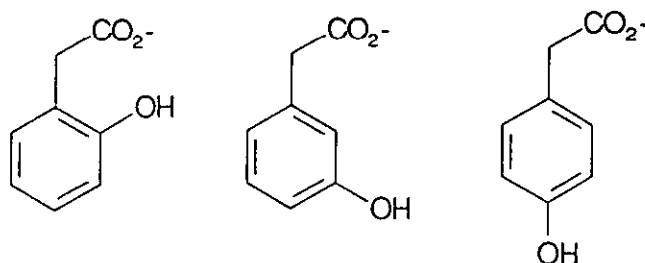


**Figure 1.9** The hydroxyphenylacetic acids.

Meyer *et al.* [84] reported the separation of *cis/trans* isomers of a prolyl peptide bond by capillary zone electrophoresis. The molecular arrangement observed in peptide chemistry resembles the configuration of *cis/trans* isomers. The partial double bond character of the peptide bond maintains the backbone of polypeptides in two preferred directions of propagation. Usually the rapid interconversion between the two forms is too fast for successful separation, however the Ala-Phe-Ψ[CS-N]-Pro-Phe-4-nitroanilide thioxo peptide isomerises much slower and so is suitable for separation by CE. The two forms were separated at 30 °C and by increasing the temperature the

separation could be destroyed by interconversion between the two forms. The UV spectra of the two forms were compared and no differences in the spectra of the pure forms and the mixture were observed. The two isomers were compared by molecular modelling, and the energetically preferred conformations of the isomers showed that the *cis* conformer had a cylindrical shape with an average length of 11.5 Å and width of 9.5 Å was calculated. The *trans* conformer had a near spherical shape with average lengths for length and width of 11.3 Å and 10.4 Å respectively. The differences in the electrophoretic properties of the peptides were thus explained by the smaller cylindrical molecule hydrodynamically adjusting its orientation to give a smaller frictional force than the spherical molecule and hence the *cis* isomer had a higher electrophoretic mobility. For an alternative peptide, Ala-Gly-Ψ[CS-N]-Pro-Phe-4-nitroanilide the differences were found to be much smaller and together with an increased isomerisation rate the absence of peak splitting for this compound was rationalised.

## 1.5 Present Study.

The aim of the present study was to investigate the influence of structural and physical properties of analytes on electrophoretic mobility in CE, to enable the relative mobilities of related analytes to be predicted. This would be valuable for the pharmaceutical analyst working in method development as separation could be easily rationalised from the physical properties of compounds. In particular, the effects of molecular size and shape on isomeric and closely related compounds were to be investigated. The work of Rowe *et al.* [76] investigating the effects of size and shape on the mobility of monosubstituted alkylpyridines was taken as a starting point for investigations. The optimisation of separations for these related compounds and the collection of accurate mobilities for the compounds would allow the testing of published models relating to the size/shape and charge on analytes. Additional models would then be developed where necessary. It was proposed to also investigate a wider range of analytes with different charges and functionalities and to compare separations achieved by differences in the shape of analytes with separations by liquid chromatography.



## Chapter 2. Experimental.

### 2.1 Introduction.

In this chapter general experimental details are provided for the analysis of compounds by capillary electrophoresis and the associated techniques used to obtain experimental data.

### 2.2 Capillary Electrophoresis.

#### 2.2.1 Chemicals.

Distilled water was purified to 18 M $\Omega$  using an ELGA MAXIMA water purification system. All alkylpyridines were obtained from Aldrich (Poole, UK) with the exception of 2-propylpyridinium bromide which was obtained from Lancaster (Morecambe, UK). The alkylbenzoic acids were obtained from Aldrich (Poole, UK) except for 4-nonylbenzoic acid and 4-decylbenzoic acid which were prepared by the hydrolysis of 4-nonylbenzoyl chloride and 4-decylbenzoyl chloride (Avocado, Lancaster). Alkylanilines were used as received from Aldrich (Poole, UK). Ortho-phosphoric acid, citric acid and boric acid were obtained from BDH (Poole, UK). Lithium hydroxide and sodium hydroxide was obtained from Fisons Scientific Apparatus (Loughborough, UK).

#### 2.2.2 Apparatus.

All capillary electrophoresis work was carried out on a P/ACE 2050 system (Beckman Instruments, High Wycombe, UK) with the exception of the analysis of 2-(3-pentenylpyridine) which was analysed on a P/ACE 5000 DAD system (Beckman). Data was recorded at 254 nm for the alkylpyridines using a

A (N,N-bis[2-hydroxyethyl]glycine) buffer (BICINE) was obtained by preparing a 50 mM solution of BICINE and adjusting the pH of the solution to pH 8.5 using lithium hydroxide (1 M). Samples were loaded onto a fused silica capillary by a 2 s pressure injection and separated at 25°C using a voltage of 15 kV. Electroosmotic flow was measured using thiourea.

#### Method D    Lithium Borate Buffer.

Lithium borate buffers were obtained by preparing a 50 mM solution of boric acid and adjusting the pH of the solution to pH 8.5 using lithium hydroxide (1 M). Samples were loaded onto fused silica capillaries and also bonded capillaries using a 2 s pressure injection and separated at 25°C using voltages of 15 kV or 30 kV. Electroosmotic flow was measured using thiourea as a marker and benzoic acid was used as an internal standard.

Modifications of the lithium borate buffer were also investigated. A sodium borate buffer was prepared by substituting sodium hydroxide (1 M) for the lithium hydroxide (1 M) and the ionic strength of the buffers was varied by taking solutions of lithium hydroxide and sodium hydroxide (both 50 mM) and adjusting the pH to 8.5 using boric acid (1 M).

## **2.3 Molecular Modelling of CE Separations.**

### **2.3.1 Equipment**

The molecular modelling package SYBYL (Tripos Assoc. Inc., USA) was used for all computer modelling on an Evans and Sutherland workstation. The spreadsheet package Excel v4.0 (Microsoft Inc., USA) was used for numerical calculations on a Toshiba T4400SXC personal computer.

5 Hz collection rate and at 214 nm for the benzoic acids using a 5 Hz collection rate. An IBM 433/DX microcomputer with System Gold v8.0 Personal Chromatograph (Beckman) software installed was used for data collection.

For the alkylpyridine work, fused silica capillaries of 50  $\mu\text{m}$  and 75  $\mu\text{m}$  internal diameter (i.d.) were used (Beckman). For the benzoic acid work three different capillaries were used: a fused silica capillary of 50  $\mu\text{m}$  i.d. (Composite Metal Services Ltd., Worc.), a 75  $\mu\text{m}$  i.d. CElect<sup>TM</sup> H 75 (C1) and a 75  $\mu\text{m}$  i.d. CElect<sup>TM</sup> H 275 (C18) (both Supelco Inc., USA). Each capillary had an inlet to outlet length of 57 cm and an inlet to detector length of 50 cm.

Electrophoretic mobilities of all analytes were determined using the following equation (equation 2.1),

$$\mu_e = \frac{lL}{Vt} - \mu_{eof} \quad (2.1)$$

where  $l$  is the length from inlet to detector,  $L$  is the total capillary length,  $V$  is the operating voltage,  $t$  is the migration time and  $\mu_{eof}$  is the electroosmotic mobility.

### 2.2.3 Methods for Alkylpyridine and Alkylaniline Separations.

Stock solutions of 1 mg mL<sup>-1</sup> of alkylpyridine and alkylanilines were made up in de-ionised water, and samples for injection were prepared each day by taking 50  $\mu\text{L}$  of the sample stock solution and diluting it in 4.4 mL of de-ionised water.

### Method A. Lithium Phosphate Buffers

A lithium phosphate buffer was prepared by taking the required molarity of ortho-phosphoric acid (10-100 mM) and adjusting the pH to 2.5 using lithium hydroxide. Samples were loaded by a 2 s pressure injection and separated at 25°C using a voltage of 15 kV. Pyridine and acridine were used as internal markers and electroosmotic flow was measured by using the fast marker technique described in chapter 3.

### Method B. Lithium Citrate Buffers.

For these separations the method is as for method A, except that the buffer was prepared from 50 mM citric acid and adjusted to the required pH using lithium hydroxide (1 M). Separation times were adjusted as required and the electroosmotic flow was determined using acetone as an additional standard.

### Method C. Sodium Phosphate Buffer.

A sodium phosphate buffer system was used for the study of the dimethylpyridines at pH 6.5. 50 mM sodium hydrogen phosphate was adjusted to pH 6.5 with hydrogen chloride (1M). The samples were analysed as in method A using acetone as the electroosmotic flow marker compound.

#### **2.1.4 Methods for Alkylbenzoic Acid Separations**

Stock solutions of  $1 \text{ mg mL}^{-1}$  alkylbenzoic acids were made up in de-ionised water, and samples for injection were prepared each day by taking 50  $\mu\text{L}$  of the sample stock solution and diluting it in 4.4 mL of de-ionised water.

#### Method D. (N,N-bis[2-Hydroxyethyl]-glycine) Buffer.

A (N,N-bis[2-hydroxyethyl]glycine) buffer (BICINE) was obtained by preparing a 50 mM solution of BICINE and adjusting the pH of the solution to pH 8.5 using lithium hydroxide (1 M). Samples were loaded onto a fused silica capillary by a 2 s pressure injection and separated at 25°C using a voltage of 15 kV. Electroosmotic flow was measured using thiourea.

#### Method D Lithium Borate Buffer.

Lithium borate buffers were obtained by preparing a 50 mM solution of boric acid and adjusting the pH of the solution to pH 8.5 using lithium hydroxide (1 M). Samples were loaded onto fused silica capillaries and also bonded capillaries using a 2 s pressure injection and separated at 25°C using voltages of 15 kV or 30 kV. Electroosmotic flow was measured using thiourea as a marker and benzoic acid was used as an internal standard.

Modifications of the lithium borate buffer were also investigated. A sodium borate buffer was prepared by substituting sodium hydroxide (1 M) for the lithium hydroxide (1 M) and the ionic strength of the buffers was varied by taking solutions of lithium hydroxide and sodium hydroxide (both 50 mM) and adjusting the pH to 8.5 using boric acid (1 M).

### **2.3 Molecular Modelling of CE Separations.**

#### **2.3.1 Equipment**

The molecular modelling package SYBYL (Tripos Assoc. Inc., USA) was used for all computer modelling on an Evans and Sutherland workstation.

The spreadsheet package Excel v4.0 (Microsoft Inc., USA) was used for numerical calculations on a Toshiba T4400SXC personal computer.

### 2.3.2 Method

Bond lengths, bond angles and molecular co-ordinates for the analytes of interest were calculated using SYBYL. The charge distributions for the alkyipyridines were also obtained using SYBYL by applying the Hückel model to the charged analyte. Molecular co-ordinates were then fed into a spreadsheet in order to obtain the centre of mass of the compounds, calculated from the formulae (2.2),

$$\bar{x} = \frac{\sum mx}{\sum m} \quad \bar{y} = \frac{\sum my}{\sum m} \quad (2.2)$$

where  $m$  is the mass of each individual atoms with co-ordinates  $x$  and  $y$ . By substituting mass for charge, the centre of charge of the analyte was also found (2.3),

$$x' = \frac{\sum qx}{\sum q} \quad y' = \frac{\sum qy}{\sum q} \quad (2.3)$$

where  $q$  is the partial charge on individual atoms and  $x$  and  $y$  are the co-ordinates of atoms. Thus, a representation of the analyte was obtained showing the centre of mass, centre of charge and the analytes' direction of travel in the electric field (discussed in chapter 6), (Figure 2.1 for 2-ethylpyridine).

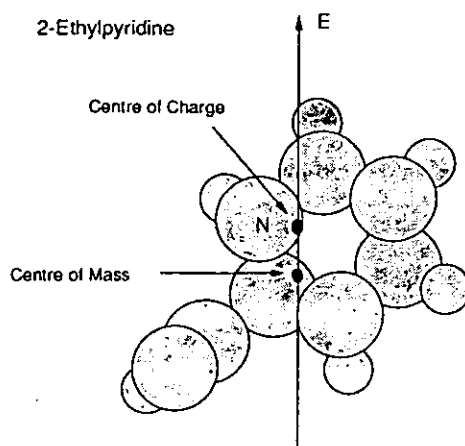


*Figure 2.1 Representation of the centre of mass and centre of charge for 2-ethylpyridine.*

The distance between the centre of mass and the centre of charge, defined as the radius of inertial rotation,  $R_i$ , was calculated by applying the simple formula (2.4),

$$R_i = \sqrt{(\bar{x} - x')^2 + (\bar{y} - y')^2} \quad (2.4)$$

To obtain the radius of rotation,  $R_{rot}$ , the analyte was redrawn on a grid with the charge-mass axis lined up with the grid (Figure 2.2 for 2-ethylpyridine). The space occupied by the atoms was then drawn in, using the Van der Waals' radii from SYBYL.

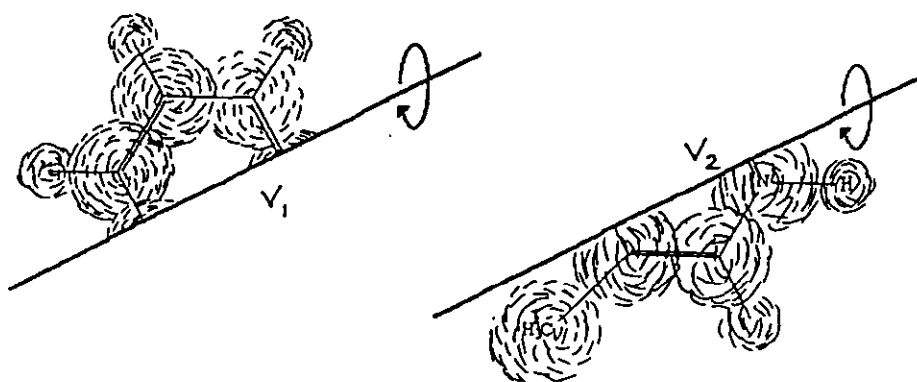


Figure 2.2 The calculation of rotated volume for 2-ethylpyridine.

The volume of rotation was then obtained for the analyte, by calculating the volumes of the two halves split by the charge-mass axis. The volume of rotation for each half was calculated by applying the equation (2.5),

$$V = \pi \sum_{l,m} (m_1 - m_2) l_1 \quad (2.5)$$

The two halves were summed and the cubed root was taken to obtain the radius of rotation for each analyte (2.6),

$$R_{rot} = \sqrt[3]{V_1 + V_2} \quad (2.6)$$

## 2.4 Potentiometric Titration.

### 2.4.1 Chemicals.

The preparation and standardisation of HCl (Fisons), KOH (Volucon<sup>TM</sup> Rhône Poulenc), ethylenediamine dihydrochloride (Fluka, used for electrode



calibration) were carried out using the procedures described by Avdeef *et al.* [85, 86]. Alkylpyridine samples (Aldrich) were used as received.

### 2.4.2 Apparatus.

The instrument used to perform the pKa analysis was a PCA 101 (Sirius Analytical Instruments Limited, Forest Row, East Sussex, UK), which consisted of an Intel 8088/8087 and Phillips 80552 distributed processors, a pH sensing circuit, a semi-micro combination pH electrode, an overhead stirrer, a precision dispenser and a six way valve for dispensing reagents and titrants: (0.5 M HCl, 0.5 M KOH, 0.15 M KCl), and SDS surfactant cleaner. A 10 cm polyimide clad quartz capillary (0.5 mm i.d) serves as a dispenser tip. Teflon FEP tubing is used throughout. The instrument moves the electrode/stirrer/dispenser tip assembly in and out of sample, buffer and wash solutions. A weighed sample of analyte (1-10 mg) was added manually; the diluent and all other reagents were added automatically.

### 2.4.3 Method.

The methods used for electrode calibration, determination of acidity errors and corrections for the carbonate from carbon dioxide were carried out as described by Avdeef *et al.* [85] and these methods were followed as a standard procedure to calibrate the instrument at the start of each working day.

The alkylpyridine sample (10 mg) was diluted with HCl (10 mL, 0.02 M). The samples were introduced into the PCA 101 and the initial pH was measured. The pH of the sample was adjusted to pH 2 by the automated addition of HCl (0.5 M). Once a stable initial pH was obtained, diluents were added automatically to perform the titration. The instrument calculated the volume of titrant to add (in the range of 0.0004-0.25 mL) to maintain an approximate 0.2 pH unit separation between successive data points. The pH of the solution was measured after the completion of 3 s vigorous stirring by

taking a sequence of 15 pH readings, one reading every 0.3 s. At the end of the sequence, pH versus time was fitted to a straight line. If the slope of fit was greater than 0.01 pH min<sup>-1</sup> in magnitude, the sequence of pH measurement was repeated. All refinements of data were performed directly by the instrument.

*Estimation of pKa values* - The difference curve (which is a measure of the average number of bound protons versus pH) was used to estimate ionisation constants. For a single substance X in solution:

$$\bar{n}_H = ([HCl] - [KOH] + nX - [H^+] + K_w/[H^+])/X \quad (2.7)$$

where  $\bar{n}_H$  is the average number of bound protons,  $n$  is the number of dissociable protons introduced into the solution by the substance X (e.g.  $n = 0$  for pyridine and for phosphoric acid introduced as NaH<sub>2</sub>PO<sub>4</sub>  $n = 2$ ),  $K_w = 10^{-13.75}$  at 25 °C and 0.2M ionic strength and [Y] is the concentration of the respective substances. The difference curve clearly reveals pK<sub>a</sub> values and overlapping pK<sub>a</sub> values can also be easily estimated from such curves.

## 2.5 pKa Estimation

### 2.5.1 Equipment.

For the calculation of estimated pK<sub>a</sub> values, the molecules of interest were drawn using Isis/Draw (Molecular Design Limited), and then converted using ConSystant (Exographics, New Jersey, USA) into SMILES form where the computational program pKalc (CompuDrug Chemistry Ltd.) could estimate the pK<sub>a</sub> values. pKalc estimates pK<sub>a</sub> values based on the work of Perrin *et al.* [87].

## 2.6 NMR Spectroscopy.

The sample of 2-(3-pentenyl)pyridine was used as received from Aldrich (Poole, UK). Deuterated chloroform was obtained from a departmental source.  $^1\text{H}$  NMR Spectra were run in deuterated chloroform on a 250 MHz AC250 Brüker NMR spectrometer.

## 2.7 Gas-Liquid Chromatography.

A sample of 2-(3-pentenyl)pyridine was used as received from Aldrich (Poole, UK). A dilute solution of 2-(3-pentenyl)pyridine in dichloromethane was analysed by GC-MS on a Fisons GC 8000 gas chromatograph coupled to a MD 800 mass spectrometer using a DB 5 ms column isothermally at 100 °C.

## Chapter 3.

### Evaluation of fundamental parameters

#### 3.1 Introduction.

The electrophoretic mobilities of compounds were to be determined and in many cases the values were very similar. Therefore it was necessary to investigate parameters that affect the mobilities of compounds so that quoted values were as independent of experimental conditions as possible. In order to measure electrophoretic mobilities the migration times and the magnitude of the electroosmotic flow must be measured. The repeatability and reproducibility of these measurements are investigated. Corrections for changes in parameters such as temperature, electroosmotic flow velocity and buffer ionic strength were investigated. Investigations at low pH were investigated and then applied to the analyses at high pH.

#### 3.2 Analysis and markers at pH 2.5.

##### 3.2.1 The Repeatability of Migration Times.

The analysis of compounds by capillary electrophoresis using a fused silica capillary has been shown to lead to poor repeatability of the migration times of analytes [88-97]. Thus workers have suggested the use of internal standards in the analysis of compounds by CE [90, 98, 99] and also the quotation of electrophoretic mobility rather than migration time as a measure of an analytes electrophoretic properties [88, 94-97, 100-102].

With fifty consecutive injections of pyridine analysed using method A, the migration time of pyridine drifted between 7 and 7.35 minutes (Figure 3.1). This drift in migration time was attributable mainly to nonrepeatable electroosmotic flow velocity due to the surface conditions at the capillary wall.

A general trend of decreasing pyridine migration time was observed, which corresponds to a decrease in EOF velocity, with periodic increases in pyridine migration time. This periodic increase in analyte migration time may be related to the introduction of fresh buffer vials to the CE system. Reasons why this could lead to the increase in migration time could be a difference in the temperature of the fresh buffer vials, or inactivity of the CE system between runs could lead to non-equilibrium conditions developing at the fused silica surface of the capillary.

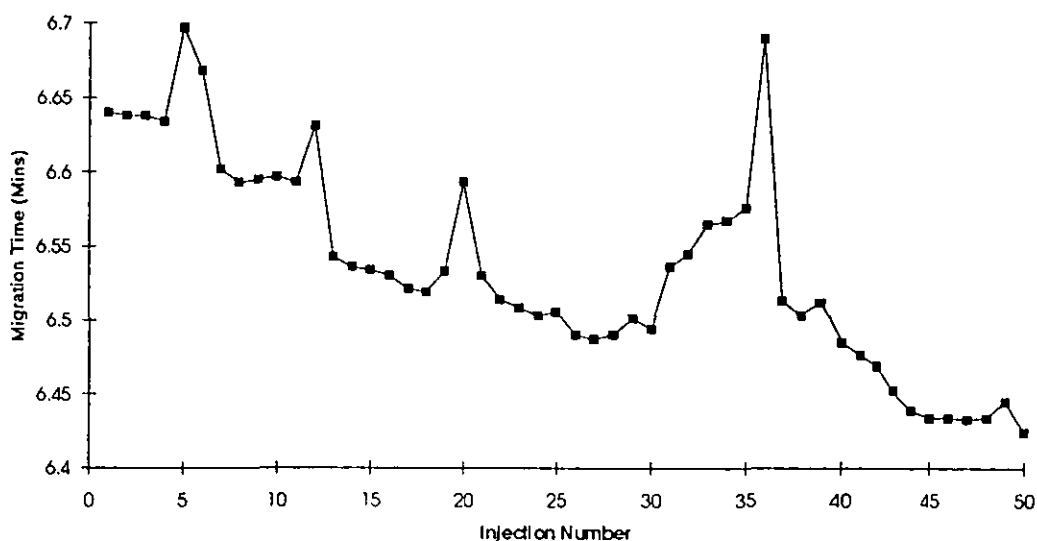


**Figure 3.1** *Repeatability of pyridine migration time in a fused silica capillary. 40 mM lithium phosphate buffer, pH 2.5, 2 s injection, 15 kV applied voltage*

Between each sample injection and analysis a capillary wash programme was applied, involving a 0.5 minute high pressure wash with 0.1 M lithium hydroxide and a 3 minute high pressure wash with the run buffer. The caustic lithium hydroxide wash changes the conditions inside the capillary considerably and this wash was removed from the rinse cycle to investigate whether it was the cause of the non-equilibrium conditions inside the capillary.

Similar drifts in migration time were observed without the wash and so it was concluded that the drifts in migration time was a fundamental property

of the separation system and that it was not possible to accurately forecast the absolute migration time of an analyte on any one run.

Thus it is necessary to apply corrections to account for the effects of the electroosmotic flow instability and also the effects of effective field strength. Electroosmotic flow must be measured which can be done by including a neutral marker compound that shows a suitable detector response.

### 3.2.2 Measurement of Electroosmotic Mobility.

The apparent electrophoretic mobility of a compound is the sum of its own electrophoretic mobility and the electroosmotic flow (EOF) within the capillary, thus in order to measure electrophoretic mobilities, the EOF must be determined.

The EOF velocity is related to the ionisation of silanol groups at the capillary surface. Counter-ions build up at the capillary surface to retain electroneutrality and it is the migration of these cations that causes the bulk flow. To measure the EOF velocity, neutral compounds with a suitable detector response are used. Typical markers include benzyl alcohol and acetone. However when the EOF was measured at pH 2.5, EOF times of between thirty and ninety minutes were observed. In order to exploit the rapid separation times offered by capillary zone electrophoresis, it is undesirable to wait long periods of time for a measurement of electroosmotic flow.

Thus the development of a fast electroosmotic flow marker was proposed, by using a positively charged (and so fast migrating molecule) in place of the neutral marker. For this study, it was proposed to relate acridine (the fast marker) to benzamide (the uncharged EOF marker). Acridine (Figure

3.2) was chosen because its electrophoretic mobility and functionality was similar to the compounds being studied but it did not co-migrate with other analytes.

Acridine has a fixed conformation and so changes in operating conditions were not expected to affect its electrophoretic mobility (with the exception of high pH values, where de-protonation takes place).

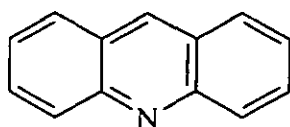


*Figure 3.2 Structure of Acridine.*

Repeated measurements of the electroosmotic flow showed that a variation in electroosmotic flow occurred, and that it was influenced by the operating conditions. A corresponding variation was experienced for the migration times of pyridine, 2,3-cyclohexenopyridine and acridine.

Data were collected at ionic strengths of 10 mM - 100 mM using the lithium phosphate buffer system. For each ionic strength the migration times of benzamide and acridine were plotted against each other to give graphs relating the acridine migration time to the migration time of the neutral marker benzamide (Figure 3.3).

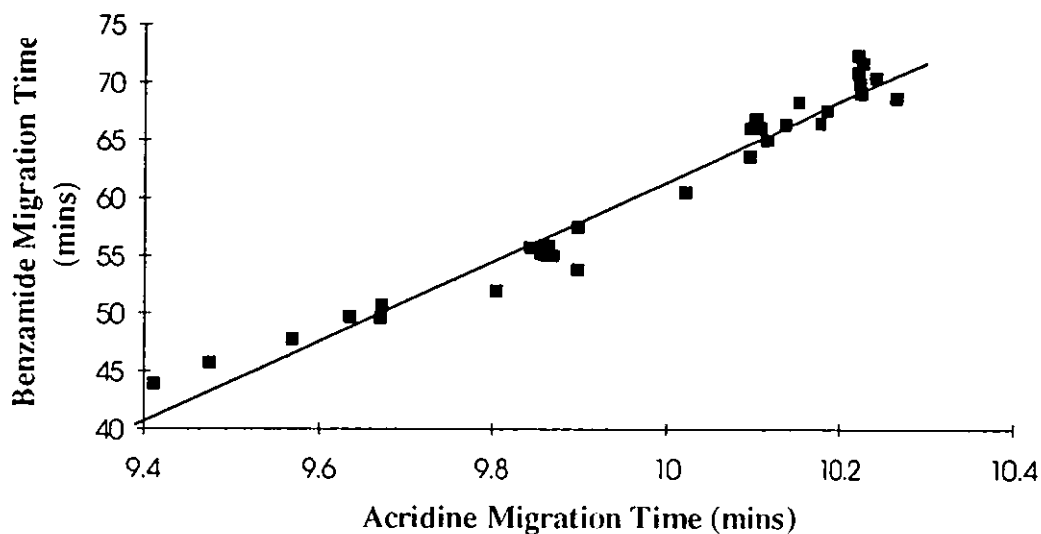


*Figure 3.3 Acridine migration time plotted against benzamide migration time. 40 mM lithium phosphate buffer, pH 2.5, 15 kV applied voltage.*

Linear regression yields equations that can be used to relate the benzamide migration time to the mobility of acridine thus providing a method to calculate electroosmotic flow for each individual run (Table 3.1). A normal measurement of the EOF was made between each set of runs to check and also to provide more data for the EOF calibration graphs.

The observed increase in electroosmotic flow with decreasing ionic strength of the buffer is due to the strength of the zeta potential at the capillary walls and is in agreement with the observations of other workers [36], and the literature relationships are applied to these results in the next chapter.



**Table 3.1** *Linear regression analysis relating the migration time of acridine to the migration time of benzamide.*

*Lithium Phosphate buffers, pH 2.5, 15 kV applied voltage.*

Regression Analysis.				
Ionic Strength	Gradient	Intercept	Correlation Coefficient	Sample Size
10 mM	6.48	-26.5	0.9212	32
20 mM	13.2	-79.6	0.9629	32
40 mM	34.4	-283	0.9601	36
60 mM	29.2	-239	0.9944	28
80 mM	46.7	-424	0.9950	28
100 mM	66.7	-650	0.9714	28

For six measurements of electroosmotic flow, the calculated electroosmotic flow from the regression analysis and the measured benzamide migration time (actual electroosmotic flow) are compared (Table 3.2). The error between calculated and actual EOF values is of the order of 3 %. For a typical EOF time of 60 minutes and an analyte migration time of 7 minutes the electroosmotic flow will make up approximately 12% of the overall migration time. Thus the error incurred by applying the fast marker was estimated at approximately 0.4%.

The repeatability of migration times and the electroosmotic flow can be attributed to the fundamental properties of the silica capillary walls with their exposed silanol groups. Such a system is highly susceptible to cation and analyte absorption as well as protonation and so one either has to alter the surface of the capillary to control EOF or to overcome these problems with a practical approach. Working at low pH it is impractical to measure the full

EOF for each run made because of the time involved. The fast marker method provides a compromise between long analysis times or imprecise EOF values. Because of the strong capillary dependence on EOF, in order to set up a EOF calibration graph, experimental measurements have to be made. However, once data is collected, then it is possible to make less frequent measurements.

**Table 3.2** *Comparison between electroosmotic flow calculated from acridine migration times and the actual electroosmotic flow measured using benzamide as a neutral marker. 40 mM lithium phosphate buffer, pH 2.5, 15 kV applied voltage.*

Acridine Migration Time (Mins)	Calculated EOF (Mins)	Actual EOF (Mins)
10.02	61.688	60.457
9.897	57.457	57.459
9.672	49.717	50.711
9.634	48.410	49.659
9.583	46.656	48.480
9.897	57.457	53.811

### 3.2.3 Pyridine as an Internal Standard.

The results obtained by using acridine as a fast electroosmotic flow marker provided a means of breaking down the actual electrophoretic migrations into a true electrophoretic migration and the electroosmotic mobility. However, when the mobility data for pyridine was tabulated, a systematic decrease in the electrophoretic mobilities was observed (Figure 3.4). The pyridine mobility showed a drift of about 2-3 % over the range studied, and the system appeared to never be reaching an equilibrium

condition. The reason for the drift in pyridine mobility was unclear, the error associated with the calculation of EOF was estimated at only 0.4%. Other workers have associated such drifts with buffer depletion or electrode processes [88, 89]. Therefore, it was necessary to correct mobilities by using an internal standard.

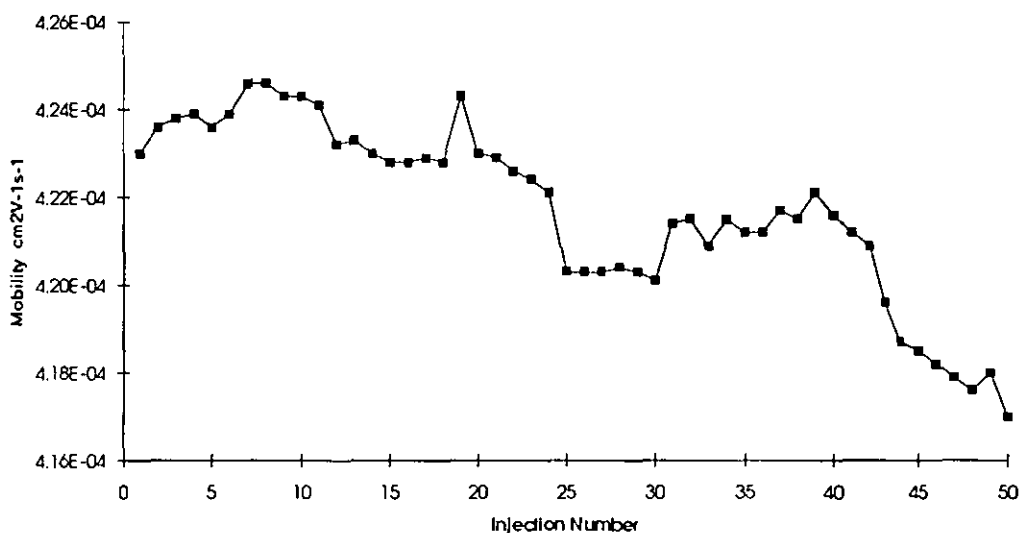


**Figure 3.4** *Uncorrected pyridine mobility, pH 2.5, 40 mM lithium phosphate buffer, 15 kV applied voltage.*

In order to perform a correction, standard values for the electrophoretic mobility of pyridine at each ionic strength are needed. Since no data was available in the literature, this was done by measuring the mobility of pyridine at ionic strengths of 10 mM - 100 mM in consecutive runs using the same conditions for each measurement. Once corrections are made to the mobilities of other analytes, all electrophoretic mobilities are relative to these standard measurements so it was necessary to get the best measurements possible. For this reason, a 10 minute buffer wash was used between each measurement to minimise analyte absorption effects. The values obtained are shown in Table 3.3.

Pyridine was to be used as the internal standard for corrections and so was included in runs at each ionic strength. 2,3-Cyclohexenopyridine and acridine were also included in the mixture to allow testing of the quality of the corrections against actual experimental values.

**Table 3.3** *Experimental electrophoretic mobility of standards.  
Lithium Phosphate buffers, pH 2.5, 15 kV applied voltage.*

Buffer Ionic Strength	Electrophoretic Mobility ( $\text{cm}^2\text{V}^{-1}\text{s}^{-1}$ )			
	Pyridine	2,3-Cyclohexenopyridine	Acridine	EOF
10 mM	4.399 e-04	3.101 e-04	2.795 e-04	1.829 e-04
20 mM	4.298 e-04	3.004 e-04	2.706 e-04	1.305 e-04
40 mM	4.176 e-04	2.891 e-04	2.602 e-04	9.787 e-05
60 mM	4.115 e-04	2.849 e-04	2.563 e-04	6.354 e-05
80 mM	4.047 e-04	2.798 e-04	2.515 e-04	5.554 e-05
100 mM	3.993 e-04	2.758 e-04	2.477 e-04	4.668 e-05

The electrophoretic mobilities of all analytes were determined by calculating the raw mobilities using the calculated EOF during the run, and adjusting these values using pyridine as the internal standard (Example 3.1). Over fifty injections, the corrected mobilities of 2,3-cyclohexenopyridine and acridine was found to be stable (Figure 3.5).

---

*Example 3.1 - Calculation of 2,3-cyclohexenopyridine mobility.*

*Migration times of 6.452 mins for pyridine, 9.039 mins for 2,3-cyclohexenopyridine and 9.923 mins for acridine were obtained in a run.*

- 1. The EOF was calculated as 58.4 mins using the regression equation for the 40 mM lithium phosphate buffer,  $EOF = 34.4(T_{acridine}) - 283$ .*
- 2. Since  $\mu_e = \mu_a - \mu_{eof}$  the uncorrected 2,3-cyclohexenopyridine mobility is calculated as  $2.964 \text{ e-}4 \text{ cm}^2\text{V}^{-1}\text{s}^{-1}$  and the uncorrected pyridine mobility is calculated as  $4.230 \text{ e-}4 \text{ cm}^2\text{V}^{-1}\text{s}^{-1}$ .*
- 3. The value for 2,3-cyclohexenopyridine can now be corrected using the standard pyridine mobility of  $4.176 \text{ e-}4 \text{ cm}^2\text{V}^{-1}\text{s}^{-1}$ .*

*Corrected 2,3-cyclohexenopyridine mobility,*

$$(2.964/4.230)*4.176 \text{ e-}4 = 2.926 \text{ e-}4 \text{ cm}^2\text{V}^{-1}\text{s}^{-1}.$$

---

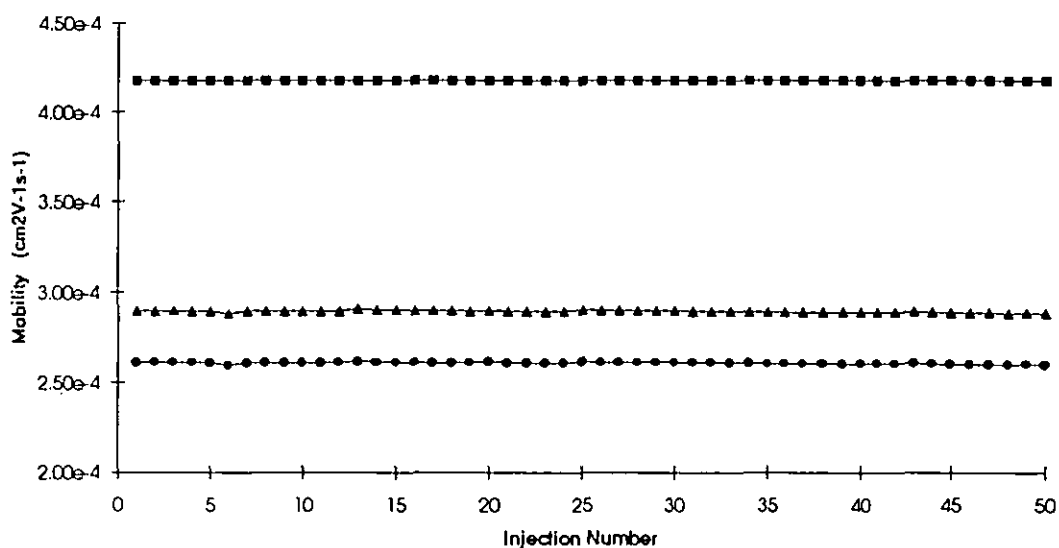


**Figure 3.5** Corrected electrophoretic mobility values. ■ - Pyridine; Δ - 2,3-cyclohexenopyridine; ◆ - acridine. 40 mM lithium phosphate buffer, pH 2.5, 15 kV applied voltage.

Relative standard deviations (RSDs) of 0.16% and 0.18% were obtained for 2,3-cyclohexenopyridine and acridine respectively for the fifty injections shown in figure 3.5. During the analysis of compounds, six replicate intra-run injections were performed, which involved injecting sample from the identical sample vials using the same buffer vials for separation. The intra-run RSD for the corrected electrophoretic mobility of 4-ethylpyridine was 0.03% (Table 3.5) and the corresponding inter-run RSD for 6 injections of acridine was 0.13% (Table 3.6). Inter-run replicates used fresh sample solutions for each injection and fresh buffers for these injections.

**Table 3.5** *Intra-run reproducibility for six injections of 4-ethylpyridine. 40 mM lithium phosphate buffer, pH 2.5, 2 s injection, 15 kV applied voltage, mobilities calculated using calculated EOF values and corrected using pyridine as an internal standard.*

	<b>4-Ethylpyridine - Intra-run replicates</b>	
Uncorrected Pyridine Mobility $\text{cm}^2\text{V}^{-1}\text{s}^{-1}$	Uncorrected 4-ethylpyridine mobility $\text{cm}^2\text{V}^{-1}\text{s}^{-1}$	Corrected 4- ethylpyridine mobility $\text{cm}^2\text{V}^{-1}\text{s}^{-1}$
4.233 e-4	3.442 e-4	3.395 e-4
4.230 e-4	3.441 e-4	3.397 e-4
4.228 e-4	3.440 e-4	3.398 e-4
4.228 e-4	3.439 e-4	3.397 e-4
4.229 e-4	3.439 e-4	3.396 e-4
4.228 e-4	3.437 e-4	3.395 e-4
Average Mobility Standard Deviation <b>RSD</b>		3.396 e-4 0.001072 e-4 <b>0.03%</b>

**Table 3.6** *Inter-run reproducibility for six injections of acridine. 40 mM lithium phosphate buffer, pH 2.5, 2 s injection, 15 kV applied voltage, mobilities calculated using calculated EOF values and corrected using pyridine as an internal standard.*

Acridine	Inter-Run	
Uncorrected pyridine Mobility $\text{cm}^2\text{V}^{-1}\text{s}^{-1}$	Uncorrected acridine mobility $\text{cm}^2\text{V}^{-1}\text{s}^{-1}$	Corrected acridine mobility $\text{cm}^2\text{V}^{-1}\text{s}^{-1}$
4.238 e-4	2.652 e-4	2.613 e-4
4.243 e-4	2.652 e-4	2.610 e-4
4.229 e-4	2.644 e-4	2.611 e-4
4.203 e-4	2.629 e-4	2.612 e-4
4.217 e-4	2.638 e-4	2.612 e-4
4.187 e-4	2.611 e-4	2.604 e-4
Average Mobility		2.610 e-4
Standard Deviation		0.003288 e-4
<b>RSD</b>		<b>0.13%</b>

### 3.2.4 Summary.

The repeatability of migration times in capillary electrophoresis was shown to be poor because of changes in the EOF. By using acridine as a fast electroosmotic flow marker the electroosmotic flow was calculated rapidly, thus allowing the calculation of analyte mobilities. Drifts in mobility were observed with time, and these drifts were corrected for by the use of an internal standard, giving inter-run reproducibility of electrophoretic mobilities below 0.5% RSDs.



### 3.3 The Effects of Temperature at pH 2.5.

An important parameter that must be controlled in capillary electrophoresis is the temperature inside the capillary. The Beckman P/ACE is equipped with liquid cooling to control the external temperature of the capillary. In this section the effectiveness of this system to control buffer temperature is investigated. By analysing the mobility of pyridine at different levels of applied power, the effect of Joule heating in the system was investigated. The overall temperature rise was also estimated at different ionic strengths of the buffer.

#### 3.3.1 Power Dissipation Experiments.

By changing the amount of power applied to the capillary it is possible to apply different heating forces to the capillary being studied. Thus as more power is applied the effectiveness of the cooling system to dissipate the heat generated is investigated. Experiments were set up to measure changes in the mobility of pyridine at different power levels (W) (Table 3.7). It was necessary to conduct these experiments without applying the corrections applied to pyridine mobility in the previous section. In most cases six repetitions were investigated, but at 0.1 W only three repetitions were conducted due to analysis times in excess of 2 hours, and one experiment failed at 0.7 W.

**Table 3.7** *Mobility of pyridine against power dissipated. 40 mM Lithium Phosphate buffer, pH 2.5, Voltage adjusted to give the Power levels indicated.*

Repetition Number	Electrophoretic Mobility of Pyridine ( $\text{cm}^2\text{V}^{-1}\text{s}^{-1}$ )				
	Power 0.1 W	Power 0.3 W	Power 0.5 W	Power 0.7 W	Power 0.9 W
Rep 1	4.0433 e-4	4.0798 e-4	4.0287 e-4	4.1746 e-4	4.1607 e-4
Rep 2	-	4.0577 e-4	4.0797 e-4	4.1874 e-4	4.1679 e-4
Rep 3	4.01659 e-4	4.1847 e-4	4.2461 e-4	4.2274 e-4	4.2508 e-4
Rep 4	4.2347 e-4	4.1785 e-4	4.2276 e-4	4.2413 e-4	4.2464 e-4
Rep 5	-	4.1616 e-4	4.1629 e-4	4.2296 e-4	4.2581 e-4
Rep 6	-	4.1838 e-4	4.1873 e-4	-	4.2788 e-4

A plot of electrophoretic mobility against power dissipated should give a linear relationship which allows one to correct electrophoretic mobilities to zero power dissipation [78]. However, the graph using the data from table 3.7 gave a essentially random scatter of points (Figure 3.6). These results indicated that either the errors in measuring mobility without the use of an internal standard were bigger than the variation in electrophoretic mobility with power dissipated in the capillary or that the cooling system was dealing adequately with the heating forces within the capillary.

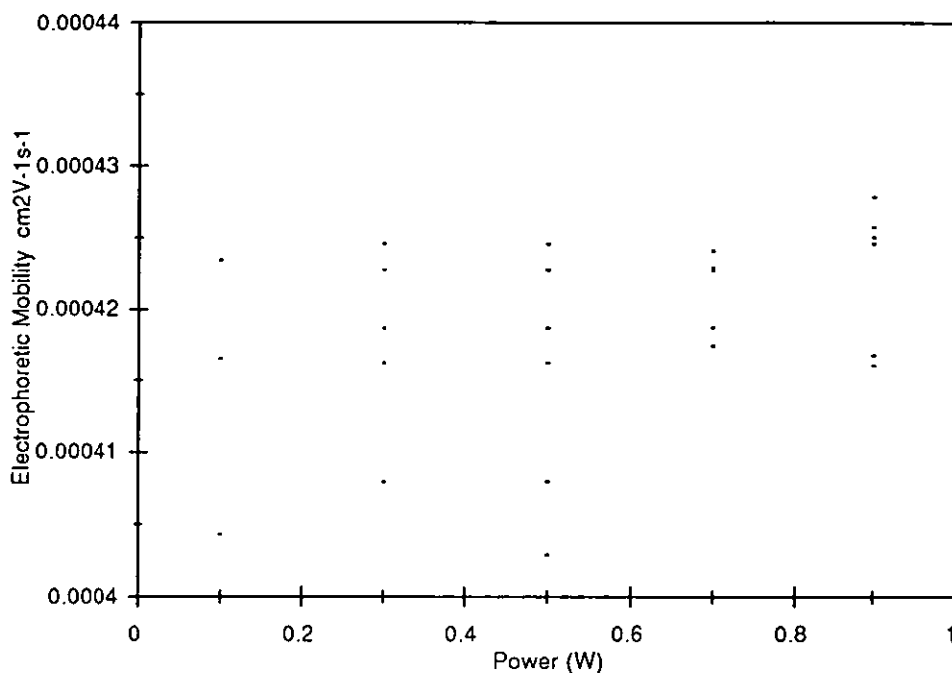


*Figure 3.6 Plot showing pyridine mobility against power dissipated.  
40 mM lithium phosphate buffer.*

### 3.3.2 Estimation of Capillary Temperature.

In section 1.2.3 the effects of temperature were reviewed and the overall temperature rise in the capillary during electrophoresis was shown to depend on basic equations of heat transfer (equation 1.11) [44-46]. This equation can be used to estimate the temperature rise within the capillary. The rate of power generation  $Se$  is given by (3.1),

$$Se = \frac{I^2}{\kappa_e} \quad (3.1)$$

where  $I$  is the current density and  $\kappa_e$  is the electrical conductivity of the electrolyte solution. Both properties are easily obtained experimentally since the current density  $I$  is related to the electrical driving current  $i$  by (3.2) and

the electrical conductivity of the electrolyte solution is related to the applied field and driving current by (3.3)

$$I = \frac{i}{\pi R_1^2} \quad (3.2)$$

$$\kappa_e = \frac{i}{\pi R_1^2 E} \quad (3.3)$$

Thus, combining (3.1-3.3) with equation (1.11), the following expression (3.4) giving the overall temperature rise across the capillary is obtained,

$$T_0 - T_a = \frac{i^2}{2\pi^2 R_1^2 \kappa_e} \left( \frac{1}{2k_b} + \frac{1}{k_g} \ln\left(\frac{R_2}{R_1}\right) + \frac{1}{k_p} \ln\left(\frac{R_3}{R_2}\right) + \frac{1}{R_3 h} \right) \quad (3.4)$$

The values of the current data and electrical conductivity were measured and calculated for the lithium phosphate buffer system at ionic strengths between 10 mM and 100 mM (Table 3.8) in a capillary of 75  $\mu\text{m}$  i.d ( $R_1$  was 37.5  $\mu\text{m}$ ) and 200  $\mu\text{m}$  o.d ( $R_2$  approx. 95  $\mu\text{m}$  and  $R_3$  approx. 100  $\mu\text{m}$ ). The outer temperature of the capillary was thermostatted to 25  $^\circ\text{C}$ . The thermal conductivity of fused silica and polyimide has been measured in the literature [77] as 1.50  $\text{Wm}^{-1}\text{K}^{-1}$ , and 1.55  $\text{Wm}^{-1}\text{K}^{-1}$  respectively and a typical value for the heat transfer coefficient  $h$  between polyimide and surrounding was measured as 10,000  $\text{W/m}^2\text{C}$  [50]. The thermal conductivity of the buffer may be determined using an iterative method using the conductivity of water as a starting point. A polynomial expression relating the thermal conductivity of water to temperature was reported by Grossman based on literature data [77],

$$\lambda_w = 0.5605 + (1.998.e-3) T - (7.765.e-6) T^2 \quad (3.5)$$

**Table 3.8** *Current and electrical conductivity in a 57 cm long, 75  $\mu\text{m}$  internal diameter capillary for a 15 kV applied voltage and buffer ionic strengths between 10 mM and 100 mM.*

Buffer Ionic Strength (mM)	Current ( $\mu\text{A}$ )	Conductivity ( $\Omega\text{m}$ )
10	19.0	0.192533
20	24.7	0.250293
40	32.8	0.332373
60	42.6	0.431275
80	52.7	0.534027
100	62.7	0.539030

The values for the electrical conductivity of the buffer at different ionic strengths were used in equation (3.2) to estimate the temperature rise in the capillary by the iterative method described (Example 3.2). Three iterations proved to be sufficient to obtain consistent results in each case. The estimated buffer temperature during electrophoresis are shown in Table 3.9.

---

**Example 3.2** *Outline of iterative steps.*

1. Use conductivity of water at 25 °C and other values in equation (4) to obtain a value for the electrolyte temperature.
  2. Use obtained value of the electrolyte temperature from step 1. in equation (7) to find a new thermal conductivity of the electrolyte.
  3. Use the value from step 2 in step 1 and repeat until a consistent value for the temperature is obtained.
-

**Table 3.9** *Estimated buffer temperature in a 57 cm long, 75  $\mu\text{m}$  internal diameter capillary for a 15 kV applied voltage and buffer ionic strengths between 10 mM and 100 mM*

Ionic Strength mM	Estimated Temperature °C
10	25.162
20	25.211
40	25.280
60	25.365
80	25.451
100	25.632

### 3.3.3 Summary.

The increase in temperature across the ionic strength range was small when compared to other CE systems described in the literature which are cooled by natural or forced convection [47,48, 52]. The increases in temperature were of the same order of magnitude as observed by Wätzig [51], and it was concluded that since electrophoretic mobilities were studied at fixed ionic strengths, corrections for temperature between sets of compounds was unnecessary. A linear relationship between ionic strength and estimated temperature was obtained of slope  $4.88 \times 10^{-3}$  and intercept 25.1 °C, correlation coefficient 0.967.

### 3.4 Analysis at pH 8.5.

#### 3.4.1 Analysis and markers at pH 8.5.

Negatively charged ions were analysed at high pH under conditions of strong electroosmotic flow, thus the EOF velocity was easily determined by including a neutral marker compound, in this case thiourea. A charged marker compound was also included at this pH which was benzoic acid. The repeatability of migration time was poor (Figure 3.8).

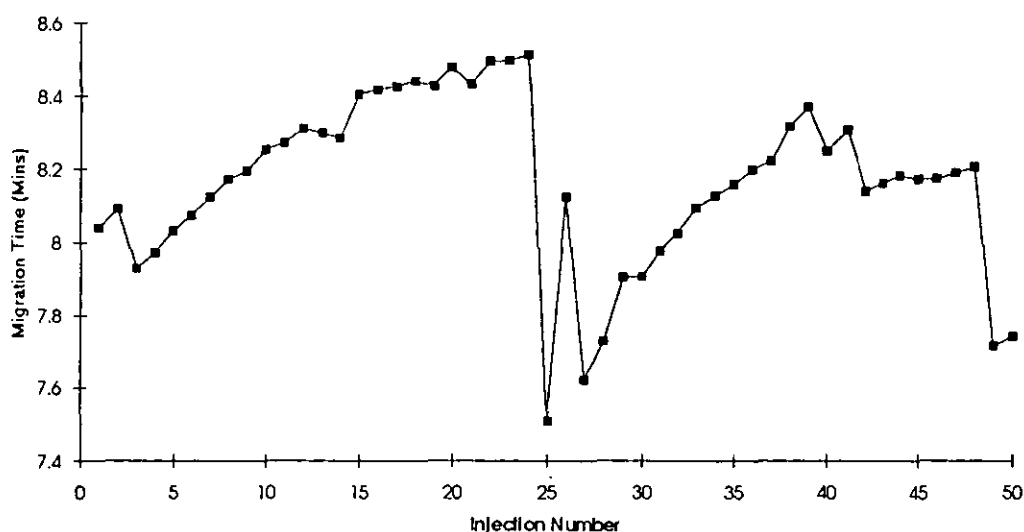


**Figure 3.7** Repeatability of benzoic acid migration time. 50 mM Lithium borate buffer, pH 8.5. Fused silica capillary, 15 kV applied voltage.

The thiourea marker used to calculate the EOF showed a corresponding change to the migration time of benzoic acid (Figure 3.8). However, when the electrophoretic mobilities of benzoic acid were calculated, the same pattern of drifts in mobility were observed. (Figure 3.9). The migration time drift and electrophoretic mobility drift correspond closely for benzoic acid. The graphs of benzoic acid migration time and electrophoretic mobility are more closely related than the corresponding graphs for pyridine, which may be due to the large electroosmotic flow at high pH having a more significant overall effect.

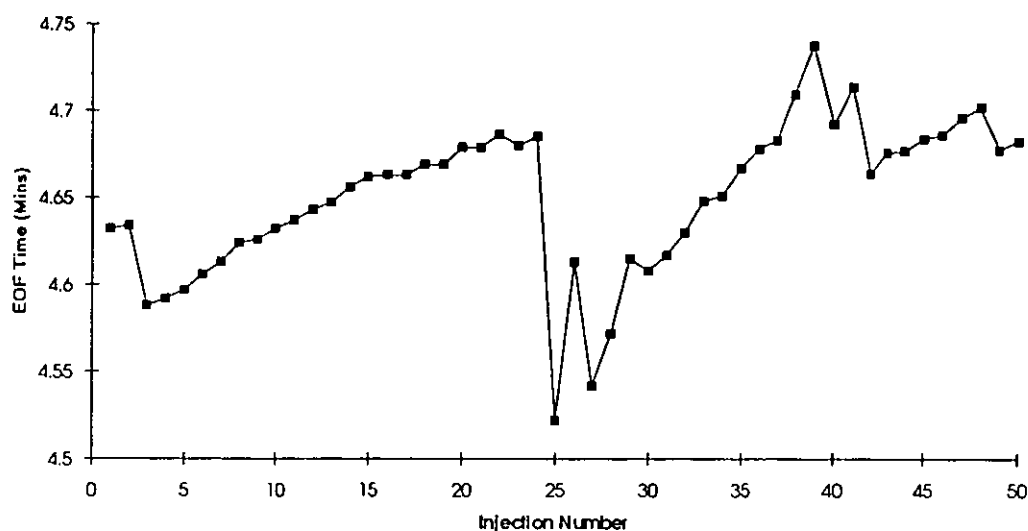


**Figure 3.8** Repeatability of EOF time. Thiourea neutral marker, 50 mM Lithium borate buffer, pH 8.5. Fused silica capillary, 15 kV applied voltage.

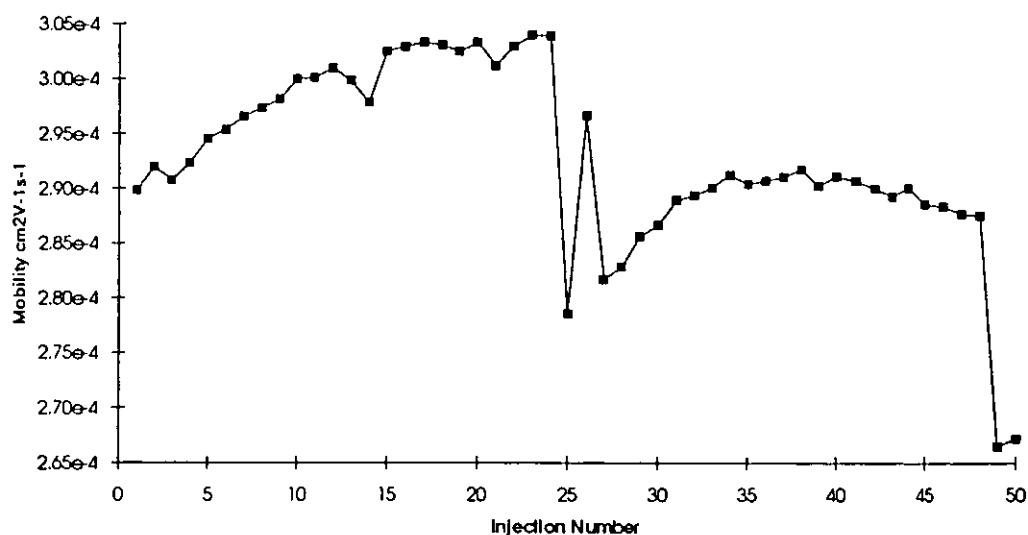


**Figure 3.9** Uncorrected electrophoretic mobility of benzoic acid. 50 mM Lithium borate buffer, pH 8.5. Fused silica capillary, 15 kV applied voltage.



In order to calculate stable values for the electrophoretic mobility of species, it was necessary to use benzoic acid as an internal standard. An average value for the benzoic acid mobility of  $2.996 \text{ e-4 cm}^2\text{V}^{-1}\text{s}^{-1}$  was used to correct electrophoretic mobilities throughout the rest of the study.

Intra-run reproducibility for six replicate injections (as defined for the alkylpyridines) was calculated for 4-ethylbenzoic acid at 0.05% (Table 3.10) and inter-run reproducibility for six repetitions of 4-methylbenzoic acid at 0.09% (Table 3.11). These figures agree closely with the data obtained for the alkylpyridines and indicate that electrophoretic mobilities may be accurately measured.

**Table 3.10** *Intra-run reproducibility for six injections of 4-ethylbenzoic acid. 50 mM lithium borate buffer, pH 8.5, 2 s injection, 15 kV applied voltage, uncorrected mobilities adjusted for electroosmotic flow. Corrected mobilities adjusted for electroosmotic flow and using benzoic acid as an internal standard.*

	4-Ethylbenzoic acid - Intra-run replicates	
Uncorrected benzoic acid mobility $\text{cm}^2\text{V}^{-1}\text{s}^{-1}$	Uncorrected 4-ethylbenzoic acid mobility $\text{cm}^2\text{V}^{-1}\text{s}^{-1}$	Corrected 4-ethylbenzoic acid mobility $\text{cm}^2\text{V}^{-1}\text{s}^{-1}$
-2.989 e-4	-2.566 e-4	-2.572 e-4
-2.996 e-4	-2.575 e-4	-2.575 e-4
-2.989 e-4	-2.569 e-4	-2.575 e-4
-3.002 e-4	-2.580 e-4	-2.575 e-4
-3.016 e-4	-2.592 e-4	-2.575 e-4
-3.005 e-4	-2.583 e-4	-2.575 e-4
Average		-2.574 e-4
Standard Deviation		1.226 e-7
RSD		0.05 %

**Table 3.11** *Inter-run reproducibility for six injections of 4-methylbenzoic acid. 50 mM lithium borate buffer, pH 8.5, 2 s injection, 15 kV applied voltage, uncorrected mobilities adjusted for electroosmotic flow. Corrected mobilities adjusted for electroosmotic flow and using benzoic acid as an internal standard.*

	4-Methylbenzoic acid - Inter-Run Replicates	
Uncorrected benzoic acid mobility $\text{cm}^2\text{V}^{-1}\text{s}^{-1}$	Uncorrected 4-methylbenzoic acid mobility $\text{cm}^2\text{V}^{-1}\text{s}^{-1}$	Corrected 4-methylbenzoic acid mobility $\text{cm}^2\text{V}^{-1}\text{s}^{-1}$
-2.974 e-4	-2.712 e-4	-2.732 e-4
-2.969 e-4	-2.712 e-4	-2.737 e-4
-3.002 e-4	-2.740 e-4	-2.735 e-4
-2.989 e-4	-2.726 e-4	-2.732 e-4
-2.987 e-4	-2.721 e-4	-2.729 e-4
-2.979 e-4	-2.716 e-4	-2.731 e-4
Average		-2.733 e-4
Standard Deviation		2.578 e-7
<b>RSD</b>		<b>0.09%</b>

### 3.4.2 Effects of Temperature.

The investigations into heating effects at low pH are applicable to the system at high pH as the principal physical factor governing heating is the current carried within the capillary. For the 50 mM lithium borate buffer used at pH 8.5 and an applied voltage of 30 kV, the current measured was typically 17 - 18  $\mu\text{A}$ , giving similar amounts of power dissipation to the lower ionic

strength lithium phosphate buffers used at low pH. Thus only very small increases in temperature were expected.

### 3.5 Summary.

Analysis of alkyipyridines at low pH showed that the repeatability of migration time in CE was poor. In order to obtain reproducible results it is necessary to measure electroosmotic flow and a method for rapidly estimating large EOF values is presented. Electrophoretic mobilities when corrected with an internal standard gave extremely reproducible results. The effects of temperature were shown to be small in the system being investigated and it is likely that the corrections applied would also correct for any aberrant changes in temperature. The data for the alkybenzoic acids at high pH on migration times and electrophoretic mobilities needed the same corrections applied to them as for the analysis of the alkyipyridines at low pH. The accurate determination of electrophoretic mobilities allows more detailed investigations in future chapters.

## Chapter 4.

### Separations of Alkylpyridines.

#### 4.1 Introduction

The first group of compounds that were investigated were the alkylpyridines. At low pH their separations were based on the size and shape of the compounds and the effects of experimental parameters such as buffer ionic strength and temperature were investigated. Separations can also be performed based on the optimisation of charge difference between ions, and these alternative separations were compared for the dimethylpyridines.

#### 4.2 Separations at low pH.

The main study on separations of alkylpyridines was performed at pH 2.5. At this pH it was expected that differences in charge between analytes would be eliminated since the alkylpyridines'  $pK_a$  values were in the range 4.5-6.5. Using the Hendersson-Hasselbach [105] equation to calculate the effective charge on analytes gave charges at pH 2.5 of +1 for the alkylpyridines. Full  $pK_a$  data is reviewed in Appendix A.

Separations of the homologous series of the 2-alkylpyridines gives a separation based on molecular size of analytes with the smaller alkylpyridines migrating faster than larger alkylpyridines (Figure 4.1)

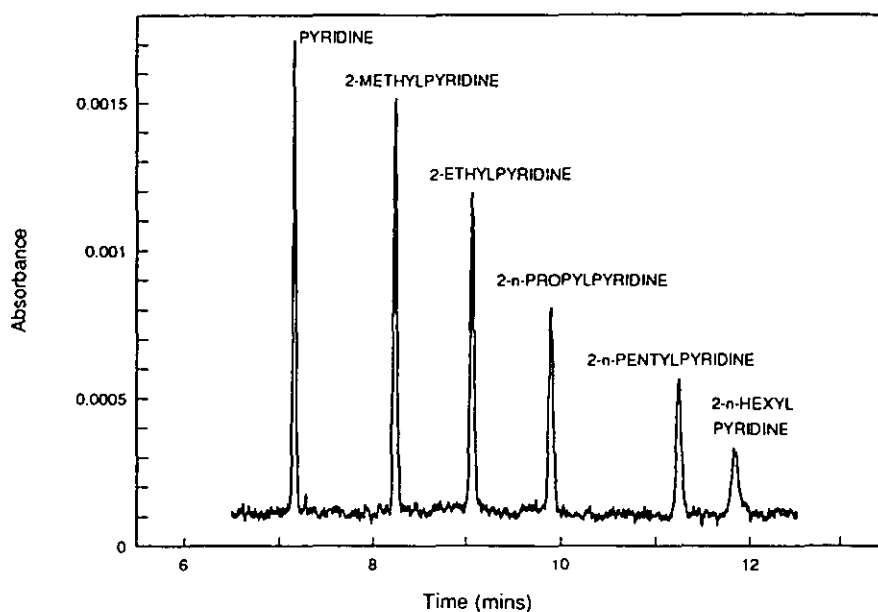


**Figure 4.1** Separation of the 2-alkylpyridines. 40 mM lithium phosphate buffer, pH 2.5, 15 kV applied voltage.

In addition to separations based on size, separations of positional isomers were observed such as the separation of 2-, 3- and 4- ethylpyridines (Figure 4.2).

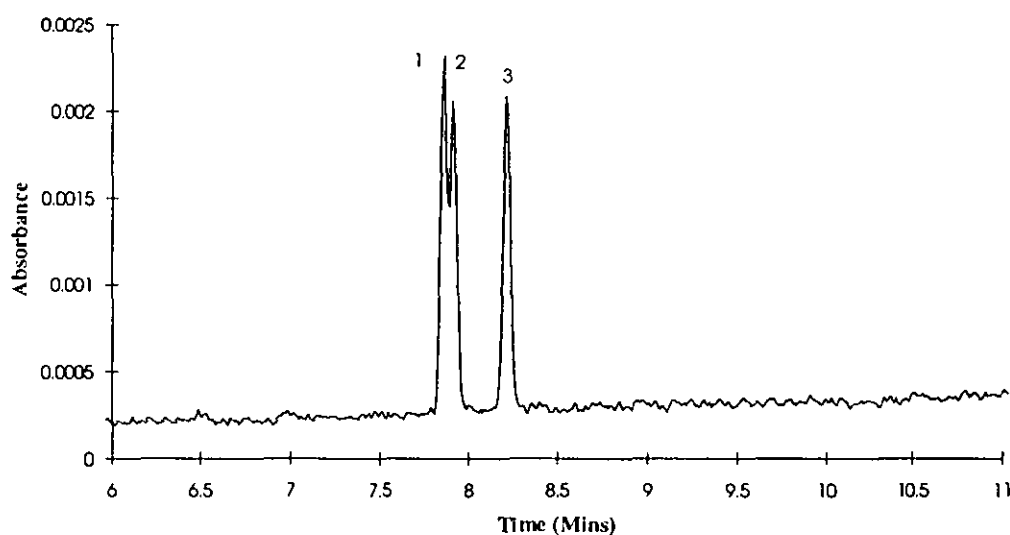


**Figure 4.2** Separation of Ethylpyridines. 40 mM Lithium Phosphate Buffer, pH 2.5, 15 kV applied voltage. 1 - 4-ethylpyridine, 2 - 3-ethylpyridine, 3 - 2-ethylpyridine.

A migration order of 4-ethylpyridine, 3-ethylpyridine, 2-ethylpyridine was observed. Similar separations were observed for the methylpyridines, but 3- and 4- methylpyridine were unresolved. The isomeric propylpyridines also gave rise to a separation with n-propylpyridinium bromide, 4-n-propylpyridine, 4-isopropylpyridine and 2-n-propylpyridine being resolved (Figure 4.3).

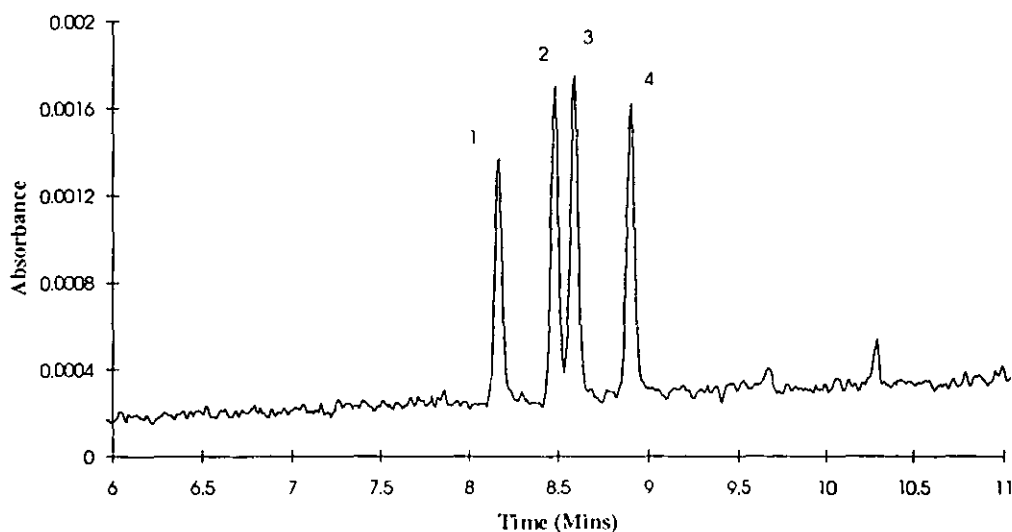


**Figure 4.3** *Separation of Propylpyridines. 40 mM Lithium Phosphate Buffer, pH 2.5, 15 kV applied voltage. 1 - N-Propylpyridinium bromide, 2 - 4-propylpyridine, 3- 4-isopropylpyridine, 4 - 2-propylpyridine.*

Thus for the propylpyridines, a separation between 4-n-propylpyridine and its isopropyl branched chain is observed. Separations of many more structural isomers could be achieved (Table 4.1). Full mobility data is presented in Appendix 1.

**Table 4.1** Electrophoretic mobility of alkylpyridines. 40 mM Lithium phosphate buffer, pH 2.5, 15 kV applied voltage.

Compound	Mobility $\text{cm}^2\text{V}^{-1}\text{s}^{-1}$	Compound	Mobility
Pyridine	4.176 e-4	2-Propylpyridine	2.923 e-4
2-Methylpyridine	3.581 e-4	4-Propylpyridine	3.097 e-4
3-Methylpyridine	3.722 e-4	3-Butylpyridine	2.848 e-4
4-Methylpyridine	3.722 e-4	2-Pentylpyridine	2.534 e-4
2-Ethylpyridine	3.222 e-4	2-Hexylpyridine	2.391 e-4
3-Ethylpyridine	3.366 e-4	4-isoPropylpyridine	3.059 e-4
4-Ethylpyridine	3.397 e-4	n-Propylpyridinium bromide	3.249 e-4
3,4-Dimethylpyridine	3.349 e-4	3-Ethyl-4-methylpyridine	3.071 e-4
3,5-Dimethylpyridine	3.285 e-4	5-Ethyl-2-methylpyridine	2.976 e-4
2,6-Dimethylpyridine	3.168 e-4	6-Ethyl-2-methylpyridine	2.904 e-4
2,4-Dimethylpyridine	3.196 e-4	Z-2,3-pentenylpyridine	2.640 e-4
2,5-Dimethylpyridine	3.236 e-4	E-2,3-pentenylpyridine	2.602 e-4
2,3-Dimethylpyridine	3.236 e-4		

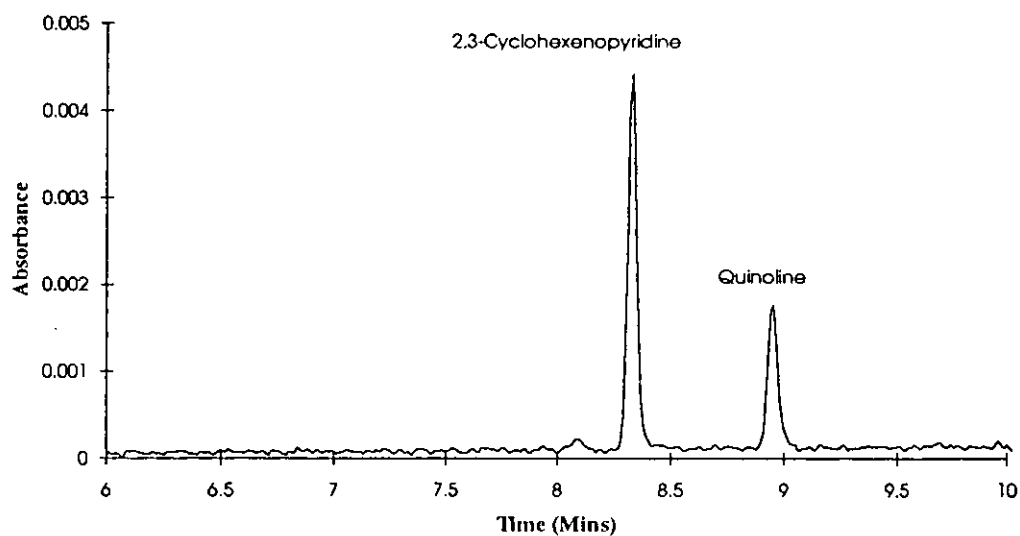


**Figure 4.4** Separation of 2,3-cyclohexenopyridine and quinoline. 40 mM lithium phosphate buffer, pH 2.5, 15 kV applied voltage.

2,3-cyclohexenopyridine and quinoline, which differ by only two molecular mass units gave a well resolved separation (Figure 4.4). There are structural differences between 2,3-cyclohexenopyridine and quinoline and this could account for the separations. 2,3-cyclohexenopyridine has a fused hexene ring in a half chair conformation whereas quinoline is a flat aromatic structure.

Thus a relationship between size and electrophoretic mobility has been shown (Figure 4.1), with additional separations of analytes of identical sizes being observed (Figures 4.2-4.4). The factors causing differential mobilities of compounds is shown clearly for the mono-alkylpyridines, where analytes migrated according to size, but bands of positional isomers were resolved (Figure 4.5).

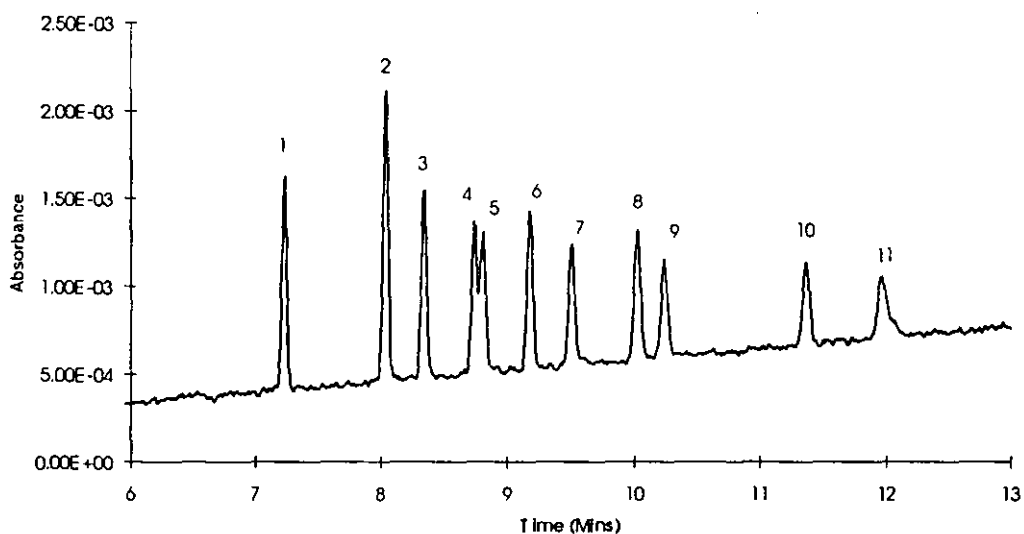


**Figure 4.5** Separation of the *n*-monoalkylpyridines. (40 mM lithium phosphate buffer, pH 2.5, 15 kV applied voltage. 1 - Pyridine, 2 - 3-methylpyridine and 4-methylpyridine, 3 - 2-methylpyridine, 4 - 4-ethylpyridine, 5 - 3-ethylpyridine, 6 - 2-ethylpyridine, 7 - 4-propylpyridine, 8 - 2-propylpyridine, 9 - 3-butylpyridine, 10 - 2-pentylpyridine, 11 - 2-hexylpyridine.



### 4.3 The Effects of Ionic Strength.

#### 4.3.1 General Trends.

In section 3.2 the compounds pyridine and acridine were investigated as markers to correct electrophoretic mobilities. 2,3-cyclohexenopyridine was also included in these analyses. The electrophoretic mobilities for the compounds pyridine, 2,3-cyclohexenopyridine, acridine and benzamide (the electroosmotic flow marker) form the basis for investigations into the effects of buffer and ionic strength. At this stage the mobilities used were measured using benzamide as the electroosmotic flow marker and taken from Table 3.3. These values were plotted against ionic strength (Figure 4.6).

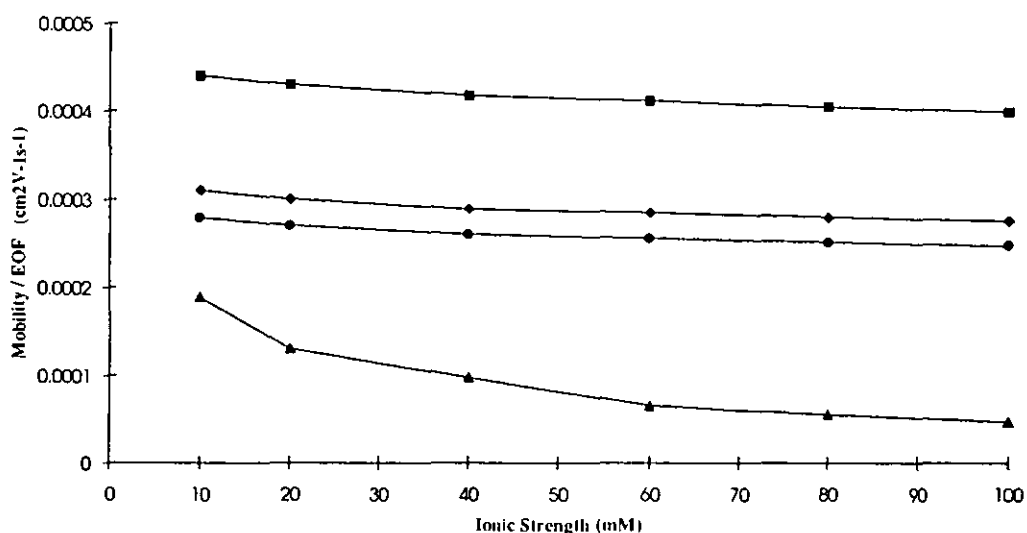


**Figure 4.6** *The effects of ionic strength on electrophoretic mobility and electroosmotic flow. Lithium phosphate buffers, pH 2.5, 15 kV applied voltage. (■) Pyridine, (◆) 2,3-cyclohexenopyridine, (●) acridine, (Δ) buffer electroosmotic mobility.*

### 4.3.2 Electroosmotic Mobility.

The changes in electroosmotic mobility (Figure 4.5) are broadly in line with theory and literature observations [36]. Over the range studied the relationship between (Ionic Strength)<sup>-1/2</sup> and EOF gives a linear relationship with correlation coefficient of 0.9869. Curvature at low ionic strengths seen by Salomon [36] is not observed probably due to the lowest value studied at 10 mM not being low enough for a significant effect. The relationship between ionic strength and the inverse of EOF gives a linear fit with correlation coefficient of 0.9890 but the curvature at high ionic strengths observed by Salomon [36] was not observed.

### 4.3.3 Electrophoretic Mobility.

The effect of ionic strength on electrophoretic mobility of analytes depends on the interaction between buffer salts and analyte and so can be a complex function. An expression has been derived which has its origins in the Debye-Hückel theory [105],

$$\mu_e = \frac{3.10^8 Q_{eff}}{\eta \sqrt{I}}$$

where  $Q_{eff}$  is the effective charge on the analyte and  $I$  is the ionic strength of the buffer. The relative separations of pyridine, 2,3-cyclohexenopyridine and acridine show no difference over the range studied (Figure 4.6), indicating no significant differences in the environments about their positive charge with ionic strength. A fit of mobility against  $I^{1/2}$  does not show a linear relationship, with a curvature at lower ionic strengths (Figure 4.7). This may be accounted for by the fact that  $Q_{eff}$  is almost certainly changing as the concentration of buffer salts surrounding the analyte ion are changed by varying the ionic strength of the buffer.

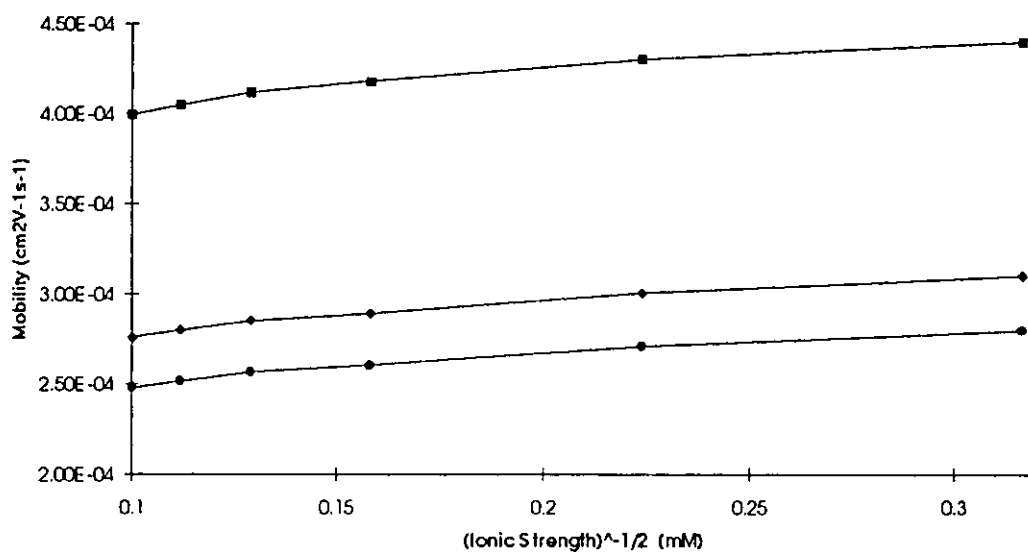


**Figure 4.7** Relationship between analyte mobility and  $(\text{Ionic strength})^{-1/2}$ . (■) Pyridine, (◆) 2,3-cyclohexenopyridine, (●) acridine.

#### 4.3.4 Effects of Ionic Strength on Separations.

The relative separations of pyridine, 2,3-cyclohexenopyridine and acridine showed no changes over the ionic strength range studied. For further investigations into the effects of ionic strength the corrected mobilities of compounds as described in section 3.2 were used. For all positional isomers studied, no overall change in migration order was observed with changes in ionic strength of the background electrolyte. However, by comparing mobilities of analytes relative to the mobility of pyridine, any changes in the buffer-analyte interaction with changes in ionic strength can be probed.

The separation of the ethylpyridines relative to the mobility of pyridine showed little difference in the relative mobilities of 3-ethylpyridine and 4-ethylpyridine in the region 20 mM to 100 mM (Figure 4.8). An increase in mobility at 10 mM can be observed which may be attributable to a decrease in the size of the buffer-analyte complex.

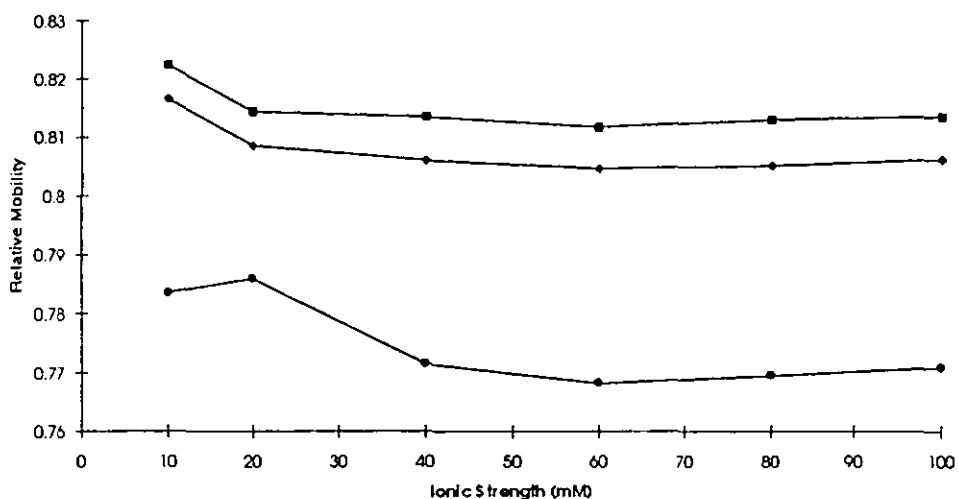


**Figure 4.8** Relative mobilities of the ethylpyridines. ● 2-ethylpyridine, ◆ 3-ethylpyridine, ■ 4-ethylpyridine.

The trend for 2-ethylpyridine shows little difference in relative mobility between 40 mM to 100 mM buffer ionic strength, but an increase in relative mobility is observed at 20 mM buffer ionic strength. This is probably indicative of a steric effect which could be due to the exclusion of ions at this ionic strength. However, since the changes were small compared with the overall separation of the positional isomers, the significance was reasoned to be small. The pattern of the 2-substituted alkylpyridines showing slight discrepancy in relative mobility to their 3- and 4- substituted isomers at low ionic strengths is repeated for the methylpyridines and the propylpyridines (Figure 4.9 and 4.10), with the effect becoming more significant with increasing chain length.

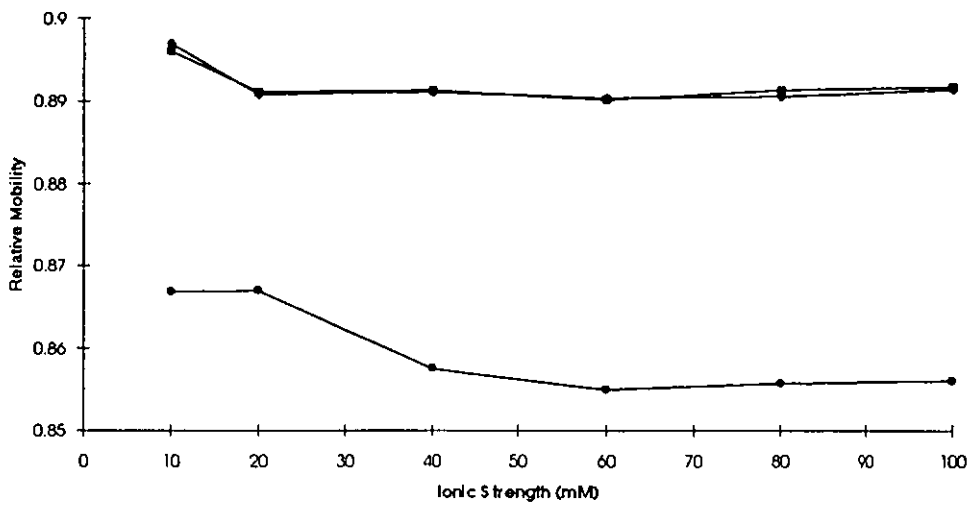


**Figure 4.9** Relative mobilities of the methylpyridines. ● 2-methylpyridine, ◆ 3-methylpyridine, ■ 4-methylpyridine.

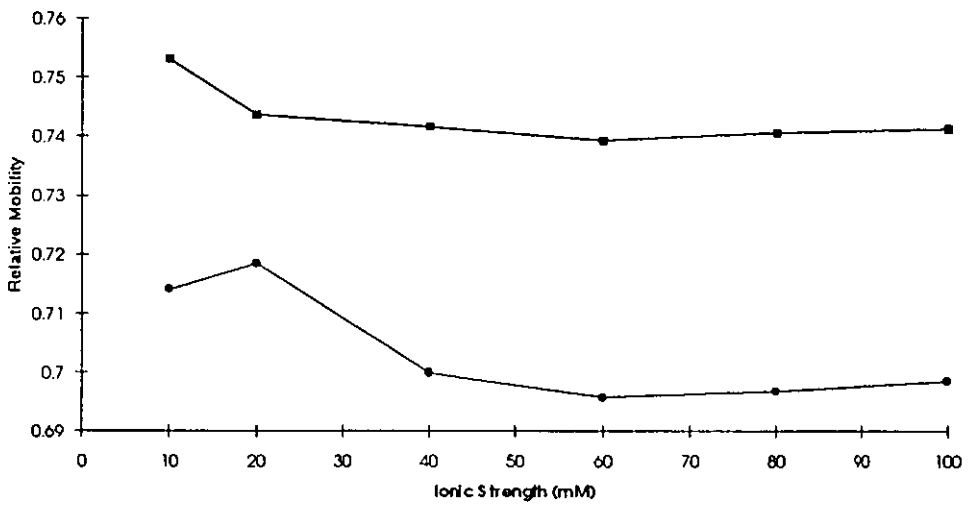


**Figure 4.10** Relative mobilities of the propylpyridines. ● 2-propylpyridine, ■ 4-propylpyridine.

#### 4.4 The Effects of Temperature

The inner capillary temperature affects a range of properties influencing a separation including buffer viscosity, the ionisation constants of analytes and electroosmotic flow. It was intended to investigate the effects of temperature on the separations by comparing the electrophoretic mobilities of compounds with respect to the supporting buffer viscosities measured by rheometry. However the fast marker technique could not be used with changes in temperature due to the influence of temperature on EOF leading to the need to run a series of measurements at each different temperature. Thus, a lithium citrate buffer of pH 4.0 was used to give an acceptable electroosmotic flow.

*Table 4.2 Electrophoretic mobilities of the isomeric ethylpyridines measured in a 40 mM lithium citrate buffer, pH 4.0, 30 kV applied voltage, at temperatures of 25-50 °C. Supporting buffer viscosity measured using a torque rheometer system between 20-50 °C at a temperature gradient of 0.1 °C/12 s.*

Buffer temperature °C	Buffer viscosity Pas	2-Ethylpyridine mobility $\text{cm}^2\text{V}^{-1}\text{s}^{-1}$	3-Ethylpyridine mobility $\text{cm}^2\text{V}^{-1}\text{s}^{-1}$	4-Ethylpyridine mobility $\text{cm}^2\text{V}^{-1}\text{s}^{-1}$
25	1.70 e-3	3.025 e-4	3.103 e-4	3.194 e-4
30	1.62 e-3	3.380 e-4	3.456 e-4	3.518 e-4
35	1.51 e-3	3.622 e-4	3.708 e-4	3.781 e-4
40	1.40 e-3	3.988 e-4	4.092 e-4	4.160 e-4
45	1.31 e-3	4.361 e-4	4.446 e-4	4.542 e-4
50	1.18 e-3	4.643 e-4	4.713 e-3	4.792 e-4
<b>Regression analysis</b>	Gradient Intercept Correlation coefficient	-0.313 8.38 e-4 0.923	-0.312 8.45 e-4 0.991	-0.313 8.54 e-4 0.991

The mobilities of the isomeric ethylpyridines were compared to the viscosity of the citrate buffer (Table 4.2, Figure 4.11). No change in the relative separations was observed with temperature and a good correlation between the measured electrophoretic mobility and viscosity was observed as would be expected from section 1.2 (equation 1.4). Thus, separations of isomeric compounds did not show a strong dependence on temperature.

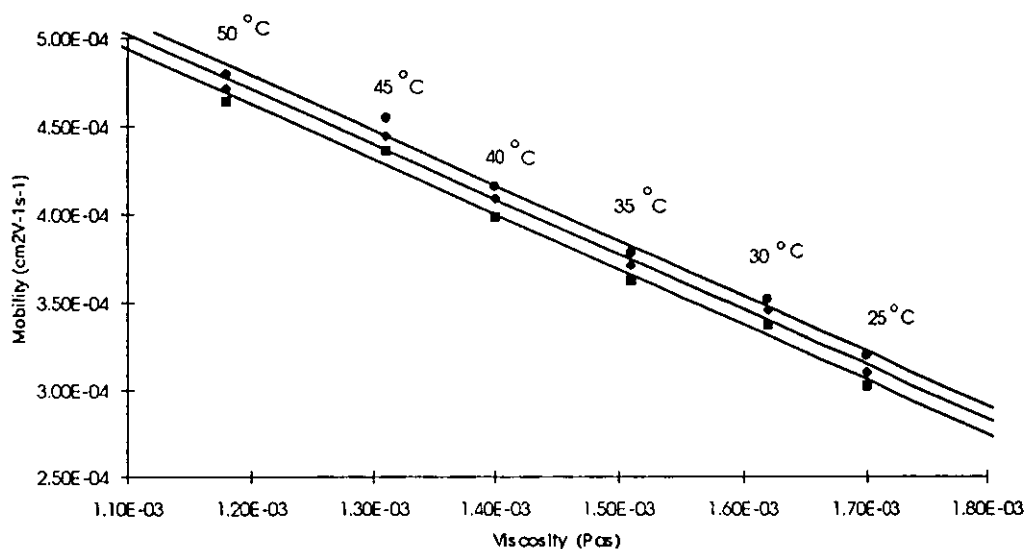


**Figure 4.11** The inverse relationship between electrophoretic mobility of analytes and the supporting buffer viscosity. 40 mM Lithium citrate buffer, pH 4.0, 30 kV applied voltage, at temperatures of 25-50 °C. Supporting buffer viscosity measured using a torque rheometer system between 20-50 °C at a temperature gradient of 0.1 °C/12 s.

## 4.5 Separation of The Dimethylpyridines across the pH Range.

### 4.5.1 Introduction.

Separations have been presented that show separations based on the size of analytes. The charge on analytes also has an important influence on the separations of compounds. The separation of the dimethylpyridines across the pH range provided a comparison between the two modes of separation.

### 4.5.2 Separations at pH 2.5.

A partial separation of the dimethylpyridines (DMP) could be achieved at pH 2.5 (Figure 4.13), where each of the isomers bears a full positive charge because the pH is much lower than their  $pK_a$  values. In order to improve the baseline separation the ionic strength of the background electrolyte was varied from 10 mM-100 mM and it was concluded that an optimal separation was obtained at about 40-60 mM. At lower ionic strengths, the electroosmotic flow in the capillary increases, and so the time window for separation decreased. At higher ionic strengths, Joule heating effects were observed, leading to band broadening of the dimethylpyridine peaks. Both these effects contributed to a loss in resolution.

The migration order at pH 2.5 was determined by spiking studies as 3,4-DMP, 3,5-DMP, 2,3-DMP  $\approx$  2,5-DMP, 2,4-DMP, 2,6-DMP. This order did not correspond to the order of  $pK_a$  values determined by potentiometric titration (Table 4.3) [103]. The electrophoretic mobility of the dimethylpyridines at low pH,  $\mu_{2.5}$  was calculated (Table 4.4).



**Table 4.3** *pKa* values for the dimethylpyridines determined by potentiometric titration [103].

Compound	Literature pKa
2,6-Dimethylpyridine	6.77
2,4-Dimethylpyridine	6.72
2,3-Dimethylpyridine	6.60
3,4-Dimethylpyridine	6.52
2,5-Dimethylpyridine	6.47
3,5-Dimethylpyridine	6.25

**Table 4.4** *Electrophoretic mobilities of the fully charged dimethylpyridines at pH 2.5, 40 mM lithium phosphate buffer, 15 kV applied voltage.*

Compound	Electrophoretic Mobility $\text{cm}^2\text{V}^{-1}\text{s}^{-1}$
3,4-Dimethylpyridine	3.349 e-4
3,5-Dimethylpyridine	3.285 e-4
2,3-Dimethylpyridine	3.236 e-4
2,5-Dimethylpyridine	3.236 e-4
2,4-Dimethylpyridine	3.196 e-4
2,6-Dimethylpyridine	3.168 e-4

By adding 0.1% hydroxypropylmethylcellulose (HPMC) to the buffer the viscosity of the background electrolyte is increased [104] increasing the migration time of compounds and potentially increasing the discrimination between isomers. However, no significant improvement in resolution was

obtained. The temperature of the background electrolyte was then reduced from 25 °C to 15 °C and a small increase in resolution was observed. However, 2,3-DMP and 2,5-DMP still did not separate and it was concluded that they had identical mobilities.

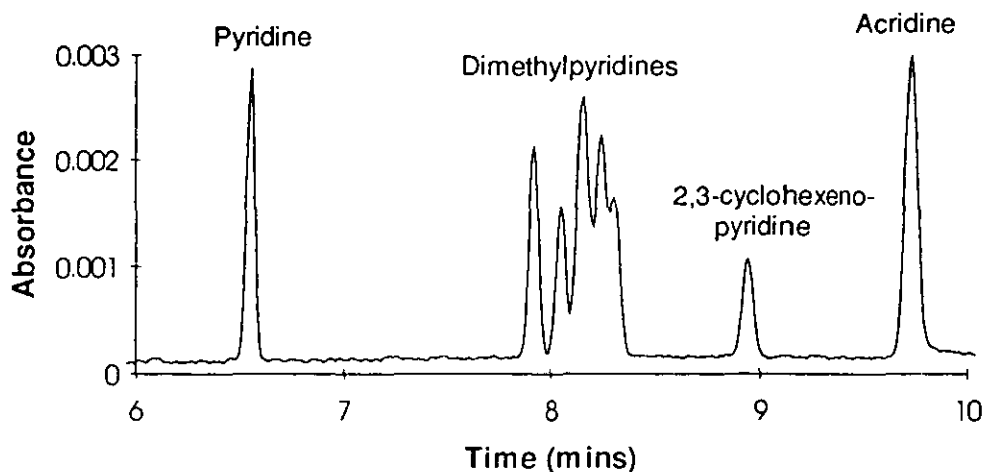


*Figure 4.13 Separation of the dimethylpyridines and standards at low pH, 40 mM lithium phosphate buffer, pH 2.5, 15 kV applied voltage.*

#### 4.5.3 Prediction of Mobility Profile from $pK_a$ Values

The partial charge on each of the dimethylpyridines was calculated across a broad pH range from their reported  $pK_a$  values [103] (Table 4.3) and the Henderson-Hasselbalch equation [105] (equation 4.1). Since the electrophoretic mobility of each isomer should be a product of their fully charged mobility (at pH 2.5) and their partial charge at the pH being studied, the mobility of the dimethylpyridines can be predicted across the pH range (Figure 4.14).

$$q_{eff} = \frac{1}{1 + 10^{pH - pK_a}} \quad (4.1)$$

where  $q_{eff}$  is the partial charge on the analyte, pH is the buffer pH and  $pK_a$  is the ionisation constant of the analyte.

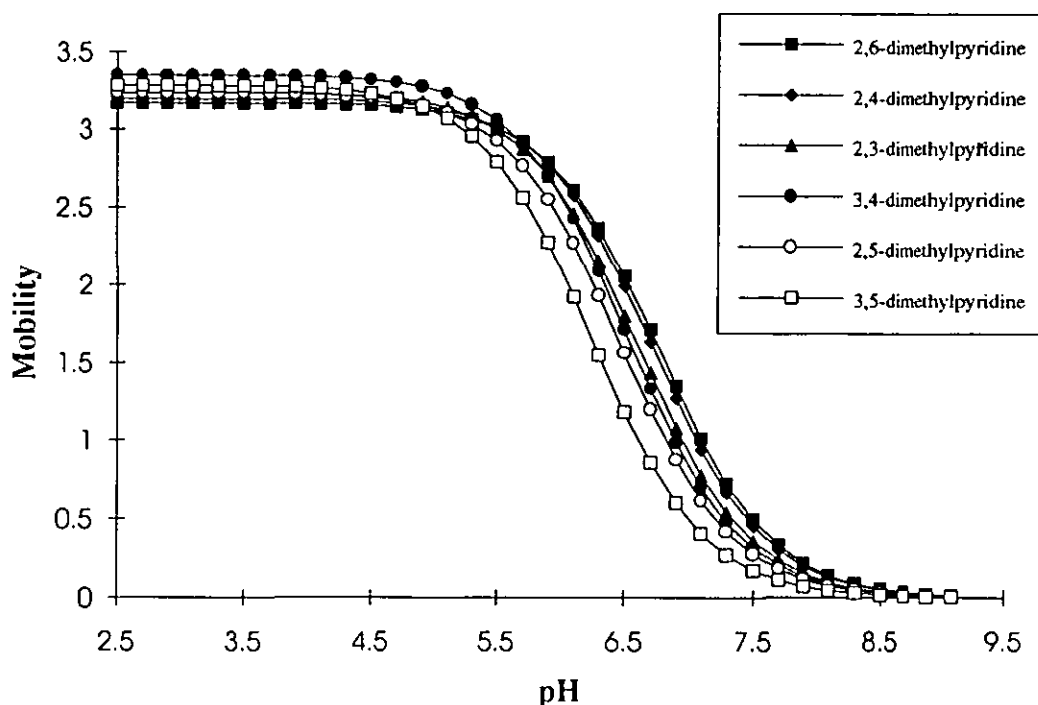


*Figure 4.14 Variation in predicted mobility with pH based on the analytes mobility at pH 2.5 and their partial charge at each pH..*

These predictions suggest that points of co-migration of isomers should occur at particular pH values and the order of elution will be reversed on either side of these points. The pH of maximum mobility difference, which occurs at pH 6.5, should give the optimum separation. In the intermediate pH range of between 4 - 6, there should be points where the mobilities of pairs of analytes should coincide. This was confirmed by separating the mixture at a number of pH values between pH 4.5-5.77 (Figure 4.15).

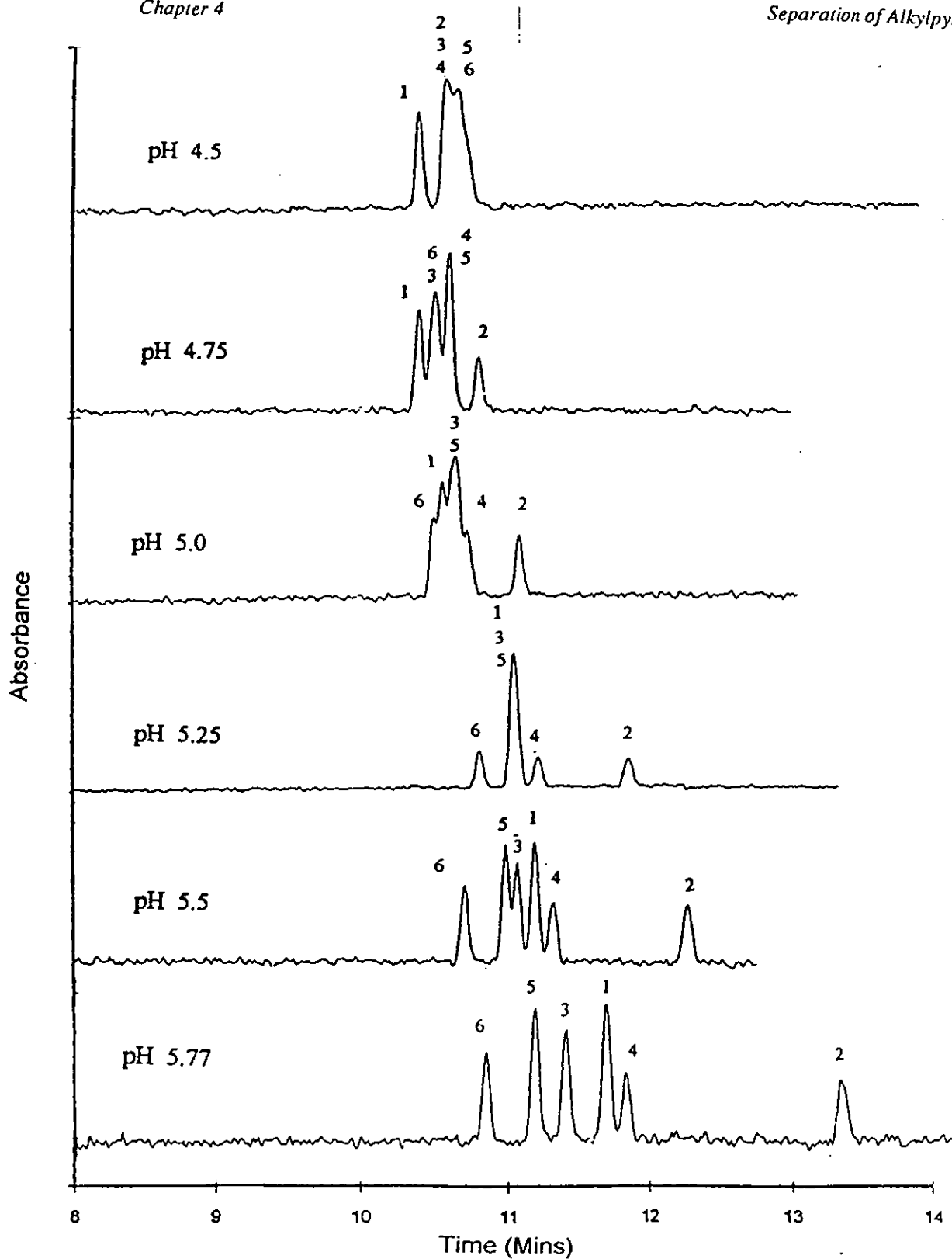


**Figure 4.15** Electropherograms showing the change in migration order across the pH range. 1 - 3,4-DMP; 2 - 3,5-DMP; 3 - 2,3-DMP; 4 - 2,5-DMP; 5 - 2,4-DMP; 6 - 2,6-DMP

At pH 4.5, the mobility order was 3,4-DMP, 3,5-DMP  $\approx$  2,3-DMP  $\approx$  2,5-DMP, 2,4-DMP  $\approx$  2,6-DMP which was the same order as at pH 2.5, suggesting that the separation was still determined by the shape of the analytes. As the pH was raised, the migration order becomes scrambled as the charges on the different isomers were reduced by different extents. For example at pH 4.75, the 2,3-DMP, 2,6-DMP and 3,5-DMP isomers co-migrated. As the pH was raised further, the differences in the partial charge on the DMPs became the dominant factor, and at pH 5.5 the migration order was 2,6-DMP, 2,4-DMP, 2,5-DMP, 3,4-DMP, 2,3-DMP, 3,5-DMP in agreement with the order predicted from  $pK_a$  data.

#### 4.5.4 Separation at pH 6.5

The separation in a lithium phosphate buffer pH 6.5 produced baseline separation of all six dimethylpyridines (Figure 4.16) and the mobility order follows the predicted separation (Figure 4.14).

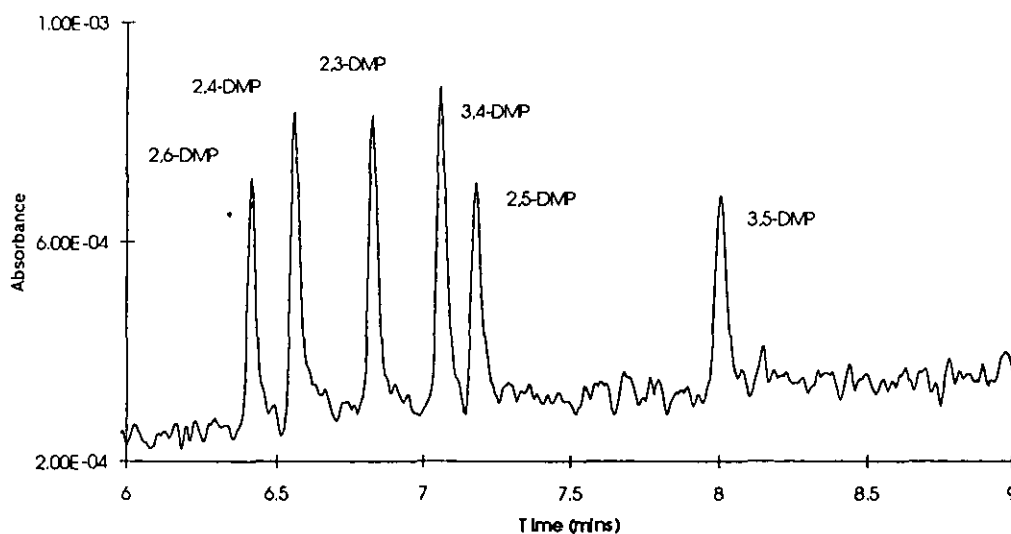


**Figure 4.16** Separation of the DMPs, 50 mM Lithium Phosphate buffer, 25 °C, pH 6.5. 1 - 3,4-DMP; 2 - 3,5-DMP; 3 - 2,3-DMP; 4 - 2,5-DMP; 5 - 2,4-DMP; 6 - 2,6-DMP

The electrophoretic mobilities for each isomer were calculated from the experimental values and were compared with the predicted values for the partial charge and electrophoretic mobility (Table 4.5). As can be seen the relative order of migration was predicted correctly but the absolute values of the electrophoretic mobility were all smaller than the predicted values with differences between 7% to 30%, with an average deviation of 15%. These differences are probably caused because the pH of the background electrolyte was slightly higher than the intended value. As can be seen in Figure 4.15, at pH 6.5 the mobilities are very sensitive to changes in pH and would change markedly with only a small discrepancy in the actual value compared to the nominal value.

**Table 4.5** Comparison between calculated and experimental mobilities of the dimethylpyridines at pH 6.5.

Compound	Experimental Mobility $\text{cm}^2\text{V}^{-1}\text{s}^{-1}$	Predicted Mobility $\text{cm}^2\text{V}^{-1}\text{s}^{-1}$	Partial Charge
2,6-Dimethylpyridine	1.947 e-4	2.06 e-4	0.651
2,4-Dimethylpyridine	1.848 e-4	1.99 e-4	0.624
2,3-Dimethylpyridine	1.630 e-4	1.80 e-4	0.557
3,4-Dimethylpyridine	1.464 e-4	1.71 e-4	0.512
2,5-Dimethylpyridine	1.386 e-4	1.56 e-4	0.483
3,5-Dimethylpyridine	0.912 e-4	1.18 e-4	0.360

In summary, the six isomeric dimethylpyridines were separated by free zone capillary electrophoresis across the pH range 2.5-6.5. The order of elution changed with pH of the buffer. The relative order of migration and the electrophoretic mobilities over a range of pH values could be predicted from

the separation of the fully charged species and the calculated partial charges based on their  $pK_a$  values and pH of the buffer.

#### 4.6 Separation of Z- and E- 2-(3-pentenyl)pyridine)

2-(3-Pentenyl)pyridine is marketed as a mixture of isomers and in solution at pH of 2.5 the isomers can readily be separated by CE in 11 minutes (Figure 4.17). Little method development was required, as 2-(3-pentenyl)pyridine was fully protonated under these conditions.

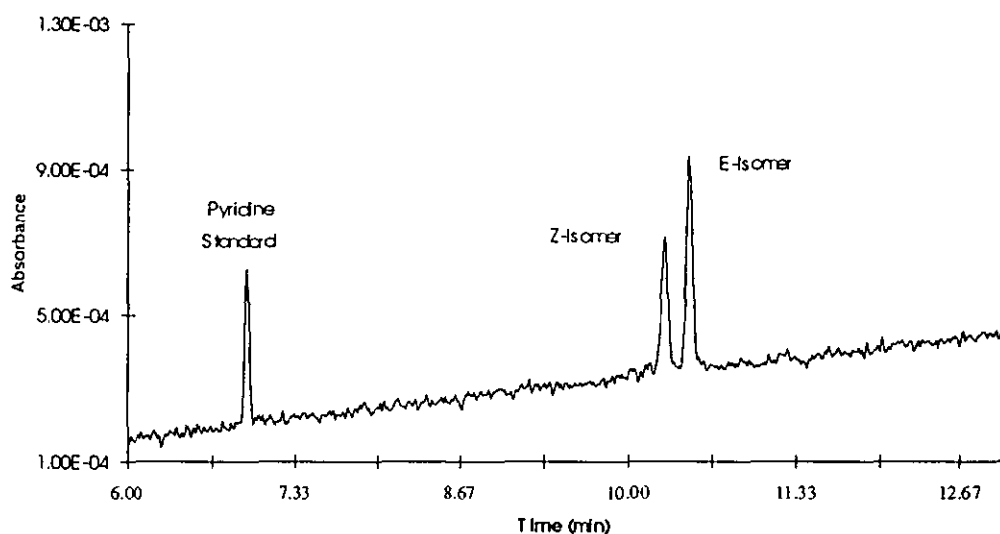


**Figure 4.17** Separation of Z- and E- 2-(3-pentenyl)pyridine. 40 mM lithium phosphate buffer, pH 2.5, 15 kV applied voltage.

It was not possible to directly assign structures to the peaks in the electropherogram because the individual isomers were not available to assign the peaks. However, as electrophoretic mobility increases with decreasing size of the analyte it should be possible to use the size and shape to predict the migration order of the isomers. When the lengths of the side chains were investigated by molecular modelling, it was found that the *E* isomer was fully extended with a length from the *ortho*-hydrogen on the pyridine ring to the end

of the sidechain of 10.2 Å. The corresponding measurement for the *Z* isomer was 9.2 Å (Figure 4.18).

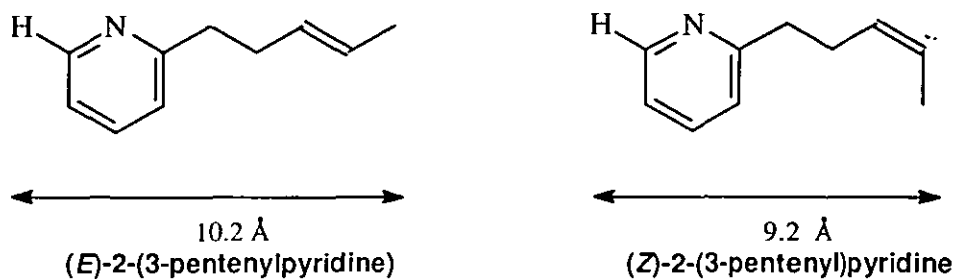


**Figure 4.18** Molecular widths of 2-(3-pentenyl)pyridine isomers

Since a smaller ion would be expected to migrate fastest, the smaller peak at 10.11 min was predicted to correspond to the *Z* isomer and the second peak at 10.31 min to the *E* isomer. These assignments agreed with the expected ratio of the isomers based on the greater thermodynamic stability of the *E* isomer.

In order to quantify the proportion of the two isomers, the absorbance of the analytes are required. Because of the similarity of the chromophore it was expected that the spectra would be effectively identical and this was confirmed using a CE system equipped with a diode array detector. Both peaks gave identical spectra with a maximum absorbance at 265 nm. It was also necessary to correct the peak areas by division by their migration times, in order to take account of the unequal residence time of the analytes in the detection window [106]. Using this correction, the mean proportions over 6 runs was 40.9% for the minor isomer and 59.1% for the major isomer with a standard deviation of 0.9%. The precision of these measurements is in agreement with the work of Altria, who reported precision's of 1-2% relative standard deviations [106].

Confirmation of the assignment of the isomers can be obtained by using  $H^1$ -nuclear magnetic resonance spectroscopy to independently determine the



proportion of the isomers (Table 4.6). The shifts of the terminal methyl groups adjacent to the double bonds are different for the *Z* and *E* isomers, and each are split due to the adjacent protons. Coupling across the double bond was also observed, which split each methyl signal into a doublet of doublets and can be used to identify the isomers (Figure 4.19). The larger peaks showed a long-range coupling of 1.1 Hz and were therefore assigned to the *E* isomer, whereas the small peaks had a coupling of 0.6 Hz typical of a *Z* isomer [107].

**Table 4.6** Tabulation of  $^1\text{H}$  NMR data for 2-(3-pentenyl)pyridine.

Description	Chemical Shift $\delta$ / ppm	Integration Ratio
Doublet	1.559	–
Doublet	1.638	–
Multiplets	2.43	2H
Triplet	2.84	2H
Multiplets	5.60	2H
Multiplets	7.10	2H
Triplet of Doublets	7.58	1H
Doublet of Doublets	8.53	1H

It was also predicted that the methyl group in the *Z* isomer would be more shielded than in the *E* isomer, thus it would occur at a higher field as was observed. The heights of the two methyl signals were compared to give relative concentrations of each isomer in the sample, giving a percentage of (*Z*)-2-(3-pentenyl)pyridine of 38% and (*E*)-2-(3-pentenyl)pyridine of 62% in agreement with the CE assignments.

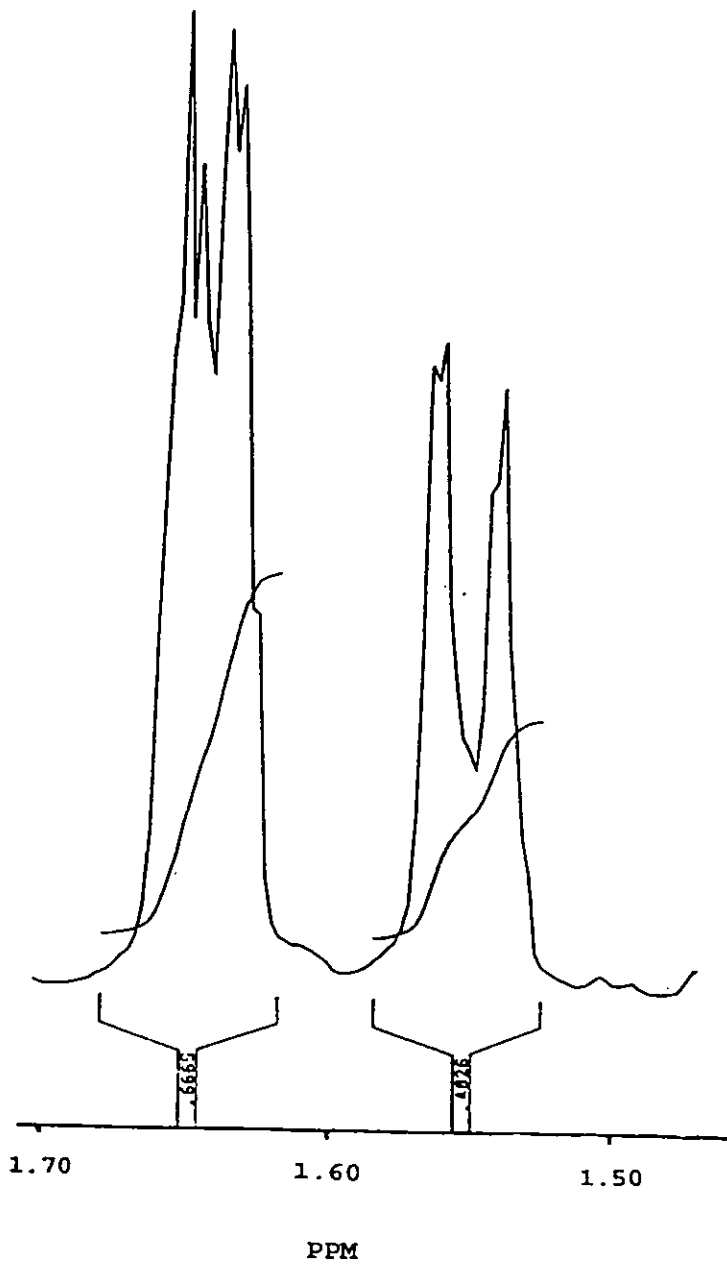


*Figure 4.19  $^1\text{H}$ -nuclear magnetic resonance spectroscopy shifts of the methyl signal for 2-(3-pentenyl)pyridines.*

In order to ensure that the two peaks were isomers and not homologues or other derivatives a sample of 2-(3-pentenyl)pyridine was also investigated by GC/MS. At 100°C under isothermal conditions, major peaks were obtained at 16.0 minutes and 17.1 minutes, which had identical mass spectra with molecular ions ( $m/z$  147), corresponding to 2-(3-pentenyl)pyridines. A minor impurity was also present. The proportions of the major peaks differed from those observed by the other techniques which was attributed to thermal equilibration of the isomers.

In conclusion, the *Z* and *E* isomers of 2-(3-pentenyl)pyridine can be separated according to their shape by capillary electrophoresis. By considering the shape of the molecules, it was possible to predict the order of migration which was subsequently confirmed by NMR Spectroscopy.

#### 4.7 Summary.

The alkylpyridines show a separation based on analyte size at low pH. Differences in the mobilities of positional isomers were noted, and these differences show little change when changing the ionic strength and temperature of the supporting buffer. Predictions of mobility based on structural modelling are presented later. The separation of the dimethylpyridines across a pH range shows the competing nature of the two mechanisms of separation and provides evidence that the separations at low pH are not based on charge effects. Proton magnetic resonance spectroscopy identified the *Z*- and *E*- isomers of 2-(3-pentenyl)pyridine and using simple molecular modelling on the electrophoretic separation, the isomers could be identified.

## Chapter 5.

### Separations of Substituted Benzenes and Related Compounds

#### 5.1 Introduction.

In order to test the theory introduced for the alkylpyridines in chapter 6 some substituted benzenes and related compounds were investigated. These compounds were of interest as the ionisable atoms were moved from a position on the aromatic ring to substituted groups. Compounds such as the alkylanilines are cations and so were analysed under the same conditions as the alkylpyridines. The alkylbenzoic acids are anions and so were analysed as negatively charged ions at high pH.

#### 5.2 Separations of Alkylbenzoic Acids .

##### 5.2.1 Separations at high pH.

Anions can be analysed by CE with the direction of the electric field in the same direction as for the analysis of cations by utilising the properties of the fused silica capillaries to give high EOF mobilities. Thus when a voltage is applied the anions move towards the anode (injection end) of the capillary (Figure 5.1). However, since the EOF is high they are dragged along in the bulk flow through the capillary and so reach the detector at the cathode end of the capillary. The flow of cations and ions in the capillary can be envisaged as downstream movement in a flow for cations and an upstream movement in a flow for anions.

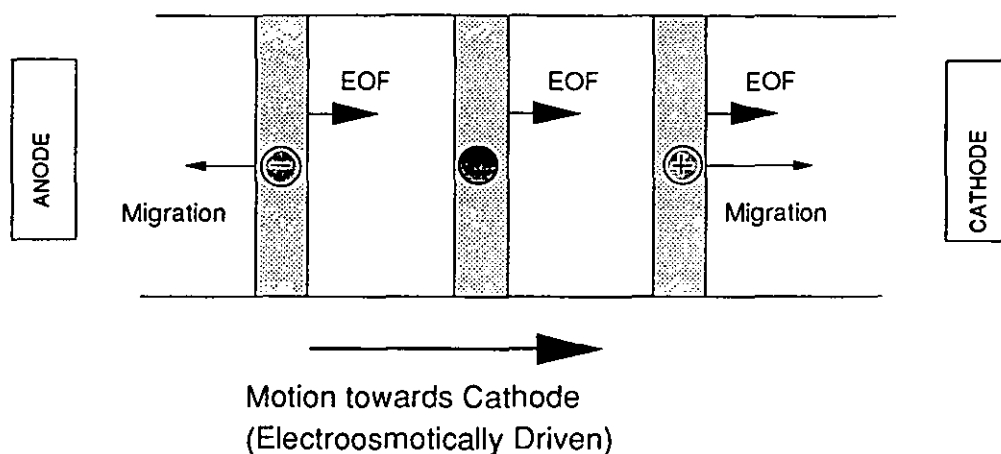


**Figure 5.1** *Movement of cations and anions under the application of an electric field to a fused silica capillary.*

### 5.2.2 BICINE Buffer.

A BICINE (N,N-bis[2-hydroxyethyl]-glycine) buffer of pH 8.5 was initially used to investigate the separations of alkylbenzoic acids. This buffer gives a small current flow in the capillary to minimise Joule heating. Very little separation of the methylbenzoic acids (Figure 5.2) and dimethylbenzoic acids (Figure 5.3) could be achieved.

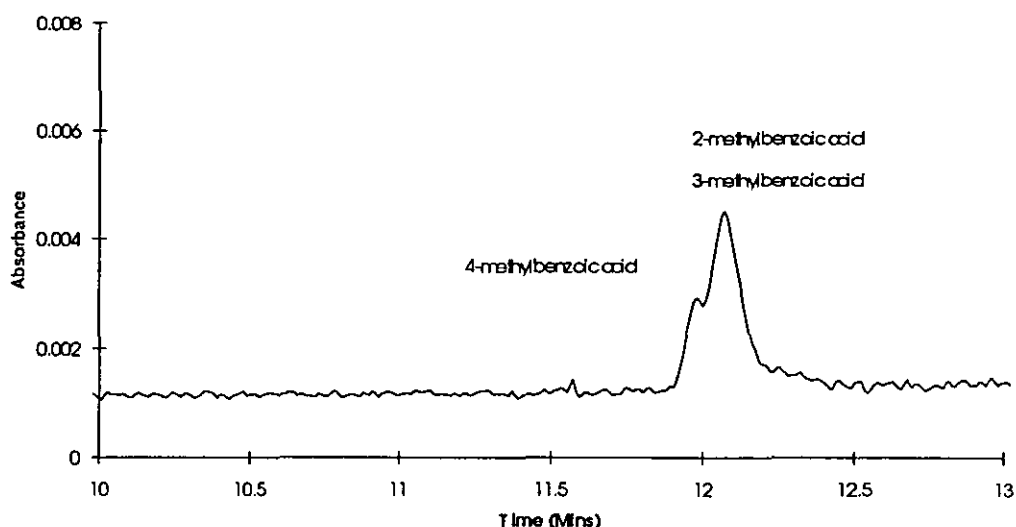


**Figure 5.2** Separation of 2-,3- and 4-methylbenzoic acids. 50 mM BICINE buffer, pH 8.5, 15 kV applied voltage.

There are several possible reasons for poorer separations than for the alkyipyridines. They could be inherently less likely to separate, or the time window could be too small to allow sufficient separation (due to the high EOF generated at this pH). The relationship between EOF mobility, analyte mobility and the resolution of species has been investigated [56]. Maximum resolution should be achieved when analyte mobility approaches the EOF mobility, although in practice this results in long analysis times and such long analysis times can allow band broadening of peaks due to molecular diffusion.

Another reason for the poor resolution could be the size of the BICINE-analyte complex. Since the BICINE buffer has a high molecular mass a strong analyte-buffer interaction would give migrating complexes with only small differences in size for positional isomers, thus the effect from the large counterion would swamp the small differences in shape. Thus the buffer was changed to investigate the effect of the buffer on separations.

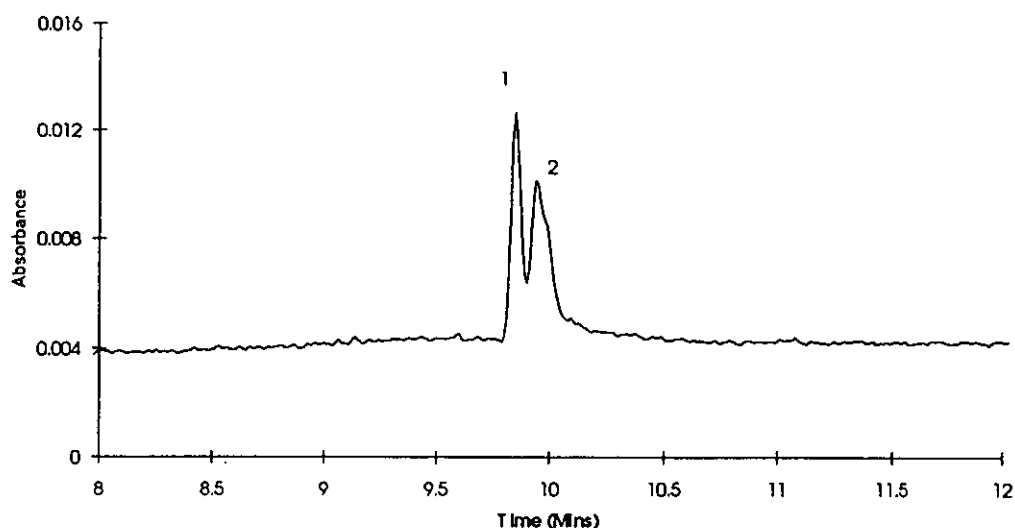


**Figure 5.3** Separation of the dimethylbenzoic acids. 50 mM BICINE buffer, pH 8.5, 15 kV applied voltage. 1 - 2,4-Dimethylbenzoic acid and 2,6-Dimethylbenzoic acid. 2 - 3,5-Dimethylbenzoic acid, 3,4-Dimethylbenzoic acid, 2,5-Dimethylbenzoic acid, 2,3-Dimethylbenzoic acid.

### 5.2.3 Lithium Borate buffer.

The selection of the buffer can change the separations of compounds dramatically in CE, mainly by influencing the efficiency of peaks [4]. A general guide for selection of the buffer is to pick a similar sized of ion and counter ion to the analytes being studied to minimise the effects of peak tailing and fronting. Thus, a borate buffer was a good alternative to the BICINE buffer used in the previous section.

Benzoic acid was included as an internal standard for the analysis. Since it bears a full negative charge at pH 8.5 and it was the smallest of all the alkylbenzoic acid ions being investigated, it was expected that benzoic acid would have the largest migration time. All the other alkylbenzoic acids were

expected to migrate between the EOF marker and the benzoic acid peak therefore a time window available for separation could be measured.

At 15 kV applied voltage, twelve repeat injections of thiourea (the EOF marker) and benzoic acid gave average migration times of 4.68 mins (RSD 0.77%) and 7.99 mins (RSD 1.15%) respectively. This gave a separation window of only 3.31 minutes for all the alkylbenzoic acids to separate. Actual separations of positional isomers were largely unchanged from the BICINE buffer, and separations were poor with no baseline resolution of species compared with the corresponding alkyipyridines at low pH. For the methylbenzoic acids a migration order of 3-methylbenzoic acid, 2-methylbenzoic acid 4-methylbenzoic acid was observed but the 3-methylbenzoic acid and 2-methylbenzoic acid again co-migrated. Mobility orders were determined by spiking studies and individual injections with the EOF marker and the benzoic acid marker. Differences in the measured electrophoretic mobilities of 2-methylbenzoic acid and 3-methylbenzoic acid were observed (Appendix I). This mobility order has no connection with  $pK_a$  data and does not have an obvious similarity with the isomeric methylpyridines.

Iodo-substituted benzoic acids were investigated as it was thought that the bulkier iodo groups might have a stronger influence on separations. However separations followed the same mobility order as the methylbenzoic acids with again with no baseline resolution between isomers.

The electrophoretic mobilities of the compounds were obtained (Table 4.1 for examples and full data in Appendix I using benzoic acid as an internal marker compound as described in chapter 3 (Section 3.4).



### 5.2.4 Alkyl Bonded Capillaries.

By reducing the electroosmotic flow in the capillary, the time window available for separation can be increased due to the analytes being swept through the capillary at a slower rate [108]. The EOF can be decreased by reducing the pH of the supporting buffer but this often results in changing the effective charge on analytes due to their own ionisation constants. An alternative way to reduce electroosmotic flow is to coat the surface of the fused silica capillary. Alkyl bonded capillaries have less silanol groups on the surface of the capillary and so electroosmotic flow is reduced [108] as well as wall absorption effects being minimised for compounds such as proteins [38, 39].

Using a C1 capped capillary with the lithium borate buffer system and an applied voltage of 15 kV, as for the fused silica capillary, average migration times of 7.81 minutes (RSD 1.62%) and 29.3 mins (RSD 0.12%) for twelve injections of thiourea and benzoic acid respectively were obtained, increasing the time window for separation to 21.5 minutes.

However, for the separations of compounds, any improvement in the time window for separation was largely negated by the fact that increased band broadening of peaks occurred due to increased residence time of compounds in the capillaries. When applied to the dimethylbenzoic acids, an additional peak was observed for the dimethylbenzoic acids (Figure 5.4). Only small differences were observed in the electrophoretic mobility of compounds measured in the fused silica and the C1 capillary was observed (Appendix I). The only exceptions were the longer chain alkylbenzoic acids which are treated in the next section.

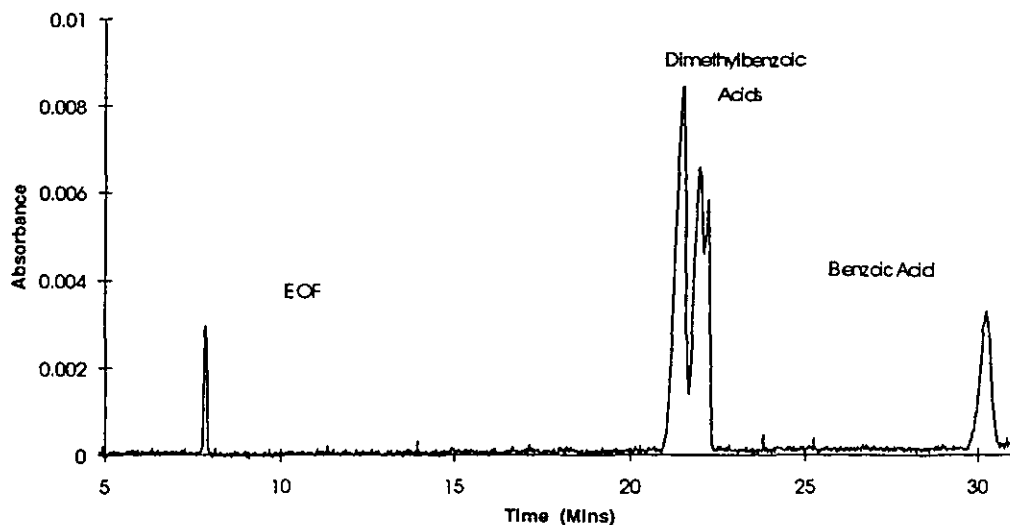


**Figure 5.4** Separation of the dimethylbenzoic acids; 15 kV applied voltage, 50 mM Lithium Borate, pH 8.5, C1 Capped Capillary. Labels

By increasing the applied voltage to 30 kV, migration times of 3.7 mins and 12.2 mins were obtained for thiourea and benzoic acid, respectively, giving a time window for separation of 8.5 minutes. This represented an acceptable analysis time and a reasonable window for separation. However, resolution was largely unchanged from the applied voltage of 15 kV for the C1 capped capillary, and for short chain alkylbenzoic acids, the electrophoretic mobilities obtained were the same as for the fused silica capillary.

### 5.3 Retention of Alkylbenzoic acids in Alkyl Bonded Capillaries.

The use of alkyl bonded capillaries was also applied to longer alkyl chained alkylbenzoic acids and this led to some interesting effects related to interactions between the capillary wall and the alkyl side chains on the benzoic acids. The compounds were studied in three different capillaries, a C1 capped capillary, a C18 capped capillary and also a fused silica capillary in order to make comparisons between the different capillaries.

### 5.3.1 Fused Silica Capillary Separations.

Separation of the 4-n-alkylbenzoic acids using a fused silica capillary gave a migration order of 4-decylbenzoic acid to 4-methylbenzoic acid as the compounds are attracted to the anode and so migrate against the electroosmotic flow (Table 5.1), as described in the previous sections.

**Table 5.1** *Electrophoretic mobilities of the 4-n-alkylbenzoic acids. 50 mM lithium borate buffer, pH 8.5, 15 kV applied voltage for fused silica capillary, 30 kV applied voltage for C1 and C18 capped capillaries.*

Compound	Fused Silica Capillary ( $\text{cm}^2\text{V}^{-1}\text{s}^{-1}$ )	C1 Capillary ( $\text{cm}^2\text{V}^{-1}\text{s}^{-1}$ )	C18 Capillary ( $\text{cm}^2\text{V}^{-1}\text{s}^{-1}$ )
4-methylbenzoic acid	-2.738 e-4	-2.732 e-4	-2.732 e-4
4-ethylbenzoic acid	-2.573 e-4	-2.575 e-4	-2.574 e-4
4-propylbenzoic acid	-2.424 e-4	-2.420 e-4	-2.417 e-4
4-butylbenzoic acid	-2.298 e-4	-2.302 e-4	-2.300 e-4
4-pentylbenzoic acid	-2.193 e-4	-2.203 e-4	-2.198 e-4
4-hexylbenzoic acid	-2.067 e-4	-2.124 e-4	-2.112 e-4
4-heptylbenzoic acid	-1.979 e-4	-2.106 e-4	-2.072 e-4
4-octylbenzoic acid	-1.948 e-4	-2.201 e-4	-2.070 e-4
4-nonylbenzoic acid	-1.892 e-4	-2.636 e-4	-2.301 e-4
4-decylbenzoic acid	-1.880 e-4	-2.631 e-4	

### 5.3.2 C1 Capillary Separations.

For the C1 capillary, the mobility initially decreased with carbon number as expected and then unexpectedly for chain lengths greater than octyl the mobilities of compounds started to increase. (Figure 5.5). This anomalous behaviour was attributed to an interaction between the capillary wall for alkylbenzoic acids with chain lengths of six carbons and above. The interaction of the longer chain acids with the bonded-phase on the wall of the column increases the migration time of compounds in the capillary. This gives the analytes an apparent increase in electrophoretic mobility as they appear to have moved more rapidly against the EOF carrying them to the detector. In addition a noticeable decrease in the efficiency of these higher chain length alkylbenzoic acids was observed, supporting a wall interaction mechanism (Figure 5.6). This behaviour is as would be expected in open tubular liquid chromatography [109] with poor efficiencies due to mass transfer effects.

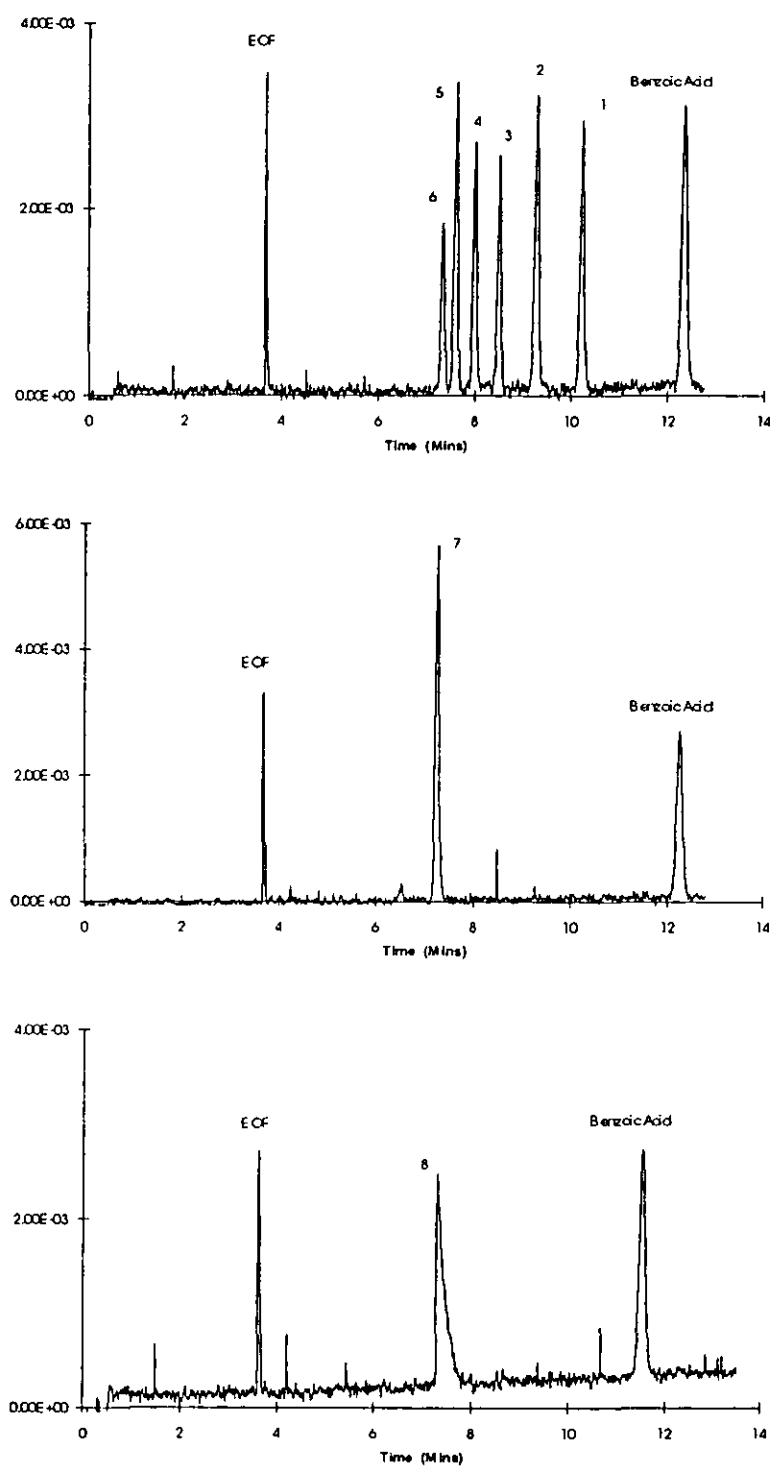


**Figure 5.5** Electropherograms showing the apparent increase in mobility of higher chain length alkylbenzoic acids. *CI* capped capillary, 50 mM lithium borate buffer, 30 kV applied voltage. Labels 1-8 represent the number of carbon atoms in the side chain (methyl - octyl).

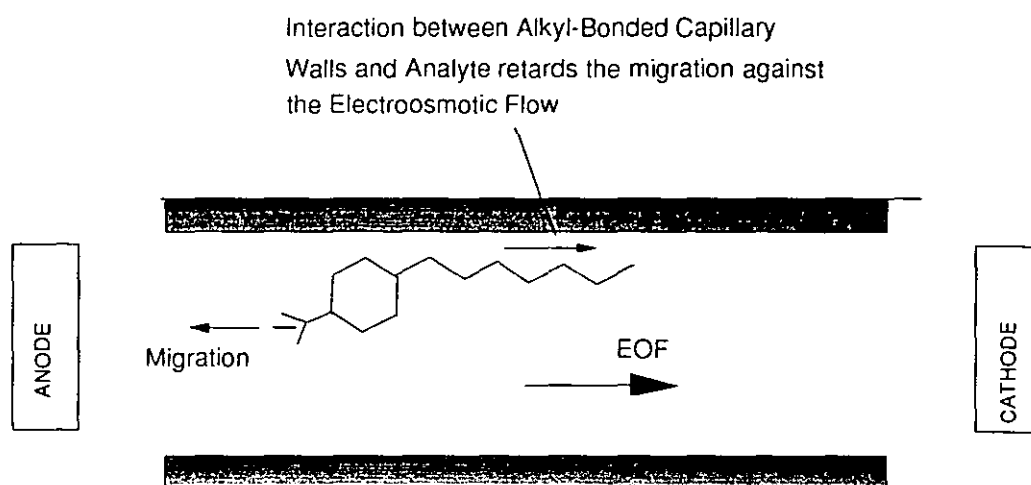


**Figure 5.6** *The forces acting on the longer chain benzoic acids in capped capillaries.*

### 5.3.3 C18 Capillary.

The C18 alkyl bonded capillary gave similar results to the C1 capillary with an effective increase in the mobilities of 4-hexylbenzoic acid and above again being observed. 4-decylbenzoic acid could not be detected possibly because it was so strongly retained that it never actually reached the detector. The electrophoretic mobility as a function of chain length is shown in Figure 5.7.

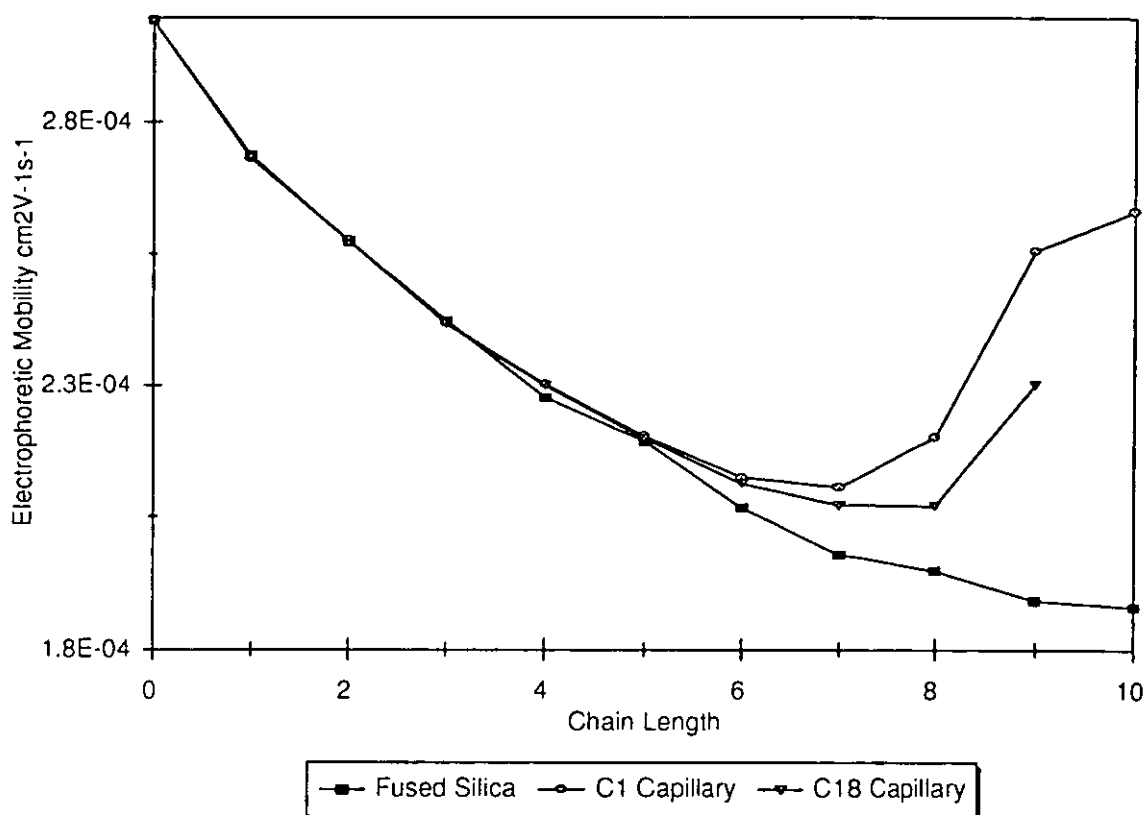


**Figure 5.7** *Mobility of  $n$ -alkylbenzoic acids as a function of alkyl chain length. 50 mM lithium borate buffer, pH 8.5.*

Reasons for the interaction between analytes and the C1 capillary wall being stronger than the corresponding interaction for the C18 capillary were unclear and difficult to determine experimentally. It is possible that in the C1 capillary analytes interact on the surface of the capillary by bending the negatively charged moiety away from the capillary surface, whereas for the C18 capillary that analytes actually fit into hydrophobic pockets created by the C18 chains. This could explain the possible reason why the retention between nonylbenzoic acid and decylbenzoic acid is similar in the C1 capillary whereas in the C18 capillary decylbenzoic acid could not be detected.

### 5.3.4 Effect of Organic Modifier.

To confirm that the increase in electrophoretic mobilities of higher chain alkylbenzoic acids was caused by a wall interaction, the effects of adding organic modifier to the buffer were investigated. By adding organic modifier to the running buffer, the affinity between the stationary phase and the alkylbenzoic acids should be decreased, and therefore less retention between higher chain homologues and the capillary walls should occur. Acetonitrile was added at 5%, 7.5% and 10% v/v concentrations. As the acetonitrile concentration increased the measured mobility values of 4-hexylbenzoic acid to 4-decylbenzoic acid decreased relative to their values in unmodified buffer indicating that their interaction with the capillary wall had been reduced (Figure 5.8).

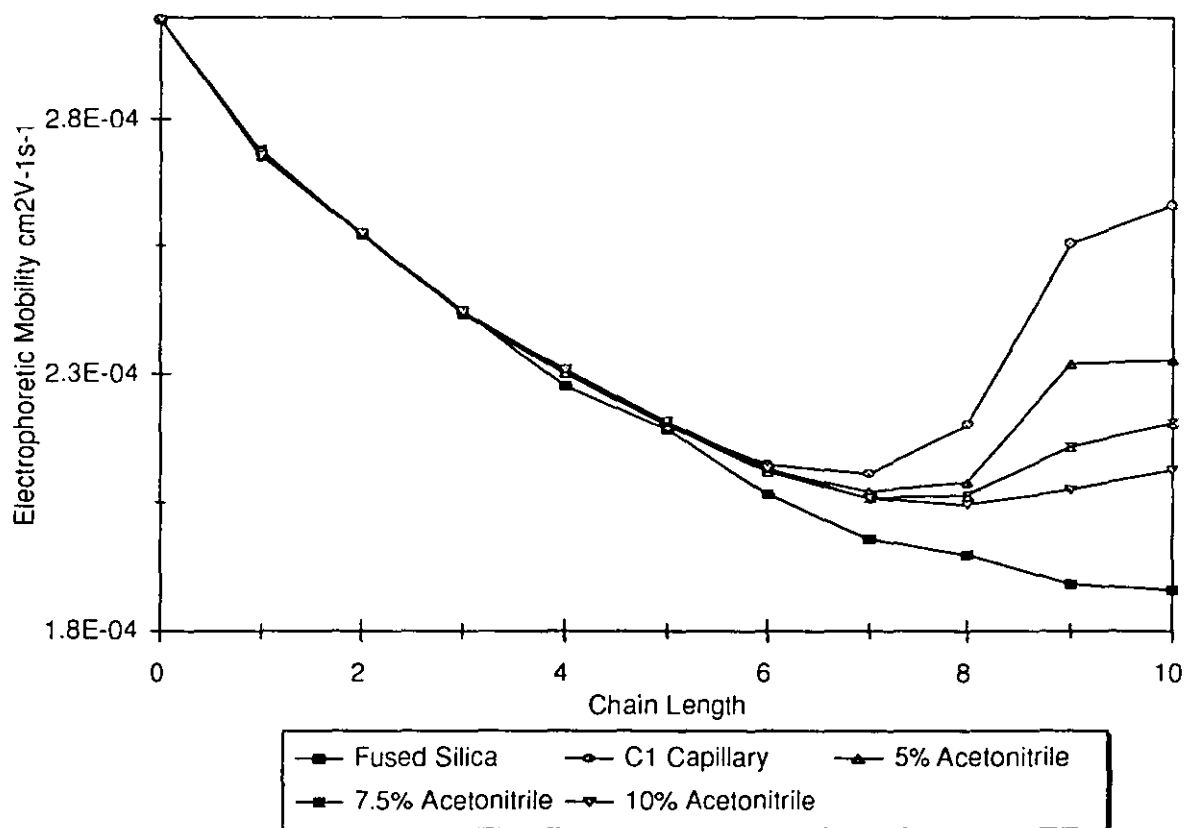


**Figure 5.8** The effect of the addition of acetonitrile to the running buffer in the C1 alkyl bonded capillary on alkylbenzoic acids.



### 5.3.5 Pressure Driven Separations.

By applying a pressure to the end of the capillary with no voltage applied, a hydrodynamic flow of liquid can be established within the capillary. Compounds can be swept in this way from the injection end of the capillary past the detector, effectively giving a open tubular capillary HPLC system. This configuration was used as a further confirmation that the interactions occurring in the capillary were due to an interaction between analyte and capillary wall. For any separation of analytes to occur there must be an interaction between the stationary phase in the capillary (the coated capillary wall) and the analytes. The C1 and C18 capillaries were investigated.

For the C1 capillary, injection of benzoic acid followed by the application of the low pressure rinse function (with no voltage) resulted in detection of benzoic acid in approximately 7 minutes. Systematic injection of the alkylbenzoic acids resulted in peaks at the same retention time for 4-methylbenzoic acid to 4-heptylbenzoic acid. However 4-octylbenzoic acid was retained and gave a peak at approximately 8 minutes. The peaks were much broader than electrophoretic separations with poor peak shape characteristic of band broadening in a wide bore column due to poor mass transport [111] (Figure 5.9).

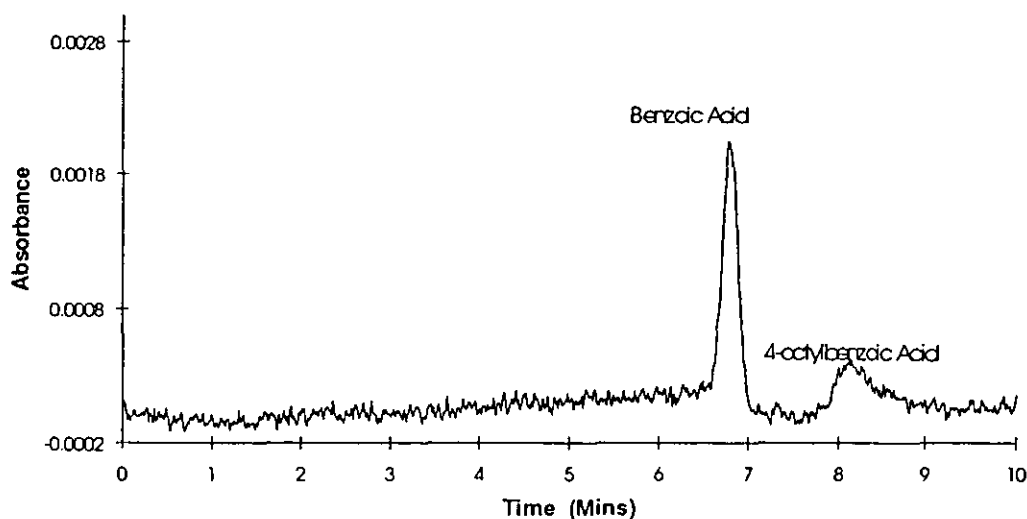


**Figure 5.9** Separation of benzoic acid and 4-octylbenzoic acid by pressure application.

4-Nonylbenzoic acid could also be detected as a broad peak at a retention time of approximately 10 minutes, but 4-decylbenzoic acid was not detected, probably because the peak was too broad to distinguish from baseline noise. The C18 capillary gave similar results with 4-octylbenzoic acid and 4-nonylbenzoic acid being detected. The capacity factors were then calculated for the pressure driven separations (Table 5.2).

The capacity factors for the interactions observed under electrophoresis could also be calculated. For electrophoretic separations, the equation for capacity factor must be modified as the measured migration time will contain components for EOF, migration and retention. Therefore to calculate capacity factors due to chromatographic retention, it is necessary to consider the difference between the unretained electrophoretic mobility of an analyte (i.e. the analyte mobility in the fused silica capillary) and the retained electrophoretic mobility. Hence the equation for capacity factor is modified to (4.1),

$$k = \frac{\mu_r - \mu_u}{\mu_u} \quad (4.1)$$

where  $\mu_r$  is the retained mobility and  $\mu_u$  is the unretained mobility of the analyte. Good agreement between the hydrostatic and electrophoretic retention factors were obtained (Table 5.2) indicating that the retentions of benzoic acids under the application of an electric field can be correlated with the retention obtained by open tubular liquid chromatography.

**Table 5.2** *Chromatographic retention factors for the retention component of the wall interactions for 4-nonylbenzoic acid and 4-decylbenzoic acid using pressure and CE flows.*

Sample	Pressure $k$	Electrophoretic $k$
<i>C1 Capillary</i>		
4-octylbenzoic acid	0.18	0.13
4-nonylbenzoic acid	0.37	0.35
<i>C18 Capillary</i>		
4-octylbenzoic acid	6.9 e-2	6.3 e-2
4-nonylbenzoic acid	0.30	0.22

### 5.3.6 Separation of Neutral Compounds.

The partitioning effect observed between buffer and capillary wall gave rise to the possibility of separating neutral compounds by open tubular capillary electrochromatography. Using the same lithium phosphate buffer as for the benzoic acids hexanophenone ( $k = 1.25$ ) (Figure 5.10) and heptanophenone ( $k = 1.58$ ) were separated from the electroosmotic flow but as with the acids the peak shapes were poor. The plug flow obtained for the electroosmotic flow gives narrow bands of compounds, however band broadening is observed due to poor mass transport.

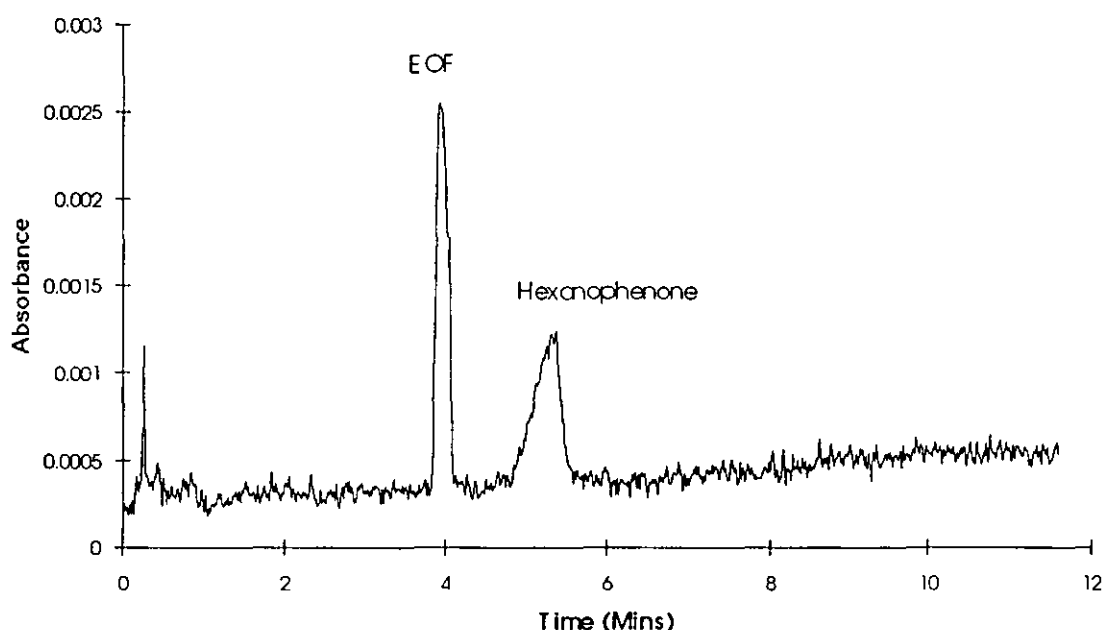


**Figure 5.10** Separation of Hexanophenone from the Electroosmotic Flow; 30 kV applied voltage, C18 capillary. 50 mM lithium phosphate buffer, pH 8.5

Longer alkyl chain analytes such as octanophenone were investigated but since they were more highly retained, very broad peaks were again observed.

## 5.4 Separations of Alkylanilines

The anilines investigated have similar ionisation constants to the alkyipyridines studied in chapter 4 (Appendix II), thus they were good test compounds for comparison as they could be studied under exactly the same conditions as used for the alkyipyridines. Structurally they have similar overall sizes and charge distributions to the alkylbenzoic acids as the ionisable atom is located on a group external to the aromatic ring (Figure 5.11).

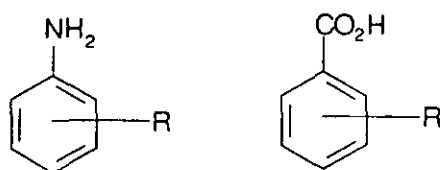


*Figure 5.11 Structural similarities of Alkylbenzoic acids and Alkylanilines.*

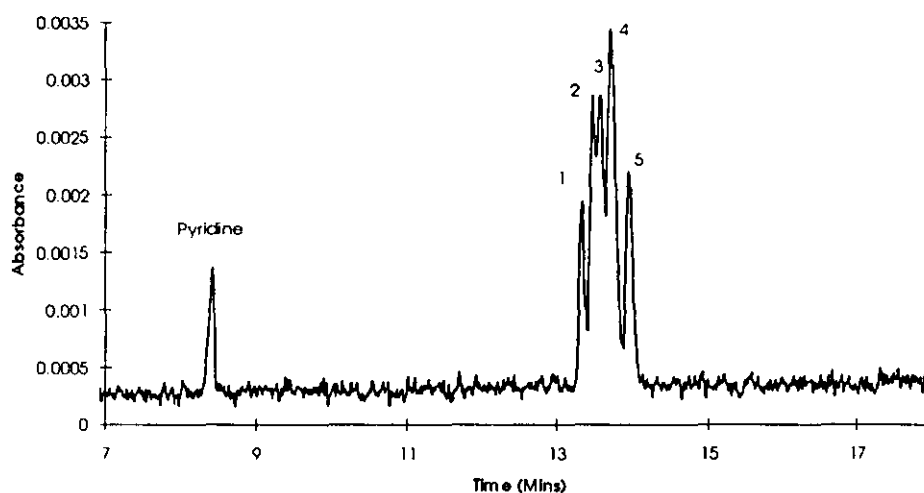


*Figure 5.12 Separation of the Dimethylanilines; 40 mM Lithium Phosphate buffer, pH 2.5, 15 kV applied voltage. 1 - 3,4-Dimethylaniline, 2 - 2,3-dimethylaniline, 3 - 2,5-dimethylaniline, 4 - 3,5-dimethylaniline and 2,4-Dimethylaniline, 6 - 2,6-dimethylaniline.*

Only a limited number of the n-alkylanilines were available for investigation, but the main compounds of interest were the dimethylanilines

as the three sets of dimethylsubstituted compounds from the anilines, pyridines and acids could be compared. Separation of the dimethylanilines gave a separation similar to the separation of the dimethylpyridines (Figure 5.12).

Aniline and some N-alkylanilines were also included in the sample set to give a wider spread of molecular weights. Electrophoretic mobilities (Table 5.3) were determined by the methods described for the alkylpyridines, determining electroosmotic flow using the fast marker technique and correcting mobilities using pyridine as an internal marker.

*Table 5.3 Mobility data for the alkyilanilines.*

Compound	Electrophoretic Mobility $\text{cm}^2\text{V}^{-1}\text{s}^{-1}$
3,4-Dimethylaniline	2.708 e-4
2,3-Dimethylaniline	2.677 e-4
2,5-Dimethylaniline	2.651 e-4
3,5-Dimethylaniline	2.620 e-4
2,4-Dimethylaniline	2.620 e-4
2,6-Dimethylaniline	2.580 e-4
Aniline	3.255 e-4
N-methylaniline	3.098 e-4
N-propylaniline	3.796 e-4
1-amino-5,6,7,8-tetrahydronaphthalene	3.587 e-4

## 5.5 Multi-functional Compounds.

Nicotinic acid, *iso*-nicotonic acid and picolinic acid are all pyridine compounds with carboxylic acid side groups. These compounds were of particular interest as they can carry a charge at both low and high pH. At low pH, the nitrogen in the ring is charged and so the uncharged carboxylic group should act in a similar way to other side chains possibly giving selectivity in separations between the isomers. At high pH, the side chain becomes charged and differences in structure between isomers was expected to be much smaller.

### 5.5.1 Separation at pH 2.5.

The addition of a carboxylic group to a pyridine ring causes the second pKa of the compound to be lowered considerably to 2.03 for nictotinic acid, 1.74 for *isonicotinic* acid and 1.06 for picolinic acid. Therefore the analysis at pH 2.5 separated the nicotinic acids with only partial positive charges, giving lower electrophoretic mobilities than would be expected for compounds of similar size (Table 5.4). Using the Hendersson - Hasselbach equation [105] and the ionisation constants of the compounds, the mobility of the fully protonated compounds can be predicted (Table 5.4). The ionisation constants of 6-methylnicotinic acid and 2-methylnicotinic acid were not available in the literature so the fully charged mobilities could not be estimated.

**Table 5.4** Electrophoretic mobilities of the Nicotinic Acids at pH 2.5. 40 mM lithium phosphate buffer, pH 2.5, 15 kV applied voltage.

Compound	Mobility at pH 2.5 $\text{cm}^2\text{V}^{-1}\text{s}^{-1}$	Ionisation Constants	Fully charged Mobility $\text{cm}^2\text{V}^{-1}\text{s}^{-1}$
Nicotinic Acid	0.9091 e-4	4.83, 2.03	3.592 e-4
IsoNicotinic Acid	0.6272 e-4	4.96, 1.74	4.235 e-4
6-Methylnicotinic Acid	1.1036 e-4		
2-Methylnicotinic Acid	0.8152 e-4		

From the predicted fully ionised ion mobilities, the nicotinic acid shows a lower mobility than isonicotinic acid. This shows a reversal in mobility order than for the monosubstituted alkyipyridines studied earlier where a general trend of 2-substituted groups having lower mobilities than 3-substituted groups was observed.

### 5.5.2 Separation at pH 8.5.

All the acid groups are fully ionised at pH 8.5 thus no corrections to the mobility for partial charges were necessary. Nicotinic acid and isonicotinic acid peaks had the same migration time as the internal standard benzoic acid and it was concluded that they all had the same electrophoretic mobilities (Table 5.5).



**Table 5.5** *Electrophoretic mobilities of the Nicotinic Acids at pH 8.5. 50 mM lithium borate buffer, pH 8.5, fused silica capillary, 15 kV applied voltage.*

Compound	Mobility $\text{cm}^2\text{V}^{-1}\text{s}^{-1}$
Nicotinic acid	-2.996 e-4
<i>Iso</i> Nicotinic acid	-2.996 e-4
6-Methylnicotinic acid	-2.713 e-4
2-Methylnicotinic acid	-2.682 e-4

From the results, no resolution between nicotinic acid and isonicotinic acid is lost when analysing the compounds at high pH. The structural differences between the isomers in anionic form are small, with the situation of the nitrogen lone pair the only difference. Picolinic acid was analysed at both low and high pH however no peak in the electropherograms was apparent. At low pH this may be attributable to the compound having effectively no charge ( $\text{pK} = 1.06$ ) and thus very long migration times, but it is unclear why the compounds were not detected at pH 8.5. Detection was attempted at 254 nm and 214 nm.

## 5.6 Summary.

Separations of alkylbenzoic acids at high pH were largely the same in different buffer systems with small differences between the electrophoretic mobilities of species. When alkyl bonded capillaries were used in an attempt to increase resolution between isomers by increasing the time window for separations to be performed, an increased band broadening was experienced. Higher molecular weight alkylbenzoic acids showed chromatographic retention in the alkyl bonded capillaries and these modifications to separations have been investigated in detail. Such separations are of interest due to the developing interest in capillary electrochromatography in the separation science community. The alkylanilines and nicotinic acids were studied as they have physical and chemical properties somewhere between the alkylbenzoic acids and the alkylpyridines.

## Chapter 6.

### Modelling of Alkylpyridine Separations.

#### 6.1 Introduction.

In this chapter the nature of the separations of alkylpyridines is investigated further. The separations of the alkylpyridines are based on physico-chemical parameters and the literature models for size-mobility effects are examined. A model is introduced to account for the separation of structural isomers. The model is tested on a range of different sized alkylpyridines and also on the doubly charged aminoalkylpyridines.

#### 6.2 Existing Models.

The basic relationships relating the size of analytes to their electrophoretic properties were reviewed in Chapter One. These relationships have been tested on the analytes investigated in this study and their results are presented here.

##### 6.2.1 Offord's Relationship.

Offord's relationship (Section 1.4.2) [80] is modelled on the effective surface area of analytes and relates mobility to the inverse of molecular weight to the power of two thirds (equation 6.1),

$$\mu_e = \frac{k'Z}{M^{2/3}} \quad (6.1)$$

Offord's relationship was calculated and plotted against the measured electrophoretic mobilities for pyridine, methylpyridines, ethylpyridines,

dimethylpyridines, propylpyridines, methyl-ethylpyridines, 3-butylpyridine, 2-pentylpyridine and 2-hexylpyridine (Figure 6.1, mobility data from Appendix I). A good fit is obtained for Offord's relationship with a correlation coefficient of 0.964, slope 85.58 and intercept -0.47.

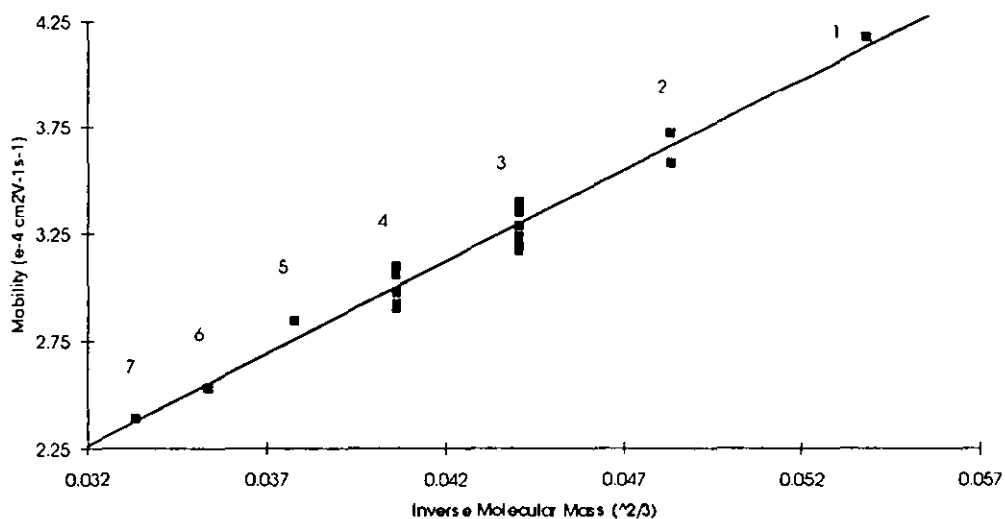


**Figure 6.1** *Offord's Relationship relating mobility to molecular weight. Points represent (1) pyridine, (2) methylpyridines, (3) ethylpyridines and dimethylpyridines, (4) propylpyridines and methyl-ethylpyridines, (5) 3-butylpyridine, (6) 2-pentylpyridine and (7) 2-hexylpyridine*

The vertical lines of points show that discrimination between positional isomers is not accounted for, since the analytes have been treated as spherical molecules. Extensions to Offord's relationship allow different shapes to be accounted for by varying the molecular mass index [80]. The main disadvantage of this approach is that only ideal shapes can be modelled, thus in order to model non-ideal shapes strict boundaries relating to the shapes of analyte would have to be applied. It was considered that the shapes of the alkylpyridines did not conform to these regular shapes and so could not be easily modelled by such an approach.

### 6.2.2 The Van der Waals Model.

The van der Waals model relates the electrophoretic mobility of analytes to the inverse of their hydrodynamic radii by the following basic equation based on the Stokes' relationship for the frictional force on a moving spherical analyte in a viscous medium (equation 6.2) (Section 1.2.1) [23],

$$\mu_E = \frac{q}{6\pi\eta r} \quad (6.2)$$

Using the measured electrophoretic mobilities of pyridine, methylpyridines, ethylpyridines, dimethylpyridines, propylpyridines, methyl-ethylpyridines, 3-butylpyridine, 2-pentylpyridine and 2-hexylpyridine a linear correlation coefficient of 0.968 (slope  $3.53 \times 10^{-3}$ , intercept  $-5.36 \times 10^{-4}$ ) was obtained for the relationship between van der Waals radii and mobility (Appendix I), which is comparable with literature data for mono-substituted alkylpyridines (Figure 6.2) [76].

The good fit obtained between van der Waals radii and electrophoretic mobility indicates that the van der Waals model works well. However, no discrimination between positional isomers is obtained which can be seen from the vertical lines of points, so the model does not explain or predict differences in migration of positional isomers.

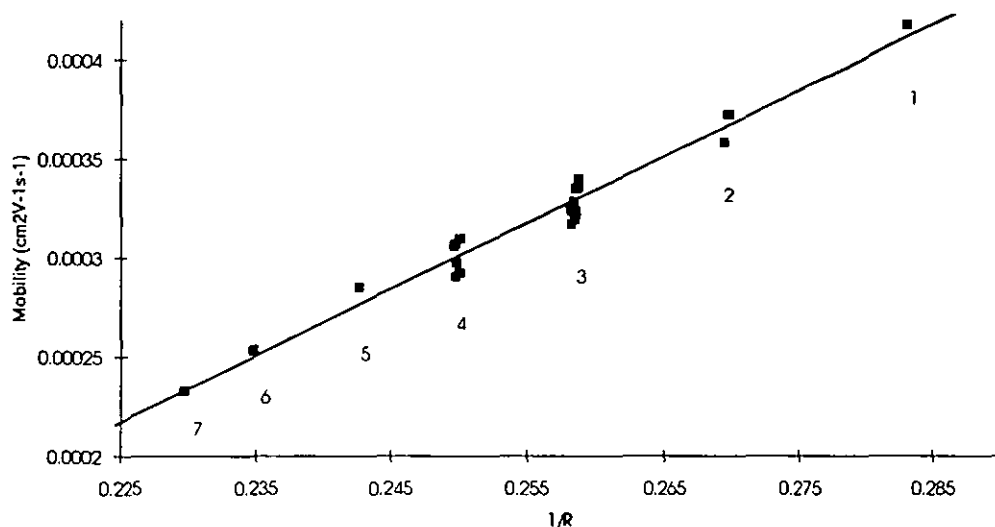


**Figure 6.2** *Mobility of alkylpyridines against the inverse of the van der Waals radii. Electrophoretic mobilities obtained experimentally by CE and van der Waals radii by molecular modelling. Points represent (1) pyridine, (2) methylpyridines, (3) ethylpyridines and dimethylpyridines, (4) propylpyridines and methyl-ethylpyridines, (5) 3-butylpyridine, (6) 2-pentylpyridine and (7) 2-hexylpyridine*

It should be noted that the basic equation for electrophoresis (6.2) relates the electrophoretic mobility to the inverse of the hydrodynamic radius of a particle rather than the van der Waals radius. The hydrodynamic radius is the effective radius that the analyte occupies under the conditions of analysis thus it includes contributions from the rotations of analytes and their interactions with counter-ions and other substances. Thus although the van der Waals relationship does not account for geometric isomers this is due to the van der Waals volumes being used in the calculations. The van der Waals volumes of analytes are the cubed root of the volume that the static ions fills and so they do not take account of interactions with other molecules and molecular translation and rotation.

Since the model using the van der Waals radii of analytes fits well to a first approximation and such radii are simple to calculate, it was proposed to

use this model as a starting point and to add in other effects as and when they were found to be significant. Thus the equation for electrophoretic mobility can be modified to (equation 6.3),

$$\mu_e = \frac{q}{6\pi \eta} \left( \frac{1}{R_{vdw}} + f(a) + f(b) + f(c) + \dots \right) \quad (6.3)$$

where  $\mu_e$  is the electrophoretic mobility,  $R_{vdw}$  is the van der Waals radii,  $q$  is the charge on the analyte,  $\eta$  is the BGE viscosity and  $f(x)$  are functions relating to additional molecular properties.

### 6.3 Molecular Properties of Analytes and their Relationship with Electrophoretic Mobility.

The nature of the relaxation and electrophoresis effects [77] (as reviewed in Chapter 1) are the fundamental properties which produce the retardation of ions in capillary electrophoresis. The relaxation effect relates to the asymmetric separation of charge between the analyte and surrounding counterions, causing a coulombic retardation force. The electrophoresis effect relates to the bulk flow of background electrolyte and water over the surface of the analyte, causing a frictional retardation of the analyte. Thus, in order to model the behaviour of separations it is these effects that must be accounted for.

#### 6.3.1 The Relaxation Effect and Charge Distribution.

The relaxation effect is dependant on the coulombic force between the analyte and the asymmetric distribution of counterions, thus it is dependent on the charge of the analyte. For a non-spherical ion it is also likely that the

position and distribution of charge throughout the ion will play a role in the strength of this effect. For the alkylpyridines, delocalisation of the positive charge across the aromatic ring occurs. The Hückel model [110] was therefore used to investigate the charge distributions for the alkyl substituted pyridines by modelling the distribution of the single positive charge in the analytes.

The charge distribution for pyridine shows that approximately 40% of the positive charge is located on the nitrogen atom, and the remaining charge is distributed on the 2-, 4- and 6- atoms, each bearing 20% of the charge (Figure 6.3).

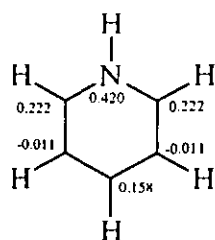


*Figure 6.3 Hückel charge distribution showing the partial positive charges for pyridine.*

Adding methyl groups to the 2-, 3- and 4- positions gave rise to only very small changes to the charge distributions (Figure 6.4), and it was concluded that these small changes in the charge distributions could not account for the separation of geometric isomers. Furthermore, differences in the partial charges did not match differences in electrophoretic mobility of analytes.



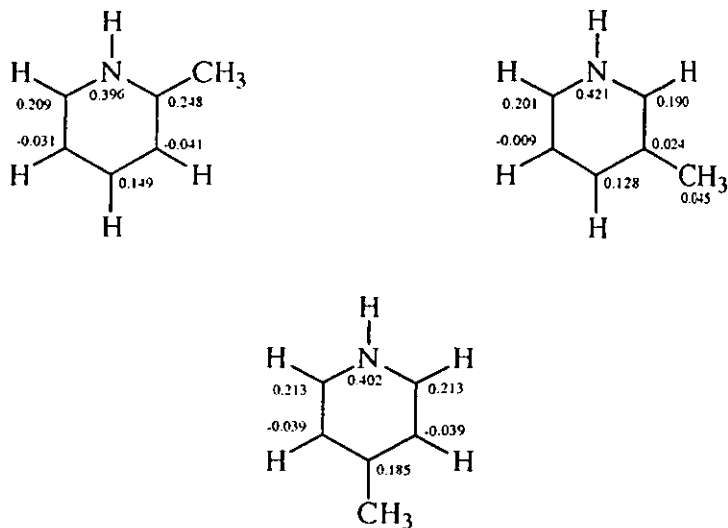


**Figure 6.4** Hückel charge distribution showing the partial positive charges for the methylpyridines.

Identical charge distribution patterns were obtained for longer side chain alkylpyridines. Since the charge is distributed about the pyridine ring with little difference between positional isomers, it was considered that the coulombic retardation caused by the relaxation effect would probably be non-specific between different positional isomers. Shielding of the positive charge in the aromatic ring by the delocalised electron clouds could also lead to reduced retardation of the ions.

### 6.3.2 The Electrophoresis Effect and Restricted Rotation.

The electrophoresis effect relates to bulk flow of background electrolyte over the surface of the analyte, and so one would expect analytes of identical volume (and charge) to migrate with the same electrophoretic mobilities. The relationship between the mobility of peptides and molecular weight [80] investigated by Offord modelled this effect.

Non-spherical shapes of molecules were treated by applying different indices to account for different shapes [81]. Much of the work implicitly

assumes an orientation of the ions to describe the different shapes. For example, Waldron and Waldron-Edward described different frictional ratios for the migration of prolate and oblate ellipsoids [82]. By rotating either ellipsoid through  $90^\circ$  the ellipsoids can be interchanged. Thus, a model was developed to take account of molecular orientation and its effect on the electrophoretic mobility (Section 6.4).

### 6.3.3 Analyte Interactions.

Other analyte interactions must also be considered when describing the migration behaviour of the alkylpyridines. For instance, it may be possible that alkylpyridines form micelles and thus reasons for differences in migration behaviour can be explained in this way. However, no evidence was obtained to suggest that these kinds of interactions occur and for the size of alkyl chains studied micelle formations is not usually observed [111]. One would expect the more polar ions to form micelles, which would indicate strong micelle formation for long chained 4-alkylpyridines, and weaker formations for short chained alkylpyridines. No obvious patterns of this sort were observed. Also, when the ethylpyridines were studied at different concentrations, no concentration dependent selectivity changes were observed.

## 6.4 A Model for Restricted Rotation of Analytes.

It was proposed that the differences in electrophoretic mobility of analytes may be a consequence of the molecular orientation of the analytes under electrophoresis. In free solution, molecules are free to move in both translational and rotational directions and so each molecule has translational and rotational diffusion coefficients. Under electrophoresis the electrical force is experienced by the charged moiety of the analyte causing migration. The whole molecular ion experiences a balancing frictional force related to the

flow of counter ions over the surface of the whole ion and this frictional force always occurs in the opposite direction to the direction of the electric field [22]. Thus the molecular ion will align with the charged moiety pointing in the direction of the electric field. The rest of the molecular ion is dragged under the frictional force related to movement through the buffer (Figure 6.5). Under such conditions, two out of the three axes available for free rotation will become hindered.

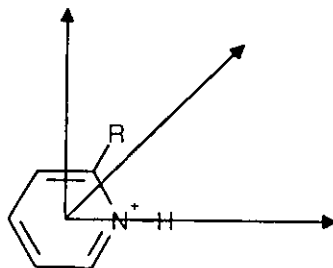


*Figure 6.5 Restricted rotation of the alkylpyridines.*

Thus only one axis is left available for free rotation. The other two rotations will be hindered to some extent, although perhaps only to a very small extent. Thus the average volume occupied by an ion under electrophoresis may be smaller than under conventional diffusion.

The axis running through the centre of charge and the centre of mass, gives the direction of travel of an analyte. The volume swept out by the remaining unhindered rotation about this axis was calculated and converted to a radius  $R_{rot}$ . Furthermore, the distance between the centre of charge and the centre of mass, defined as the inertial radius ( $R_i$ ), gives a measure of the force required to rotate an ion against the applied electric field.

The restricted radii of rotation and inertial rotation were calculated for the methylpyridines, ethylpyridines and the dimethylpyridines (Table 6.1) using the calculation procedures outlined in Section 2.2. Graphical representations of the compounds and their respective centres of charge and

mass (Figure 6.6), clearly show the different location of centre of charge and centre of mass for positional isomers. Thus, different values are obtained for the rotated and inertial radii.

**Table 6.1** Radii calculations for the methylpyridines, ethylpyridines and dimethylpyridines.

Compound	$R_{vdw}$ (Å)	$R_{rot}$ (Å)	$R_i$ (Å)	Electrophoretic Mobility $\text{cm}^2\text{V}^{-1}\text{s}^{-1}$
2-methylpyridine	3.712	5.19	0.58	3.581 e-4
3-methylpyridine	3.708	4.80	0.85	3.721 e-4
4-methylpyridine	3.709	4.70	1.15	3.722 e-4
2-ethylpyridine	3.868	5.30	0.97	3.222 e-4
3-ethylpyridine	3.864	5.01	0.97	3.366 e-4
4-ethylpyridine	3.864	4.94	1.54	3.397 e-4
2,6-dimethylpyridine	3.873	5.08	0.53	3.168 e-4
2,5-dimethylpyridine	3.873	5.18	0.69	3.236 e-4
2,3-dimethylpyridine	3.867	5.23	0.87	3.236 e-4
2,4-dimethylpyridine	3.869	5.20	0.70	3.196 e-4
3,5-dimethylpyridine	3.869	5.08	0.88	3.285 e-4
3,4-dimethylpyridine	3.867	5.04	0.89	3.349 e-4

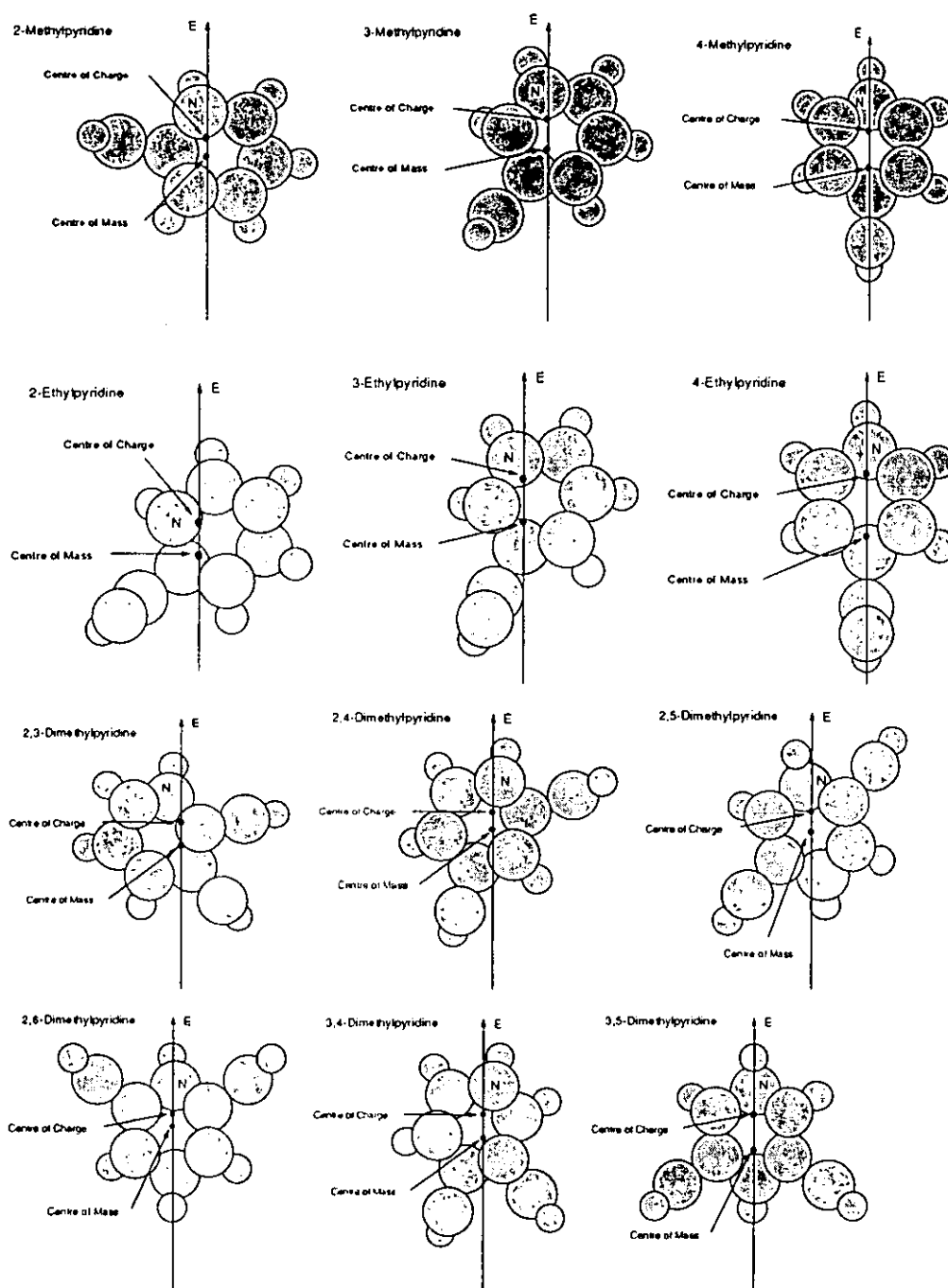


**Figure 6.6** Graphical representations of the modelling of the methylpyridines, ethylpyridines and dimethylpyridines.  $R_1$  is the distance between centre of charge and centre of mass and  $R_{rot}$  is the radius obtained by rotating the molecules about the charge mass axis.

The general trend of the mobility being inversely proportional to the radii of analytes is supported through observations of the rotated radii versus mobility. For the methylpyridines and the ethylpyridines, the CE data gave a mobility order of 4-, 3- and 2-alkylpyridines. For the methylpyridines, 2-methylpyridine has the largest rotated radius of 5.19Å, which would give it the lowest mobility. 4-methylpyridine and 3-methylpyridine have smaller but similar rotated radii and co-migration of these species was observed. The ethylpyridines follow a similar pattern. The situation for the dimethylpyridines is more complex. They showed only small differences in their mobilities and it was thought that differences in mobility could also relate to the ease of rotation against the electric field. This group of molecules represented a challenging set of compounds to investigate by multi-linear regression.

## 6.5 Multi-Linear Regression Analysis.

The modelling data and mobility data for the methylpyridines, ethylpyridines and dimethylpyridines were investigated by multi-linear regression. A semi-empirical method based on equation 6.2 was used. In order to build up information on the quality of fit it is necessary to investigate each part of the equation separately and to obtain a correlation for each part. Thus each combination of the molecular radii (Table 6.1) and their relationship with the electrophoretic mobilities (Appendix I) were investigated.

### 6.5.1 van der Waals model.

Applying the van der Waals model for the twelve alkylpyridines to be used as the data set for investigation gave a linear regression equation (6.4).

$$\mu_e = (33.2 \times 10^{-4}) \frac{1}{R_{vdw}} - (4.06 \times 10^{-4}) \quad (6.4)$$

No discrimination between isomers was observed as expected and a linear correlation coefficient of 0.831 provides a measure to compare other models by. The correlation coefficient is lower for this restricted set of compounds than for the set investigated in Figure 6.2 because the sets of compounds of only two distinct molecular weight were deliberately chosen in order to try minimise the effects in the regression analysis of the size-mobility relationship which could potentially overwhelm the more subtle shape effects that were observed.

### 6.5.2 van der Waals model including $1/R_{rot}$ .

Multiple linear regression analysis of mobility against  $1/R_{vdw}$  and  $1/R_{rot}$  yielded a regression equation with correlation coefficient of 0.921, but the mobility order of the dimethylpyridines was not correctly predicted.

### 6.5.3 van der Waals model including $1/R_i$ .

Similar analysis of mobility against  $1/R_{vdw}$  and  $1/R_i$  yielded a regression equation with correlation coefficient 0.934. The mobility order of the dimethylpyridines was again not correctly described. These results indicated that all the molecular radii should be used simultaneously.

### 6.5.4 van der Waals model including $1/R_{rot}$ and $1/R_i$

Multi linear regression using the three different radii gave the following regression equation (6.5),

$$\mu_e = 3.213e^{-3} \frac{1}{R_{vdw}} + 0.571e^{-3} \frac{1}{R_{rot}} - 0.013e^{-3} \frac{1}{R_i} - 0.599e^{-3} \quad (6.5)$$

An adjusted correlation coefficient of 0.965 is a considerable improvement over the value of 0.831 obtained for the van der Waals model. Full statistical data (Table 6.2) shows that the  $R_{vdw}$  is by far the most significant term, relating to the size-mobility van der Waals relationship. The other two terms have smaller effects, yet it is these terms that provided selectivity between positional isomers. The plot of experimental mobility against predicted mobility for the van der Waals model shows vertical lines for positional isomers (Figure 6.7) but using the additional molecular dimensions the points were spread out (Figure 6.8) from these vertical bands seen previously. The points fall within 95% confidence limits.

**Table 6.2** *Statistical data for the multiple regression analysis of electrophoretic mobility against  $R_{vdw}$ ,  $R_{rot}$  and  $R_i$ . Electrophoretic mobility of compounds measured in 40 mM lithium phosphate buffer, pH 2.5, 15 kV applied voltage.*

Dependant Variable : Electrophoretic Mobility ( $\mu_e$ )				
Parameter	Estimate	Standard Error	T Statistic	P-Value
1/ $R_{vdw}$	3.213 e-3	2.971 e-4	10.814	0
1/ $R_{rot}$	5.705 e-4	2.302 e-4	2.478	0.04
1/ $R_i$	-1.270 e-5	3.893 e-6	-3.263	0.01
Constant	-5.990 e-4	5.783 e-5	-10.359	0



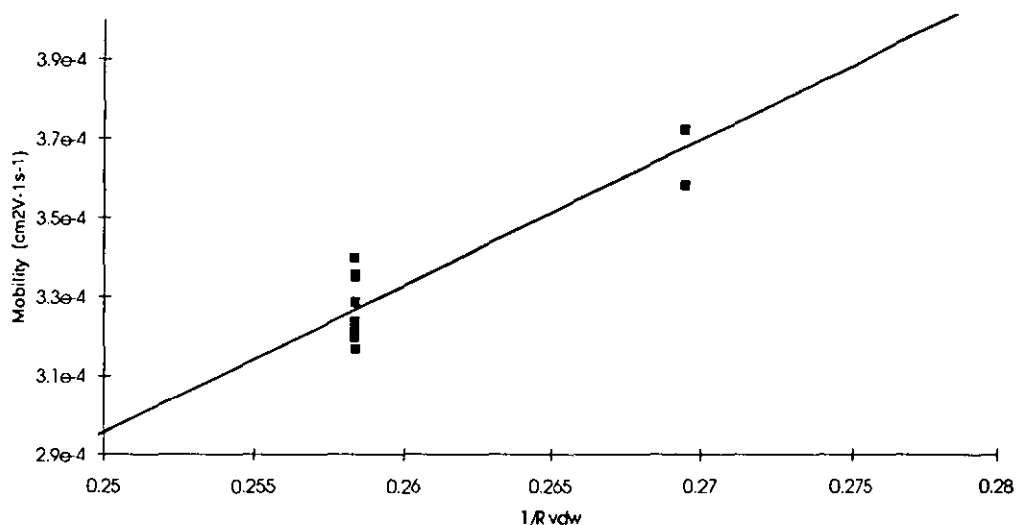


**Figure 6.7** Regression analysis for mobility versus  $1/R_{vdw}$ , in the analysis of the methylpyridines, ethylpyridines and dimethylpyridines (Regression equation 6.4).

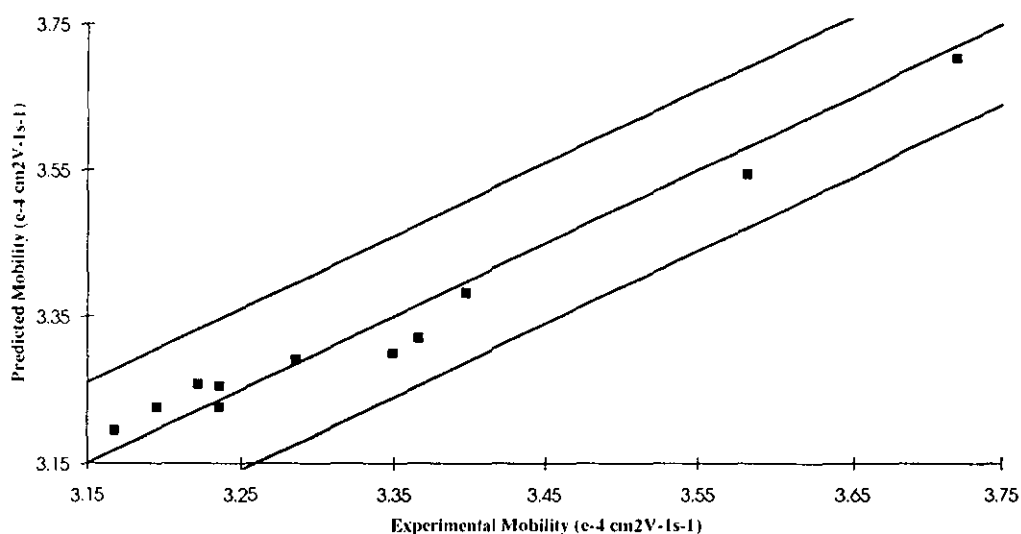


**Figure 6.8** Regression analysis for mobility versus  $1/R_{vdw}$ ,  $1/R_{rot}$  and  $1/R_i$  in the analysis of the methylpyridines, ethylpyridines and dimethylpyridines (Regression equation 6.5). Confidence intervals shown are 95%.

Using multi-linear regression with a model containing all three radii, the correct migration order of the dimethylpyridines was obtained (Table 6.2). This is an important improvement over the single and two term models which gave incorrect migration order predictions.

**Table 6.3** Comparisons between predicted mobilities calculated by molecular modelling and experimental mobilities measured by CE in 40 mM lithium phosphate buffer, pH 2.5, 15 kV applied voltage.

Analyte	Experimental Mobility $\text{cm}^2\text{V}^{-1}\text{s}^{-1}$	Predicted Mobility $\text{cm}^2\text{V}^{-1}\text{s}^{-1}$
3,4-dimethylpyridine	3.349 e-4	3.303 e-4
3,5-dimethylpyridine	3.285 e-4	3.295 e-4
2,3-dimethylpyridine	3.236 e-4	3.257 e-4
2,5-dimethylpyridine	3.236 e-4	3.233 e-4
2,4-dimethylpyridine	3.196 e-4	3.232 e-4
2,6-dimethylpyridine	3.168 e-4	3.195 e-4
2-methylpyridine	3.581 e-4	3.544 e-4
3-methylpyridine	3.721 e-4	3.704 e-4
4-methylpyridine	3.722 e-4	3.774 e-4
2-ethylpyridine	3.222 e-4	3.258 e-4
3-ethylpyridine	3.366 e-4	3.321 e-4
4-ethylpyridine	3.397 e-4	3.382 e-4

### 6.5.5 Effects of Ionic Strength.

In section 4.3, the effect of ionic strength on the separations of analytes were investigated. Although changes in mobility order of compounds were not observed, there were some changes in the relative separations at 20 mM buffer ionic strength. These were attributed to changes in the analyte-buffer interaction with a steric or relaxation effect being more significant at this ionic strength. In the development of the molecular modelling the electrophoretic mobility values at 40 mM ionic strength buffers were used in all calculations

and analyses. The multi-linear regression analysis using all three calculated radii for each analyte was also investigated across the ionic strength range using the electrophoretic mobility data (Appendix I). For the general equation (6.6) the values of the constants were calculated (Table 6.4).

$$\mu_e = A \frac{1}{R_{vdw}} + B \frac{1}{R_{rot}} + C \frac{1}{R_I} + D \quad (6.6)$$

**Table 6.4** Multi-linear regression constants across the buffer ionic strength range. Constants A, B, C and D relate to the general equation 6.6.

Ionic Strength	A	B	C	D
10 mM	32.3 e-4	4.92 e-4	-0.132 e-4	-5.64 e-4
20 mM	34.1 e-4	3.05 e-4	-0.139 e-4	-5.85 e-4
40 mM	32.1 e-4	5.71 e-4	-0.127 e-4	-5.99 e-4
60 mM	30.9 e-4	6.41 e-4	-0.117 e-4	-5.89 e-4
80 mM	29.8 e-4	6.74 e-4	-0.105 e-4	-5.72 e-4
100 mM	2.92 e-4	6.78 e-4	-0.100 e-4	-5.61 e-4

Some general changes are evident. The values of A, related to the van der Waals radii ( $R_{vdw}$ ) of compounds, decreases with increasing ionic strength, while the values of B, related to the restricted rotation ( $R_{rot}$ ), increase with increasing ionic strength. As the ionic strength of the supporting buffer increases, more counterions are available to interact with the analyte ions, and thus it may be expected that the effects of the size of ions (related to A) may become less significant. Properties that are related to asymmetric effects such as  $R_{rot}$  may become more significant with increasing buffer concentration, as was observed.

However, an anomaly is shown at the 20 mM ionic strength, with the value of A higher than the general trend suggests, and consequently the value of B is lower. This behaviour mirrors the effects observed in the relative separations of isomeric methylpyridines, ethylpyridines and propylpyridines observed in section 4.3 and is presumably related to steric effects.

## 6.6 Extensions to other Analytes.

The regression equation obtained for the twelve alkylpyridines investigated in the previous section was tested on the other alkylpyridine analytes available, whose electrophoretic mobility had been measured (Appendix I).

### 6.6.1 Other positional isomers and longer chain alkylpyridines.

The rotated radii and inertial radii for an extended number of analytes were calculated in the same way as for the methylpyridines and ethylpyridines (Table 6.5). By substituting these values into the regression equation (6.5) obtained for the methyl, ethyl and dimethylpyridines, electrophoretic mobilities for these compounds were predicted.

**Table 6.5** Radii calculations for other alkylpyridines.

Compound	$R_{vdw}$ (Å)	$R_{rot}$ (Å)	$R_I$ (Å)
2-Vinylpyridine	4.495	5.454	0.540
4-Vinylpyridine	4.495	4.858	1.130
N-propylpyridinium bromide	4.740	4.821	0.430
2-propylpyridine	4.740	5.251	1.290
4- <i>iso</i> -propylpyridine	4.736	4.857	1.562
4-propylpyridine	4.759	4.820	1.621
2,4,6-trimethylpyridine	4.802	5.293	0.907
3-ethyl-4-methylpyridine	4.744	5.321	1.156
5-ethyl-2-methylpyridine	4.733	5.319	0.938
6-ethyl-2-methylpyridine	4.733	5.567	0.492
3-butylpyridine	4.942	5.122	1.832
2-pentylpyridine	5.112	5.380	1.470
2-hexylpyridine	5.270	5.459	1.728
2-'butylpyridine	4.933	5.295	1.052
4-'butylpyridine	4.933	4.830	1.886
2,4,6-'butylpyridine	6.119	5.732	0.737

**Table 6.6** Comparison between electrophoretic mobilities of the Vinylpyridines predicted by molecular modelling and measured experimentally by CE in 40 mM lithium phosphate buffer, pH 2.5, 15 kV applied voltage.

Compound	Predicted Mobility $\text{cm}^2\text{V}^{-1}\text{s}^{-1}$	Experimental Mobility $\text{cm}^2\text{V}^{-1}\text{s}^{-1}$
2-Vinylpyridine	3.178 e-4	3.388 e-4
4-Vinylpyridine	3.429 e-4	3.597 e-4

The mobility order of 2-vinylpyridine and 4-vinylpyridine are correctly predicted. (Table 6.6). The vinylpyridines had higher mobilities than the corresponding ethylpyridines, but since there was very little difference in the calculated rotated radii, the predicted mobilities were only slightly higher than those for 2-ethylpyridine and 4-ethylpyridine. This is due to limitations in the model used to calculate the rotated radii of compounds. Alkyl chains are approximated to straight line chains thus no significant difference between an ethyl and a vinyl group is observed. In solution, the ethyl groups can rotate and so occupy more space than the vinyl groups thus resulting in lower overall mobilities.

The mobility order of 2-propylpyridine and 4-propylpyridine is also predicted from the molecular modelling (Table 6.7). The model is not able to correctly predict the mobility of 4-*isopropyl*pyridine relative to 4-propylpyridine. However the compounds have only a small difference in mobilities and the differences in predicted mobilities were similarly small. Modifications in the model to tackle branched chains are presented in the next section. N-Propylpyridinium bromide had a quite different predicted mobility to the experimental value. One possible clue why such a different value is obtained is given from the positions of centre of charge and centre of mass obtained by molecular modelling. For all other compounds, the centre of charge is in front of the centre of mass, whereas for N-propylpyridinium bromide the situation is reversed (Figure 6.9).

**Table 6.7** Comparison between electrophoretic mobilities predicted by molecular modelling and measured experimentally for the propylpyridines.

Compound	Predicted Mobility $\text{cm}^2\text{V}^{-1}\text{s}^{-1}$	Experimental Mobility $\text{cm}^2\text{V}^{-1}\text{s}^{-1}$
2-propylpyridine	3.051 e-4	2.923 e-4
4-propylpyridine	3.177 e-4	3.097 e-4
4-isopropylpyridine	3.125 e-4	3.059 e-4
N-propylpyridinium bromide	2.941 e-4	3.249 e-4

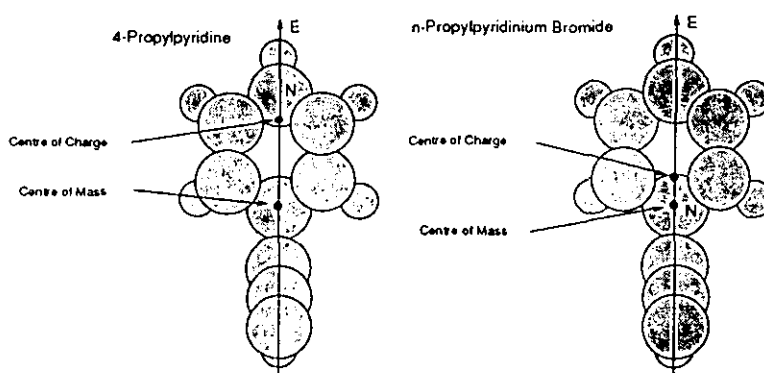


**Figure 6.9** Centre of charge locations for 4-propylpyridine and n-propylpyridinium bromide.

The ethylmethylpyridines and 2,4,6-trimethylpyridine are closely related in size to the propylpyridines, with di-substituted and tri-substituted rings. The mobility order for the ethylmethylpyridines is correctly predicted (Table 6.8), with the biggest difference between 5-ethyl-2-methylpyridine and 6-ethyl-2-methylpyridine being accentuated in the predicted mobilities. The 2,4,6-trimethylpyridine predicted mobility is close to its experimental mobility, and lies in the correct order with 3-ethyl-4-methylpyridine and 5-ethyl-2-methylpyridine, although the low value for the predicted mobility obtained for

6-ethyl-2-methylpyridine does not correspond with the predicted 2,4,6-trimethylpyridine value. The pattern of mobility orders of the mono-substituted, di-substituted and tri-substituted propylpyridines compare well.

**Table 6.8** Comparison between electrophoretic mobilities predicted by molecular modelling and measured experimentally for the ethylmethylpyridines and 2,4,6-trimethylpyridine.

Compound	Predicted Mobility $\text{cm}^2\text{V}^{-1}\text{s}^{-1}$	Experimental Mobility $\text{cm}^2\text{V}^{-1}\text{s}^{-1}$
3-ethyl-4-methylpyridine	2.980 e-4	3.071 e-4
5-ethyl-2-methylpyridine	2.954 e-4	2.976 e-4
6-ethyl-2-methylpyridine	2.784 e-4	2.904 e-4
2,4,6-trimethylpyridine	2.937 e-4	2.849 e-4

Other compounds available for study were the larger sized alkylpyridines, 3-butylpyridine, 2-pentylpyridine and 2-hexylpyridine, of which positional isomers were not available. Predicted and experimental mobilities compared well (Table 6.9), mainly because of the dominant van der Waals size term ( $1/R_{\text{vdw}}$ ) in the regression equation.

**Table 6.9** Comparison between electrophoretic mobilities predicted by molecular modelling and measured experimentally for 3-butylpyridine, 2-pentylpyridine and 2-hexylpyridine.

Compound	Predicted Mobility $\text{cm}^2\text{V}^{-1}\text{s}^{-1}$	Experimental Mobility $\text{cm}^2\text{V}^{-1}\text{s}^{-1}$
3-butylpyridine	2.771 e-4	2.851 e-4
2-pentylpyridine	2.504 e-4	2.526 e-4
2-hexylpyridine	2.391 e-4	2.363 e-4



The graph of experimental mobility against predicted mobility for all the derivatives shows these patterns clearly (Figure 6.10). Most points lie within the 95% confidence intervals. Notable aberrant points, such as the vinylpyridines and n-propylpyridinium bromide have been discussed.

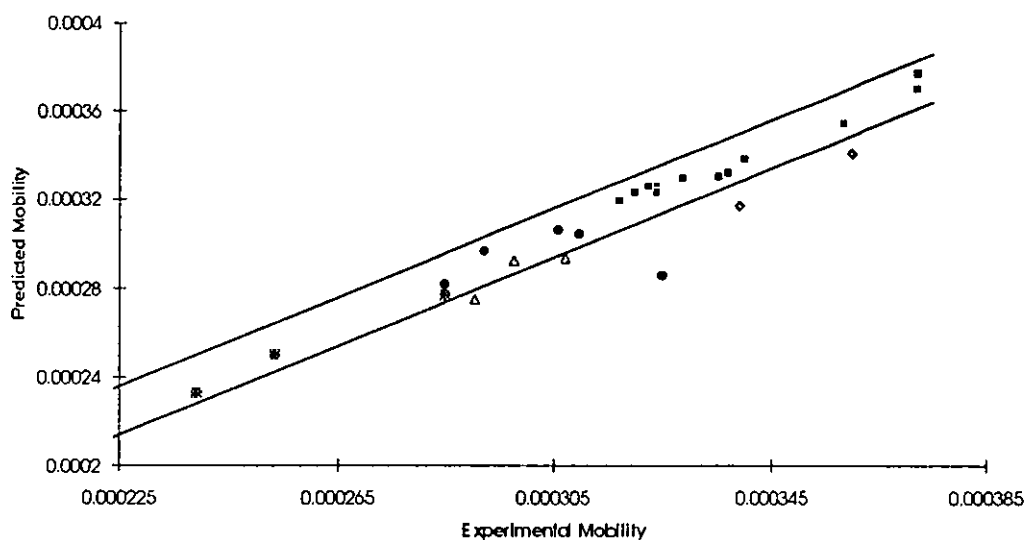


*Figure 6.10 Comparison between electrophoretic mobilities predicted by molecular modelling and measured experimentally for the alkylpyridines.*

## 6.6.2 Chain branching.

4-*Iso*-Propylpyridine.

For simplicity, the model used to predict the mobilities of the alkylpyridines approximated alkyl chains as straight lines. However the model was shown to be unable to account for differences in the branching of alkyl chains for 4-*n*-propylpyridine and 4-*iso*-propylpyridine. Thus, in order to model the migration behaviour of branched chains the chain branching was maintained rather than reduce the alkyl chain to a single line. For 4-isopropylpyridine this is a better representation of the ion as the isopropyl group is likely to sit out of the plane of the pyridine ring (Figure 6.11).

The rotated radii and the inertial radii of 4-*isopropylpyridine* were calculated using the modified branched chain model, and the difference in the obtained values was in the rotated radii (Table 6.10) which is larger for the branched chain model. Thus, the predicted mobility using the branched chain model is lower than for the straight chain model.

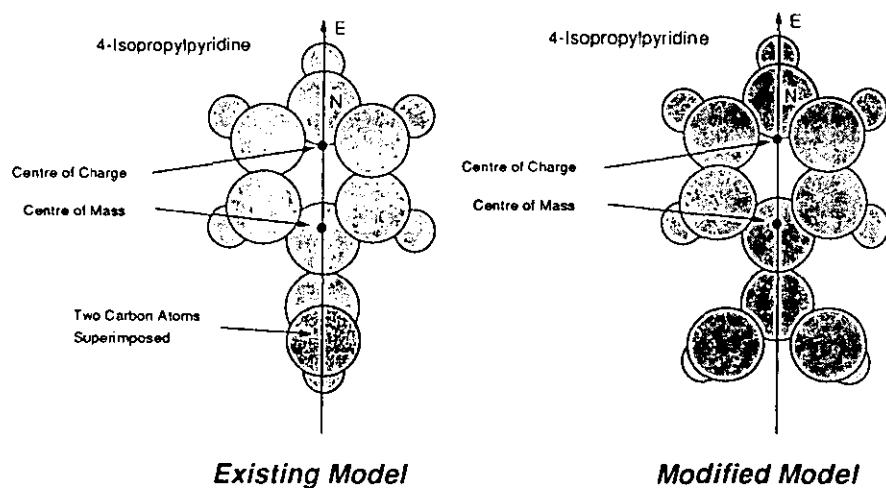


**Figure 6.11** Representations of 4-isopropylpyridine showing the model for restricted rotation and the need to show chain branching.

Using the branched chain model for 4-*isopropylpyridine* and the straight chain model for 4-*n*-propylpyridine the mobility order of these alkylpyridines

is correctly predicted. The predicted value of the mobility of 4-isopropylpyridine is lower than the experimental because the model has been developed by the regression analysis of compounds modelled by the straight chain method. Both models represent a simplification because of the conformational mobility of alkyl chains.

**Table 6.10** *Modelling of 4-isopropylpyridine. Straight chain model approximates the isopropyl group to a straight line and the branched chain model maintains the chain branching.*

4-isopropylpyridine	$R_{vdw}$ Å	$R_{rot}$ Å	$R_i$ Å	Predicted Mobility $\text{cm}^2\text{V}^{-1}\text{s}^{-1}$	Experimental Mobility $\text{cm}^2\text{V}^{-1}\text{s}^{-1}$
Straight Chain Model	4.736	4.857	1.540	3.076 e-4	3.059 e-4
Branched Chain Model	4.736	5.143	1.540	2.982 e-4	3.059 e-4

### 2-(1-ethylpropyl)pyridine.

2-(1-Ethylpropyl)pyridine is a structural isomer of 2-*n*-pentylpyridine and analysis by CE showed that it had a higher electrophoretic mobility of  $2.650 \text{ e-4 cm}^2\text{V}^{-1}\text{s}^{-1}$  compared to  $2.534 \text{ e-4 cm}^2\text{V}^{-1}\text{s}^{-1}$  for 2-*n*-pentylpyridine. On this occasion, the straight chain model gives the best prediction of electrophoretic mobility (Table 6.11).

**Table 6.11** *Modelling of 2-(1-ethylpropyl)pyridine. Straight chain model approximates the isopropyl group to a straight line and the branched chain model maintains the chain branching.*

Compound	$R_{vdw}$ Å	$R_{tot}$ Å	$R_i$ Å	Predicted Mobility $\text{cm}^2\text{V}^{-1}\text{s}^{-1}$	Experimental Mobility $\text{cm}^2\text{V}^{-1}\text{s}^{-1}$
Ethylpropylpyridine Straight Chain Model	5.112	4.999	1.182	2.561 e-4	2.650 e-4
Ethylpropylpyridine Branched Chain Model	5.112	5.422	1.182	2.474 e-4	2.650 e-4
2-Pentylpyridine	5.112	5.380	1.470	2.504 e-4	2.534 e-4

### 6.6.3 2-(3-pentenyl)pyridine.

2-(3-Pentenyl)pyridine was obtained as a mixture of *Z* and *E* isomers. Previous treatment of the modelling of the isomers electrophoretic mobilities (Section 4.6) [112] investigated the distance between the end of the alkyl chain and the ortho hydrogen to predict mobility orders based on the shorter distance for the *Z* isomer giving it a smaller size and thus higher mobility.

The model for restricted rotation was investigated for *Z*-2-(3-pentenyl)pyridine and *E*-2-(3-pentenyl)pyridine. In modelling the alkene group, the differences in the bond were maintained so as to give the greatest possible difference between the two isomers. The isomers were thus modelled in the conformations shown in Figure 6.12.

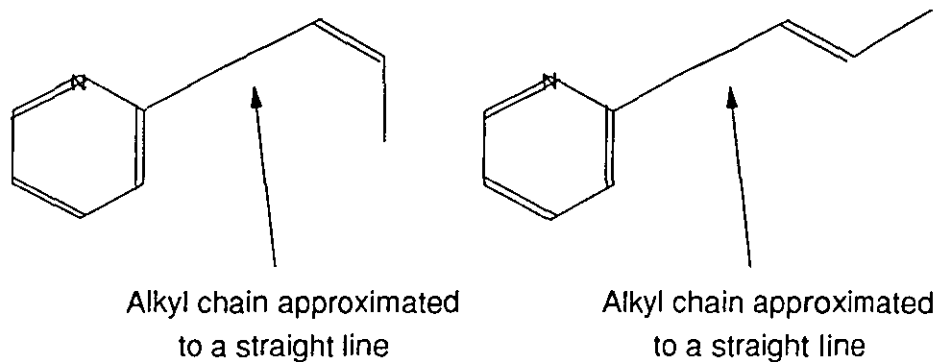


**Figure 6.12** Conformations of *Z*-2-(3-pentenyl)pyridine and *E*-2-(3-pentenyl)pyridine used for molecular modelling.

The predicted mobilities of the two isomers are lower than the actual observed mobilities (Table 6.12). This is due to the modifications of the model used (as represented in Figure 6.12). The mobility order is predicted correctly and the difference between the mobilities of the two isomers is 1.9% for the predicted values and 1.5% for the experimental values.

**Table 6.12** Modelling data for *E*-2-(3-pentenyl)pyridine and *Z*-(2-3-pentenyl)pyridine.

2-(3-Pentenyl)pyridine	$R_{vdw}$ Å	$R_{rot}$ Å	$R_i$ Å	Predicted Mobility $\text{cm}^2\text{V}^{-1}\text{s}^{-1}$	Experimental Mobility $\text{cm}^2\text{V}^{-1}\text{s}^{-1}$
<i>E</i> -Isomer	5.088	5.877	1.602	2.450	2.602
<i>Z</i> - Isomer	5.088	5.571	1.408	2.496	2.640

## 6.7 Aminoalkylpyridines.

The aminoalkylpyridines were of interest because two ionisable groups were available on each compound and so further investigations into the effects of shape and charge location could be studied from their mobilities.

### 6.7.1 Van der Waals' model.

Doubly charged aminoalkylpyridines migrate faster than their correspondingly sized alkylpyridines because they bear double the charge of the alkylpyridines at pH 2.5 (Table 6.13). The relationship between Van der Waals' radii of compounds and mobility was investigated for the aminoalkylpyridines (Figure 6.13). Linear regression of mobility versus Van der Waals' radii gave a slope of  $3.65 \times 10^{-3}$ , intercept  $-2.78 \times 10^{-4}$ , with a correlation coefficient of 0.850. This is a steeper slope than obtained for a corresponding group of alkylpyridines which gave slope  $2.928 \times 10^{-3}$ , intercept  $-3.151 \times 10^{-4}$  and a correlation coefficient of 0.972 (in this instance the monosubstituted alkylpyridines were used for comparisons).

:

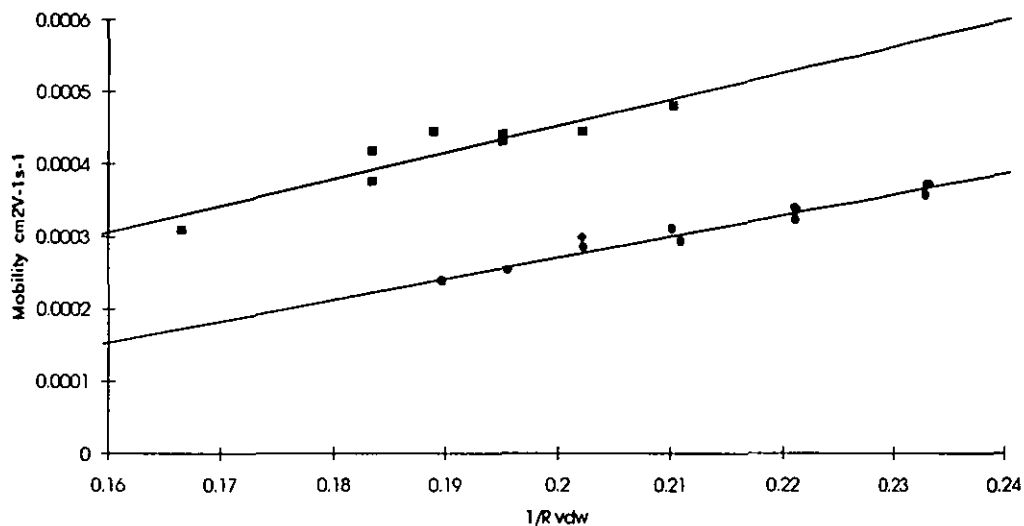


**Figure 6.13** Comparison between the mobilities of the alkylaminopyridines (■) and the mono-substituted alkylpyridines (●). 2-(dimethylaminomethyl)pyridine (◆) bears only one positive charge due to its ionisation constant.

**Table 6.13** Properties of the aminoalkylpyridines. Electrophoretic mobilities determined by CE in a lithium phosphate buffer, pH 2.5, 15 kV applied voltage. Ionisation constants determined by potentiometric titration,  $R_{vdw}$  by molecular modelling.

Compound	Mobility $\text{cm}^2\text{V}^{-1}\text{s}^{-1}$	Ionisation Constants	$R_{vdw}$ Å	Molecular Mass
2-(N-aminoethyl)pyridine	4.787 e-4	9.62, 3.98	4.756	107.6
4-(N,N-diethylaminoethyl)pyridine	4.176 e-4	9.46, 5.02	5.450	161.9
2-(N,N-diethylaminoethyl)pyridine	3.761 e-4	9.62, 3.64	5.450	161.9
3-(N-methylaminobutyl)pyridine	4.449 e-4	10.4, 5.46	5.293	148.3
2-(N-methylaminoethyl)pyridine	4.439 e-4	9.43, 4.33	4.946	121.0
2-(N,N-dimethylaminoethyl)pyridine	4.404 e-4	9.08, 3.72	5.125	134.6
2-(ethylaminoethyl)pyridine	4.310 e-4	9.98, 4.80	5.124	134.6
2-(N,N-dibutylamino)ethyl)pyridine	3.088 e-4	9.68, 3.80	6.003	216.3
2-(dimethylaminomethyl)pyridine	2.990 e-4	8.21, 1.42	4.946	121.0

Theoretically since the aminoalkylpyridines have double the charge of the alkylpyridines, they should have double the electrophoretic mobility of a similarly sized alkylpyridines. Therefore it is necessary to normalise the charge on the aminoalkylpyridines in order to compare mobilities between species. This is done by calculating the effective charge on the aminoalkylpyridines at pH 2.5 using the Hendersson-Hasselbach equation [105] and correcting the mobilities for differences in charge (mobility/charge) (Table 6.14).

*Table 6.14 Normalised electrophoretic mobilities for the aminoalkylpyridines 40 mM lithium phosphate buffer, pH 2.5, 15 kV applied voltage.*

Compound	Effective charge	Normalised Mobility $\text{cm}^2\text{V}^{-1}\text{s}^{-1}$
2-(2-aminoethyl)pyridine	1.968	2.432 e-4
4-(N,N-diethylaminoethyl)pyridine	1.997	2.091 e-4
2-(N,N-diethylaminoethyl)pyridine	1.932	1.947 e-4
3-(N-methylaminobutyl)pyridine	1.999	2.226 e-4
2-(N-methylaminoethyl)pyridine	1.956	2.269 e-4
2-(N,N-dimethylaminoethyl)pyridine	1.942	2.268 e-4
2-(N-ethylaminoethyl)pyridine	1.958	2.201 e-4
2-(N,N-dibutylaminoethyl)pyridine	1.952	1.582 e-4
2-(dimethylaminomethyl)pyridine	1.077	2.776 e-4

The normalised electrophoretic mobilities of the aminoalkylpyridines were generally lower than similarly sized alkylpyridines (Figure 6.14), and the regression analysis showed differences in the gradient and intercept of the regression lines (Table 6.15).



**Table 6.15** Regression results for the relationship between the electrophoretic mobility of aminoalkylpyridines and mono-substituted alkylpyridines and their size measured by Van der Waals' radii of compounds.

Compound group	Gradient	Intercept	Correlation coefficient
Aminoalkylpyridines (Standard Errors)	3.649 e-3 (6.24 e-4)	-2.780 e-4 (1.19 e-4)	0.850
Mono-substituted alkylpyridines	2.928 e-3 (1.66 e-4)	-3.151 e-4 (3.582 e-5)	0.972
Normalised aminoalkylpyridines	1.858 e-3 (2.605 e-4)	-1.414 e-4 (4.977 e-5)	0.895

The aminoalkylpyridines contain two ionisable nitrogen atoms, one within the pyridine ring and the other as an amine group which for the group of compounds studied are either primary or secondary. The different functionality of the amino group may lead to different buffer-analyte interactions and therefore lower normalised mobilities with interactions between buffer and analyte from both protonated nitrogens.

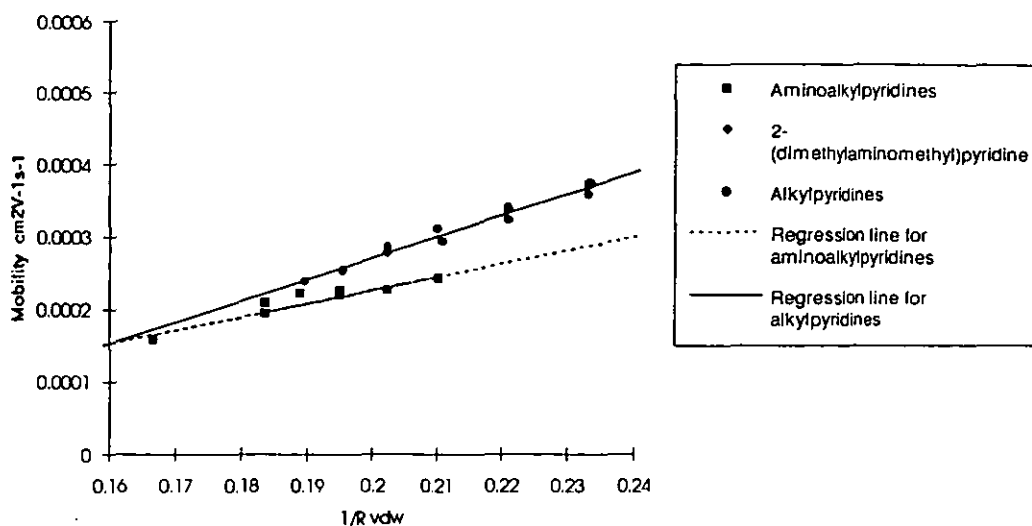


**Figure 6.14** Comparison between the normalised mobilities of the aminoalkylpyridines and the mono-substituted alkyipyridines.

### 6.7.2 Relationship with molecular mass.

A similar graph is obtained for the relationship between molecular weight to the power of two thirds and mobility for the aminoalkylpyridines (Figure 6.15).

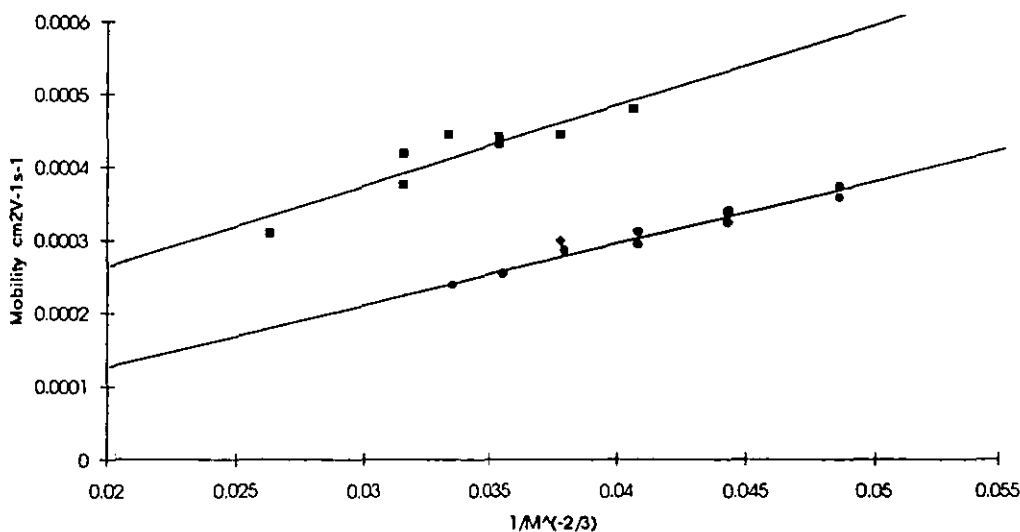


**Figure 6.15** Comparison between the mobilities of the alkylaminopyridines (■) and the mono-substituted alkyipyridines (●) related to their molecular masses. 2-(dimethylaminomethyl)pyridine (◆) bears only one positive charge due to its ionisation constant.

### 6.7.3 Separations of Isomers.

Of the nine aminoalkylpyridine analytes studied there were three pairs of isomeric compounds. One such set, 4-(*N,N*-diethylaminoethyl)pyridine and 2-(*N,N*-diethylaminoethyl)pyridine are positional isomers (Figure 6.16)

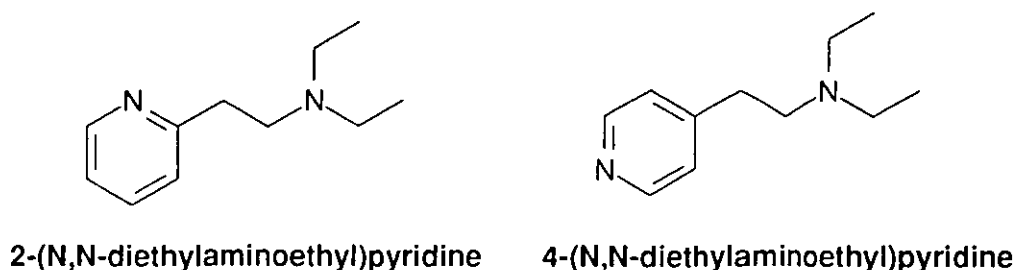
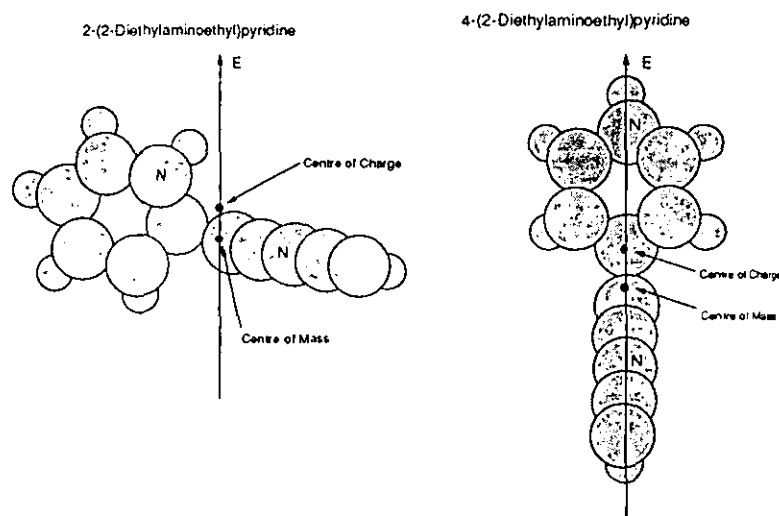


Figure 6.16 Structure of 2-(*N,N*-diethylaminoethyl)pyridine and 4-(*N,N*-diethylaminoethyl)pyridine

Table 6.16 Radii calculations for the aminoalkylpyridines.

Compound	$R_{vdw}$ (Å)	$R_{rot}$ (Å)	$R_i$ (Å)
2-(2-diethylaminoethyl)pyridine	5.450	6.556	0.444
4-(2-diethylaminoethyl)pyridine	5.450	4.882	0.617
2-(2-dimethylaminoethyl)pyridine	5.124	5.705	0.479
2-(2-ethylaminoethyl)pyridine	5.124	5.887	0.444
2-(2-methylaminoethyl)pyridine	4.946	5.323	0.711
2-(2-dimethylaminomethyl)pyridine	4.946	4.888	1.864
2-(2-aminoethyl)pyridine	4.756	5.016	1.021
3-(4-methylaminobutyl)pyridine	5.293	6.458	0.322
2-(2-dibutylaminoethyl)pyridine	6.003	5.365	1.048

Modelling 2-(N,N-diethylaminoethyl)pyridine and 4-(N,N-diethylaminoethyl)pyridine gave differences in the values of  $R_{rot}$  and  $R_i$  (Table 6.16, Figure 6.17). The values were used in regression equation (6.5) to give normalised predicted mobilities (Table 6.17). As can be seen the mobility order of the aminoalkylpyridines isomers was predicted correctly and the size of the predicted mobility was slightly larger for 4-(N,N-diethylaminoethyl)pyridine and smaller for 2-(N,N-diethylaminoethyl)pyridine. The correct prediction of mobility order for the aminoalkylpyridines indicates that the reduction of two discrete charges in the ions to one single point is a good method for approximating the migration behaviour of multiply charged analytes.



**Figure 6.17** Graphical representations of the modelling of the 4-(2-diethylaminoethyl)pyridine and 2-(2-diethylaminoethyl)pyridine.  $R_i$  is the distance between centre of charge and centre of mass and  $R_{rot}$  the radius obtained by rotating the molecules about the charge-mass axis.

**Table 6.17 Comparison between the predicted and experimental normalised mobilities of the aminoalkylpyridines.**

Compound	Predicted (Normalised) Mobility $\text{cm}^2\text{V}^{-1}\text{s}^{-1}$	Experimental (Normalised) Mobility $\text{cm}^2\text{V}^{-1}\text{s}^{-1}$
2-(N,N-diethylaminoethyl)pyridine	1.472 e-4	1.947 e-4
4-(N,N-diethylaminoethyl)pyridine	2.131 e-4	2.091 e-4
2-(N,N-dimethylaminoethyl)pyridine	2.248 e-4	2.268 e-4
2-(N-ethylaminoethyl)pyridine	2.196 e-4	2.201 e-4
2-(N-methylaminoethyl)pyridine	2.613 e-4	2.269 e-4
2-(N,N-dimethylaminomethyl)pyridine	2.820 e-4	2.820 e-4
2-(2-aminoethyl)pyridine	2.971 e-4	2.432 e-4
3-(N-methylaminobutyl)pyridine	1.818 e-4	2.226 e-4
2-(N,N-dibutylaminoethyl)pyridine	1.617 e-4	1.582 e-4

2-(N,N-Dimethylamino)ethyl)pyridine and 2-(N-ethylaminoethyl)-pyridine are structurally very similar with the only difference being secondary and primary amine groups respectively (Figure 6.18). Thus it was expected that there would be a smaller difference in electrophoretic mobility between these isomers than for the (N,N-diethylaminoethyl)pyridine positional isomers. This was observed (Table 6.17).

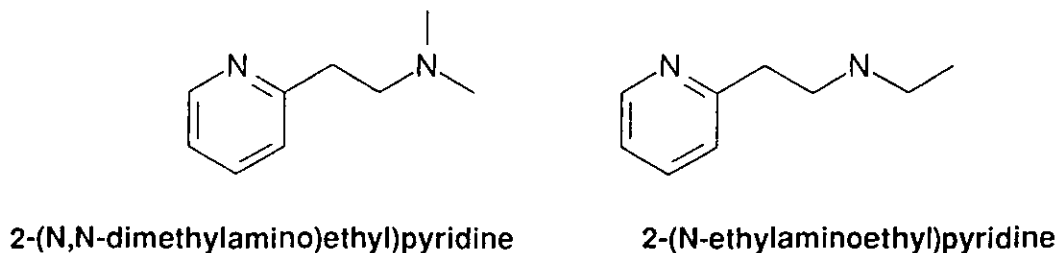
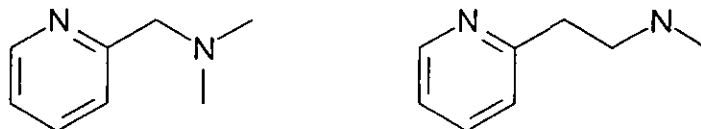


**Figure 6.18 Structures of 2-(2-dimethylamino)ethyl)pyridine and 2-(ethylaminoethyl)pyridine.**

2-(N-methylaminoethyl)pyridine and 2-(dimethylaminomethyl)-pyridine are structural isomers but they carry quite different charges due to the proximity of the nitrogen atoms in the compounds (Figure 6.19). For 2-(dimethylaminomethyl)pyridine one single positive charge is carried by the amine side chain.



2-(dimethylaminomethyl)pyridine    2-(N-methylaminoethyl)pyridine

*Figure 6.19 Structures of 2-(dimethylaminomethyl)pyridine and 2-(N-methylaminoethyl)pyridine*

Modelling of these structural isomers showed the reasonably similar shapes of the analytes under electrophoresis (Figure 6.20), although the charges on the analytes were quite different (Table 6.13). The normalised mobility order was correctly predicted for these isomers (Table 6.17) indicating that the mobility order of analytes with different charges can be predicted.

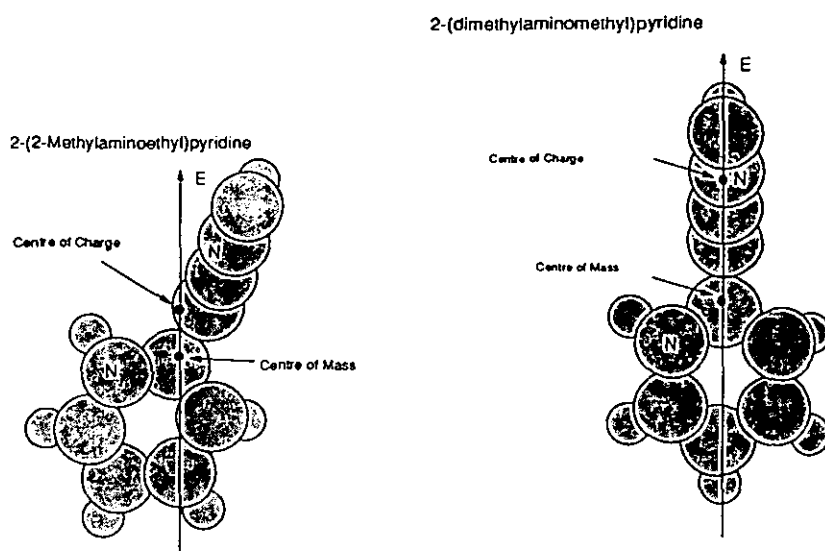


*Figure 6.20 Graphical representations of the modelling of the 2-(N,N-dimethylaminomethyl)pyridine and 2-(N-methylaminoethyl)pyridine.  $R_1$  is the distance between centre of charge and centre of mass and  $R_{rot}$  the radius obtained by rotating the molecules about the charge-mass axis.*

## 6.8 Summary.

The literature models for the size dependence of analytes on electrophoretic mobility were tested for the alkylpyridines studied in chapter 4. These models could not account adequately for structural isomers and so a model based on the restricted rotation of charged non-spherical analytes in the electric field was introduced. For the methylpyridines, ethylpyridines and dimethylpyridines the measured data was used to produce a mobility equation using multi-linear regression. This equation was tested on singly charged alkylpyridines and was found to generally predict the mobility orders of structural isomers well. Aminoalkylpyridines can bear two positive charges and these compounds were also modelled in the same way. The mobility order of structural isomers could again be correctly predicted thus indicating that multiple charges on compounds could be accounted for.

## Chapter 7

### Modelling of Substituted Benzenes and Related Compounds.

#### 7.1 Introduction.

The separation and modelling of the alkyipyridines showed that electrophoretic mobility could be predicted for structural isomers. In this chapter the relationship of structure and electrophoretic mobility is investigated for compounds that have other functionalities. Alkylanilines are closely related structures to the alkyipyridines and have the advantage that they can be analysed under the same conditions as for the alkyipyridines. Alkylbenzoic acids were also investigated in this case under conditions of high EOF.

#### 7.2 Alkylanilines.

##### 7.2.1 Literature Relationships and comparisons with the Alkyipyridines.

Alkylanilines were analysed under the same conditions as the alkyipyridines, therefore any differences observed in the mobility behaviour of the two sets of compounds may be attributed to the properties of the analytes being studied. The relationship between measured electrophoretic mobility (Appendix I) and molecular weight (Offord's parameter) for aniline, N-methylaniline, the dimethylanilines, N,n-propylaniline and 1-amino-5,6,7,8-tetrahydronaphthalene showed a poor correlation for the ten compounds taken as the regression set ( $r^2 = 0.7097$ , Slope =  $5.783 \times 10^{-4}$ , Intercept  $3.61 \times 10^{-5}$ ,  $n = 10$ ) (Figure 7.1). There is an insufficient number of compounds to properly evaluate the relationship between substitution on the nitrogen and electrophoretic mobility, however some patterns were observed. Aniline and the dimethylanilines, which are primary amines showed generally lower



mobilities than N-methylaniline and N-propylaniline, which are secondary amines. The other analyte studied, 1-amino-5,6,7,8-tetrahydronaphthalene is a primary amine, however it behaved as a secondary amine.

A possible reason for the lower mobilities of primary amines could be the interaction between analyte and buffer. The primary amines have less steric hindrance around the nitrogen atom than secondary amines and so can interact more strongly with charged counterions. This would result in a larger analyte-counterion complex and a greater contribution from the relaxation effect, resulting in primary amines exhibiting lower mobilities.

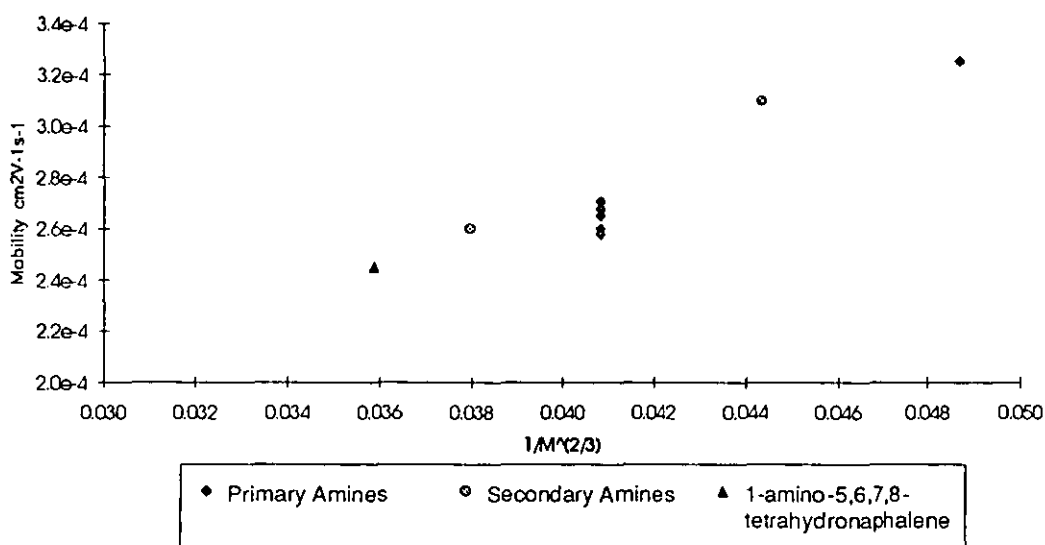


**Figure 7.1** Relationship between mobility and molecular mass for some alkyanilines. 40 mM Lithium phosphate buffer, pH 2.5, 15 kV applied voltage.

The electrophoretic mobilities of the alkyanilines were also compared to the electrophoretic mobilities of the alkyipyridines using Offord's relationship (Figure 7.2). The alkyipyridines had higher electrophoretic mobilities than alkyanilines of equivalent molecular mass. This behaviour was again attributed to the alkyanilines being able to interact more strongly with counterions generating an effectively larger analyte ion. For the alkyipyridines charge

delocalisation occurs, which probably reduces the analyte - counterion interactions. This effect was also observed for the aminoalkylpyridines which contain an amine function, with their normalised mobilities being lower than the equivalently sized alkylpyridines.

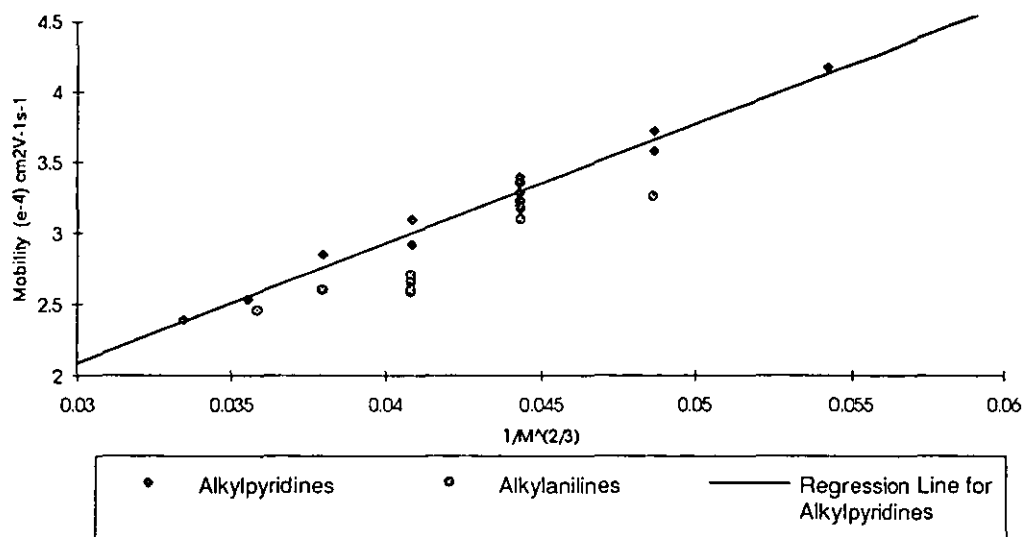


**Figure 7.2** Comparison between the electrophoretic mobilities of the alkylpyridines and the alkylanilines using their relationship with molecular mass.

The relationship between electrophoretic mobility and the van der Waals volumes of the molecules showed a similar pattern, with the mobilities of the alkylpyridines being higher than those of the alkylanilines (Figure 7.3).

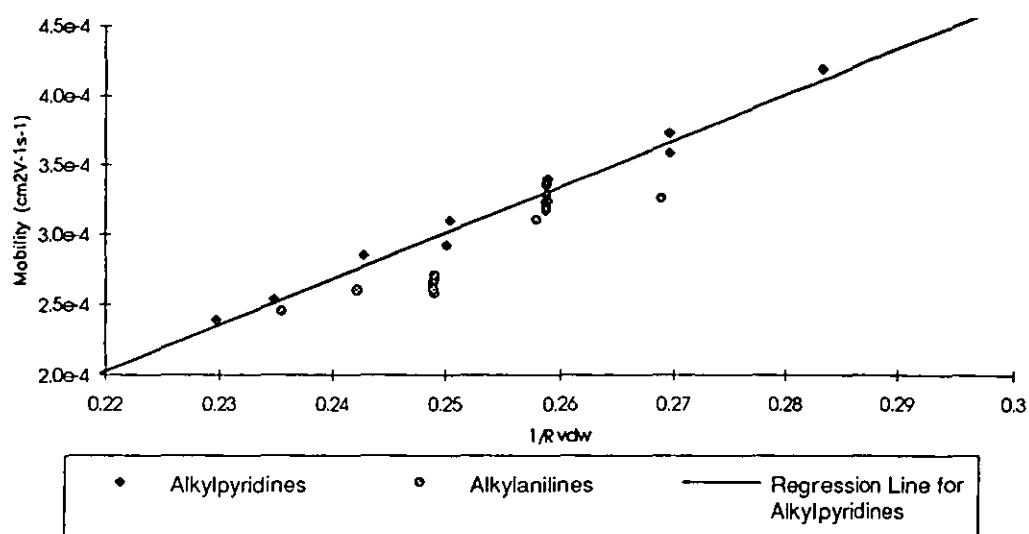


**Figure 7.3** Comparison between the mobilities of the alkylpyridines and the alkylanilines and their van der Waals molecular radii.

### 7.2.2 Modelling of the Dimethylanilines.

The dimethylanilines (DMAs) are structural analogues of the dimethylpyridines. As with the dimethylpyridines, the use of literature models to describe their electrophoretic mobilities gave vertical lines of points, indicating no discrimination of their mobilities. The dimethylanilines showed a similarity in mobility order to the dimethylpyridines (Table 7.1, Figure 5.12), indicating that the effects governing their relative separations are of a similar nature to the alkylpyridines. However, one notable difference was the mobility of 3,5-dimethylaniline, which had a lower mobility relative to its structural isomers compared to its corresponding structural isomer, 3,5-dimethylpyridine.

**Table 7.1** *Electrophoretic mobilities of the dimethylanilines (DMA) and the dimethylpyridines (DMP) in order of decreasing mobility. 40 mM lithium phosphate buffer, pH 2.5, 15 kV applied voltage.*

Compound	Electrophoretic Mobility $\text{cm}^2\text{V}^{-1}\text{s}^{-1}$	Compound	Electrophoretic Mobility $\text{cm}^2\text{V}^{-1}\text{s}^{-1}$
3,4-DMA	2.708 e-4	3,4-DMP	3.349 e-4
2,3-DMA	2.677 e-4	3,5-DMP	3.285 e-4
2,5-DMA	2.651 e-4	2,3-DMP	3.236 e-4
3,5-DMA	2.620 e-4	2,5-DMP	3.236 e-4
2,4-DMA	2.620 e-4	2,4-DMP	3.196 e-4
2,6-DMA	2.580 e-4	2,6-DMP	3.168 e-4

The rotated and inertial radii of the DMAs were calculated in the same way as for the alkylpyridines (Table 7.2). One obvious feature is that the inertial radii  $R_i$  values are much bigger than for the dimethylpyridines because of the greater distance between the centre of mass and centre of charge. This results in higher mobilities being predicted for the DMAs using the regression equation developed for the alkylpyridines (equation 6.5). However, the relative differences between isomers was of most interest and some correlation between experimental and predicted mobility orders (Table 7.2) was observed with 3,4-DMA predicted as having the greatest mobility and 2,6-DMA the smallest mobility.

**Table 7.2** *Calculated radii values for the dimethylanilines and their predicted electrophoretic mobilities using the model for restricted rotation developed for the alkyipyridines.*

Compound	$R_{vdw}$ (Å)	$R_{rot}$ (Å)	$R_i$ (Å)	Experimental Mobility $\text{cm}^2\text{V}^{-1}\text{s}^{-1}$	Predicted Mobility $\text{cm}^2\text{V}^{-1}\text{s}^{-1}$
3,4-DMA	4.015	5.166	3.050	2.708 e-4	3.074 e-4
2,3-DMA	4.015	5.325	2.569	2.677 e-4	3.030 e-4
2,5-DMA	4.017	5.351	2.493	2.651 e-4	3.023 e-4
3,5-DMA	4.017	5.351	2.849	2.620 e-4	3.030 e-4
2,4-DMA	4.016	5.215	2.696	2.620 e-4	3.056 e-4
2,6-DMA	4.015	5.351	2.139	2.580 e-4	3.019 e-4

Reasons for the apparent difference in relative mobility order between 3,5-dimethylaniline and 3,5-dimethylpyridine are unclear. One possible explanation may be due to the effects of 2-substitution in the anilines causing steric hindrance around the positive charge leading to higher overall mobilities than compounds unsubstituted in this position. Thus, 3,5-dimethylaniline would have an effectively lower electrophoretic mobility than other isomers. However, this behaviour was not observed for 3,4-dimethylaniline.

### 7.3 Aminoalkylbenzenes.

A number of aminoalkylbenzenes containing two amine groups were available for analysis. 1,4-dimethylbenzenediamine, 1,3-dimethylbenzenediamine and 2-(4-aminophenyl)ethylamine were all expected to bear double positive charges at pH 2.5 based on the  $\text{pK}_a$  values (Appendix II) whereas N-phenylethylenediamine was expected to have a single positive charge (Figure 7.3).

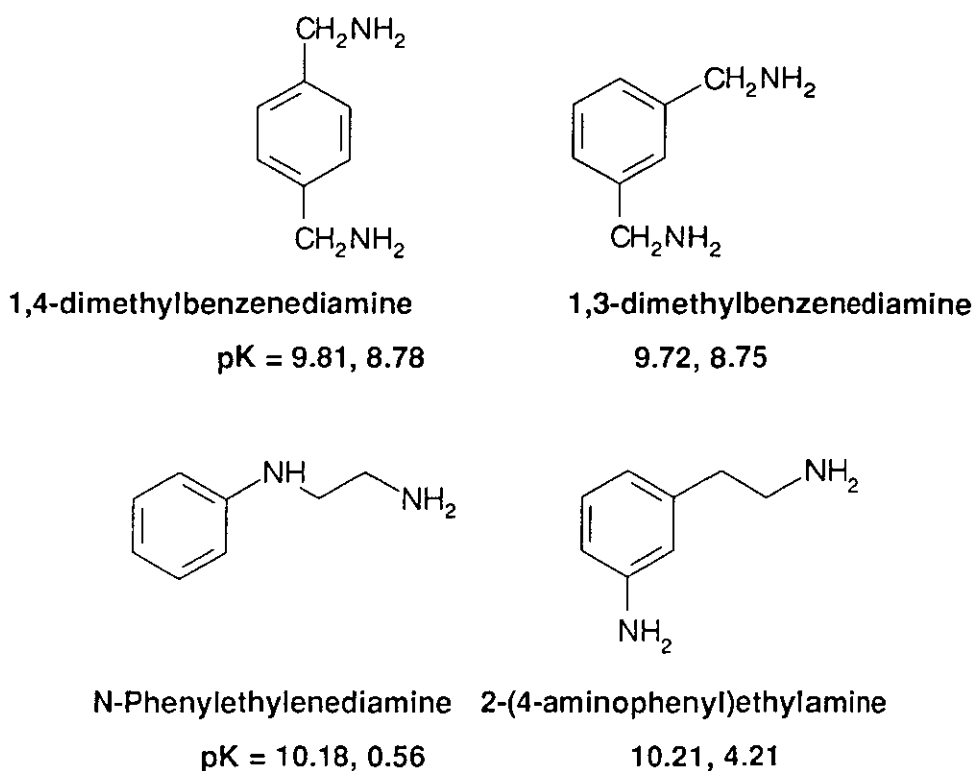


**Figure 7.3** Structures and predicted [115] pK values for the aminobenzenes.

The electrophoretic mobilities of the compounds were normalised to correct for charge differences and the relationship between mobility and molecular mass was investigated (Figure 7.4). The doubly charged compounds, 1,3-dimethylbenzenediamine, 1,4-dimethylbenzenediamine and 2-(4-aminophenyl)ethylamine all exhibited lower electrophoretic mobilities than both the corresponding alkyipyridines and alkyanilines of similar size. For these compounds, two primary amine groups are ionised. Based on the results for the alkyanilines the doubly charged amino groups should interact strongly with counterions in the buffer, thus giving lower overall mobilities than for the other functionalities investigated earlier. N-Phenylethylenediamine showed a relatively higher mobility, which corresponds with the alkyipyridine mobilities. However, it is likely that the predicted  $pK_a$  value is too low and in fact that some partial protonation of the second amine group occurs. The model again does not discriminate between structural isomers.

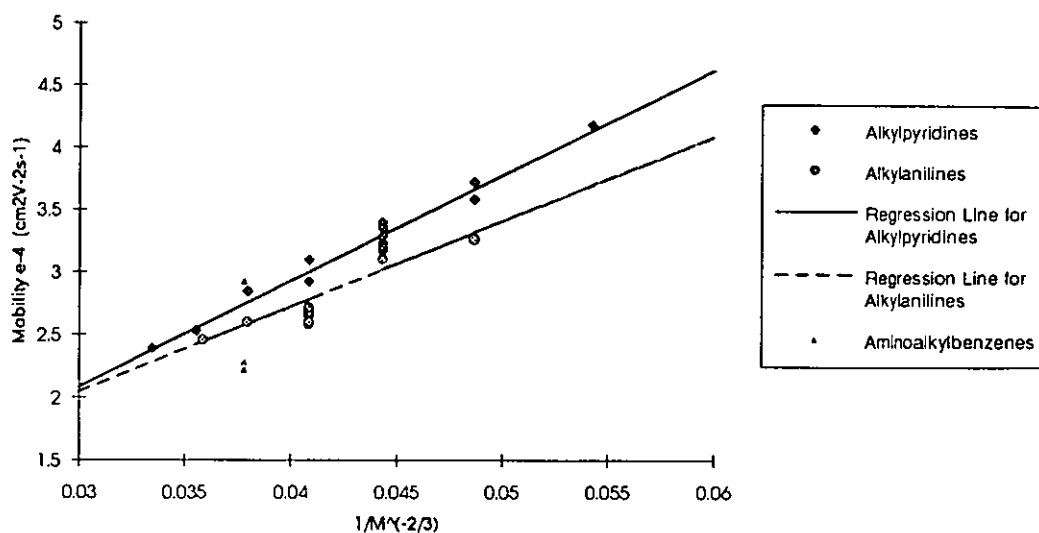


**Figure 7.4** *Offord's relationship between molecular mass and mobility for the aminoalkylbenzenes compared with the alkylpyridines and alkylanilines. Mobilities have been normalised for charge.*

#### 7.4 Dual Functionality Compounds.

Some pyridine compounds with carboxylic acid substituent groups were also analysed. These compounds can carry a charge on either the nitrogen atom or the carboxyl group at either low or high pH respectively and thus can be used to probe the effects of the position of charge on mobility. At pH 2.5, it was necessary to correct the mobilities of compounds for the partial charge as full positive charges were not present (Table 4.4). Nicotinic acid was thus shown to have a lower corrected mobility than *isonicotinic acid* showing a reversal in mobility order than for the alkylpyridines. The mobilities compared to size were also shown to be higher than for the alkylpyridines (Figure 7.5). It is unclear whether this is because of the normalisation of

mobilities or due to the structural properties of the analytes. The mobility order of the nicotinic acids may be reversed due to the carboxyl group shielding the positive charge on the analyte from interaction with buffer.

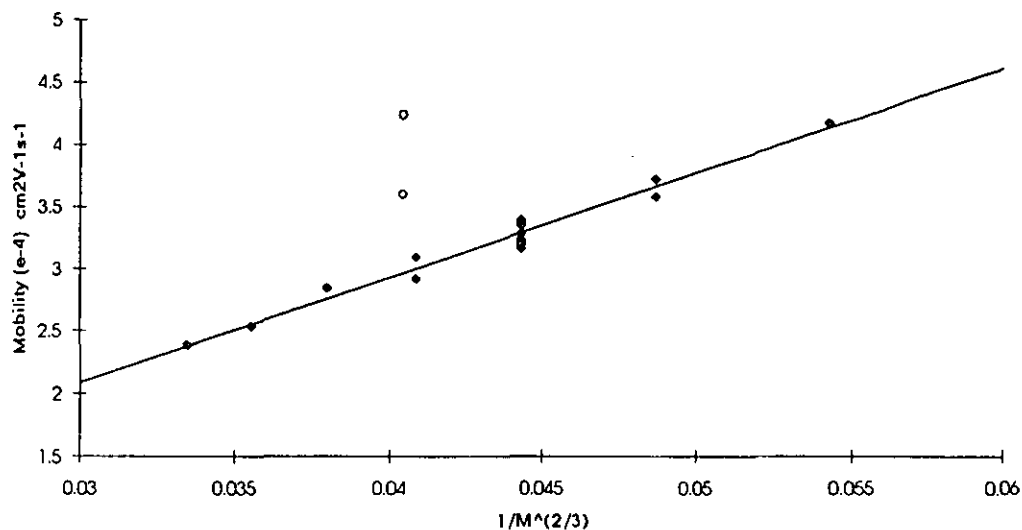


**Figure 7.5** Relationship between molecular mass and mobility for the nicotinic acid and isonicotinic acid with the alkylpyridines. Mobilities have been normalised for charge. 40 mM lithium phosphate buffer, pH 2.5, 15 kV applied voltage.

No separation of the nicotinic acids was achieved at pH 8.5 with the compounds co-migrating with benzoic acid. This is probably due to the compounds being ionised on the carboxyl group rather than the aromatic ring structure and thus the only structural difference in the ionised forms is the lone pair of electrons on the nitrogen. Comparison of the electrophoretic mobilities at pH 2.5 and pH 8.5 shows that the nicotinic acids have higher normalised mobilities at low pH than at high pH. The compounds were analysed at the different pH values using different buffers which may account for the differences or the differences may be due to the exposed nature of the carboxyl group allowing strong analyte-buffer interactions. The carboxyl functionality is further investigated for the benzoic acids.



## 7.5 Study of the Alkylbenzoic acids.

### 7.5.1 Literature Relationships.

The electrophoretic mobilities of the methylbenzoic acids, 4-ethylbenzoic acid, dimethylbenzoic acids, 4-propylbenzoic acid, 4-*isopropyl*benzoic acid, 4-butylbenzoic acid-4-decylbenzoic acid (Appendix I) fit Offord's relationship with regression analysis showing a good correlation between mobility and molecular mass (Gradient =  $6.9 \times 10^{-3}$ , Intercept =  $1.2 \times 10^{-5}$ ,  $r^2 = 0.9853$ ,  $n = 21$ ). A slight curvature was observed for higher molecular weight compounds in a fused silica capillary which may be related to the hydrophobicity of the larger alkylbenzoic acids causing conformational changes in the structures of the compounds. Thus, using a different molecular index may account for this curvature [81]. No discrimination between structural isomers was observed by the model, although the differences in mobility between structural isomers were generally smaller than for the alkylpyridines.

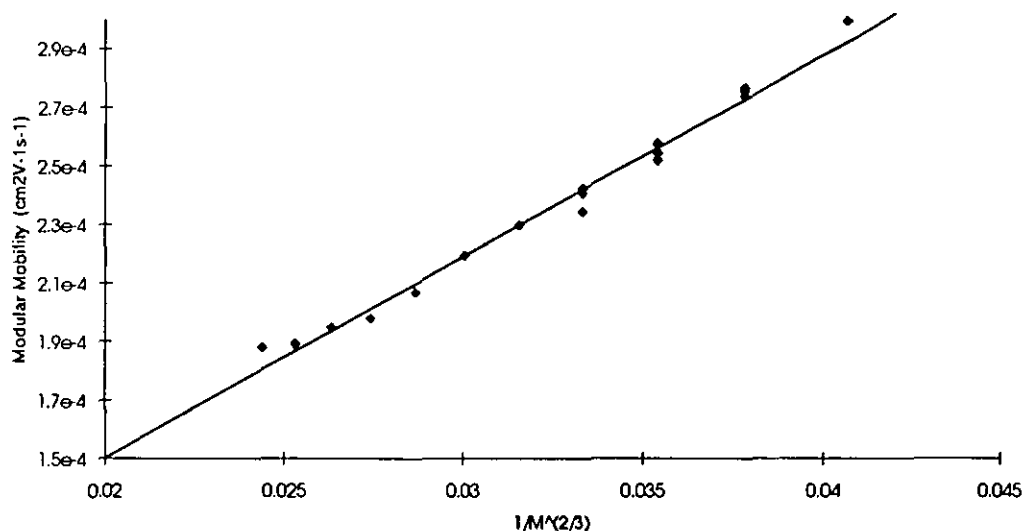


**Figure 7.6** *Offord's relationship between alkylbenzoic acid mobility and molecular mass. 50 mM lithium borate buffer, pH 8.5, 15 kV applied voltage.*

Comparison of the modular mobilities of the alkylbenzoic acids with the results obtained for the alkyipyridines of similar ionic strength showed the benzoic acids to have similar electrophoretic mobilities to alkyipyridines of similar molecular weights, although the gradient for the alkylbenzoic acids was smaller (Figure 7.7). Thus for the homologous series of alkylbenzoic acids the difference in mobility between carbon units is smaller than for the alkyipyridines.

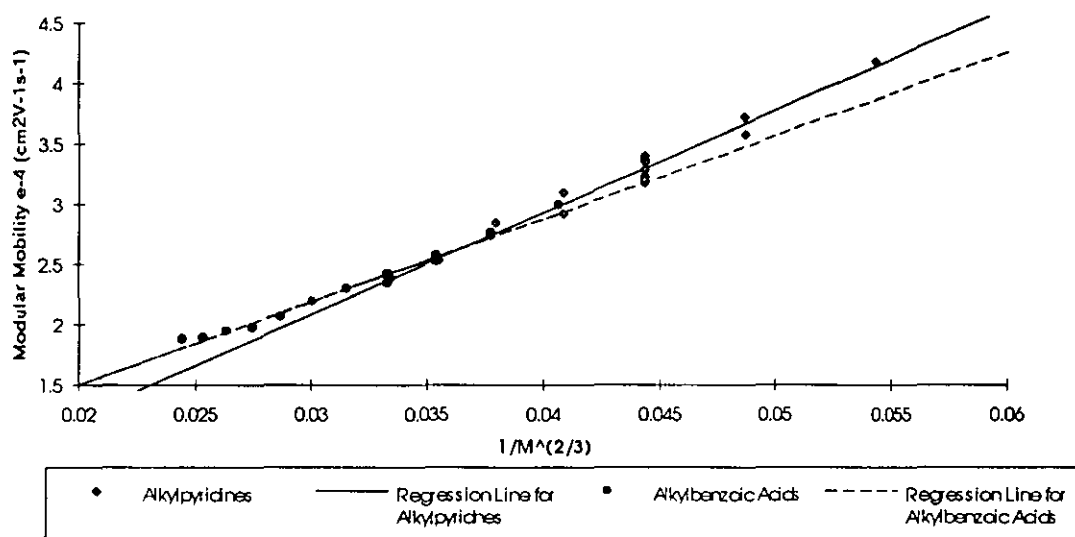


**Figure 7.7** Comparison of Offord's parameter for the alkylbenzoic acids and the alkyipyridines.

The relationship between the electrophoretic mobility and the van der Waals radii of the benzoic acids was also investigated (Figure 7.8). A similar result, to that for the relationship with molecular mass, was obtained, with again curvature of the values for higher molecular weight alkylbenzoic acids.

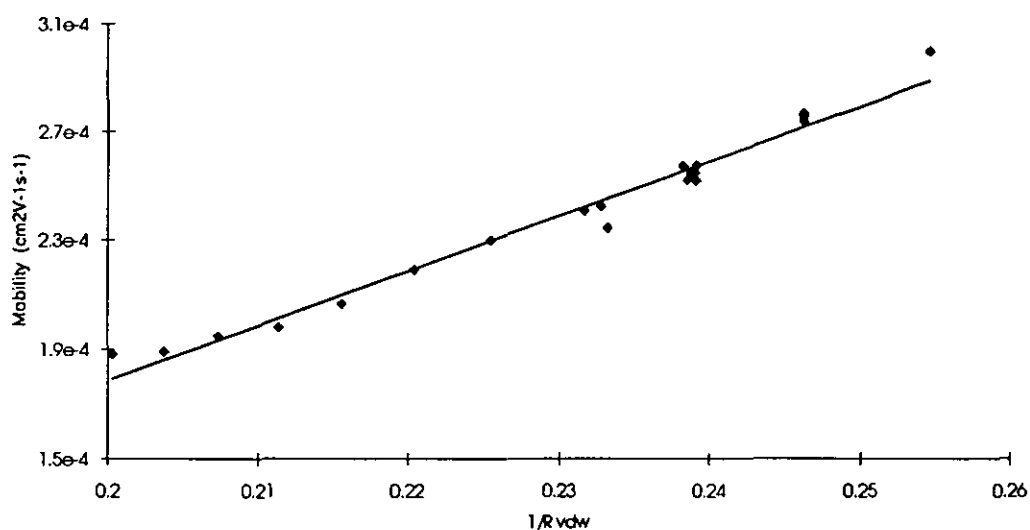


**Figure 7.8** *Mobility of alkylbenzoic acids against 1/Rvdw. 50 mM lithium borate buffer, pH 8.5, 15 kV applied voltage.*

The modular mobility of the alkylbenzoic acids were also compared with the mobility of the alkylpyridines in a plot of mobility against the inverse of the van der Waals radii (Figure 7.9). Both sets of compounds followed the general trend of an inverse relationship between mobility and size, but there was a clear difference in the gradient of the lines (Table 7.3), and the statistical data suggests that these differences are real. Since both sets of compounds bear either full positive or full negative charges they should theoretically have the same electrophoretic mobility.

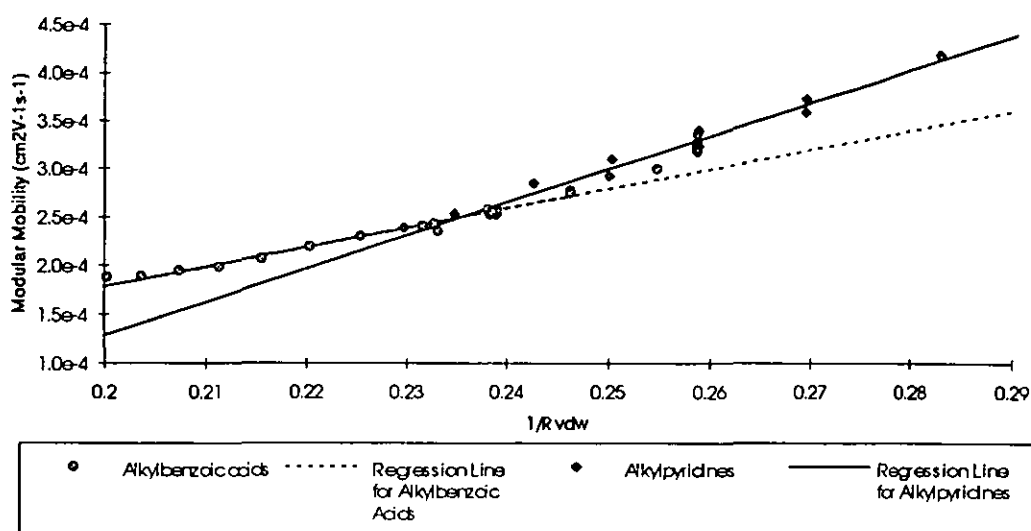


**Figure 7.9** Comparison between the alkyipyridines and alkylbenzoic acids plotted against their van der Waals radii.

**Table 7.3** Regression analysis for the relationship between electrophoretic mobility and van der Waals radii (from Figure 7.9).

Compound Set	Gradient	Intercept	Correlation Coefficient	Sample Size
Alkylbenzoic acids (Standard Error)	2.010 e-3 (7.36 e-5)	-2.235 e-4 (1.70 e-5)	0.975	21
Alkylpyridines (Standard Error)	3.416 e-3 (12.9 e-5)	-5.548 e-4 (3.28 e-5)	0.967	21

It was important to distinguish whether such differences in the gradients of the plots were due to structural differences between the different sets of compounds or the conditions under which the compounds were analysed. One of the main differences between the two sets of compounds is the buffer that the compounds were analysed in to maintain the correct pH for the ionisation of compounds. To investigate whether a change in buffer could affect the gradient of the mobility-size plot, the benzoic acids were studied in different buffers. Since the alkylpyridines were studied in a lithium phosphate buffer, two lithium phosphate buffers of pH 8.2 were prepared, the first taking 40 mM phosphoric acid and adjusting the pH with 1 M lithium hydroxide, the second taking 40 mM lithium hydroxide and adjusting the pH with 1 M orthophosphoric acid. Also since the alkylbenzoic acids were expected to interact with counterions in solution, a sodium phosphate buffer was prepared to investigate the effects of a different counterion.

The electrophoretic mobility values of benzoic acid and the homologous series 4-methylbenzoic acid to 4-hexylbenzoic acid in different buffers were found to be slightly different. The mobility-size plot shows that essentially the same gradient for each buffer was obtained with a RSD of 1.6 % between different buffers (Table 7.4 and Figure 7.10), but that slightly different intercepts were apparent with an RSD between buffers of 2.75 %. The gradients were slightly different to the value obtained for the complete set of compounds (Table 7.3) since only a selection of *n*-alkylbenzoic acids were included in this study. Electrophoretic mobilities of compounds were not corrected using the internal standard benzoic acid to maintain the mobility differences between different buffers.

**Table 7.4** Regression analysis for the benzoic acid mobility versus  $1/R_{vdw}$  plots, using different buffer compositions.

Buffer	Slope	Intercept	Correlation Coefficient
Lithium Borate (Borate 50 mM)	2.29 e-3	-2.87 e-4	0.996
Lithium Phosphate (Phosphate 40 mM)	2.34 e-3	-3.11 e-4	0.994
Lithium Phosphate (Lithium 40 mM)	2.23 e-3	-2.96 e-4	0.992
Sodium Phosphate (S odium 40 mM)	2.26 e-3	-2.99 e-4	0.993

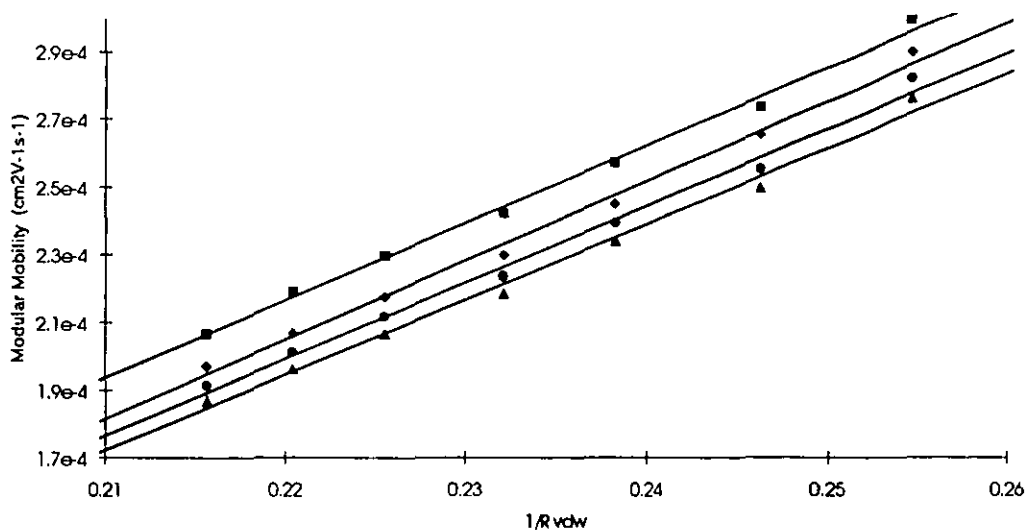


**Figure 7.10** The effect of different buffers on the mobility of benzoic acids and the 4-*n*-alkylbenzoic acids from 4-methylbenzoic acid to 4-hexylbenzoic acid.. [ ■ Lithium Borate buffer (Borate 50 mM); ◆ Lithium Phosphate Buffer ( $\text{Li}^+$  40 mM); ● Sodium Phosphate Buffer ( $\text{Na}^+$  40 mM); Δ Lithium Phosphate Buffer (Phosphate 40 mM)]

When compared to the gradient obtained for the alkyipyridines (Table 7.3), the differences between gradients obtained for the benzoic acid mobility-size plots for the four different buffers were small. This indicated that the gradient of this line is not controlled by the buffer system alone and thus must be related to properties of the analyte molecule itself. The relative differences obtained in different buffer systems for the benzoic acids may be compared with the relative differences between electrophoretic mobilities of the alkyipyridines at different ionic strengths.

It has been shown (Section 7.3) that for the compounds containing amino groups that the electrophoretic mobilities of compounds were found to be generally lower than the electrophoretic mobilities of alkyipyridine compounds. This was attributed to the increased interaction between analyte and buffer. For the benzoic acids it was expected that a strong interaction between buffer and analyte could occur due to the exposed carboxyl group not being sterically shielded from ion-counterion interactions. This would be expected to lead to lower electrophoretic mobility values for the alkyibenzoic acids, and might also explain the different gradients between the sets of compounds.

### 7.5.2 Shape Modelling of the Alkyibenzoic Acids.

The alkyibenzoic acids were modelled in an identical way to the alkyipyridines to model the effective size of the ions in solution and the electrophoretic retardation of the ions. For the methylbenzoic acids, the following values were obtained assuming the distribution of the negative charge to be located on the carboxyl group (Table 7.5).

Table 7.5 Radii values obtained for the methylbenzoic acids.

Compound	Mobility	$R_{vdw}$	$R_{rot}$	$R_i$
2-methylbenzoic acid	-2.756 e-4	4.054	5.298	2.412
3-methylbenzoic acid	-2.767 e-4	4.058	5.317	2.732
4-methylbenzoic acid	-2.738 e-4	4.058	5.116	2.874

The rotated radii,  $R_{rot}$ , of 2- and 3- methylbenzoic acids are very similar but the  $R_i$  values, which are a measure of the analytes' ability to rotate against the force of electrical alignment differ, with the 3- and 4-methylbenzoic acids having higher values than 2-methylbenzoic acid. Applying the model developed for the alkyipyridines, the mobility of the methylbenzoic acids is not correctly predicted (Table 7.6). The actual electrophoretic mobilities of the species' is predicted to be higher than the actual values, as was observed for other compound functionalities such as the alkylanilines where the  $R_i$  values were generally larger than for the alkyipyridines. The mobilities of 2-methylbenzoic acid and 3-methylbenzoic acid were predicted to be identical and this agreed with the very similar experimental results, with these peaks always co-migrating. However, the predicted mobility for the 4-methylbenzoic acid which is higher than the other isomers, showed a lower experimental electrophoretic mobility than its structural isomers.



**Table 7.6.** *Comparison between experimental and predicted electrophoretic mobilities for the methylbenzoic acids.*

Compound	Predicted Mobility $\text{cm}^2\text{V}^{-1}\text{s}^{-1}$	Experimental Mobility $\text{cm}^2\text{V}^{-1}\text{s}^{-1}$
2-methylbenzoic acid	-2.959 e-4	-2.756 e-4
3-methylbenzoic acid	-2.959 e-4	-2.767 e-4
4-methylbenzoic acid	-3.003 e-4	-2.738 e-4

A possible explanation for the differences in migration behaviour of the methylbenzoic acids is due to the way in which the compounds interact with buffer. The electrophoresis effect was modelled to take account of the flow of counterions over analyte molecule, however the relaxation effect, which is caused by the coulombic interaction between buffer counterion and analyte ion was not modelled. For benzoic acid, the region where the asymmetric distribution of counterions would build up is around the carboxyl group and particularly on the opposite side to the direction of travel of the analyte (Figure 7.11).

Such a distribution of counterions would be sensitive to the substitution at the 2-position as groups would point into this region of counterions. If a region was sterically blocked then a smaller interaction between analyte ion and counterion would result, giving a higher overall mobility for the analyte. Representations for the isomeric methylbenzoic acids show the possible interaction between analyte ion and counterion (Figure 7.12).

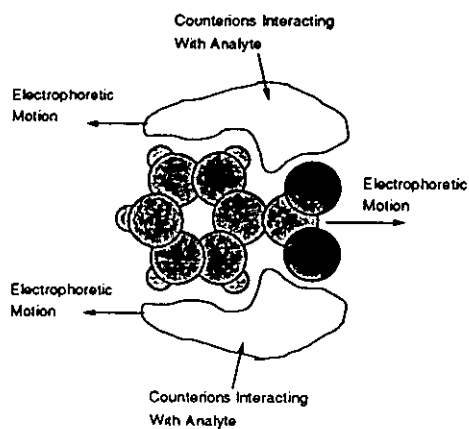


Figure 7.11 Asymmetric distribution of counterions around benzoic acid.

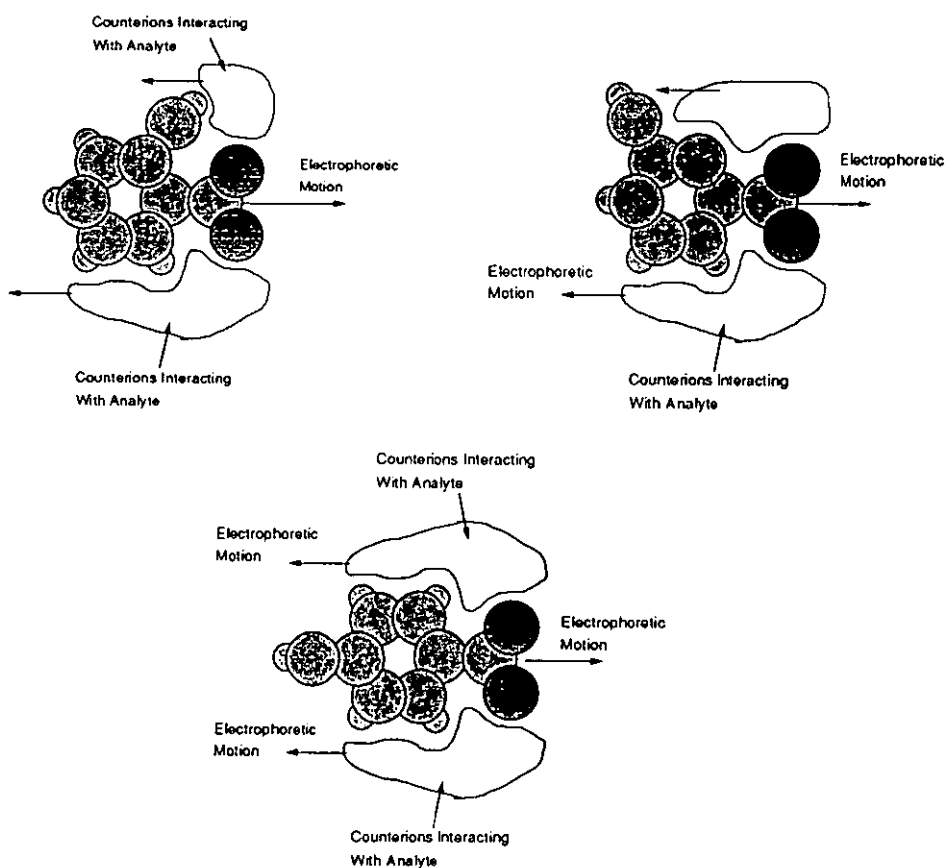


Figure 7.12 The interaction of counterions with the methylbenzoic acids.

Thus the mobility order expected from consideration of the relaxation/steric effects would predict a mobility order of 2-methylbenzoic acid, 3-methylbenzoic acid, 4-methylbenzoic acid. The actual separations probably include contributions from both effects.

The buffers used to analyse the benzoic acids contained sodium and potassium which are relatively small counterions. For the analysis of the alkyipyridines, phosphate and citrate ions were the comparative counterions used, thus the interactions could also be stronger for these smaller counterions.

Other alkbenzoic acid isomers also had quite different mobility orders to alkyipyridines and so the model developed for the alkyipyridines was unable to account for these compounds. In order to model the mobilities of these compounds, other factors would have to be considered.

## 7.6 Summary.

Sets of compounds of similar functionalities were found to fit literature relationships relating to the size or mass of analyte ions. When these sets of compounds were compared to others of different functionality, differences were observed which were attributed to the interaction between analyte ions and counterions in solution. Thus, when compared to the alkyipyridines studied in chapter 6, analytes containing amino groups exhibited generally lower electrophoretic mobilities.

Some correlation between the mobility orders of the isomeric dimethylanilines and the dimethylpyridines was observed, although for the alkybenzoic acids, scrambling of mobility orders was obtained. It was proposed that this behaviour was again related to increased analyte-counterion interaction for the alkybenzoic acids.

## Chapter 8.

### Conclusions.

Much of the work investigated in CE has been application based. This project set out to investigate some of the effects of size, shape and charge on electrophoretic mobility with an aim of being able predict electrophoretic mobility to aid the pharmaceutical analyst in method development. Literature models proved to be capable of describing the effect of analyte size on electrophoretic mobility for homologous compounds, However they failed to describe the shape effects that enabled structural isomers to be separated, and to describe the differences between electrophoretic mobilities of compounds of different functionalities.

The use of marker techniques to quote accurate electrophoretic mobilities of compounds provided the foundations for future investigations. Analysis of the alkyipyridines showed a unique selectivity in separations which were correlated with structural properties to provide a quantitative predictive model for the electrophoretic mobilities of alkyipyridines. The models were based on the Van der Waals' radii of compounds, their radii when aligned in the applied electric field and the distance between the calculated centres of mass and charge.

Analysis of related compounds such as the aminoalkyipyridines, alkyilanilines and aminobenzenes showed that the different functionalities of the compounds affects their electrophoretic mobility behaviour. Such behaviour was attributed to increased interaction of analyte and buffer leading to the lowered mobilities of compounds. Thus, it is believed that the charge delocalisation of the positive charge in the alkyipyridines together with

shielding of the positive charge from aromatic electrons reduces the contribution of the buffer to the alkyipyridines.

Alkylbenzoic acids were also analysed. For such compounds the ions are retarded by the flow of counterions over their surface as modelled for the alkyipyridines and also the effects of coulombic interactions between analyte and counterion, the effect observed for aminoalkyipyridines. Thus two mechanisms of separation of structural isomers are established which compete against one another. It is believed that the coulombic interaction dominates leading to a different selectivity of separations than for alkyipyridines. Separations of these compounds are thus determined by the amount of steric hindrance around the location of the charged moiety. Greater steric hindrance leads to lowered analyte - counterion interactions and hence to higher electrophoretic mobilities.

The mobility behaviour has been described qualitatively. Future models able to take account of sets of molecules that vary in functionality would have to be developed to take account of the interaction between buffer and analyte thus the steric hindrance around charges would have to be considered.

Alkyl bonded capillary columns showed some chromatographic retention properties when analysing alkylbenzoic acids by CE. Equations for calculating capacity factors of charged compounds relative to their analysis in uncoated fused silica capillaries were introduced and shown to give values close to the open tubular LC values obtained. With the recent advent of packed capillary electrochromatography there is much interest in the combination of electrophoretic and chromatographic techniques and with improvements in detection performance and miniaturisation open tubular systems may offer an attractive alternative to working with packed capillaries.

## References.

1. D.W.A. Sharp, *Dictionary of Chemistry*, Penguin, London, 1988, 155.
2. A.T. Andrews, *Electrophoresis - Theory, Techniques and Biomedical and Clinical Applications*, Second Ed., Oxford University Press, 1986.
3. R. Virtanen, *Acta Polytech. Scand.*, 123 (1974) 1.
4. F.E.P. Mikkers, F.M. Everaerts and T.P.E. Verheggen, *J. Chromatogr.*, 169 (1979) 11.
5. J.W. Jorgenson and K.D. Lukacs, *Anal. Chem.*, 53 (1981) 1298.
6. W. Steuer and I. Grant, *Nachr. Chem. Tech. Lab.*, 38 (1990) M1.
7. R.P. Oda, T.C. Spelsberg and J.P. Landers, *LC-GC*, 12 (1994) 50.
8. J. Snopek, I. Jelinek and E. Smolková-Keulemansová, *J. Chromatogr.*, 452 (1988) 571.
9. A.G. Ewing, R.A. Wallingford and T.M. Olefirowicz, *Anal. Chem.*, 61 (1989) 1.
10. R.A. Wallingford and A.G. Ewing, *Adv. Chromatogr.*, 29 (1989) 1.
11. W.G. Kuhr, *Anal. Chem.*, 62 (1990) 403R.
12. D.M. Goodall, D.K. Lloyd and S.J. Williams, *LC-GC*, 3 (1990) 28.
13. W.G. Kuhr and C.A. Monnig, *Anal. Chem.*, 64 (1992) 389R.
14. G. Schomburg, *Chromatographia*, 30 (1990) 500.
15. J. Vanantwerp, *Abstracts of papers of the American Chem. Soc.*, 202 (1991) 137.
16. T.E. Wheat, K.A. Lilley and J.F. Banks, *Abstracts of papers of the American Chem. Soc.*, 211 (1991) 116.
17. K.D. Altria, *J. Chromatogr.*, 735 (1996) 43.
18. K.D. Altria, J. Elgey, P. Lockwood and D. Moore, *Chromatographia*, 42 (1996) 332.
19. K.D. Altria, P. Frake, I. Gill, T. Hadgett, M.A. Kelly and D.R. Rudd, *J. Pharm. Biomed. Analysis*, 13 (1995) 951.

20. S.F.Y. Li, C.L. Ng and C.P Ong, *Adv. Chromatogr.*, 35 (1995) 199.
21. S.R. Rabel and J.F. Stobaugh, *Pharm. Res.*, 10 (1993) 171.
22. C.J.O.R. Morris and P. Morris, *Separation methods in Biochemistry*, Pitman Publishing Ltd., London, 1976, Chapter 12, p. 709.
23. P.W. Atkins, *Physical Chemistry*, Oxford University Press, 4 Ed., Oxford.
24. J.T. Overbeek and P.h. Wiersema, *Electrophoresis*, Academic Press Inc., New York, 1967, Vol.2, 1.
25. D.H. Heiger, *High Performance Capillary Electrophoresis - An Introduction*, 1992, Hewlett-Packard Company.
26. S.F.Y. Li, *Capillary Electrophoresis - Principles, Practices and Applications (Journal of Chromatography Library, Vol 52)*, Elsevier, Amsterdam, 1992.
27. P. Camilleri, *Capillary Electrophoresis: Theory and Practice*, 1993, CRC Press.
28. K. Salomen, D.S. Burgi and J.C. Helmer, *J. Chromatogr.*, 559 (1991) 69-80.
29. A.J. Bard and L.R. Faulkner, *Electrochemical Methods. Fundamentals and Applications*, Wiley, New York, 1980.
30. R.K. Iler, *The Chemistry of Silica*, Wiley, New York, 1979.
31. J.E. Dickens, J. Gorse, J.A. Everhart and M. Ryan, *J. Chromatogr.*, 657 (1994) 401.
32. S. Fujiwara and S. Honda, *Anal. Chem.*, 59 (1987) 487.
33. J. Gorse, A.T. Balchunas, D.F., Swaile and M.J. Sepaniak, *J. High Res. Chromatogr. Commun.*, 11 (1988) 554.
34. J. Lui, K. Cobb and M. Novotny, *J. Chromatogr.*, 468 (1988) 55.
35. M.M. Bushey and J.W. Jorgenson, *J. Microcol. Sep.*, 1 (1989) 125.
36. K. Salomen, D.S. Burgi and J.C Helmer, *J. Chromatogr.*, 549 (1991) 375.

37. G.J.M. Bruin, J.P. Chang, R.H. Kuhlman, K. Zegers, J.C. Kraak and H. Poppe, *J. Chromatogr.*, 471 (1989) 429.
38. M.X. Huang, *Amer. Biotech. Lab.*, 13 (1995) 80.
39. G.M. Janini, R.J. Fischer, L.E. Henderson, H.J. Issaq, *J. Liq. Chromatogr.*, 18 (1995) 3615.
40. E.L. Cussler, *Diffusion: Mass Transfer in Fluid Systems*, (1984), Cambridge University Press, England.
41. G.K. Vemulapalli, *Physical Chemistry*, (1993) Prentice-Hall, London.
42. A.Kolin, *J. Appl. Phys.*, 25 (1954) 1442.
43. S. Hjerten, *Chromatogr. Rev.*, 9 (1967) 122.
44. J.P. Holman, *Heat Transfer*, International Edition, McGraw-Hill, New York, 1985.
45. M.N. Ozisik, *Heat Transfer - A Basic Approach*, McGraw-Hill, New York, 1985.
46. W.H. McAdams, *Heat Transmisson*, 3rd Edition, McGraw-Hill, New York, 1985.
47. J.H. Knox and K.A. McCormack, *Chromatographia*, 38 (1994) 215.
48. J.H. Knox and K.A. McCormack, *Chromatographia*, 38 (1994) 207.
49. J.H. Knox, *Chromatographia*, 26 (1988) 329.
50. A.E. Jones and E. Grushka, *J. Chromatogr.*, 466 (1989) 225.
51. H. Wätzig, *Chromatogrpahia*, 33 (1992) 445.
52. K.L. Davis, K.K. Liu, M.Lanan and M.D. Morris, *Anal. Chem.*, 65 (1993) 293.
53. J. Vindevogel and P. Sandra, *Introduction to Micellar Electrokinetic Chromatography*, 1992, Hüthig, Heidelberg.
54. S. Terabe, T. Yashima, N. Tanaka and M. Araki, *Anal. Chem.*, 60 (1988) 1673.
55. S. A. C. Wren, *J. Microcol. Sep.*, 3 (1991) 147.
56. W. Friedl and E. Kenndler, *Anal. Chem.*, 65 (1993) 2003.



57. J.L. Beckers, F.M. Everaerts and M.T. Ackermans, *J. Chromatogr.*, 537 (1991) 407.
58. J. A. Cleveland Jr., M. H. Benko, S. J. Gluck and Y. M. Walbroehl, *J. Chromatogr.*, 652 (1993) 301.
59. J.H. Jumppanen, H. Sirén, M.L. Riekkola and O. Söderman, *J. Microcol. Sep.*, 5 (1993) 451.
60. S. Terabe, O. Shibata and T. Isemura, *J. High Res. Chromatogr.*, 14 (1991) 52.
61. Y. Walbroehl and J.W. Jorgenson, *J. Microcol. Sep.*, 1 (1989) 41.
62. P.E. Jackson, P.R. Haddad, *TrAC*, 12 (1993) 231.
63. I.Z. Atamna, C.J. Metral, G.M. Muschik and H.J. Issaq, *J. Liq. Chromatogr.*, 13 (1990) 2517.
64. J.L. Beckers, T.P.E.M. Verheggen and F.M. Everaerts, *J. Chromatogr.*, 452 (1988) 591.
65. L. Gross and E.S. Yeung, *Anal. Chem.*, 62 (1990) 427.
66. T. Tsuda, K. Nomura and G. Nakagawa, *J. Chromatogr.*, 264 (1983) 385.
67. S. Fanali, L.Ossicini, F. Foret, P. Bocek, *J. Microcol. Sep.*, 1 (1989) 190.
68. M.B. Amran, M.D. Lakkis, F.Lagarde, M.J.F. Lroy, J.F. Lopez-Sanchez and G.Rauret, *Fesenius J. Anal. Chem.*, 345 (1993) 420.
69. W.C., Brumley, *J. Chromatogr.*, 603 (1992) 267.
70. B.F. Kenny, *J. Chromatogr.*, 546 (1991) 423.
71. L. Kelly and R.J. Nelson, *J. Liq. Chromatogr.*, 16 (1993) 2103.
72. W.C. Brumley and C.M. Brownrigg, *J. Chromatogr.*, 646 (1993) 377.
73. M. W. F. Nielen, *J. Chromatogr.*, 542 (1991) 173.
74. R.R. Chadwick and J.C. Hsieh, *Anal. Chem.*, 63 (1991) 2377.
75. M. Korman, J. Vindevogel and P. Sandra, *J. Chromatogr.*, 645 (1993) 366.

76. R.C. Rowe, S.A.C. Wren and A.G. McKillop, *Electrophoresis*, 15 (1994) 635..
77. P.D. Grossman and J.C. Colburn, *Capillary Electrophoresis - Theory and Practice*, 1992, Academic Press Inc., London.
78. M.A. Surway, D.M. Goodall, S.A.C. Wren and R.C. Rowe, *J. Chrom.*, In Press.
79. L.P. Ribeiro, *Paper Electrophoresis*, 1961, Elsevier, Amsterdam.
80. R.E. Offord, *Nature*, 211 (1966) 591.
81. C.R. Cantor and P.R. Schimmel, *Biophysical Chemistry Part 2*, W H Freeman, New York, 1980.
82. F. Perrin, *J. Phys. Chem.*, 7 (1936) 1.
83. J.T. Edward and D. Waldron-Edward, *J. Chromatogr.*, 20 (1965) 563.
84. S. Meyer, A. Jabs, M. Schutkowski and G. Fischer, *Electrophoresis*, 15 (1994) 1151.
85. A. Avdeef, J.J. Butcher, *Anal. Chem.*, 50 (1978) 2137.
86. A. Avdeef, D.L. Kearney, J.A. Brown, A.R. Jr. Chemotti, *Anal. Chem.*, 54 (1982) 2322.
87. D.D. Perrin, Boyd Dempsey and E.P. Serjeant, *pK<sub>a</sub> Prediction for Organic Acids and Bases*, (1981) Chapman and Hall, London.
88. J.H. Jumppanen and M.L. Riekkola, *Anal. Chem.*, 67 (1995) 1060.
89. I.E. Valkó, J.H. Jumppanen, H. Sirén and M.L. Riekkola, *Proceedings of the eighteenth international symposium on capillary chromatography*, Riva del Garda, 1996.
90. J. Yang, S. Bose and D.S. Hage, *J. Chromatogr.*, 735 (1996) 209.
91. M.A. Strege and A.L. Lagu, *J. Liq. Chromatogr.*, 16 (1993) 51.
92. J. Frenz, S.L. Wu and W.S. Hancock, *J. Chromatogr.*, 480 (1989) 379.
93. T. Dülfer, R. Herb, H. Herrmann and U. Kobold, *Chromatographia*, 30 (1990) 675.

**Appendix I.**  
**Tabulation of Electrophoretic Mobility Data.**

*Table I.i 10mM Lithium phosphate buffer pH 2.5; fused silica capillary,  
applied voltage 263 Vcm<sup>-1</sup>.*

<i>Compound</i>	<i>Electrophoretic Mobility cm<sup>2</sup> V<sup>-1</sup> s<sup>-1</sup></i>	<i>Compound</i>	<i>Electrophoretic Mobility cm<sup>2</sup> V<sup>-1</sup> s<sup>-1</sup></i>
Pyridine	4.399 e-4	2,4,6-Trimethylpyridine	3.030 e-4
2-Methylpyridine	3.813 e-4	3-Ethyl-4-methylpyridine	3.282 e-4
3-Methylpyridine	3.946 e-4	5-Ethyl-2-methylpyridine	3.179 e-4
4-Methylpyridine	3.942 e-4	6-Ethyl-2-methylpyridine	3.089 e-4
2-Ethylpyridine	3.447 e-4	N-propylpyridinium bromide	3.437 e-4
3-Ethylpyridine	3.592 e-4	Z-2-(3-pentenyl)pyridine	2.879 e-4
4-Ethylpyridine	3.618 e-4	E-2-(3-pentenyl)pyridine	2.834 e-4
2-Propylpyridine	3.141 e-4	2-(2-aminoethyl)pyridine	5.386 e-4
4-Propylpyridine	3.313 e-4	2-(2-diethylaminoethyl)pyridine	4.364 e-4
4- <i>iso</i> Propylpyridine	3.275 e-4	4-(2-diethylaminoethyl)pyridine	4.660 e-4
3-Butylpyridine	3.080 e-4	3-(4-methylaminobutyl)pyridine	5.033 e-4
2-Pentylpyridine	2.725 e-4	2-(2-methylaminoethyl)pyridine	5.043 e-4
2-Hexylpyridine	2.578 e-4	2-(2-dimethylamino)ethyl)pyridine	4.939 e-4
3,4-Dimethylpyridine	3.577 e-4	2-(2-ethylaminoethyl)pyridine	4.659 e-4
3,5-Dimethylpyridine	3.520 e-4	2-(2-dibutylamino)ethyl)pyridine	3.480 e-4
2,3-Dimethylpyridine	3.477 e-4	2-(dimethylaminomethyl)pyridine	3.146 e-4
2,4-Dimethylpyridine	3.433 e-4	2-(1-ethylpropyl)pyridine	2.703 e-4
2,6-Dimethylpyridine	3.384 e-4		
2,5-Dimethylpyridine	3.477 e-4		

**Table I.ii** 20 mM Lithium phosphate buffer pH 2.5; fused silica capillary, applied voltage 263 Vcm<sup>-1</sup>.

<i>Compound</i>	<i>Electrophoretic Mobility cm<sup>2</sup> V<sup>-1</sup> s<sup>-1</sup></i>	<i>Compound</i>	<i>Electrophoretic Mobility cm<sup>2</sup> V<sup>-1</sup> s<sup>-1</sup></i>
Pyridine	4.298 e-4	2,4,6-Trimethylpyridine	2.941 e-4
2-Methylpyridine	3.726 e-4	3-Ethyl-4-methylpyridine	3.194 e-4
3-Methylpyridine	3.829 e-4	5-Ethyl-2-methylpyridine	3.106 e-4
4-Methylpyridine	3.830 e-4	6-Ethyl-2-methylpyridine	3.016 e-4
2-Ethylpyridine	3.378 e-4	N-propylpyridinium bromide	3.338 e-4
3-Ethylpyridine	3.475 e-4	Z-2-(3-pentenyl)pyridine	2.751 e-4
4-Ethylpyridine	3.500 e-4	E-2-(3-pentenyl)pyridine	2.712 e-4
2-Propylpyridine	3.088 e-4	2-(2-aminoethyl)pyridine	5.160 e-4
4-Propylpyridine	3.196 e-4	2-(2-diethylaminoethyl)pyridine	4.082 e-4
4- <i>iso</i> Propylpyridine	3.167 e-4	4-(2-diethylaminoethyl)pyridine	4.437 e-4
3-Butylpyridine	2.949 e-4	3-(4-methylaminobutyl)pyridine	4.737 e-4
2-Pentylpyridine	2.710 e-4	2-(2-methylaminoethyl)pyridine	4.806 e-4
2-Hexylpyridine	2.570 e-4	2-(2-dimethylaminoethyl)pyridine	4.649 e-4
3,4-Dimethylpyridine	3.467 e-4	2-(2-ethylaminoethyl)pyridine	4.405 e-4
3,5-Dimethylpyridine	3.407 e-4	2-(2-dibutylaminoethyl)pyridine	3.260 e-4
2,3-Dimethylpyridine	3.360 e-4	2-(dimethylaminomethyl)pyridine	3.012 e-4
2,4-Dimethylpyridine	3.320 e-4	2-(1-ethylpropyl)pyridine	2.616 e-4
2,6-Dimethylpyridine	3.282 e-4		
2,5-Dimethylpyridine	3.360 e-4		

**Table I.iii** 40 mM Lithium phosphate buffer pH 2.5; fused silica capillary, applied voltage 263 Vcm<sup>-1</sup>.

<i>Compound</i>	<i>Electrophoretic Mobility cm<sup>2</sup> V<sup>-1</sup> s<sup>-1</sup></i>	<i>Compound</i>	<i>Electrophoretic Mobility cm<sup>2</sup> V<sup>-1</sup> s<sup>-1</sup></i>
Pyridine	4.176 e-4	2,4,6-Trimethylpyridine	2.849 e-4
2-Methylpyridine	3.581 e-4	3-Ethyl-4-methylpyridine	3.071 e-4
3-Methylpyridine	3.721 e-4	5-Ethyl-2-methylpyridine	2.976 e-4
4-Methylpyridine	3.722 e-4	6-Ethyl-2-methylpyridine	2.904 e-4
2-Ethylpyridine	3.222 e-4	N-propylpyridinium bromide	3.249 e-4
3-Ethylpyridine	3.366 e-4	Z-2-(3-pentenyl)pyridine	2.640 e-4
4-Ethylpyridine	3.397 e-4	E-2-(3-pentenyl)pyridine	2.602 e-4
2-Propylpyridine	2.923 e-4	2-(2-aminoethyl)pyridine	4.787 e-4
4-Propylpyridine	3.097 e-4	2-(2-diethylaminoethyl)pyridine	3.761 e-4
4-isoPropylpyridine	3.059 e-4	4-(2-diethylaminoethyl)pyridine	4.176 e-4
3-Butylpyridine	2.848 e-4	3-(4-methylaminobutyl)pyridine	4.449 e-4
2-Pentylpyridine	2.534 e-4	2-(2-methylaminoethyl)pyridine	4.439 e-4
2-Hexylpyridine	2.391 e-4	2-(2-dimethylamino)ethyl)pyridine	4.404 e-4
3,4-Dimethylpyridine	3.349 e-4	2-(2-ethylaminoethyl)pyridine	4.310 e-4
3,5-Dimethylpyridine	3.285 e-4	2-(2-dibutylamino)ethyl)pyridine	3.088 e-4
2,3-Dimethylpyridine	3.236 e-4	2-(dimethylaminomethyl)pyridine	2.990 e-4
2,4-Dimethylpyridine	3.196 e-4	2-(1-ethylpropyl)pyridine	2.521 e-4
2,6-Dimethylpyridine	3.168 e-4	2-'butylpyridine	2.748 e-4
2,5-Dimethylpyridine	3.236 e-4	4-'butylpyridine	2.838 e-4
		2,4,6-tri'butylpyridine	1.809 e-4

**Table I.iv** 60 mM Lithium phosphate buffer pH 2.5; fused silica capillary, applied voltage 263 Vcm<sup>-1</sup>.

<i>Compound</i>	<i>Electrophoretic Mobility cm<sup>2</sup> V<sup>-1</sup> s<sup>-1</sup></i>	<i>Compound</i>	<i>Electrophoretic Mobility cm<sup>2</sup> V<sup>-1</sup> s<sup>-1</sup></i>
Pyridine	4.115 e-4	2-(2-aminoethyl)pyridine	4.609 e-4
2-Methylpyridine	3.518 e-4	2-(2-diethylaminoethyl)pyridine	3.623 e-4
3-Methylpyridine	3.664 e-4	4-(2-diethylaminoethyl)pyridine	4.020 e-4
4-Methylpyridine	3.663 e-4	3,4-Dimethylpyridine	3.295 e-4
2-Ethylpyridine	3.161 e-4	3,5-Dimethylpyridine	3.231 e-4
3-Ethylpyridine	3.311 e-4	2,3-Dimethylpyridine	3.182 e-4
4-Ethylpyridine	3.340 e-4	2,4-Dimethylpyridine	3.140 e-4
2-Propylpyridine	2.863 e-4	2,6-Dimethylpyridine	3.122 e-4
4-Propylpyridine	3.042 e-4	2,5-Dimethylpyridine	3.182 e-4
3-Butylpyridine	2.795 e-4		
2-Pentylpyridine	2.554 e-4		
2-Hexylpyridine	2.476 e-4		

**Table I.v** 80 mM Lithium phosphate buffer pH 2.5; fused silica capillary, applied voltage 263 Vcm<sup>-1</sup>.

<i>Compound</i>	<i>Electrophoretic Mobility cm<sup>2</sup> V<sup>-1</sup> s<sup>-1</sup></i>	<i>Compound</i>	<i>Electrophoretic Mobility cm<sup>2</sup> V<sup>-1</sup> s<sup>-1</sup></i>
Pyridine	4.047 e-4	2-(2-aminoethyl)pyridine	4.425 e-4
2-Methylpyridine	3.463 e-4	2-(2-diethylaminoethyl)pyridine	3.481 e-4
3-Methylpyridine	3.604 e-4	4-(2-diethylaminoethyl)pyridine	3.892 e-4
4-Methylpyridine	3.607 e-4	3,4-Dimethylpyridine	3.246 e-4
2-Ethylpyridine	3.114 e-4	3,5-Dimethylpyridine	3.182 e-4
3-Ethylpyridine	3.258 e-4	2,3-Dimethylpyridine	3.132 e-4
4-Ethylpyridine	3.290 e-4	2,4-Dimethylpyridine	3.089 e-4
2-Propylpyridine	2.820 e-4	2,6-Dimethylpyridine	3.089 e-4
4-Propylpyridine	2.997 e-4	2,5-Dimethylpyridine	3.132 e-4
3-Butylpyridine	2.752 e-4		
2-Pentylpyridine	2.448 e-4		
2-Hexylpyridine	2.304 e-4		

**Table I.vi** 100 mM Lithium phosphate buffer pH 2.5; fused silica capillary, applied voltage 263 Vcm<sup>-1</sup>.

<i>Compound</i>	<i>Electrophoretic Mobility cm<sup>2</sup> V<sup>-1</sup> s<sup>-1</sup></i>	<i>Compound</i>	<i>Electrophoretic Mobility cm<sup>2</sup> V<sup>-1</sup> s<sup>-1</sup></i>
Pyridine	3.993 e-4	2-(2-aminoethyl)pyridine	4.303 e-4
2-Methylpyridine	3.418 e-4	2-(2-diethylaminoethyl)pyridine	3.396 e-4
3-Methylpyridine	3.560 e-4	4-(2-diethylaminoethyl)pyridine	3.803 e-4
4-Methylpyridine	3.561 e-4	3,4-Dimethylpyridine	3.206 e-4
2-Ethylpyridine	3.078 e-4	3,5-Dimethylpyridine	3.142 e-4
3-Ethylpyridine	3.219 e-4	2,3-Dimethylpyridine	3.091 e-4
4-Ethylpyridine	3.248 e-4	2,4-Dimethylpyridine	3.055 e-4
2-Propylpyridine	2.789 e-4	2,6-Dimethylpyridine	3.055 e-4
4-Propylpyridine	2.960 e-4	2,5-Dimethylpyridine	3.091 e-4
3-Butylpyridine	2.749 e-4		
2-Pentylpyridine	2.416 e-4		
2-Hexylpyridine	2.278 e-4		



**Table I.vii** 50 mM Lithium borate buffer pH 8.5; fused silica capillary, applied voltage 263 Vcm<sup>-1</sup>.

<i>Compound</i>	<i>Electrophoretic Mobility cm<sup>2</sup> V<sup>-1</sup> s<sup>-1</sup></i>	<i>Compound</i>	<i>Electrophoretic Mobility cm<sup>2</sup> V<sup>-1</sup> s<sup>-1</sup></i>
Benzoic acid	-2.996 e-4	3,5-Dimethylbenzoic acid	-2.520 e-4
2-Methylbenzoic acid	-2.756 e-4	2,5-Dimethylbenzoic acid	-2.548 e-4
3-Methylbenzoic acid	-2.767 e-4	2,6-Dimethylbenzoic acid	-2.520 e-4
4-Methylbenzoic acid	-2.738 e-4	2,4-Dimethylbenzoic acid	-2.519 e-4
4-Ethylbenzoic acid	-2.573 e-4	3,4-Dimethylbenzoic acid	-2.543 e-4
4-Propylbenzoic acid	-2.424 e-4	2,3-Dimethylbenzoic acid	-2.578 e-4
4- <i>iso</i> Propylbenzoic acid	-2.407 e-4	2,4,6-Trimethylbenzoic acid	-2.345 e-4
4-Butylbenzoic acid	-2.298 e-4	2-Aminobenzoic acid	-2.955 e-4
4-Pentylbenzoic acid	-2.193 e-4	3-Aminobenzoic acid	-2.811 e-4
4-Hexylbenzoic acid	-2.067 e-4	4-Aminobenzoic acid	-2.777 e-4
4-Heptylbenzoic acid	-1.979 e-4	2-(dimethylamino)benzoic acid	-1.387 e-4
4-Octylbenzoic acid	-1.948 e-4	3-(dimethylamino)benzoic acid	-2.461 e-4
4-Nonylbenzoic acid	-1.892 e-4	4-(dimethylamino)benzoic acid	-2.417 e-4
4-Decylbenzoic acid	-1.880 e-4	2-(methylamino)benzoic acid	-2.739 e-4
2-Iodobenzoic acid	-2.662 e-4	4-(methylamino)benzoic acid	-2.546 e-4
3-Iodobenzoic acid	-2.666 e-4		
4-Iodobenzoic acid	-2.647 e-4		

**Table I.viii** 50 mM Lithium borate buffer pH 8.5; C1 capped capillary, applied voltage 263 Vcm<sup>-1</sup>.

<i>Compound</i>	<i>Electrophoretic Mobility cm<sup>2</sup> V<sup>-1</sup> s<sup>-1</sup></i>	<i>Compound</i>	<i>Electrophoretic Mobility cm<sup>2</sup> V<sup>-1</sup> s<sup>-1</sup></i>
Benzoic acid	-2.996 e-4	3,5-Dimethylbenzoic acid	-2.546 e-4
2-Methylbenzoic acid	-2.760 e-4	2,5-Dimethylbenzoic acid	-2.582 e-4
3-Methylbenzoic acid	-2.763 e-4	2,6-Dimethylbenzoic acid	-2.540 e-4
4-Methylbenzoic acid	-2.732 e-4	2,4-Dimethylbenzoic acid	-2.545 e-4
4-Ethylbenzoic acid	-2.575 e-4	3,4-Dimethylbenzoic acid	-2.570 e-4
4-Propylbenzoic acid	-2.420 e-4	2,3-Dimethylbenzoic acid	-2.591 e-4
4- <i>iso</i> Propylbenzoic acid	-2.412 e-4	2,4,6-Trimethylbenzoic acid	-2.536 e-4
4-Butylbenzoic acid	-2.302 e-4	2-Aminobenzoic acid	-2.957 e-4
4-Pentylbenzoic acid	-2.203 e-4	3-Aminobenzoic acid	e-4
4-Hexylbenzoic acid	-2.124 e-4	4-Aminobenzoic acid	-2.786 e-4
4-Heptylbenzoic acid	-2.106 e-4	2-(dimethylamino)benzoic acid	-1.260 e-4
4-Octylbenzoic acid	-2.201 e-4	3-(dimethylamino)benzoic acid	-2.479 e-4
4-Nonylbenzoic acid	-2.636 e-4	4-(dimethylamino)benzoic acid	-2.458 e-4
4-Decylbenzoic acid	-2.631 e-4	2-(methylamino)benzoic acid	-2.754 e-4
2-Iodobenzoic acid	-2.671 e-4	4-(methylamino)benzoic acid	e-4
3-Iodobenzoic acid	-2.675 e-4		
4-Iodobenzoic acid	-2.652 e-4		

**Table I.ix** 50 mM Lithium borate buffer pH 8.5; C18 capped capillary, applied voltage 263 Vcm<sup>-1</sup>.

<i>Compound</i>	<i>Electrophoretic Mobility</i> <i>cm<sup>2</sup> V<sup>-1</sup> s<sup>-1</sup></i>
Benzoic acid	-2.996 e-4
4-Methylbenzoic acid	-2.732 e-4
4-Ethylbenzoic acid	-2.574 e-4
4-Propylbenzoic acid	-2.417 e-4
4-Butylbenzoic acid	-2.300 e-4
4-Pentylbenzoic acid	-2.198 e-4
4-Hexylbenzoic acid	-2.112 e-4
4-Heptylbenzoic acid	-2.072 e-4
4-Octylbenzoic acid	-2.070 e-4
4-Nonylbenzoic acid	-2.301 e-4
4-Decylbenzoic acid	-

## Appendix II

### Survey of Ionisation Constants

The ionisation constant of a compound determines its charge at a particular pH, which is determined by the Hendersson-Hasselbach equation (II.1) [105].

$$pH = pK_a + \log \frac{[A^-]}{[HA]} \quad (\text{II.i})$$

where  $[A^-]$  is the concentration of the dissociated acid (or deprotonated base) and  $[HA]$  is the concentration of the protonated acid (or free base). For the alkylpyridines, the pH of the background electrolyte was usually 2.5. At this pH, pyridines and alkylpyridines with  $pK_a$  values typically in the region 5-6 were fully protonated. For work at higher pH values or for compounds with lower  $pK_a$  values, such as the investigation of the dimethylpyridines across the pH range (section 4.5) and the separations of aminoalkylpyridines (section 6.6), the ionisation constants must be known in order to be able to predict the partial charge on the analytes.

Ionisation constants were obtained from three sources (Tables II.i for the alkylpyridines, alkylanilines and aminoalkylpyridines, Table Iii for the alkylbenzoic acids). Literature data [115, 116] provides collections of ionisation constants for acids and bases. When comparing the published ionisation constants of closely related compounds, it is necessary to ensure that the ionisation constants were measured by the same method, preferably during the same study. Literature ionisation constants quoted in Tables II.i and II.ii were determined by potentiometric titration.

Estimated  $pK_a$  data were obtained from the program pKalc which calculates the contributions of functional groups to estimate  $pK_a$  values based on the work of Perrin [87]. It was found that these values were generally close to published values for compounds with one ionisable group although for

closely related compounds such as the dimethylpyridines some scrambling of values could occur.

The ionisation constants for the aminoalkylpyridines, with two ionisable nitrogen atoms, were also measured experimentally by potentiometric titration as described by Avdeef *et al.* [85, 86]. It was important to have reliable pKa data for these compounds since corrections to electrophoretic mobility were made, based on the effective charge on compounds at a particular pH.

**Table II.i**      *Ionisation constants for the basic compounds studied  
(Alkylpyridines, alkylanilines and aminoalkylpyridines).*

Compound	pKa Values		
	Literature [103]	Estimated [87]	Experimental
Pyridine	5.23	5.25	-
2-Methylpyridine	6.06	6.02	6.05
3-Methylpyridine	5.70	5.60	-
4-Methylpyridine	5.99	6.08	-
2-Ethylpyridine	5.99	6.02	-
3-Ethylpyridine	5.70	5.66	-
4-Ethylpyridine	6.03	6.14	-
2-Propylpyridine	5.97	6.08	-
4-Propylpyridine	6.05	6.14	-
N, <i>n</i> -Propylpyridinium bromide			
4- <i>iso</i> Propylpyridine	6.02	6.14	-
2,4,6-Trimethylpyridine	7.43	7.61	-
3-Butylpyridine	-	5.66	-
2-Pentylpyridine	6.00	6.19	-
2-(1-Ethylpropyl)pyridine		5.86	
2-(3-Pentenyl)pyridine	-	5.23	-
2-Hexylpyridine	-	6.19	-
2- <i>tert</i> -Butylpyridine	-		-
4- <i>tert</i> -Butylpyridine	5.99	6.14	-
2,4-Dimethylpyridine	6.99	6.84	-
3,5-Dimethylpyridine	6.15	5.96	-
3,4-Dimethylpyridine	6.46	6.43	-
2,3-Dimethylpyridine	6.57	6.37	-
2,6-Dimethylpyridine	6.60	6.78	-
2,5-Dimethylpyridine	6.40	6.37	-
5-Ethyl-2-ethylpyridine	-	6.43	-
6-Ethyl-2-ethylpyridine	-	6.78	-
3-Ethyl-4-ethylpyridine	-	6.49	-
2,4,6-Tri- <i>tert</i> -butylpyridine	-	7.43	-

**Table II.i** (Continued)  
*Ionisation constants for the basic compounds studied  
 (Alkylpyridines, alkylanilines and aminoalkylpyridines).*

Compound	pKa Values		
	Literature [103]	Estimated [87]	Experimental
2-(2-Aminoethyl)pyridine	9.52, 3.80	9.22, 4.57	9.68, 3.98
2-(2-Diethylaminoethyl)pyridine	-	9.29, 4.24	9.62, 3.64
4-(2-Diethylaminoethyl)pyridine	-	9.87, 4.24	9.46, 5.02
3-(4-Methylaminobutyl)pyridine	-	10.39, 5.66	10.4, 5.46
2-(2-Methylaminoethyl)pyridine	-	9.43, 4.33	9.43, 4.33
2-(2-(Dimethylamino)ethyl)pyridine	-	8.23, 4.42	9.08, 3.72
2-(2-Ethylaminoethyl)pyridine	-	9.98, 4.80	9.98, 4.80
2-(2-Dibutylaminoethyl)pyridine	-	8.95, 4.24	9.68, 3.80
2-(Dimethylaminomethyl)pyridine		6.77, 2.71	8.21, 1.42
Acridine		6.80	
1-Amino-5,6,7,8-tetrahydronaphthalene		7.34	
m-Xylylenediamine		9.72, 8.75	
p-Xylylenediamine		9.81, 8.78	
N-Phenylethylenediamine		10.18, 0.56	
2,4-Dimethylaniline	4.84		
2,6-Dimethylaniline	3.95		
3,5-Dimethylaniline	4.78		
2,3-Dimethylaniline	4.72		
2,5-Dimethylaniline	4.57		
3,4-Dimethylaniline	5.17		
N-Methylaniline	4.84		
N,n-Propylaniline	4.79		

Table II.ii Ionisation constants for the alkylbenzoic acids.

Compound	pKa Values	
	Literature [113]	Estimated [87]
Benzoic Acid		4.20
2-Methylbenzoic acid	3.93	3.88
3-Methylbenzoic acid	4.29	4.26
4-Methylbenzoic acid	4.41	4.34
4-Ethylbenzoic acid		4.35
4-Propylbenzoic acid		4.35
4- <i>iso</i> Propylbenzoic acid	4.36	4.35
4-Butylbenzoic acid		4.35
4-Pentylbenzoic acid		4.35
4-Hexylbenzoic acid		4.35
4-Heptylbenzoic acid		4.35
4-Octylbenzoic acid		4.35
4-Nonylbenzoic acid		4.35
4-Decylbenzoic acid		4.35
2,5-Dimethylbenzoic acid	4.04	3.97
3,4-Dimethylbenzoic acid	4.50	4.40
2,4-Dimethylbenzoic acid	4.30	4.08
3,5-Dimethylbenzoic acid	4.39	4.32
2,3-Dimethylbenzoic acid	3.80	3.97
2,6-Dimethylbenzoic acid	3.26	3.47
2,4,6-Trimethylbenzoic acid		3.67
2-Aminobenzoic acid	2.11, 4.95	2.05, 4.95
3-Aminobenzoic acid	3.12, 4.74	3.53, 4.32
4-Aminobenzoic acid	2.41, 4.85	3.67, 3.89
2-Dimethylaminobenzoic acid	8.51	3.77, 5.51
2-Iodobenzoic acid		2.86
3-Iodobenzoic acid		3.85
4-Iodobenzoic acid		3.99



## Appendix III.

### Study of the Alkylpyridines by HPLC.

#### 1. Introduction.

High performance liquid chromatography (HPLC) offers an alternative method for the separation of compounds to CE. In reversed-phase (RP) HPLC compounds are separated according to their partition between a non-polar stationary phase and a polar water-organic modifier mobile phase. Thus compounds separate according to their hydrophobicity which is linked to the log P [114] of the compounds, the partitioning constant for the distribution of a compound in a solvent-water mixture (usually octanol). The pH of the mobile phase in liquid chromatography can be altered by using buffers, but suppression of ionisation by organic solvents often causes a shift in  $pK_a$  values of compounds to values lower than their  $pK_a$  values in aqueous media.

Claessens et al. [115] used the probe compounds 2-hexyl- and 2-heptylpyridine in a study of eight columns. The analysis of basic compounds, such as pyridine and its derivatives can be used to probe the heterogeneity of the RP surface and changes that can occur in the surface with time.. Large differences in the asymmetry of peaks were observed with simple organic solvent-water mixtures and acetonitrile gave rise to the most asymmetric peaks. In another study by McCalley [116], relatively little difference in asymmetry when using acetonitrile-water compared to methanol-water was observed for pyridine. He also studied the performance of pyridine and pyridine derivatives [117, 118] on a range of commercially available ODS stationary phases. Significant peak shape differences were obtained for pyridine and alkyl-substituted derivatives when using a silica-based RP column. Such differences were attributed to steric

hindrance around the basic nitrogen in 2-substituted derivatives, leading to reduced silanol interactions.

In this study, the selectivity of some octadecyl silica (ODS) reversed phase columns are studied for the separations of the dimethylpyridines (DMPs) and the correlation of retention with log P values for the DMPs is investigated. The optimisation of the separation of the DMPs by variation of apparent pH of mobile phase is also investigated and comparisons are drawn with the separation of the DMPs by CE [119] at different pH values.

## 2. Experimental.

### Chemicals.

All alkyipyridines (Aldrich, Poole, UK) were used as received. Acetonitrile of HPLC grade was obtained from FSA (Loughborough, Leics. UK). Buffers were prepared from potassium dihydrogen phosphate of analytical grade (FSA) and sodium hydroxide of analytical grade (FSA).

### Apparatus.

The HPLC apparatus consisted of a two constaMetric<sup>®</sup> 3000 HPLC pumps (Milton Roy LDC, Florida, USA) and a constaMetric<sup>®</sup> 3500 HPLC pump (Milton-Roy LDC Analytical), dynamic mixer, a column temperature controller unit (Jones Chromatography), autosampler (Spark-Holland) containing a 7010-080 valve (Rheodyne), and a spectroMonitor<sup>®</sup> 5000 diode array detector (Milton-Roy LDC Analytical). A personal computer ran the system using LCtalk software (LCD Analytical).

### Methods.

Alkylpyridine stock solutions were prepared by diluting 20 mg of the alkylpyridine in water : acetonitrile mixture (10 mL, 70:30 by volume). Sample solutions were prepared by taking 0.5 mL of each alkylpyridine solution and diluting it in 10 mL of mobile phase. 20  $\mu$ L samples were injected and separated at 1 mLmin<sup>-1</sup>. UV absorbency was monitored at 254 nm.

The stationary phases were used as received and were 5  $\mu$ m particles packed in 25 cm x 4.6 mm columns. The phases used were Inertsil ODS (HICROM) Spherisorb ODS-1 (HICROM), Spherisorb ODS-B (Phasesep, Deeside), and Primesphere (Phenomenex, Macclesfield).

### **3. Results & Discussion.**

#### Study at pH 8.0.

With pKa values in the region 5-6 (Appendix II) [103] it was expected that the DMPs would be uncharged at pH 8.0. The four different stationary phases were investigated with the DMPs as test compounds. As would be expected, for the four different reversed phase materials general similarities in retention behaviour between columns was observed. For Primesphere ODS and Inertsil ODS the elution order 2,6-DMP, 2,3-DMP, 2,4-DMP, 2,5-DMP, 3,4-DMP, 3,5-DMP was observed although 2,5-DMP and 2,4-DMP were not resolved on the Inertsil ODS column. Maximum resolution of the compounds was obtained at 30% acetonitrile mobile phase. For Spherisorb ODS-B and Spherisorb ODS-1 higher retention times were observed and the elution order of 2,5-DMP and 2,4-DMP were transposed giving an elution order of 2,6-DMP, 2,3-DMP, 2,5-DMP,

2,4-DMP, 3,4-DMP, 3,5-DMP. The retention factors show this general trend in selectivity (Table III.i). Reasons for the reversal in the retention order of 2,5-DMP and 2,4-DMP are unclear.

**Table III.i**      *Retention factors for the dimethylpyridines separated on four commercially available stationary phases. 30% Acetonitrile : 70% phosphate buffer (apparent pH 8.0) mobile phase.*

Compound	Retention Factors k			
	Phenomenex Primesphere	Inertsil ODS	Spherisorb ODS-B	Spherisorb ODS-1
3,5-DMP	3.89	3.98	5.60	6.98
3,4-DMP	3.37	3.48	5.26	6.97
2,5-DMP	3.08	3.28	4.51	6.13
2,4-DMP	3.03	3.28	4.75	6.88
2,3-DMP	2.89	3.11	4.31	6.11
2,6-DMP	2.45	2.68	3.36	4.70

The separation of compounds may be related to their log P values, thus the log P of the DMPs were calculated using ProLogD. The values calculated for each isomer was the same at 1.67. Literature values were found. Only the logP values of three DMPs were available (Table III.ii) [114].

Table III.ii

Literature values of log *P* values in benzene-water [114] and *pK<sub>a</sub>* values [103] for the dimethylpyridines.

Compound	<i>pK<sub>a</sub></i>	Log <i>P</i>
2,6-DMP	6.77	1.31
2,4-DMP	6.72	1.36
2,3-DMP	6.60	-
3,4-DMP	6.52	-
2,5-DMP	6.47	-
3,5-DMP	6.25	1.51

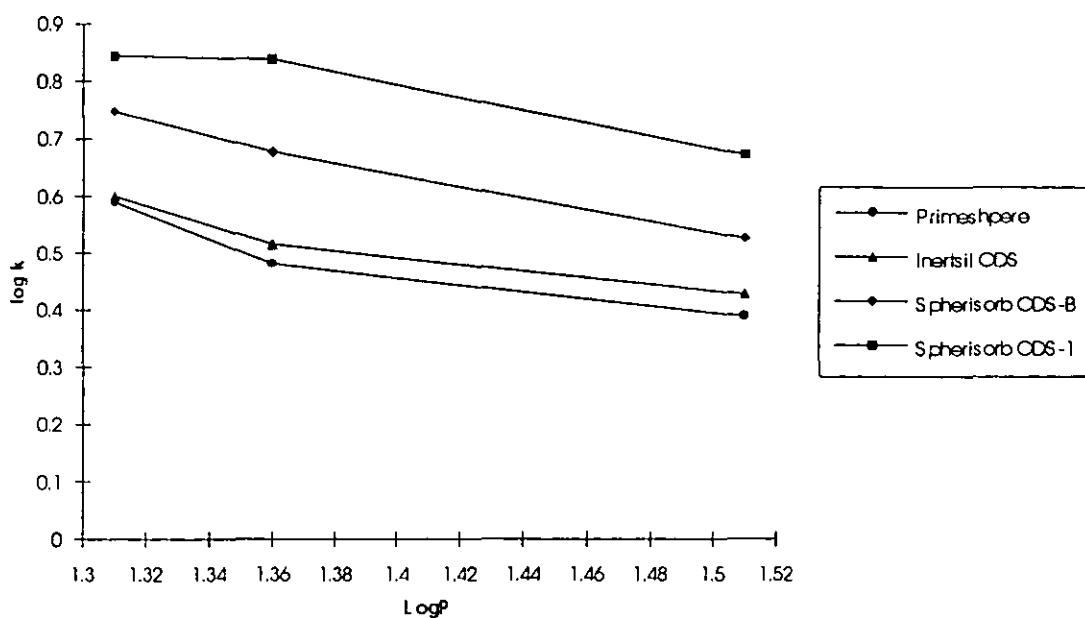


Figure III.i

The correlation between literature log *P* values and the retention factors obtained for 2,6-DMP, 2,4-DMP and 3,5-DMP.

A correlation between log P and the retention factors for the DMPs was observed (Figure III.i) for each stationary phase. However, one would expect the retention factor of a compound to increase with increasing logP based on the hydrophobicity of compounds. For the DMPs the reverse of this behaviour was observed and reasons are unclear.

#### Study across the pH range.

By varying the charge on the DMPs the effective polarity of the analytes can be changed and thus different retention times of compounds was expected. Charges on the DMPs vary according to the pKa of the analytes and thus different elution orders of compounds may occur. The pKa values of the DMPs have been quoted elsewhere [103, Table II.i] and combining the retention factors of the separation at pH 8.0 (where the DMPs were expected to be neutral) with the Hendersson-Hasselbach equation [105] (equation III.i) a retention-pH profile could be constructed (Figure III.2 for Primesphere). Such a pH profile assumes that the chromatographic retention of analytes is proportional to the charge on the analytes with the constant of proportionality being the chromatographic retention of the neutral analyte.

$$k = k_8 \left( \frac{1}{1 + 10^{\rho K_a - \text{pH}}} \right) \quad (\text{III.i})$$

where  $k$  is the retention factor of the compound at any pH and  $k_8$  is the retention factor of the compounds at pH 8. For such a relationship to hold, the compounds must be unretained at low pH ( $k = 0$ ). The retentions of the compounds were measured at pH 2.5 and found to be identical to pyridine which was used as a void volume marker at this pH.

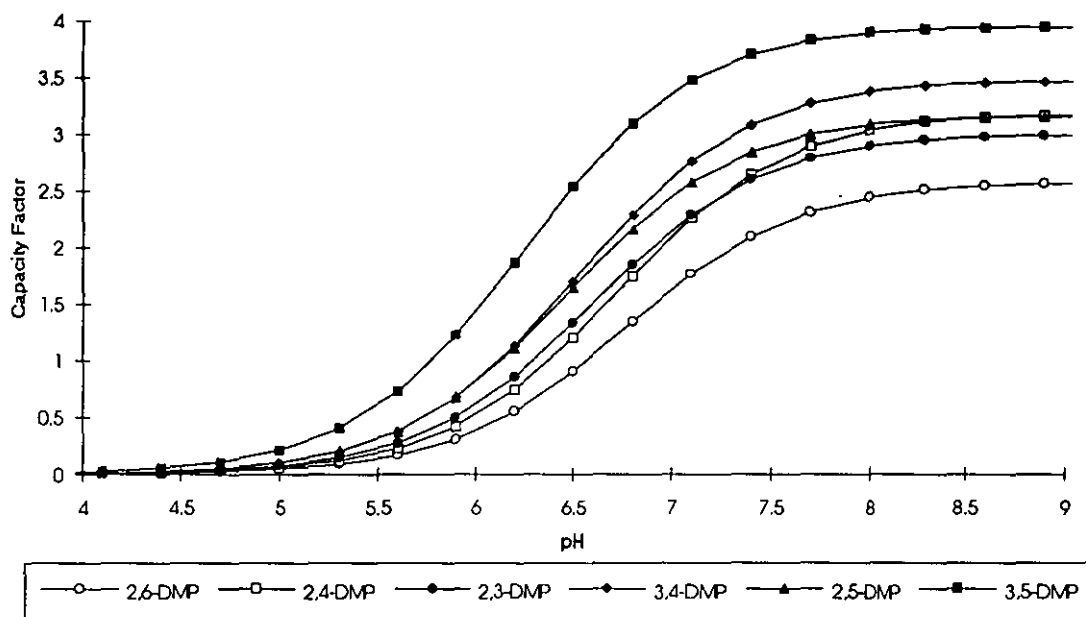


**Figure III.ii**      *Retention factor - pH profile for DMPs on Primesphere predicted from pKa data and the measured retention factors of the DMPs at pH 8.0.*

Similar curves for the predicted retention factor-pH profiles were also calculated for the other stationary phases. An optimum pH for separation of the DMPs was predicted to occur at pH 6.7 [119], based on the largest difference in effective charge between analytes. To compare the calculated retention factors (Figure III.ii) and the experimental change in retention factor with pH the retention factors of each compounds were measured at different pH values (Table III.iii) for Primesphere. The elution order of the compounds changed as predicted with an optimum separation at pH 5.8 (Figure III.3). However, the changes in retention order occurred at a lower apparent pH than was predicted which is probably due to the presence of acetonitrile in the mobile phase causing suppression of ionisation. The main reversal in elution order is for 2,4-DMP and 2,3-DMP. A previous study of the DMPs by CE showed a greater scrambling in migration order between pH 2.5 and pH 7 [119]. For HPLC, only small changes

in elution order occur because of the similarities between the mechanisms of separation since the charge on the DMPs is linked to the polarity of the compounds.

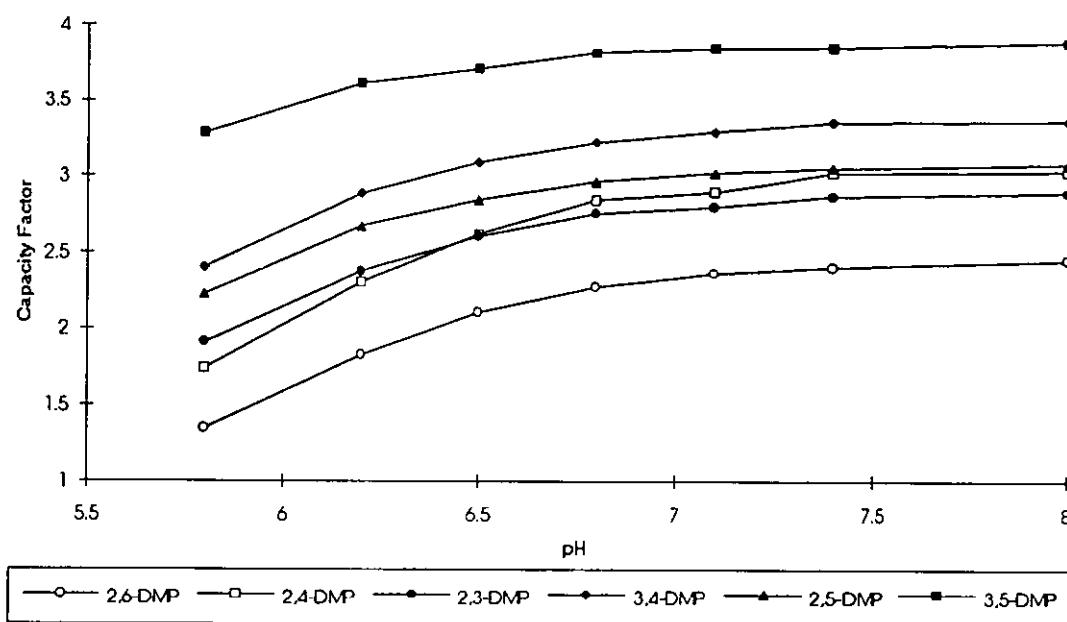


**Figure III.iii**      *Variation in retention factors for the DMPs with apparent pH of the acetonitrile : phosphate buffer mobile phase (30:70). Primesphere ODS stationary phase.*



**Table III.iii**      *Retention factors for the DMPs with different pH. Acetonitrile : phosphate buffer mobile phase (30:70), Primesphere stationary phase.*

pH	Retention Factors					
	2,6-DMP	2,4-DMP	2,3-DMP	3,4-DMP	2,5-DMP	3,5-DMP
5.8	1.35	1.74	1.91	2.40	2.23	3.29
6.2	1.83	2.31	2.38	2.89	2.67	3.61
6.5	2.10	2.62	2.60	3.09	2.84	3.71
6.8	2.27	2.84	2.75	3.22	2.96	3.82
7.1	2.36	2.89	2.80	3.29	3.02	3.84
7.4	2.40	3.02	2.87	3.36	3.05	3.85
8.0	2.45	3.03	2.89	3.37	3.08	3.89

The predicted retention factor - pH profile for Spherisorb ODS-B (Figure III.iv) and the experimental results (Figure III.5, Table III.4) also show a correlation with the optimum separation occurring at pH 5.8, a shift of approximately one pH unit from the predicted optimum. The cross over in the retention order of 2,3-DMP and 2,4-DMP is clearly seen for this stationary phase. For this stationary phase resolution of all six isomers can be achieved at either pH 8.0 or pH 5.8.

**Table III.iv**      *Retention factors for the DMPs with varying pH. 30:70 acetonitrile : water mobile phase, Spherisorb ODS-B stationary phase.*

pH	Retention Factors					
	2,6-DMP	2,4-DMP	2,3-DMP	3,4-DMP	2,5-DMP	3,5-DMP
5.8	2.14	3.05	3.13	4.10	3.59	5.06
6.2	2.77	4.00	3.86	4.85	4.18	5.51
6.5	3.05	4.39	4.09	5.11	4.40	5.64
6.8	3.26	4.62	4.32	5.39	4.48	5.84
7.1	3.34	4.74	4.31	5.34	4.52	5.73
7.4	3.37	4.77	4.32	5.28	4.54	5.64
8.0	3.36	4.75	4.31	5.26	4.51	5.60

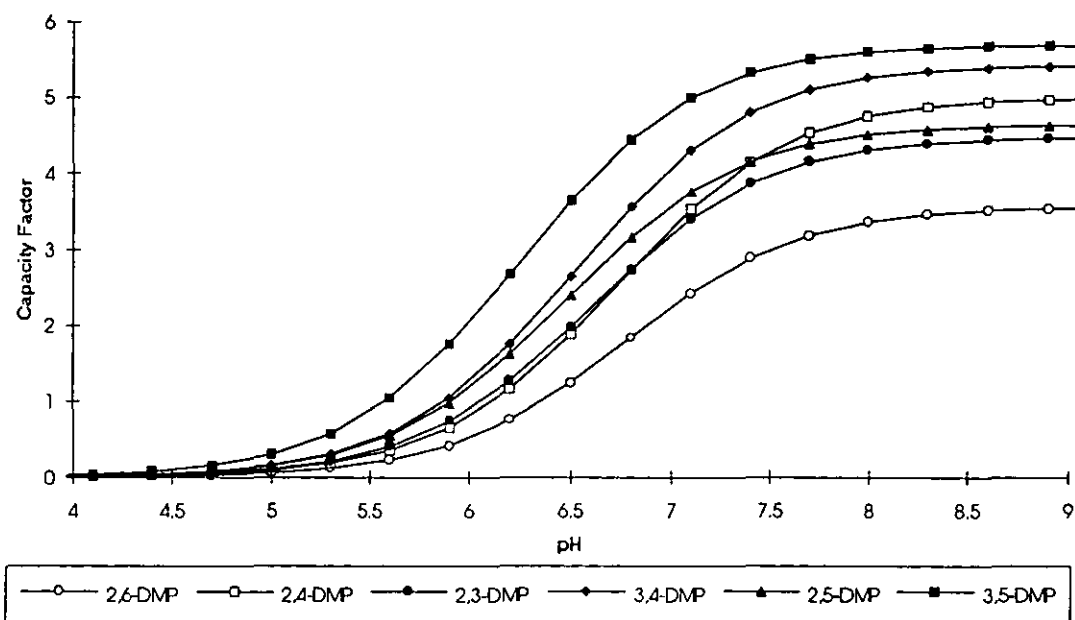


**Figure III.iv** Retention factor - pH profile for Spherisorb ODS-B predicted from pKa data and the retention factors of the DMPs at pH 8.0.

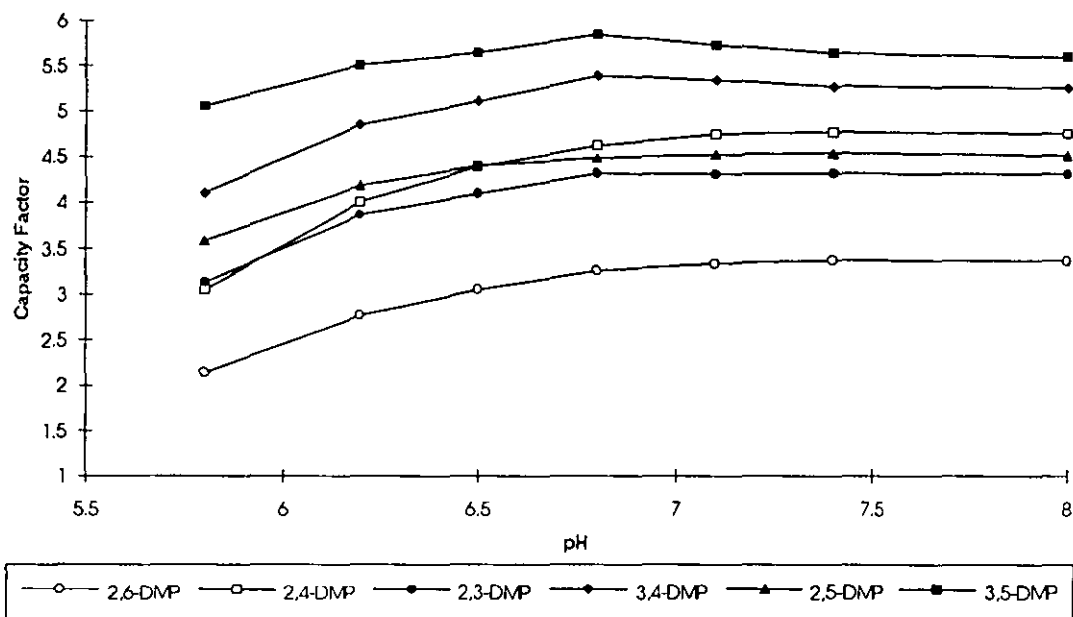


**Figure III.5** Variation in retention factors for the DMPs with apparent pH of the 30:70 acetonitrile : phosphate buffer mobile phase.

#### **4. Conclusions.**

The dimethylpyridines were separated by HPLC. As neutral molecules the DMPs were shown to elute in order of their logP values (where known) although small differences in selectivity between commercial stationary phases was observed. By adjusting the apparent pH of the buffered mobile phase differences in the elution order of the DMPs were observed, and the order of elution was governed by the differences in the dissociation constants of the compounds.

## Appendix IV

### Presentations and Publications

#### Oral Presentations

1. *Optimisation of the Separation of Six Dimethylpyridines by Capillary Electrophoresis.*  
Research Topics in Chromatography, (Chromatography and Electrophoresis Group; South East Region of the Analytical Division, University of Surrey) April 95.
  
2. *The Effects of Size and Shape on the Mobility of Analytes by Capillary Electrophoresis.*  
Zeneca Pharmaceuticals, Macclesfield, December 96.
  
3. *Prediction of Electrophoretic Mobility in Capillary Electrophoresis by Molecular Modelling.*  
Research and Development Topics in Analytical Chemistry meeting, Nottingham Trent University, 22-23 July 1996.
  
4. *Effect of Size and Shape on Electrophoretic Mobility of Analytes in Capillary Electrophoresis.*  
19th International Symposium on Chromatography, Stuttgart (September 1996).

## Poster Presentations

- 1. Molecular Size/Shape Effects in the Separation of the Dimethylpyridines and Related Compounds by Capillary Electrophoresis.*

18th International Symposium on Chromatography, Bournemouth (19-24 June 1994).
- 2. Separation and Identification of the Z and E Isomers of 2-(3-pentenyl)pyridine by Capillary Electrophoresis and Nuclear Magnetic Resonance.*

Research and Development Topics in Analytical Chemistry meeting (18-19 July 1994) and Third International Symposium on Capillary Electrophoresis (24-26 August 1994, University of York).
- 3. Molecular Charge Effects in the Separation of Substituted Pyridines by Capillary Electrophoresis.*

Poster presentation at the Third International Symposium on Capillary Electrophoresis (24-26 August 1994, University of York)
- 4. The Investigation of Substituted Pyridines by Capillary Electrophoresis and Molecular Modelling.*

HPLC '95, Innsbruck, Austria, 30 May - 2 June 1995 and SAC conference, Hull, 19-21 July 1995.
- 5. Modelling of the Diffusion Characteristics of Alkylpyridines under Electrophoresis.*

Research and Development Topics in Analytical Chemistry meeting, Hull, 18-19 July 1995.

6. *Modelling of the Shapes of Compounds by Capillary Electrophoresis.*  
Eighteenth International Symposium on Capillary Chromatography,  
Riva del Garda, Italy, 20-24 May 1996
  
7. *The Retention of Alkylbenzoic Acids in Alkyl Bonded Capillaries by Capillary Electrophoresis.*  
Eighteenth International Symposium on Capillary Chromatography,  
Riva del Garda, Italy, 20-24 May 1996
  
8. *Modelling of the Shapes of Compounds by Capillary Electrophoresis.*  
Fourth International Symposium on Capillary Electrophoresis (21-23 August 1996, University of York).

### **Publications**

1. *Molecular Size/Shape Effects in the Separation of the Monosubstituted Alkyl Pyridines using Capillary Electrophoresis.*  
Electrophoresis, 1994, 15, 635-639.
  
2. *Separation and Identification of the Z and E Isomers of 2-(3-pentenyl)pyridine by Capillary Electrophoresis and Nuclear Magnetic Resonance Spectroscopy.*  
J. Chromatogr. A, 1995, 700, 69-72
  
3. *Optimisation of the Separation of the Six Dimethylpyridines by Capillary Electrophoresis.*  
J. Chromatogr. A, 1996, 730, 321-328.



Donald C. Rowe  
 Stephen A. C. Wren  
 Andrew G. McKillop

Zeneca Pharmaceuticals, Alderley  
 Edge, Macclesfield, Cheshire

## Molecular size/shape effects in the separation of the monosubstituted alkyl pyridines using capillary electrophoresis

A series of monosubstituted alkyl pyridines have been used to investigate the presence of molecular size/shape effects in capillary electrophoresis and the applicability of various descriptors in discriminating not only between derivatives of differing chain length but also between positional isomers. Although van de Waals' radii and Offord's parameters are extremely good descriptors in predicting the relative mobilities of the derivatives, a further descriptor involving length and/or diameter of the molecule is necessary for discrimination between the positional isomers.

### Introduction

Capillary electrophoresis (CE) is fast becoming a technique complementary to HPLC for analysing small organic molecules [1]. Whereas in HPLC analytes are separated on the basis of differences in distribution, in CE the separation is on the basis of differences in mobility arising from differences in charge and molecular size. In the simplest form of CE (open tubular), the apparent mobility ( $\mu_{app}$ ) of a charged molecule in an electric field is given by the sum of its electrophoretic mobility ( $\mu_{epb}$ ) and the mobility of the background electrolyte (the electroosmotic mobility  $\mu_0$ ).

$$\mu_{app} = \mu_{epb} + \mu_0 \quad (1)$$

The electroosmotic mobility arises because of the ionisation of the silanol groups on the capillary wall and this is considerably reduced as the pH of the buffer solution is decreased. It is directly proportional to the dielectric constant ( $\epsilon$ ) and the zeta potential ( $\zeta$ ),

$$\frac{\epsilon \zeta}{\eta} \quad (2)$$

where  $\eta$  is the viscosity of the buffer.

Using a modified form of the Stokes equation for a spherical particle moving in a medium regarded as a hydrodynamic continuum, the electrophoretic mobility can be related to the electric charge  $q$  and the hydrodynamic radius  $r_s$  of the analyte,

$$\mu_{epb} = \frac{q}{6\pi r_s \eta} \quad (3)$$

However, for small organic ions 3–5 Å in radius, Edward and Waldron-Edward [2] have argued that the factor  $6\pi$  should be replaced by factor  $5\pi$ . The authors also proposed that the free solution mobility of ions in infinitely dilute aqueous solution at 25°C can be given by the equation

$$\mu_{epb} = \frac{1.14 \times 10^{-3} \times Z f}{r_s f_0} \quad (4)$$

Correspondence: Dr. R. C. Rowe, Pharmaceutical Department, Zeneca Pharmaceuticals, Hurdsfield Industrial Estate, Macclesfield, Cheshire SK10 2NA, England

where  $r_s$  is the van der Waals' radius (Å) of the ion,  $Z$  is the ionic charge in electronic units, and  $f/f_0$  is the frictional ratio for non-spherical molecules (unity for spheres, less than unity for prolate ellipsoids and greater than unity for oblate ellipsoids). This is an important equation in the field of CE since it introduces the concept of molecular size and shape.

An additional relevant equation is suggested by Offord [3] for the mobility of peptides in a fibrous media such as paper,

$$\mu_{epb} = \frac{\kappa Z}{M^{1/3}} \quad (5)$$

where  $\kappa$  is a constant and  $M$  the molecular weight of the charged species.  $M^{1/3}$  is dimensionally equivalent to the effective surface area of the molecule. Although semiempirical the equation has been shown to be applicable to a wide range of peptides including recently the capillary electrophoresis of the oligoglycines and oligoalanines [4]. In this work these concepts have been applied to the separation of the monosubstituted alkyl pyridines using CE.

### 2 Materials and methods

Work was carried out on a PACE 2100 system (Beckman Instruments, High Wycombe, UK) using a fused silica capillary (Beckman) with an internal diameter of 75  $\mu\text{m}$ , a total length of 57 cm and a length from inlet to detector of 50 cm. Samples were loaded by a 2 s pressure injection and separated at 25°C using a voltage of 15 kV. Data was recorded at 254 nm using a 2 Hz collection rate. The *n*-alkyl pyridines, obtained from Aldrich (Poole, UK), were chosen because of their water solubility, strong UV absorbance at 254 nm and  $pK_a$  values (e.g. for pyridine 5.2), i.e. they are fully protonated at pH 2.5. Stock solutions of 1 mg mL<sup>-1</sup> were made up in water before being diluted to 0.01 mg mL<sup>-1</sup> with a phosphate buffer prepared from 40 mM of lithium hydroxide (FSA, Loughborough UK) and adjusted to pH 2.5 with orthophosphoric acid (BDH, Poole, UK). Electrophoretic mobilities  $\mu_{app}$  of all derivatives were determined using the equation

$$\mu_{app} + \mu_0 = \frac{IL}{Vt} \quad (6)$$

2646

where  $l$  is the length from inlet to detector,  $L$  is the total capillary length,  $V$  is the operating voltage,  $t$  is the migration time and  $\mu_0$  is the electroosmotic mobility. Reproducibility between duplicate injections was typically  $\pm 1.5\%$ . Van der Waals' radii of all the derivatives were calculated from their van der Waals' volumes using group contribution data given by Edward and Waldron-Edward [2]. Other dimensions were calculated using molecular modelling (Alchemy II, Tripos Associated Inc.) after energy minimisation (Fig. 1).

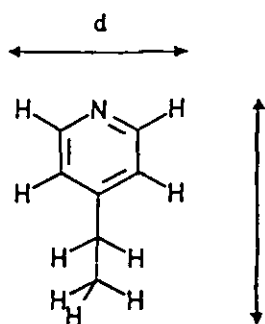


Figure 1. Dimensions of molecule measured after molecular modelling.

### 3 Results and discussion

#### 3.1 Separation efficiency

Figure 2 shows the separation of the 2, 3 and 4 methylpyridines. Spiking experiments indicated that the 2- and 4-derivatives comigrated ahead of the 3-derivatives. This is in contrast with earlier work using overload conditions (as opposed to the low sample loadings used here) where all three derivatives could be separated by optimisation of the pH and reduction of electroosmotic mobility [5]. However, in this work with different objectives resolution was maximised by operating at pH 2.5 thus minimising the electroosmotic mobility. With a mixture of 2,3 and 4 ethylpyridines all three components were separated (Fig. 3) with the fastest migrating 4-derivative being partially resolved from the 3-derivative. In all

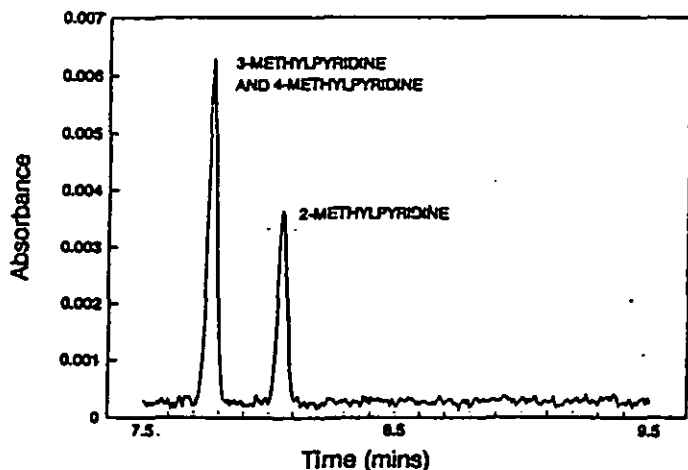


Figure 2. Separation of the 2, 3 and 4-methylpyridines showing comigration of the 3- and 4-derivatives.

subsequent experiments the 2-, 3- and 4-derivatives were run as a separate series with migration orders determined by spiking experiments.

#### 3.2 Mobility of the 2-derivatives

Figure 4 shows the separation of pyridine and the 2-methyl, ethyl, *n*-propyl, *n*-pentyl and *n*-hexyl derivatives. The components are all first-component, pyridine, having the greatest electrophoretic mobility. Note that the efficiency of separation appears to be relatively independent of the molecular weight with values for pyridine and 2-pentylpyridine being 220 000 and 190 000 theoretical plates respectively. This is consistent with the work of Kenndler and Schwer [6] who stated that under optimum conditions the efficiency should be independent of the mass and directly proportional to charge. Mobility data on the 2-derivatives (Table 1) show a decrease in mobility with increasing length of alkyl chain, with a 40% decrease in mobility and a doubling in molecular weight. While calculations of van der Waals' radii show only a 40% increase, calculations from molecular modelling indicate an increase in diameter of the molecule of some 180%. Linear regression anal-

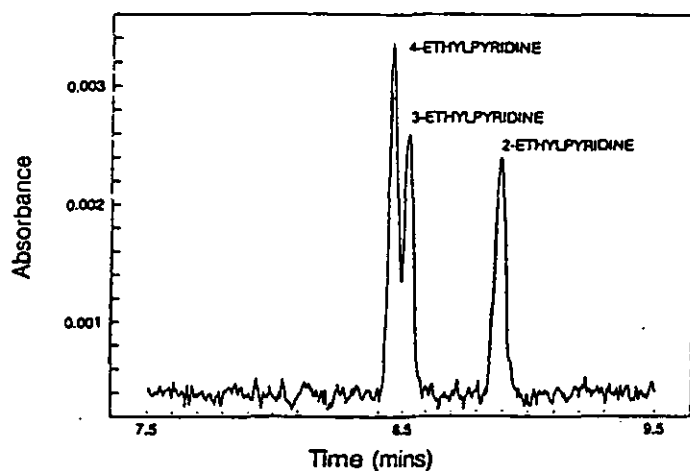


Figure 3. Separation of the 2, 3 and 4-ethylpyridines.

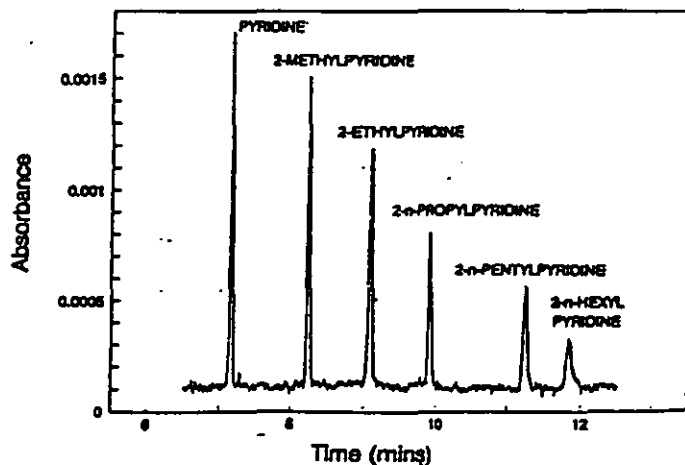


Figure 4. Separation of the 2-methyl, ethyl, *n*-propyl, *n*-pentyl and *n*-hexyl derivatives.

1. Data on 2-derivatives

Compound	Mobility $\times 10^{-4}$ $\mu/\text{cm}^2\text{V}^{-1}\text{s}^{-1}$	Molecular weight M	Van der Waals' radius ( $r_w$ ) Å	Diameter ( $d$ ) Å
benzylpyridine	4.555	79.10	2.45	4.16
ethylpyridine	3.946	93.13	2.66	5.37
propylpyridine	3.577	107.16	2.84	6.75
isopropylpyridine	3.268	121.18	3.00	8.01
butylpyridine	2.869	149.22	3.27	10.52
hexylpyridine	2.715	163.26	3.39	11.80

(Table 2) shows good correlation between mobility and the reciprocal of van der Waals' radius and diameter as well as between mobility and  $M^{-0.66}$ . The similarity in the magnitude of the gradient in respect to the variable  $1/d$  with that given by Eq. (4) would appear to be fortuitous. The good correlation in respect to the variable  $1/r_w$  implies a similar frictional ratio for all the derivatives studied. In all cases the extrapolated intercept is different from the electroosmotic mobility measured using the neutral marker benzyl alcohol ( $0.35 \times \text{cm}^2\text{V}^{-1}\text{s}^{-1}$ ).

Mobility of the 4-derivatives

These derivatives molecular modelling showed a constant diameter but an increasing length of alkyl chain. The data (Table 3) shows a decrease in mobility with increasing length of alkyl chain, with a 25% decrease in mobility and a 53% increase in molecular weight (cf. the 2-derivatives). Calculations of van der Waals' radii show an increase of 22% but an increase in length of 142%. Linear regression analysis (Table 4) shows very good correlation between mobility and the variables  $1/r_w$  and  $M^{-0.66}$  with less (but still highly significant) correlation with the reciprocal of the length. The intercept in respect to the variable  $M^{-0.66}$  is insignificantly different from zero.

Mobility of the 3-derivatives

These derivatives molecular modelling indicated a trapezoid shape (in two dimensions) (Fig. 5), with a constant length. Hence three diameters could be calculated, the maximum diameter  $d_{\text{max}}$ , the arithmetic mean

2. Regression analysis on 2-derivatives

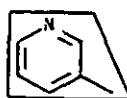
Variable	Intercept $\pm$ SE $\times 10^{-4}$	Gradient $\pm$ SE $\times 10^{-3}$	$r^2$
$1/r_w$	$-2.076 \pm 0.150$	$1.613 \pm 0.043$	0.9971
$1/d$	$+1.770 \pm 0.058$	$1.173 \pm 0.373$	0.9960
$1/M^{0.66}$	$-0.287 \pm 0.146$	$8.537 \pm 0.325$	0.9943

3. Data on 4-derivatives

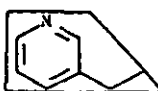
Compound	Mobility $\times 10^{-4}$ $\mu/\text{cm}^2\text{V}^{-1}\text{s}^{-1}$	Molecular weight M	Van der Waals' radius ( $r_w$ ) Å	Diameter ( $d$ ) Å
benzylpyridine	4.555	79.10	2.45	3.85
ethylpyridine	4.091	93.13	2.66	4.76
propylpyridine	3.757	107.16	2.84	6.06
isopropylpyridine	3.445	121.18	3.00	9.34

Table 4. Regression analysis on 4-derivatives

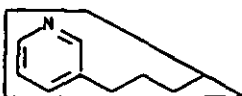
Variable	Intercept $\pm$ SE $\times 10^{-4}$	Gradient $\pm$ SE $\times 10^{-3}$	$r^2$
$1/r_w$	$-1.437 \pm 0.124$	$1.470 \pm 0.034$	0.9990
$1/d$	$+2.617 \pm 0.129$	$0.725 \pm 0.066$	0.9833
$1/M^{0.66}$	$+0.068 \pm 0.066$	$8.032 \pm 0.136$	0.9994



3-METHYLPYRIDINE



3-ETHYLPYRIDINE



3-N-BUTYLPYRIDINE

Figure 5. Schematic diagram showing the trapezoid shape of the 3-alkyl pyridines used in the study. Only the carbon skeleton is shown for clarity.

of the two diameters  $d_{\text{max}}$  or the diameter of the molecule at its centre of gravity  $d_{\text{cog}}$  (Table 5). The data (see Table 5) shows a decrease in mobility with an increase in alkyl chain length and a 30% decrease in mobility and a 70% increase in molecular weight. Dimensional changes are shown in Table 5. Linear regression analysis shows very good correlation between mobility and the variables  $1/r_w$  and  $M^{-0.66}$  (Table 6). The correlation between mobility and the reciprocal of the diameter would appear to be best for the derived diameters  $d_{\text{max}}$  and  $d_{\text{cog}}$ . As with the 4-derivatives the intercept in respect to the variable  $M^{-0.66}$  is insignificantly different from zero.

## Separation and identification of the *Z* and *E* isomers of 2-(3-pentenyl)pyridine by capillary electrophoresis and nuclear magnetic resonance spectroscopy

Andrew G. McKillop<sup>a</sup>, Roger M. Smith<sup>a,\*</sup>, Raymond C. Rowe<sup>b</sup>,  
Stephen A.C. Wren<sup>b</sup>

<sup>a</sup>Department of Chemistry, Loughborough University of Technology, Loughborough, Leics. LE11 3TU, UK

<sup>b</sup>Zeneca Pharmaceuticals, Hurdfield Industrial Estate, Macclesfield, Cheshire, SK10 2NA, UK

### Abstract

A mixture of the *Z* and *E* isomers of 2-(3-pentenyl)pyridine has been separated with baseline resolution by capillary electrophoresis. Using molecular modelling it was proposed that the smaller more rapidly migrating peak would be the *Z* isomer. This agreed with a 38:62 (*Z/E*) composition by nuclear magnetic resonance spectroscopy. The sample was also investigated by gas chromatography coupled to mass spectrometry.

### 1. Introduction

Capillary electrophoresis (CE) is rapidly developing as a complementary technique to high-performance liquid chromatography (HPLC) for the separation of small molecules [1]. Since CE is based on different physicochemical properties than HPLC, different performance characteristics are obtained, such as higher efficiencies and rapid times of separation. Together with low consumption of buffer and small sample requirements, it is clear that CE is an attractive method of separation for the pharmaceutical industry.

Separation in CE depends on the movement of the analyte ions in the applied electrical field. The electrophoretic mobility,  $\mu$ , of a particle is defined as the steady state velocity per unit field strength,  $\mu = q/f$ , where  $q$  is the charge on the analyte and  $f$  is the frictional coefficient of the

analyte. Thus, the principal parameters that can influence separation are the charge on the analyte,  $q$ , and the factors which influence the frictional coefficient,  $f$ , which are the size of the analyte and also the shape of the analyte ion.

Rowe et al. [2] have investigated the influence of size/shape on the separation of the monosubstituted alkyl pyridines. The separation of positional isomers was achieved and various molecular descriptors were investigated to predict the mobility of the analytes. Chadwick and Hsieh [3] have also reported the separation of the alkenes, fumaric acid, maleic acid, all *trans*-retinoic acid and 13-*cis*-retinoic acid. Differences in mobility were ascribed to differences in shape of the alkenes, which were regarded as spheres with different hydrodynamic radii.

Quantitative impurity content determination by CE has been shown to be of comparable precision to HPLC by Altria [4,5]. It was shown that the analytes must have the same UV chro-

\* Corresponding author.

mophores or correction factors applied, and that peak areas must be normalised by migration time in order to correct for the effect of analytes spending different residence times in the portion of the capillary that acts as the detection cell, because of the different mobilities.

In this study a mixture of the *Z* and *E* isomers of 2-(3-pentenyl)pyridine were investigated as model compounds, and the relative abundance of each isomer was determined by CE and compared to the nuclear magnetic resonance (NMR) spectrum of the sample. The sample of 2-(3-pentenyl)pyridine was also investigated by gas chromatography coupled to mass spectrometry (GC-MS).

## 2. Experimental

### 2.1. Chemicals

The sample of 2-(3-pentenyl)pyridine was used as received from Aldrich (Poole, UK) and was a mixture of the *Z* and *E* isomers.  $^1\text{H}$  NMR spectra were run in deuterated chloroform on a 250 MHz AC250 Brüker NMR spectrometer. The sample of 2-(3-pentenyl)pyridine as a dilute solution in dichloromethane was also analysed using GC-MS on a Fisons GC 8000 gas chromatograph coupled to MD 800 mass spectrometer using a DB 5 ms column isothermally at 100°C. Molecular modelling measurements were made using Nemesis Sampler (Oxford Molecular).

### 2.2. Capillary electrophoresis

Work was carried out on a P/ACE 2050 system (Beckman Instruments, High Wycombe, UK) using a fused-silica capillary of 57 cm (50 cm to detector)  $\times$  75  $\mu\text{m}$  I.D. Samples were loaded by a 2-s pressure injection at the anode and separated using a voltage of 15 kV. The external temperature of the capillary was thermostated at 25°C. The capillary was rinsed between each injection with a rinse cycle of sodium hydroxide (0.1 *M*, 2 min) and running buffer (3 mins). The peaks were detected at 254 nm using a 2 Hz

collection rate. Electrophoretic separations were performed in a phosphate buffer (40 mM) prepared from orthophosphoric acid (BDH, Poole, UK) and adjusted to pH 2.5 with lithium hydroxide (1 *M*; FSA, Loughborough, UK).

## 3. Results and discussion

2-(3-Pentenyl)pyridine is marketed as a mixture of isomers and in a solution at pH of 2.5 these can readily be separated by CE in 11 mins (Fig. 1). Little method development was required, as 2-(3-pentenyl)pyridine was fully protonated under these conditions. However, it was not possible to directly assign structures to the peaks in the electropherogram but as electrophoretic mobility increases with decreasing size of the analyte it should be possible to use molecular modelling to predict the migration order of the isomers. When the lengths of the side chains were calculated, it was found from a molecular modelling package that the *E* isomer was fully extended with a length from the *ortho*-hydrogen on the pyridine ring to the end of the sidechain of 10.2 Å. The corresponding measurement for the *Z* isomer was 9.2 Å (Fig. 2). Thus the smaller peaks at 10.11 min was predicted to correspond to the *Z* isomer and the second larger peak at 10.31 min to the *E* isomer. These assignments agreed with the expected ratio of the isomers based on the greater thermodynamic stability of the *E* isomer.

In order to quantify the proportion of the two isomers, the absorbance of the analytes are required. Because of the similarity of the chromophore it was expected that the spectra would be effectively identical and this was confirmed using a CE system equipped with a diode array detector. Both peaks gave identical spectra with a maximum absorbance at 265 nm. It was also necessary to correct the peak areas by division by their migration times, in order to take account of the unequal residence time of the analytes in the detection window. Using this correction, the mean proportions over six runs was 40.9% for the minor isomer and 59.1% for

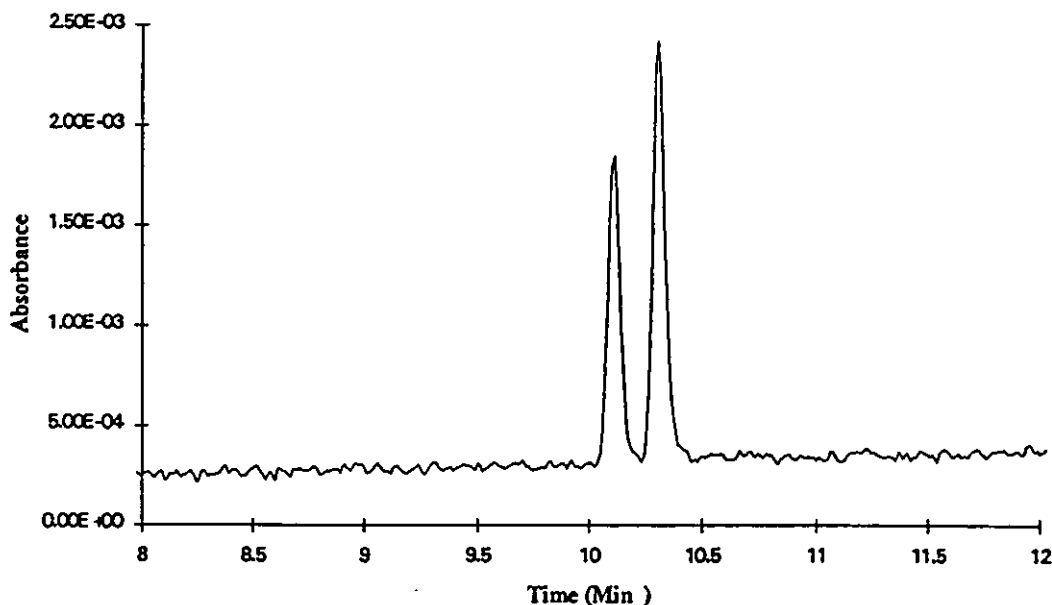


Fig. 1. Electropherogram showing the separation of (*Z*)- and (*E*)-2-(3-pentenyl)pyridine.

the major isomer with a standard deviation of 0.9%. The precision of these measurements is in agreement with the work of Altria [5], who reported precisions of 1–2% relative standard deviations.

Confirmation of the assignment of the isomers can be obtained by using  $^1\text{H}$  NMR spectroscopy to independently determine the proportion of the isomers. The shifts of the terminal methyl groups adjacent to the double bonds are different for the *Z* and *E* isomers, and each are split due to the adjacent protons. Coupling across the double bond was also observed, which split each methyl signal into a doublet of doublets and can be used to identify the isomers (Fig. 3). The

larger peaks showed a long-range coupling of 1.1 Hz and were therefore assigned to the *E* isomer, whereas the small peaks had a coupling of 0.6 Hz typical of a *Z* isomer. It was also predicted that the methyl group in the *Z* isomer would be more shielded than in the *E* isomer, thus it would occur at a higher field as was observed. The heights of the two methyl signals were compared to give relative concentrations of each isomer in the sample, giving a percentage of (*Z*)-2-(3-pentenyl)pyridine of 38% and (*E*)-2-(3-pentenyl)pyridine of 62% in agreement with the CE assignments.

In order to ensure that the two peaks were isomers and not homologues or other derivatives a sample of 2-(3-pentenyl)pyridine was also investigated by GC-MS. At 100°C under isothermal conditions, major peaks were obtained at 16.0 and 17.1 mins, which had identical mass spectra with molecular ions ( $m/z$  147), which correspond to 2-(3-pentenyl)pyridines. A minor impurity was also present. The proportions of the major peaks differed from those observed by the other techniques which was attributed to thermal equilibration of the isomers.

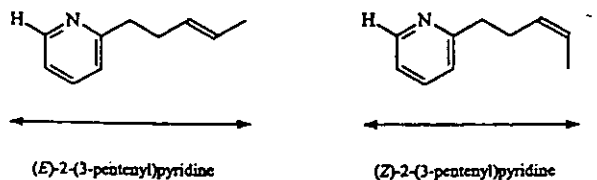


Fig. 2. Structures of (*Z*)- and (*E*)-2-(3-pentenyl)pyridine.

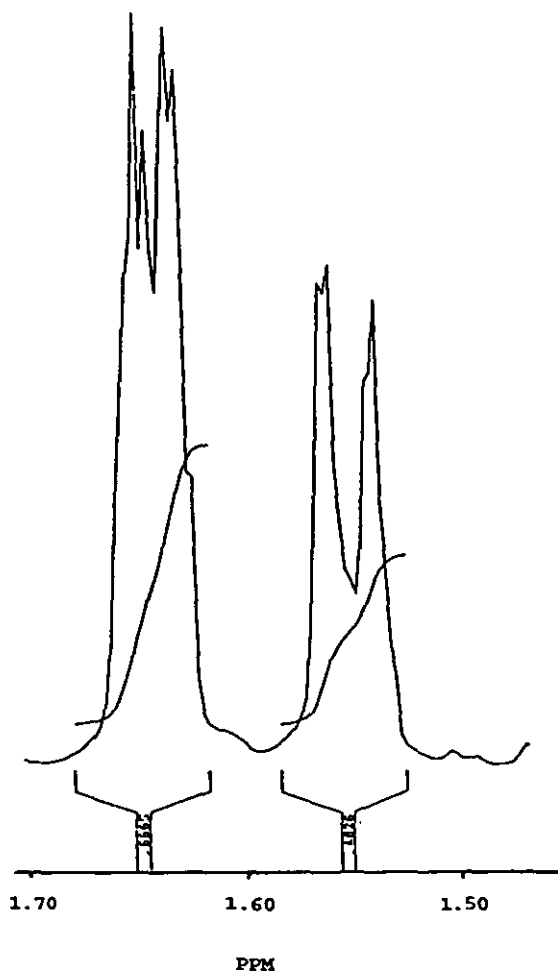


Fig. 3. Expanded methyl signals in the NMR spectrum of 2-(3-pentenyl)pyridine.

#### 4. Conclusions

The *Z* and *E* isomers of 2-(3-pentenyl)pyridine can be separated according to their shape by CE. By considering the shape of the molecules, it was possible to predict the order of migration which was subsequently confirmed by NMR spectroscopy.

#### References

- [1] C.W. Demarest, E.A. Monnot-Chase, J. Jiu and R. Weinburger, in P.D. Grossman and J.C. Colburn (Editors), *Capillary Electrophoresis – Theory and Practice*, Academic Press, San Diego, CA, 1992, Ch. 11. p. 301.
- [2] R.C. Rowe, S.A.C. Wren and A.G. McKillop, *Electrophoresis*, 15 (1994) 635.
- [3] R.R. Chadwick and J.C. Hsieh, *Anal. Chem.*, 63 (1991) 2377.
- [4] K.D. Altria, *Chromatographia*, 35 (1993) 177.
- [5] K.D. Altria, *LC·GC Int.*, 6 (1993) 616.



ELSEVIER

Journal of Chromatography A, 730 (1996) 321-328

JOURNAL OF  
CHROMATOGRAPHY A

## Optimisation of the separation of the dimethylpyridines by capillary electrophoresis

Andrew G. McKillop<sup>a</sup>, Roger M. Smith<sup>a,\*</sup>, Raymond C. Rowe<sup>b</sup>, Stephen A.C. Wren<sup>b</sup>

<sup>a</sup>*Department of Chemistry, Loughborough University of Technology, Loughborough, Leics. LE11 3TU, UK*

<sup>b</sup>*Zeneca Pharmaceuticals, Hurdsfield Industrial Estate, Macclesfield, Cheshire SK10 2NA, UK*

### Abstract

The separation of the isomers of dimethylpyridine has been studied by capillary electrophoresis. Studies at low pH where the dimethylpyridines all bear the same charge showed a partial separation probably due to size/shape effects. The charge profiles of the analytes calculated from their ionisation constants were compared with their separation between pH 2.5 and 9. The optimum resolution was found at a pH of 6.5 in the area of maximum charge difference between the dimethylpyridines.

**Keywords:** Capillary electrophoresis; Optimization; pH effects; Dimethylpyridines; Pyridines

### 1. Introduction

Capillary electrophoresis (CE) is a separation technique which has been successfully used to achieve the highly efficient separation of a vast range of analytes, ranging from biomolecules to smaller analytes, such as small organic molecules or inorganic ions [1]. Because the separation depends on the migration velocities of the analytes under the influence of the electrical field, it should be possible to predict the differences between the behaviour of even closely related compounds from their size and charge. By selecting a suitable buffer pH the analyst should be able to adjust the charge on partially ionised analytes to optimise the resolution of a mixture. If the ionisation constants ( $pK_a$  values) of the analytes are known then it should be also

possible to predict the conditions for maximum separation.

In previous studies, Terabe and co-workers studied the separation of oxygen isotopic benzoic acids as examples of closely related compounds [2]. An optimum pH for separation was calculated to be  $(pK_a - \log 2)$  based on the theoretical resolution equation in CE. The effects of applied voltage and capillary length were also investigated. Optimisation of pH in the separation of the methylpyridines was studied by Wren [3], who predicted that the maximum charge difference between two species could be calculated by taking the average of their  $pK_a$  values. The relationship between the calculated charge on an analyte and its electrophoretic mobility was investigated as well as the relationship with electroosmotic mobility. Separation of the methylpyridines was improved by the use of a cationic surfactant to suppress electroosmotic flow.

Friedl and Kenndler investigated resolution as a function of the pH of the buffer for multivalent ions,

\*Corresponding author. Tel. +44 (1509) 222 563; Fax: +44 (1509) 233 163.



including the benzenecarboxylic acids [4]. It was determined that resolution depended on two terms, the ratio of the electrophoretic mobilities and an efficiency term. Based on the  $pK_a$  values and the actual mobilities the resolution was calculated across the pH range and compared with experimental data. The effect of experimental parameters on the separation of *p*- and *m*-aminobenzoic acids was investigated by Nielen [5]. The pH was varied between 4.0 and 6.0 and the optimum resolution was found to be close to the  $pK_a$  values of the analytes. Because these analytes have two  $pK_a$  values, a reversal in migration order was observed at low pH with co-migration at pH 4.2. The effect of the partial charge on the migration rates has also been used to determine ionisation constant at low solute concentrations [6]. By studying the change in electrophoretic mobility across the pH range,  $pK_a$  values between 2.55 and 5.26 were determined to within 0.03 pH units for analyte concentrations less than 100  $\mu M$ .

Separations due to differences in the shape of closely related analytes have been observed by several workers. The separation of *cis*-retinoic acid and *trans*-retinoic acid was investigated by Chadwick and Hsieh [7] and Korman and co-workers investigated the separation of codeine and its synthesis by-products [8]. A series of mono-alkylpyridines was investigated by Rowe and co-workers and molecular descriptors were used to explain the separation [9]. A mixture of (Z) and (E) pentenylpyridines has been investigated by CE and NMR and quantified by the two techniques [10].

In this study, the resolution of a complex mixture of the six dimethylpyridine isomers has been studied by capillary electrophoresis. The mobilities of the fully charged analytes were determined at low pH and these values, together with the partial charge calculated from their ionisation constants by using the Henderson–Hasselbalch equation, were used to predict the mobility of each isomer across a wide pH range. These predictions were then compared with the experimentally determined resolution.

## 2. Experimental

### 2.1. Chemicals

Distilled water was purified to 18 M $\Omega$  using an

Elga Maxima water purification system. The dimethylpyridines (DMP), benzamide and hydroxypropylmethylcellulose (Average M.N. 86 000. HPMC) were obtained from Aldrich Chemical (Gillingham, UK). Sodium dihydrogen phosphate, citric acid and orthophosphoric acid were obtained from BDH (Poole, UK). Lithium hydroxide was obtained from Fisons Scientific Apparatus (Loughborough, UK).

### 2.2. Apparatus

The capillary electrophoresis was carried out on a P/ACE 2050 system (Beckman Instruments, High Wycombe, UK), using a fused-silica capillary (Beckman) with an internal diameter of 75  $\mu m$ , a length from inlet to detector of 50 cm and a total length of 57 cm. The capillary was thermostatted to 25°C. The electropherograms were recorded at 254 nm using a 5 Hz collection rate. An IBM 433/DX microcomputer with System Gold Personal Chromatograph (Beckman) software was used for data collection.

Buffer pH values were measured using a combination pH electrode fitted to a radiometer Copenhagen PHM 64 research pH meter.

### 2.3. Methods

A lithium phosphate buffer was prepared by making up a 40 mM solution of orthophosphoric acid and adjusting the pH to 2.5 with 1 M lithium hydroxide. A sodium phosphate buffer was prepared by making a 50 mM solution of sodium dihydrogen phosphate and adjusting the pH to 6.5 with 1 M hydrogen chloride. Lithium citrate buffer systems were prepared by making up a 40 mM citrate solution and adjusting to the required pH with 1 M lithium hydroxide.

The dimethylpyridines were used as received. Stock solutions of 1 mg ml<sup>-1</sup> were made up in de-ionised water and samples for injection were prepared each day by taking 50 ml of the DMP stock solution and diluting it in 4.4 ml of de-ionised water. Samples were loaded onto the CE column by using a 2 s pressure injection and were separated using a voltage of 15 kV.

Electrophoretic mobilities  $\mu_e$  of the analytes were determined using the equation:

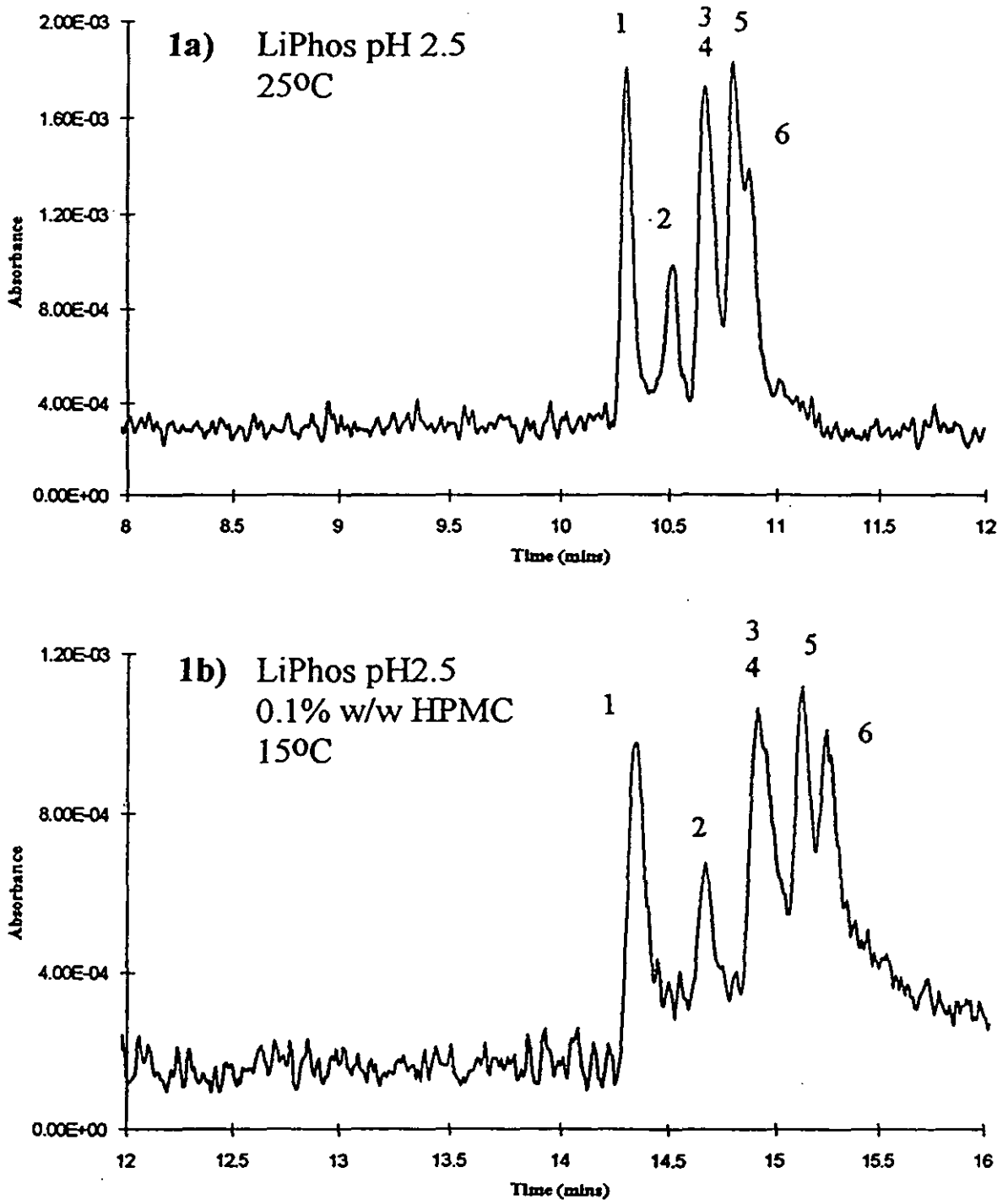


Fig. 1. Separation of the dimethylpyridines (DMP) at pH 2.5 with different buffers and temperatures: (a) 25°C 40 mM lithium phosphate buffer; b, 15°C, 40 mM lithium phosphate buffer, 0.1% w/w hydroxypropylmethylcellulose. Compounds: 1, 3,4-DMP; 2, 3,5-DMP; 3, 2,3-DMP; 4, 2,5-DMP; 5, 2,4-DMP; 6, 2,6-DMP.

Table 1  
Electrophoretic mobilities of the fully charged dimethylpyridines at pH 2.5 and their reported  $pK_a$  values

Compound	Electrophoretic mobility ( $\text{cm}^2 \text{V}^{-1} \text{s}^{-1}$ )	Literature $pK_a$ values [11]
3,4-Dimethylpyridine	$3.349 \cdot 10^{-4}$	6.52
3,5-Dimethylpyridine	$3.285 \cdot 10^{-4}$	6.25
2,3-Dimethylpyridine	$3.236 \cdot 10^{-4}$	6.60
2,5-Dimethylpyridine	$3.236 \cdot 10^{-4}$	6.47
2,4-Dimethylpyridine	$3.196 \cdot 10^{-4}$	6.72
2,6-Dimethylpyridine	$3.168 \cdot 10^{-4}$	6.77

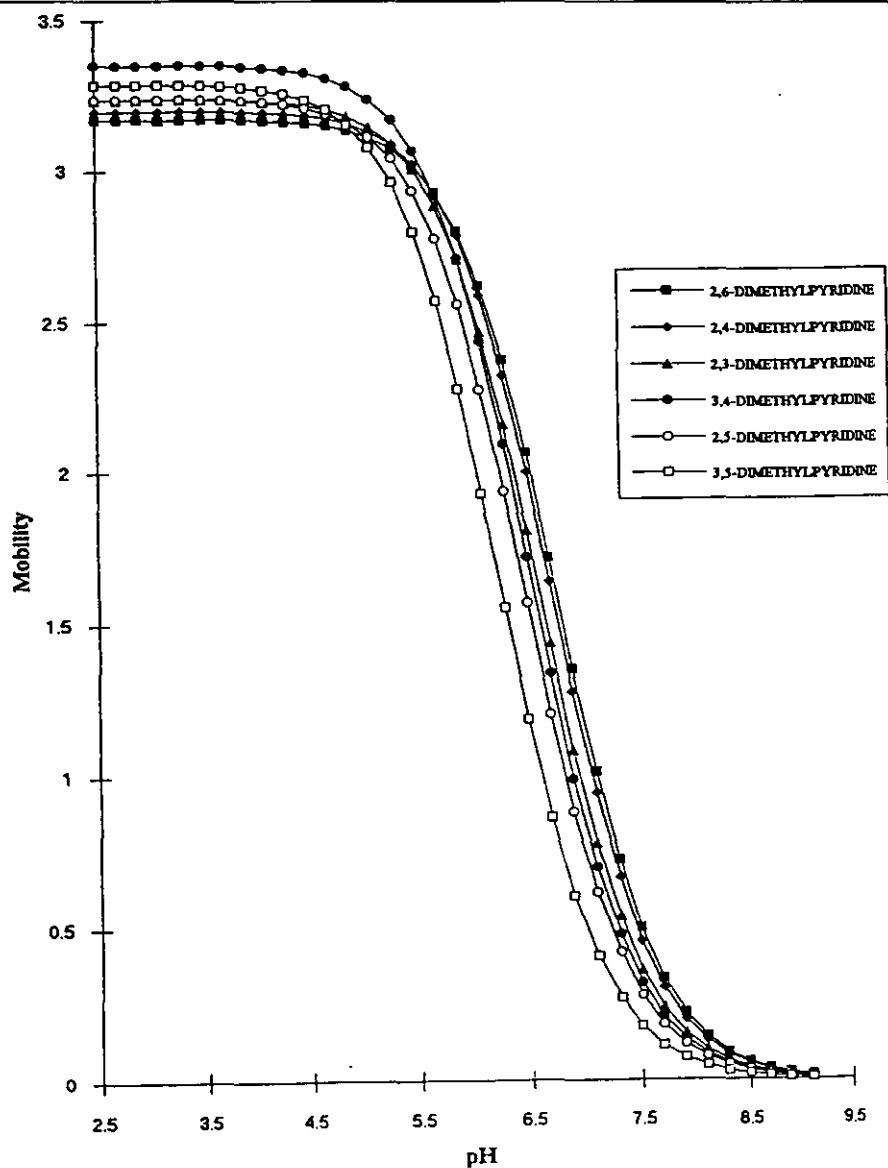


Fig. 2. Variation in predicted mobility of the dimethylpyridines with pH based on the mobilities at pH 2.5 and the partial charge on the analyte calculated from the buffer pH.

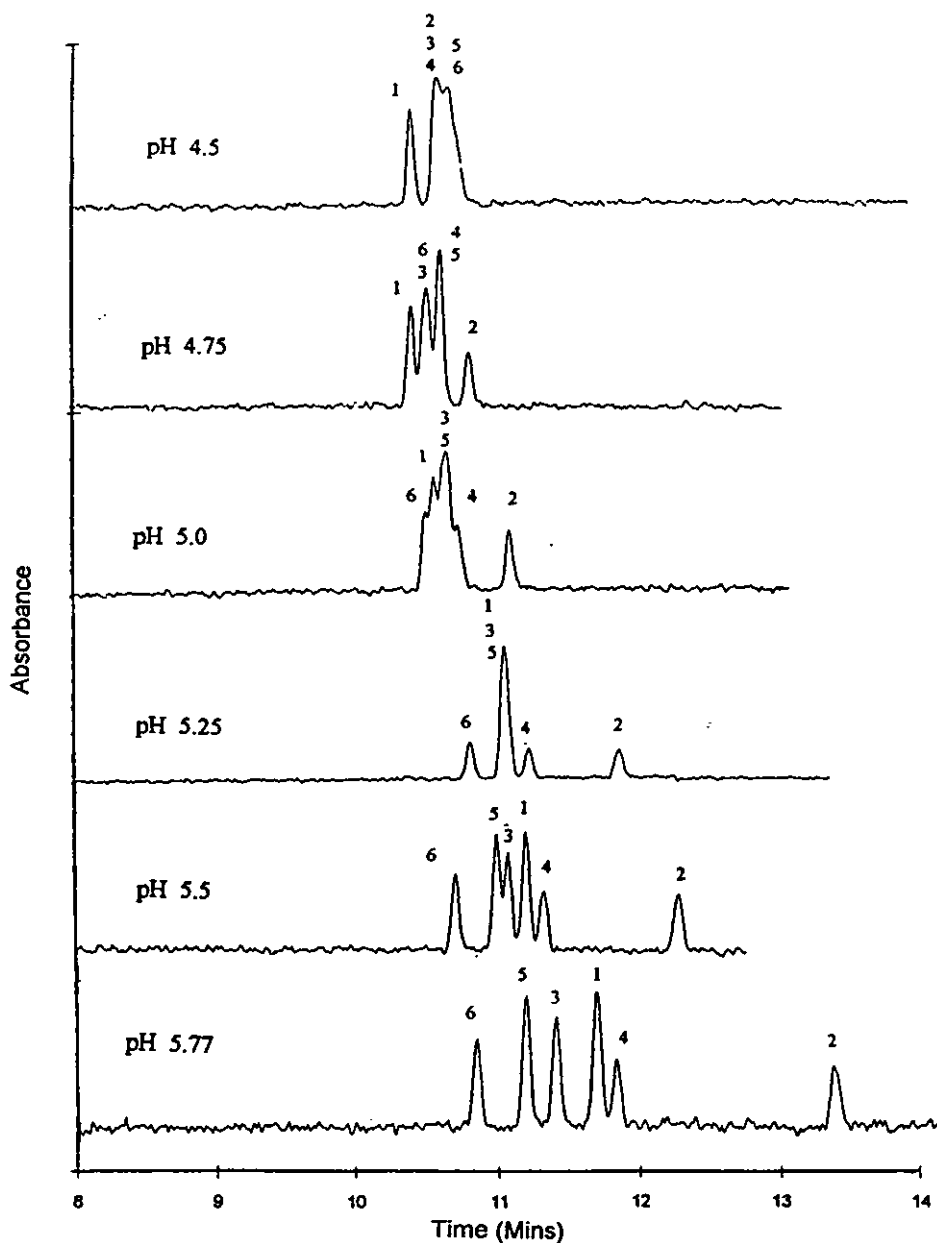


Fig. 3. Electropherograms showing the change in migration order of the dimethylpyridines at different buffer pH values. Compounds: 1, 3,4-DMP; 2, 3,5-DMP; 3, 2,3-DMP; 4, 2,5-DMP; 5, 2,4-DMP; 6, 2,6-DMP.

4) and the mobility order follows the predicted separation (Fig. 2). The mobilities for each isomer were calculated and were compared with the predicted values for the partial charge and electro-

phoretic mobility (Table 2). As can be seen the relative order of migration was predicted correctly but the absolute values of the electrophoretic mobility were all smaller than the predicted values with

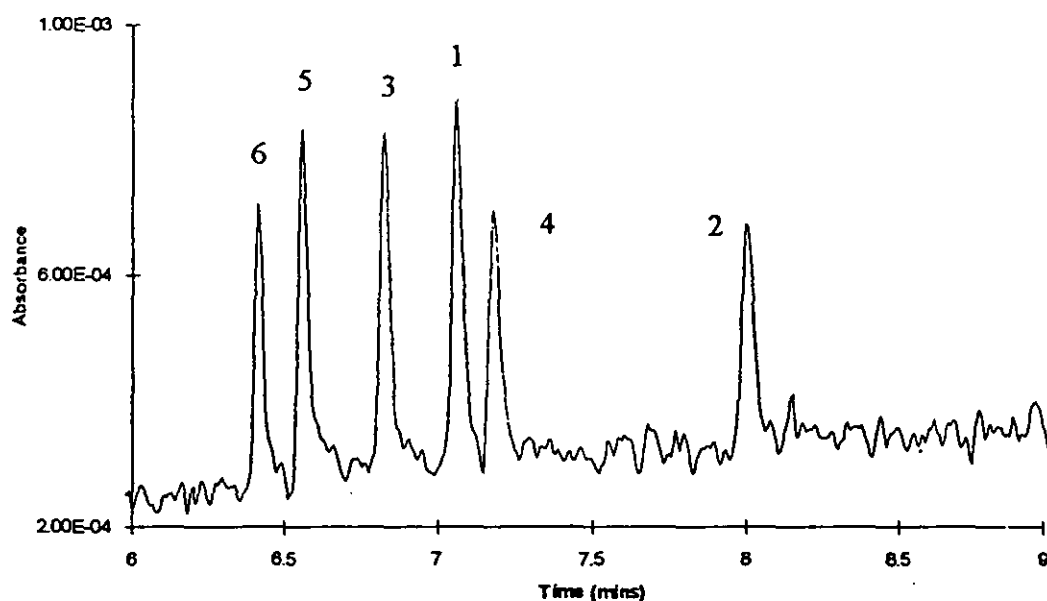


Fig. 4. Separation of the dimethylpyridines at pH 6.5. Buffer, 50 mM lithium phosphate buffer, 25°C. Compounds: 1, 3,4-DMP; 2, 3,5-DMP; 3, 2,3-DMP; 4, 2,5-DMP; 5, 2,4-DMP; 6, 2,6-DMP.

differences between 7% and 30%, with an average deviation of 15%. These differences are probably caused because the pH of the background electrolyte was slightly higher than the intended value. As can be seen in Fig. 2, at pH 6.5 the mobilities are very sensitive to pH and would change markedly with only a small discrepancy in the actual value compared to the nominal value.

#### 4. Conclusions

The six isomeric dimethylpyridines have been separated by free-zone capillary electrophoresis. The

order of elution changed with pH of the buffer and it was demonstrated that the relative order of elution and the electrophoretic mobilities over a range of pH could be predicted from the separation of the fully charged species and the calculated partial charges based on their  $pK_a$  values and the pH of the buffer.

#### Acknowledgements

The authors thank the Trustees of the Analytical Division of the Royal Society of Chemistry for a research studentship to AGM and Beckman Ltd. for the loan of a CE instrument.

Table 2  
Experimental and calculated mobilities and predicted partial charge on the dimethylpyridines at pH 6.5

Compound	Experimental mobility ( $\text{cm}^2 \text{V}^{-1} \text{s}^{-1}$ )	Predicted mobility ( $\text{cm}^2 \text{V}^{-1} \text{s}^{-1}$ )	Calculated partial charge
2,6-Dimethylpyridine	$1.947 \cdot 10^{-4}$	$2.06 \cdot 10^{-4}$	0.651
2,4-Dimethylpyridine	$1.848 \cdot 10^{-4}$	$1.99 \cdot 10^{-4}$	0.624
2,3-Dimethylpyridine	$1.630 \cdot 10^{-4}$	$1.80 \cdot 10^{-4}$	0.557
3,4-Dimethylpyridine	$1.464 \cdot 10^{-4}$	$1.71 \cdot 10^{-4}$	0.512
2,5-Dimethylpyridine	$1.386 \cdot 10^{-4}$	$1.56 \cdot 10^{-4}$	0.483
3,5-Dimethylpyridine	$0.912 \cdot 10^{-4}$	$1.18 \cdot 10^{-4}$	0.360

## References

- [1] S.F.Y. Li, *Capillary Electrophoresis—Principles, Practices and Applications* (Journal of Chromatography Library, Vol 52), Elsevier, Amsterdam, 1992.
- [2] S. Terabe, T. Yashima, N. Tanaka and M. Araki, *Anal. Chem.*, 60 (1988), 1673.
- [3] S.A.C. Wren, *J. Microcol. Sep.*, 3 (1991) 147.
- [4] W. Friedl and E. Kenndler, *Anal. Chem.*, 65 (1993) 2003.
- [5] M.W.F. Nielen, *J. Chromatogr.*, 542 (1991) 173.
- [6] J.A. Cleveland, Jr., M.H. Benko, S.J. Gluck and Y.M. Walbroehl, *J. Chromatogr. A*, 652 (1993) 301.
- [7] R.R. Chadwick and J.C. Hsieh, *Anal. Chem.*, 63 (1991) 2377.
- [8] M. Korman, J. Vindevoel and P. Sandra, *J. Chromatogr.*, 645 (1993) 366.
- [9] R.C. Rowe, S.A.C. Wren and A.G. McKillop, *Electrophoresis*, 15 (1994) 635.
- [10] A.G. McKillop, R.M. Smith, R.C. Rowe and S.A.C. Wren, *J. Chromatogr. A*, 700 (1995) 69.
- [11] D.D. Perrin, *Dissociation Constants of Organic Bases in Aqueous Solution*, International Union of Pure and Applied Chemistry, 1965, p. 155.

